PAGES 221–332

ISSN 0003–2654

THE ROYAL SOCIETY OF CHEMISTRY

1841–1991

The Analyst

A monthly international journal dealing with all branches of the theory and practice of analytical chemistry, including instrumentation and sensors, and physical, biochemical, clinical, pharmaceutical, biological, environmental, automatic and computer-based methods

Vol.116 No.3 March 1991

The Analyst

The Analytical Journal of The Royal Society of Chemistry

Editorial Manager, Analytical Journals: Judith Egan

Editor, *The Analyst*
Harpal S. Minhas
The Royal Society of Chemistry,
Thomas Graham House, Science Park,
Milton Road, Cambridge CB4 4WF, UK
Telephone 0223 420066.
Fax 0223 423623. Telex No. 818293 ROYAL.

US Associate Editor, *The Analyst*
Dr J. F. Tyson
Department of Chemistry,
University of Massachusetts,
Amherst MA 01003, USA
Telephone 413 545 0195
Fax 413 545 4490

Senior Assistant Editor
Paul Delaney

Assistant Editors
Brenda Holliday, Paula O'Riordan, Sheryl Whitewood

Editorial Secretary: Claire Harris

Advertisements: Advertisement Department, The Royal Society of Chemistry, Burlington House, Piccadilly, London, W1V 0BN. Telephone 071-437 8656. Telex No. 268001. Fax 071-437 8883.

The Analyst (ISSN 0003–2654) is published monthly by The Royal Society of Chemistry, Thomas Graham House, Science Park, Milton Road, Cambridge CB4 4WF, UK. All orders, accompanied with payment by cheque in sterling, payable on a UK clearing bank or in US dollars payable on a US clearing bank, should be sent directly to The Royal Society of Chemistry, Turpin Transactions Ltd., Blackhorse Road, Letchworth, Herts SG6 1HN, United Kingdom. Turpin Transactions Ltd., distributors, is wholly owned by the Royal Society of Chemistry. 1991 Annual subscription rate EC £246.00, USA $580, Rest of World £283.00. Purchased with *Analytical Abstracts* EC £551.00, USA $1299.00, Rest of World £634.00. Purchased with *Analytical Abstracts* plus *Analytical Proceedings* EC £648.00, USA $1527.00, Rest of World £745.00. Purchased with *Analytical Proceedings* EC £313.00, USA $738.00, Rest of World £360.00. Air freight and mailing in the USA by Publications Expediting Inc., 200 Meacham Avenue, Elmont, NY 11003.

USA Postmaster: Send address changes to: *The Analyst,* Publications Expediting Inc., 200 Meacham Avenue, Elmont, NY 11003. Second class postage paid at Jamaica, NY 11431. All other despatches outside the UK by Bulk Airmail within Europe, Accelerated Surface Post outside Europe. PRINTED IN THE UK.

Information for Authors

Full details of how to submit material fc publication in *The Analyst* are given in th Instructions to Authors in the January issue Separate copies are available on request.

The Analyst publishes papers on all aspects c the theory and practice of analytical chemistry fundamental and applied, inorganic an organic, including chemical, physical, biochem ical, clinical, pharmaceutical, biologica environmental, automatic and computer-base methods. Papers on new approaches to existin methods, new techniques and instrumentatior detectors and sensors, and new areas of appli cation with due attention to overcoming limita tions and to underlying principles are all equall welcome. There is no page charge.

The following types of papers will be con sidered:

Full research papers.

Communications, which must be on ar urgent matter and be of obvious scientifi importance. Rapidity of publication is enhancec if diagrams are omitted, but tables and formulae can be included. Communications receive pri ority and are usually published within 5–8 weeks of receipt. They are intended for brie descriptions of work that has progressed to a stage at which it is likely to be valuable tc workers faced with similar problems. A fulle paper may be offered subsequently, if justifiec by later work. Although publication is at the discretion of the Editor, communications will be examined by at least one referee.

Reviews, which must be a critical evaluation of the existing state of knowledge on a par ticular facet of analytical chemistry.

Every paper (except Communications) will be submitted to at least two referees, by whose advice the Editorial Board of *The Analyst* will be guided as to its acceptance or rejection. Papers that are accepted must not be published else where except by permission. Submission of a manuscript will be regarded as an undertaking that the same material is not being considered for publication by another journal.

Regional Advisory Editors. For the benefit of potential contributors outside the United Kingdom and North America, a Group of Regional Advisory Editors exists. Requests for help or advice on any matter related to the preparation of papers and their submission for publication in *The Analyst* can be sent to the nearest member of the Group. Currently serving Regional Advisory Editors are listed in each issue of *The Analyst.*

Manuscripts (four copies typed in double spacing) should be addressed to:

Harpal S. Minhas, Editor, *The Analyst,*
Royal Society of Chemistry,
Thomas Graham House,
Science Park, Milton Road,
CAMBRIDGE CB4 4WF, UK *or:*

Dr. J. F. Tyson
US Associate Editor, *The Analyst*
Department of Chemistry
University of Massachusetts
Amherst MA 01003, USA

Particular attention should be paid to the use of standard methods of literature citation, including the journal abbreviations defined in Chemical Abstracts Service Source Index. Wherever possible, the nomenclature employed should follow IUPAC recommendations, and units and symbols should be those associated with SI.

All queries relating to the presentation and submission of papers, and any correspondence regarding accepted papers and proofs, should be directed either to the Editor, or Associate Editor, *The Analyst* (addresses as above). Members of the Analytical Editorial Board (who may be contacted directly or via the Editorial Office) would welcome comments, suggestions and advice on general policy matters concerning *The Analyst.*

Fifty reprints are supplied free of charge.

PUBLISH IN THE ANALYST

Cambridge, 1991.

Dear Subscriber,

As a regular reader of *The Analyst* you probably know a fair amount about the journal. But did you know that *The Analyst*

- is the oldest English-language analytical science journal
- has the largest circulation of any European analytical science journal
- is truly international, going to over 90 countries worldwide, with US and Canadian sales equalling those in the UK
- accepts papers on all aspects of analytical chemistry
- is produced using full-time qualified professional editors, with a high standard of error detection (top in a recent independent survey of analytical chemistry journals)
- has no page or other charges, and provides authors with 50 free reprints
- uses peer review of submissions by two independent referees, and is backed by an internationally known editorial board
- now has a US Associate Editor, enabling North American submissions to be reviewed in their country of origin
- achieves rapid publication (5 months from acceptance to publication of papers, or 6–8 weeks for communications)?

If you did, you're probably already submitting your primary papers to *The Analyst*. If not, don't you think you should be? We welcome submissions in the areas stated below, and look forward to hearing from you.

Yours sincerely,

Harpal S. Minhas,
Editor

THE ANALYST
WELCOMES PAPERS ON:

- **Biochemical analysis**
- **Chemometrics**
- **Mass spectrometry**
- **Vibrational spectroscopy**
- **EPR and ESR**
- **Atomic & molecular absorption spectroscopy**
- **Chromatography**
- **Electrochemistry**

Editor, *The Analyst*, Harpal S. Minhas,
The Royal Society of Chemistry,
Thomas Graham House, Science Park,
Milton Road, Cambridge CB4 4WF, UK
Tel: 0223 420066. Fax: 0223 423623.
Tlx: 818293 ROYAL

US Associate Editor, Dr. J. F. Tyson,
Department of Chemistry,
University of Massachusetts, Amherst,
MA 01003, USA
Tel: 413 545 0195. Fax: 413 545 4490

ROYAL SOCIETY OF CHEMISTRY
Information Services

Editorial Manager, Analytical Journals: Judith Egan

Dilute, Neutral pH Standard of Known Conductivity and Acid Neutralizing Capacity*

David V. Peck and Richard C. Metcalf†
Environmental Programs Office, Lockheed Engineering and Sciences Company, 1050 E. Flamingo Road, Suite 209, Las Vegas, NV 89119, USA

By using the equilibrium computer program MINTEQA2, a quality control standard suitable for assessing measurement errors of pH, acid neutralizing capacity (ANC, formerly titration alkalinity) and conductivity of dilute, neutral pH solutions [ionic strength $\approx 4.6 \times 10^{-4}$ mol kg^{-1} of solvent (water)] has been developed and tested. A dilute phosphate standard is prepared as a 200-fold dilution (by mass) of 0.025 mol kg^{-1} (of solvent) KH_2PO_4 and Na_2HPO_4 standard buffer solution. At 25 °C and in equilibrium with 340 vppm (parts per million by volume) CO_2, the standard has a theoretical pH of 6.89, a calculated ANC of 125×10^{-6} equiv kg^{-1} (124.6×10^{-6} equiv dm^{-3}) and a calculated conductivity of 37.6×10^{-4} S m^{-1}. Theoretical pH and calculated ANC and conductivity values were also determined at equilibrium with laboratory CO_2 concentrations ranging between 0 and 680 vppm. The dilute phosphate standard was measured repeatedly over a 6 month period at three laboratories. Measurements agreed well with the theoretical values (mean pH = 6.87, $2s = \pm 0.100$, $n = 362$; mean ANC = 124.5×10^{-6} equiv dm^{-3}, $2s = \pm 8.78$, $n = 294$; mean conductivity = 37.7×10^{-4} S m^{-1} at 25 °C, $2s = \pm 5.22$, $n = 308$). The long-term systematic and random errors associated with the dilute phosphate standard are reduced for pH (because of reduced sensitivity to changes in CO_2), and comparable for ANC and conductivity as compared to a dilute hydrogen carbonate standard (7.0×10^{-5} mol kg^{-1} $NaHCO_3$ and 1.75×10^{-4} mol kg^{-1} KCl). For the dilute phosphate standard, among-day variation within a laboratory is the greatest source of error for ANC and conductivity measurements. For the dilute hydrogen carbonate standard, among-laboratory variation is the greatest source of error in pH measurements. Within-day variation is the greatest source of error in ANC measurements for the dilute hydrogen carbonate standard, while among-day variation within a laboratory is the greatest source of error for conductivity measurements of both dilute standards. Additional application of total speciation programs to the solving of design problems for quality control and assurance samples appears promising and justified.

Keywords: *Dilute pH standard solution; acid neutralizing capacity standard solution; conductivity standard solution; acidic precipitation standards; quality control of water analyses*

In studies of surface water acidification, pH, acid neutralizing capacity (ANC, formerly titration alkalinity) and conductivity are important indicators of acidification status. Surface waters sensitive to acidification are characterized by neutral pH values, low ANC, low conductivity and low ionic strength. These systems serve as early warning indicators of acidification, and quantitative estimates of measurement precision and bias are necessary in order to interpret correctly long-term trends in water quality. It is important to utilize appropriate standard solutions to assess the random and systematic errors associated with such measurements.

An appropriate standard solution for this purpose should have the following properties: (*i*) it should be of appropriate ionic strength and have representative levels of the chemical determinands of interest; (*ii*) it should have a composition such that it can be used as a standard for more than one determinand (for cross-checking the composition and for convenience in preparation); and (*iii*) it should provide reproducible results, over extended periods and in different geographic locations, with minimal systematic errors due to changes in sample composition.

Dilute acid standards are often used to assess the precision and bias of pH,[1] and for conductivity measurements[2] in acidification studies of surface waters and precipitation. Such standards, while of known pH, negative ANC values, and sometimes known conductivity values, are not necessarily representative of acid-sensitive surface waters. Precision and bias estimates from such standards are assumed to be representative of the precision and bias present at neutral pH, low positive ANC and low conductivity values. Little proof of the accuracy of this extrapolation is available.

In order to alleviate such concerns, dilute standards of neutral pH, low ANC and low conductivity based on carbonate compounds have been used at our laboratories.[3–5] Circumstantial evidence has indicated that some dilute, neutral pH standards made from carbonate compounds are difficult to prepare with accurate CO_2 equilibration during high-volume analyses and do not yield reproducible results, even when prepared with extreme care. The pH (and to a lesser extent, conductivity) can be influenced substantially by daily changes in ambient atmospheric CO_2 concentrations. Low pressures and temperatures during express transport in the unpressurized cargo compartment of an airplane, the size and ventilation of the laboratory rooms for analyses, and the number of respiring technicians can change the atmospheric CO_2 concentrations in equilibrium with the samples.

A dilute, neutral pH standard for assessing the precision and accuracy of pH, ANC and conductivity measurements in neutral, dilute surface waters, which meets all three of the criteria presented above, has been developed. While the standard that has been developed and is presented here is probably most applicable to dilute surface waters, the proposed method using chemical speciation computer programs has much wider applicability in the development of suitable quality control standards for a wide range of water

* Although the information in this paper has been funded in part by the United States Environmental Protection Agency under contract number 68-03-3249 to Lockheed Engineering and Sciences Company, it has not been subjected to review by the Agency. It therefore does not necessarily reflect the views of the Agency and no official endorsement should be inferred. The mention of trade names or commercial products does not constitute endorsement or recommendation for use. This work is a contribution to the United States Environmental Protection Agency's Aquatic Effects Research Program which is a part of the National Acid Precipitation Assessment Program.

† To whom correspondence should be addressed.

quality studies. The approach used in developing and verifying this standard was: selecting an appropriate reference material, developing predicted values for pH, ANC and conductivity using a chemical speciation program, confirming empirically the predicted values by repeated measurements at several laboratories, and comparing various effects on the measurement variance of the standard.

Selection of Reference Material

National Bureau of Standards [NBS, now known as the National Institute of Standards and Technology (NIST)] 0.025 mol kg^{-1} KH_2PO_4 and 0.025 mol kg^{-1} Na_2HPO_4 pH standard (6.865 pH units at 25 °C) was chosen as an appropriate stock solution. [Except where specifically noted, all concentrations are expressed as mol kg^{-1} of solvent (which is water in the case considered). However, for the concentrations of the dilute standards, there is little numerical difference between mol kg^{-1} of solvent (infrequently termed 'molality'), mol kg^{-1} of solution and mol dm^{-3}.] It was felt that if the inferences made about pH changes in previous dilute, neutral pH standards, caused by varying CO_2 concentrations, were correct, that a successful new standard would have more hydrogen ion (H^+) complexed by non-carbonate species than the previous carbonate-based standards. The NBS standard offers several advantages as a stock solution. Even when diluted, its chemical characteristics are dominated by phosphate equilibria, rather than carbonate equilibria. The reagents are commonly available with high purity at low cost. The equilibrium constants for the controlling equilibria are well known.[6–8] In undiluted form, the NBS standard has been found to change less than 0.007 pH units during 28 months of storage, although some mould or sediment was observable.[9]

A 200-fold dilution (by mass) of the NBS equimolal phosphate buffer was selected for the initial dilute, neutral pH standard, hereafter referred to as the 'dilute phosphate standard' (1.25×10^{-4} mol kg^{-1} KH_2PO_4 and Na_2HPO_4). In order to obtain estimates of the appropriate ionic strength for a dilute standard, previous trial and error dilutions of a commercial pH 7 buffer (American Scientific Products' proprietary stock solution, manufactured by Fisher Scientific, Tustin, CA. Certified to be pH = 7.00 ± 0.01 at 25 °C and NBS-traceable.) to a conductivity of less than 75×10^{-4} S m^{-1} at 25 °C were used.[10]

Development of Theoretical pH, ANC and Conductivity Values

Theoretical values for the dilute phosphate standard were calculated using the chemical speciation computer program MINTEQA2 (version A21).[8,11] (MINTEQA2 is available from the US Environmental Protection Agency's Center for Exposure Assessment Modeling, Athens, GA 30613-7799, USA.) Both DOS executable code and the FORTRAN 77 source code are provided.

[**N.B.** Use of the MINTEQA2 program was enhanced by J. Allison and J. Westall who showed us how to avoid poor estimates of initial component activities (by using the log activity of H^+ and PO_4^{3-} = −10.00) which prevented the program from converging properly during the solution of the mass balance equations. Without incorporating this critical technique, other workers will be unable to reproduce the results of the present study using MINTEQA2.]

MINTEQA2 is a hybrid, multi-component, chemical equilibrium speciation program based on the matrix computational scheme of MINEQL[12] and the database of WATEQ3.[13] It includes equilibrium constant variation with temperature using the van't Hoff equation. Individual ion activity coefficients are estimated using either the Debye–Hückel or Davies equation.[8] Considerable flexibility in assigning boundary conditions is available. This flexibility allowed rapid changes of the input conditions (*e.g.*, CO_2 partial pressure or sample temperature) during interactive design of the dilute phosphate standard solution.

The test runs in this study were performed on IBM AT or AT-compatible personal computers running at 8 or 12 MHz with 1 Mbyte of RAM and a mathematical co-processor chip. Typical runs averaged 3–5 min per sample.

In order to assess the accuracy of the computed results using the given equilibrium constants, data from well characterized pH standards, as test cases, were initially input. Table 1 shows the pH values for two common NBS concentrated buffers, calculated using MINTEQA2, compared to the reference pH values measured with the hydrogen electrode.[10] The pH values calculated from MINTEQA2 (in an atmosphere without CO_2) are within 0.01 pH units of the measured standards (measured in a hydrogen atmosphere) for seven tests carried out at 20 or 25 °C. Poor agreement (−0.25 pH units) was observed at the extreme temperature limit of NBS reference measurements at 95 °C. [This problem could be resolved by placing a seven coefficient, higher-order poly-

Table 1 Comparison between pH standards and pH values calculated using MINTEQA2

Concentration/ mol kg^{-1}	Temperature/ °C	Reference pH	Predictive error*	Calculated pH		Ionic strength with CO_2/ mol kg^{-1}
				Without CO_2	340 vppm CO_2	
NBS potassium hydrogen phthalate standard (0.05 mol kg^{-1} $KC_8H_5O_4$)—						
0.05	25	4.008†	−0.006	4.002	4.002	5.34×10^{-2}
0.05	5	3.999†	−0.008	4.007	4.007	5.33×10^{-2}
0.05	95	4.227†	−0.252	3.975	3.975	5.35×10^{-2}
0.01	25	4.117‡,§	−0.004	4.113	4.113	1.07×10^{-2}
0.01	20	4.112‡	+0.002	4.114	4.114	1.07×10^{-2}
0.001	25	4.334§,¶	−0.004	4.330	4.329	1.13×10^{-3}
NBS phosphate buffer standard (0.025 mol kg^{-1} KH_2PO_4 + 0.025 mol kg^{-1} Na_2HPO_4)—						
0.025	25	6.865†	−0.009	6.856‖	6.854‖	9.75×10^{-2}
0.025	5	6.951†	−0.026	6.925	6.922	9.82×10^{-2}
0.025	95	6.886†	−0.248	6.638	6.637	9.39×10^{-2}
0.0025	25	7.068‡	−0.001	7.067	7.046	9.89×10^{-3}
0.0025	20	7.082‡	−0.001	7.081	7.057	9.89×10^{-3}

* Error calculated as calculated pH (without CO_2) minus reference pH.
† See reference 9, p. 73.
‡ See reference 14, p. 1529.
§ See reference 15, Table 3.
¶ See reference 16, p. 1063.
‖ As an example of the differences caused by varying activity coefficient algorithms, values in both of these columns have been computed with the Davies equation. Use of the Debye–Hückel equation in MINTEQA2 yields pH values of 6.865 (without CO_2) and 6.864 (340 vppm CO_2), respectively.

nomial function relating log K and T (in K) in the MINTEQA2 database calibrated against the known NBS measurements. This was not necessary for the present work, but would not have provided any information about the accuracy of our modelling either.] The good agreement observed between the pH values calculated using MINTEQA2 and measured with a hydrogen electrode[10] convinced us of the capabilities of MINTEQA2 and of the accuracy of the equilibrium constants in the MINTEQA2 database for the phosphate buffer (especially the 10-fold dilutions by mass), on which the predictions made in this study depend (Table 1).

Acid neutralizing capacity is often calculated for surface water studies in order to compare calculated with measured ANC values.[17,18]

For an aqueous solution containing KH_2PO_4 and Na_2HPO_4 and exposed to atmospheric CO_2, the charge balance equation is:

$$[H^+] + [K^+] + [Na^+] = [HCO_3^-] + 2[CO_3^{2-}] + [H_2PO_4^-] + 2[HPO_4^{2-}] + 3[PO_4^{3-}] + [NaCO_3^-] + [NaHPO_4^-] + [KHPO_4^-] + [OH^-] \quad (1)$$

where the bracketed values are ionic concentrations.

By using the derivation, developed by Kramer,[17] of ANC for acid titrations of mixed protolyte systems, the equation to calculate ANC (expressed as equiv kg^{-1} of solvent) in the dilute phosphate standard solution is as follows:

$$ANC = [HCO_3^-] + [HPO_4^{2-}] + [OH^-] - [H^+] \quad (2)$$

This definition of ANC implies a potentiometric titration to a $H_2PO_4^-/H_2CO_3$ equivalence point.

For a given addition of H^+ during the simulated 'titration' shown in Fig. 1, the remaining ANC is calculated by:

$$\text{Remaining ANC} = 125 \times 10^{-6} \text{ equiv kg}^{-1} - [H^+_{added}] \quad (3)$$

Previous work with the 200-fold dilution of a proprietary pH 7 buffer[10] suggested that the conductivity of the solution would be consistently less than 100×10^{-4} S m^{-1} at 25 °C which enables the conductivity to be calculated from solution concentrations with minimal errors.[19] By modifying the methods of Rossum[19] and Dobos,[20] the conductivity of the standard solution was calculated by summing the contributions for each major ion of the product of the ionic concentration, calculated using the MINTEQA2 program, and the Onsager-corrected equivalent conductivity at 25 °C.[20,21]

Theoretical pH values for the 200-fold dilution (by mass) of the NBS pH 7 buffer are computed as part of the total speciation for the standard solution. Table 2 shows the speciation calculated for this standard at 25 °C in an atmosphere containing 340 vppm (parts per million by volume) of CO_2. It is apparent from this calculation that only species of concentrations between 10^{-4} (K^+, Na^+, $H_2PO_4^-$) and 10^{-5} (HCO_3^-, H_2CO_3, HPO_4^{2-}) mol kg^{-1} are controlling the equilibria of this standard. Individual ion activities were calculated using the Davies equation.[22] It should be noted that the ionic strength of this standard (4.602×10^{-4} mol kg^{-1}) is about 20 times more dilute than many commonly used neutral pH standards of known composition (Table 1).

Table 3 gives the pH results of 12 speciation calculations following that shown in Table 2, under a variety of CO_2 gas concentrations (0, 170, 340 and 680 vppm CO_2 under a total pressure of 1.013×10^5 Pa = 1 atm) and ambient temperatures (5, 15 and 25 °C). The pH values calculated at 25 °C are believed to be accurate to within ±0.01 pH units based on the test comparisons presented in Table 1. (All values in Table 3 are rounded to two decimal places from values calculated from MINTEQA2 given to three decimal places.) Uncertainties in calculating single ion activity coefficients from the Davies equation should decrease in more dilute solutions. Therefore, pH estimates for the 200-fold dilution used here should be

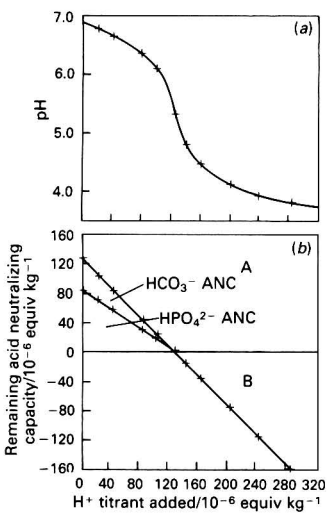

Fig. 1 (*a*) Calculated pH and (*b*) remaining ANC (by species) of a 1.25×10^{-4} mol kg^{-1} KH_2PO_4 and Na_2HPO_4 standard solution *versus* addition of H^+ from the HCl titrant during a simulated ANC titration (computed using the MINTEQA2 program, assuming an atmosphere containing 340 vppm CO_2 at 25 °C). A, H^+ neutralized during HCl addition; and B, excess of H^+ added after the equivalence point

Table 2 Calculated speciation for 1.25×10^{-4} mol kg^{-1} KH_2PO_4 and Na_2HPO_4 solution* at 25 °C in an atmosphere of 340 vppm CO_2 (speciation based on MINTEQA2 program)

Species	Calculated concentration/ mol kg^{-1}	Log of activity	Activity coefficient (γ_{Davies})
K^+	1.250×10^{-4}	−3.91	0.9757
PO_4^{3-}	3.356×10^{-10}	−9.57	0.8016
Na^+	2.500×10^{-4}	−3.61	0.9757
H^+	1.326×10^{-7}	−6.89	0.9757
CO_3^{2-}	1.551×10^{-8}	−7.85	0.9064
$H_2PO_4^-$	1.648×10^{-4}	−3.79	0.9757
OH^-	7.960×10^{-8}	−7.11	0.9757
$NaCO_3^-$	6.514×10^{-11}	−10.20	0.9757
$NaHCO_3$(aq)	5.332×10^{-9}	−8.27	1.0001
$NaHPO_4^-$	3.762×10^{-8}	−7.44	0.9757
$KHPO_4^-$	1.898×10^{-8}	−7.73	0.9757
HCO_3^-	3.981×10^{-5}	−4.41	0.9757
H_2CO_3(aq)	1.123×10^{-5}	−4.95	1.0001
HPO_4^{2-}	8.515×10^{-5}	−4.11	0.9064

* Ionic strength of solution = 4.602×10^{-4} mol kg^{-1}.

Table 3 Theoretical pH values for 200-fold dilution (by mass) of NBS phosphate buffer standard at various temperatures and concentrations of CO_2. (Theoretical values estimated using MINTEQA2 computer speciation program)

	CO_2 (vppm)			
Temperature/ °C	340 (atmospheric)*	0 (inert gas)†	170 (½ atmospheric)‡	680 (2 × atmospheric)‡
25	6.89	7.17	7.00	6.75
15	6.87	7.20	6.99	6.70
5	6.83	7.23	6.96	6.65

* Expected condition for most laboratory pH measurements.
† Conditions for standard hydrogen electrode measurements.
‡ These levels represent extremes in laboratory conditions for pH measurements.

expected to improve compared to the higher ionic strength standards presented in Table 1 for 25 °C.

The comparison of calculations with measured pH reference values given in Table 1 suggests that greater error is incurred in predicting pH using MINTEQA2 calculations as temperatures are progressively different from 25 °C. It is felt that the pH estimates are more uncertain at 5 °C than at 15 °C.

The inert gas atmosphere pH values in Table 3 have been included because those pH values should be measured with a standard hydrogen electrode (see comparison in Table 1), and also for comparison with relatively simplified pH calculations,[23] which do not include complications from CO_2 in air. The doubled and halved values of atmospheric CO_2 concentrations are included (Table 3) in order to provide the maximum variation for pH changes that can be expected from CO_2 variation for this phosphate standard, *i.e.*, 7.00 − 6.75 = 0.25 pH units at 25 °C. For a hydrogen carbonate standard (7.00×10^{-5} mol kg^{-1} $NaHCO_3$ and 1.250×10^{-4} mol kg^{-1} KCl; ANC = 70×10^{-6} equiv dm^{-3}) which has been used in earlier work,[4,5] the calculated pH is 6.84 at 680 vppm CO_2 and 7.44 at 170 vppm CO_2. This yields a maximum pH change, caused by CO_2 variation in the carbonate standard, of 0.60 pH units compared with 0.25 pH units for the dilute phosphate standard used here, which minimizes pH changes that result from p_{CO_2} changes in the laboratory atmosphere.

The calculation of the theoretical conductivity of the 1.25×10^{-4} mol kg^{-1} KH_2PO_4 and Na_2HPO_4 standard solution, designed in the present study, is given in Table 4. At 340 vppm CO_2 concentration, the theoretical conductivity of the standard is 37.6×10^{-4} S m^{-1} at 25 °C. Carbonate species make up less than 5% of the contribution to the theoretical conductivity of the phosphate standard. However, the variation in laboratory CO_2 can cause changes of conductivity in the standard of greater than 5% through changes in the concentrations of the phosphate anionic species with changing pH. Table 4 shows examples of such conductivity changes, when the standard is purged with an inert gas (0 vppm CO_2), or is at equilibrium with 170 or 680 vppm CO_2. At 0 vppm CO_2, the theoretical conductivity rises to 38.8×10^{-4} S m^{-1} at 25 °C, rather than the $37.6 - 1.8 = 35.8 \times 10^{-4}$ S m^{-1} at 25 °C obtained by subtracting the hydrogen carbonate contribution from the conductivity at 340 vppm CO_2. The 8% increase in conductivity after removing CO_2 from solution is caused by the increase in HPO_4^{2-} concentrations as pH increases during CO_2 removal. At 170 vppm CO_2 and 25 °C, the theoretical conductivity is 38.0×10^{-4} S m^{-1}, an increase of 0.4×10^{-4} S m^{-1} over the conductivity at 340 vppm CO_2. At CO_2 levels greater than normal (340 vppm CO_2), the conductivity decreases slightly. At 680 vppm and 25 °C, the theoretical conductivity is 37.0×10^{-4} S m^{-1}, a decrease of 0.6×10^{-4} S m^{-1} from the theoretical conductivity at 340 vppm CO_2.

Limiting equivalent ionic conductivities were employed from several different references[6,20,21,26] without changing the solution conductivity by more than 0.1×10^{-4} S m^{-1} at 25 °C.

Table 4 Conductivity calculations for 1.25×10^{-4} mol kg^{-1} KH_2PO_4 and Na_2HPO_4 standard solution at 25 °C

Major ion*	Concentration/ mol kg^{-1}	Equivalent concentration/ 10^{-3} equiv kg^{-1}	Limiting equivalent conductivity†/ 10^{-4} S m^2 equiv^{-1}	Onsager equivalent conductivity/ 10^{-4} S m^2 equiv^{-1}	Contribution to conductivity/ 10^{-4} S m^{-1} at 25 °C
K^+	1.25×10^{-4}	0.1250	73.5	72.6	9.08
Na^+	2.500×10^{-4}	0.2500	50.1	49.0	12.24
H^+	1.326×10^{-7}	0.00013	349.7	349.6	0.05
OH^-	7.96×10^{-8}	0.00008	197.6	197.6	0.02
$H_2PO_4^-$	1.648×10^{-4}	0.1648	32.3‡	31.4	5.18
HCO_3^-	3.981×10^{-5}	0.03981	44.5	44.1	1.75
HPO_4^{2-}	8.515×10^{-5}	0.1703	55§	54.3	9.25
	Total contribution under 340 vppm CO_2 atmosphere:				37.6
	Total contribution under inert gas atmosphere:				38.8
	Total contribution under 170 vppm CO_2 atmosphere:				38.0
	Total contribution under 680 vppm CO_2 atmosphere:				37.0

* Order of species based on MINTEQA2 output, as presented in Table 2.
† Source: reference 20.
‡ Sources: reference 24 ($32.3 \pm 0.1 \times 10^{-4}$ S m^2 equiv^{-1}); reference 25 ($31.9 \pm 0.3 \times 10^{-4}$ S m^2 equiv^{-1}).
§ As used in reference 24.

Table 5 Summary statistics for measurements of a 1.25×10^{-4} mol kg^{-1} KH_2PO_4 and Na_2HPO_4 standard, measured at three laboratories during a 6 month period. (Predicted values from the MINTEQA2 program are in parentheses, assuming 340 vppm CO_2 and 25 °C)

pH (6.89)

Laboratory	*n*	Mean	2*s*	2SE†
A	160	6.86	±0.074	±0.006
B	63	6.84	±0.174	±0.022
C	139	6.89	±0.044	±0.004
Total	362	6.87	±0.100	±0.060

ANC (125×10^{-6} equiv kg^{-1}*)

Laboratory	*n*	Mean‡	2*s*	2SE
A	112	126.2	±7.10	±0.68
B	75	125.8	±9.18	±1.06
C	107	121.7	±7.18	±0.70
Total	294	124.5	±8.78	±0.52

Conductivity (37.6×10^{-4} S m^{-1} at 25 °C)

Laboratory	*n*	Mean	2*s*	2SE
A	87	38.3	±8.06	±0.86
B	84	37.8	±3.58	±0.38
C	137	37.3	±3.36	±0.28
Total	308	37.7	±5.22	±0.30

* 125.00×10^{-6} equiv kg^{-1} = 124.64×10^{-6} equiv dm^{-3}.
† Standard error of the mean.
‡ Units of 10^{-6} equiv dm^{-3}.

However, a detailed search of primary sources revealed significant errors in some valued compilations of limiting ionic conductivities, especially the few mentioning the values of $H_2PO_4^-$ (36×10^{-4} S m^2 equiv^{-1}) and HPO_4^{2-} (57×10^{-4} S m^2 equiv^{-1}).[20] In fact, the limiting conductivity value of $H_2PO_4^-$ has been determined to be $32.3 (\pm 0.1) \times 10^{-4}$ S m^2 equiv^{-1} by Selvaratnam and Spiro[24] and $31.9 (\pm 0.3) \times 10^{-4}$ S m^2 equiv^{-1} by Marx and Fischer.[25] In the present study 32.3×10^{-4} S m^2 equiv^{-1} has been used as the limiting ionic conductivity of $H_2PO_4^-$ as has the value of 55×10^{-4} S m^2 equiv^{-1} for HPO_4^{2-} cited by Selvaratnam and Spiro.[24] We are uncomfortable with the present state of knowledge concerning the limiting equivalent conductivity of HPO_4^{2-} and think it is the most poorly known variable in our conductivity estimates.

After compiling the limiting equivalent conductivity values presented in Table 4, the Debye–Hückel–Onsager equation[27,28] was used in the present work to calculate the equivalent conductivity of each species for the theoretical concentrations as calculated with MINTEQA2. These values are termed 'Onsager equivalent conductivity' in Table 4. The product of the Onsager equivalent conductivity and the equivalent concentration of the species yields the contribution of a given species to conductivity.

The ANC values were calculated by using two different techniques during a theoretical titration of the phosphate standard to the $H_2PO_4^-/H_2CO_3$ equivalence point with HCl as the titrant. The first method calculated the ANC at each point of addition of titrant using equation (2). This theoretical titration, the plot of ANC, remaining ANC [equation (3)], and excess of H^+_{added} are shown in Fig. 1. Fig. 1 shows that most of the ANC of the solution is provided by HPO_4^{2-} and that the reference ANC value is 125.00×10^{-6} equiv kg^{-1}. The second method was a Gran analysis[22] of computed acidic pH values, which gives the same molal ANC value when H^+ activity corrections are included. On a volumetric basis, the reference ANC value is 124.64×10^{-6} equiv dm^{-3} (using the specific gravity determination of Bates[9] for the NBS concentrated buffer at 25 °C = 1.0028 kg dm^{-3} of solution).

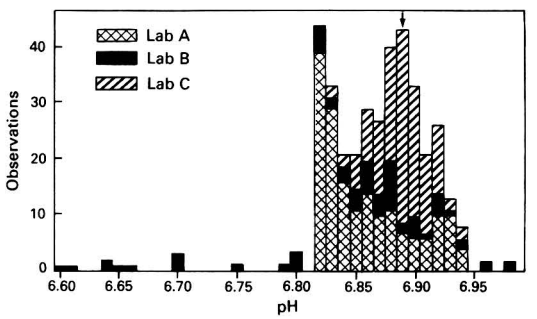

Fig. 2 Histogram of pooled pH measurements, from three laboratories, for the 1.25×10^{-4} mol kg^{-1} KH_2PO_4 and Na_2HPO_4 standard made from different aliquots of the same 0.025 mol kg^{-1} stock solution. Patterns on the bars denote measurements made at each laboratory. The arrow denotes the theoretical pH of 6.89 at 25 °C under 340 vppm CO_2

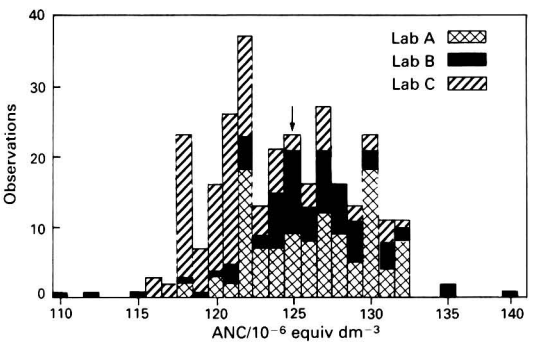

Fig. 3 Histogram of pooled ANC measurements from three laboratories for the 1.25×10^{-4} mol kg^{-1} KH_2PO_4 and Na_2HPO_4 standard solution made from different aliquots of the same 0.025 mol kg^{-1} stock solution. Patterns on the bars denote measurements made at each laboratory. The arrow denotes the theoretical ANC of 124.64×10^{-6} equiv dm^{-3} (125.00×10^{-6} equiv kg^{-1}) at 25 °C under 340 vppm CO_2

Empirical Verification of Dilute Phosphate Standard

Verification of the pH, ANC and conductivity of the dilute phosphate standard was accomplished through repeated measurements conducted at three laboratories over a 6 month period. A large volume (20 dm^3) of the NBS phosphate buffer[9] was prepared as a stock standard. The pH of the stock standard (6.865 at 25 °C) was verified by measurement with a Ross pH combination electrode. Smaller volumes (2 dm^3) of the stock standard, prepared by sub-sampling the 20 dm^3 volume, were distributed to three laboratories. During the 6 month period, each laboratory independently prepared 200-fold dilutions of the stock standard. For each day when measurements were made, repeated measurements of each dilution were conducted for pH (combination electrode), ANC (Gran titration) and conductivity. Measurements of the dilute phosphate standard were conducted in conjunction with analyses of streamwater samples.

All chemical measurement protocols followed those published by the Aquatic Effects Research Program of the United States Environmental Protection Agency.[29] Quality control samples were measured in every batch in each laboratory for each method. All laboratories used Orion Ross pH combination electrodes with an operational equilibrium of not more than 0.02 pH units change throughout a 1 min interval.[29,30] Temperature-compensated pH measurements were made at laboratory temperatures (20–25 °C) using comparable Orion 901, Orion 811 and Beckman 571 pH meters. Temperature-corrected conductivity measurements (2% per °C, corrected to 25 °C) were made at laboratory temperatures using Yellow Springs Instrument (YSI) Model 31, YSI Model 32 and Altex conductivity bridges. At our laboratory, comparable pH measurements were made using Ross pH combination electrodes and an Orion 611 pH meter. The temperature-corrected conductivity measurements in this laboratory were made with YSI Model 32 and modified Aqua Chemical PTI 10 conductivity bridges. Acid neutralizing capacity measure-

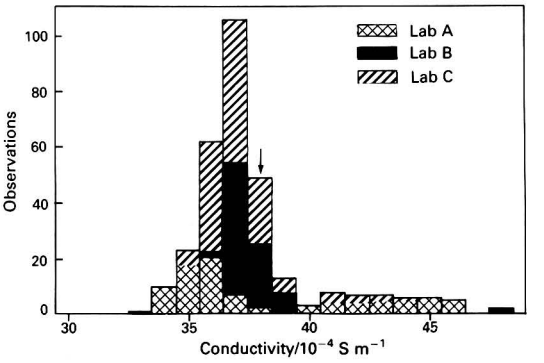

Fig. 4 Histogram of pooled conductivity measurements from three laboratories for the 1.25×10^{-4} mol kg^{-1} KH_2PO_4 and Na_2HPO_4 standard solution made from different aliquots of the same 0.025 mol kg^{-1} stock solution. Patterns on the bars denote measurements made at each laboratory. The arrow denotes the theoretical conductivity of 37.6×10^{-4} S m^{-1} at 25 °C under 340 vppm CO_2

ments were made by potentiometric titration of mixtures containing 36.0 ml of sample and 4.0 ml of 1.00 mol dm^{-3} KCl, with HCl as the titrant. Equivalence point (V_2) determination was by linear, least-squares fit of 'acid side' titration points (pH 5.3–3.5) using the Gran F_1 function to calculate V_2.[22]

Summary statistics for the measurements (Table 5) support the predicted pH, ANC and conductivity of the dilute phosphate standard. For pH, mean values from all laboratories (Table 5) were within −0.05 pH units of the predicted pH. Long-term precision estimates (calculated as 2s) from two laboratories were less than ±0.1 pH units (Table 5). The estimated precision for the third laboratory (±0.24 pH units) was influenced by several measurements (Fig. 2) between pH 6.60 and 6.80. These outlying measurements may have resulted from errors in the pH electrode reference junction, from errors in preparing the diluted standard or from contamination of the standard before measurement.

For ANC, mean values for all laboratories were within ±3 × 10^{-6} equiv dm^{-3} of the predicted ANC (Table 5). Precision estimates from all laboratories were less than ±10 × 10^{-6} equiv dm^{-3} (±8%). Only six of the 294 measurements differed from the predicted ANC by more than 10 × 10^{-6} equiv dm^{-3} (Fig. 3).

Mean values for conductivity from all laboratories (Table 5) were within 1 × 10^{-4} S m^{-1} of the predicted conductivity. Precision estimates from two laboratories were less than ±4 × 10^{-4} S m^{-1} (Table 5). The precision estimate from the third laboratory (±8.06 × 10^{-4} S m^{-1}) was influenced by a number of measurements exceeding 43 × 10^{-4} S m^{-1} (Fig. 4).

Independent conductivity measurements of the dilute phosphate standard were conducted at the LESC Las Vegas Laboratories. Three different preparations were measured using two different conductivity meters. Each preparation was measured ten times with each meter. The mean conductivity of all 60 measurements was 36.9 × 10^{-4} S m^{-1} at 25 °C (2s = ±2.43 × 10^{-4} S m^{-1}). The mean value of the measurements was within 0.7 × 10^{-4} S m^{-1} at 25 °C of the predicted value (37.6 × 10^{-4} S m^{-1} at 25 °C, Table 4). Some error in conductivity measurements may have arisen from an increase in laboratory CO_2 levels above 340 vppm. The conductivity of the dilute phosphate standard in equilibrium with 680 vppm CO_2 is predicted to be 37.0 × 10^{-4} S m^{-1} at 25 °C (Table 4). Other possible sources of error include preparation error, use of equivalent conductivity values that are incorrect for the phosphate species, use of an inappropriate algorithm for correcting the measured conductivity to 25 °C or using an incorrect cell constant.

Comparison of Dilute Phosphate Standard and Dilute Hydrogen Carbonate Standard

Both before and during the same period of time as the dilute phosphate standard was being measured, the three participating laboratories also measured a dilute hydrogen carbonate standard prepared from $NaHCO_3$ (7.0 × 10^{-5} mol kg^{-1}) and KCl (1.75 × 10^{-4} mol kg^{-1}). This standard was prepared at a single location (Las Vegas); sub-samples were distributed by overnight courier to all laboratories for analysis. Measurements were conducted on the shipped hydrogen carbonate standard solution, as opposed to measuring phosphate standards diluted from shipped stock solutions. The difference in standard preparation may be open to criticism, but the observed differences in measured pH of these hydrogen carbonate standards were the basis for initiating this study. Theoretical values of pH, ANC and conductivity for this standard were 7.14, 70 × 10^{-6} equiv dm^{-3} and 32.4 × 10^{-4} S m^{-1}, respectively, at 25 °C, assuming equilibrium with an atmosphere of 340 vppm CO_2. Measurements are summarized in Table 6.

For pH, the dilute phosphate standard could be measured more precisely and with less systematic error than the dilute hydrogen carbonate standard at all three laboratories. Mean values for the dilute hydrogen carbonate standard from two laboratories (Table 6) differed from the predicted pH value by more than −0.20 pH units. The largest such difference observed from the dilute phosphate standard (Table 5) was −0.05 pH units. Precision estimates (calculated as 2s) of pH measurements of the dilute hydrogen carbonate standard were greater than ±0.23 pH units for all three laboratories (Table 6). Precision estimates associated with the dilute phosphate standard (Table 5) were less than ±0.17 pH units for one laboratory and less than ±0.07 pH units for two laboratories. The apparent systematic error and poor precision may be due to pH changes in the standard caused by the variation in atmospheric CO_2 present in the laboratory at concentrations higher than 340 vppm CO_2. The pH of the hydrogen carbonate standard at 25 °C for 680 vppm CO_2 predicted by MINTEQA2 is 6.84 at 25 °C, and for 170 vppm CO_2, the predicted pH is 7.44.

For ANC, measurements obtained for both standards by the laboratories were comparable. For the dilute hydrogen carbonate standard, mean ANC values for two laboratories differed from the predicted ANC by less than 1 × 10^{-6} equiv dm^{-3} (Table 6). The third laboratory conducted only four ANC determinations of the dilute hydrogen carbonate standard over a very short time period (2 d). For the dilute

Table 6 Summary statistics for measurements of a dilute hydrogen carbonate standard (7.0 × 10^{-5} mol kg^{-1} $NaHCO_3$ and 1.75 × 10^{-4} mol kg^{-1} KCl), measured at three laboratories during a 6 month period. (Predicted values from the MINTEQA2 program are in parentheses, assuming 340 vppm CO_2 and 25 °C)

pH (7.14)					ANC (70 × 10^{-6} equiv kg^{-1})				
Laboratory	n	Mean	2s	2SE*	Laboratory	n	Mean	2s	2SE
A	48	6.94	±0.428	±0.062	A	70	69.2	±4.38	±0.52
B	35	7.12	±0.382	±0.064	B	4	77.4	±3.97	±1.98
C	73	6.78	±0.226	±0.026	C	98	70.1	±6.44	±0.64
Total	156	6.90	±0.432	±0.034	Total	172	69.9	±6.12	±0.46

Conductivity (32.4 × 10^{-4} S m^{-1} at 25 °C)				
Laboratory	n	Mean	2s	2SE
A	102	32.6	±3.20	±0.32
B	101	32.7	±0.75	±0.15
C	59	32.4	±0.72	±0.09
Total	262	32.6	±2.24	±0.14

* Standard error of the mean.

Table 7 Variance components for measurements of a dilute phosphate standard (1.25×10^{-4} mol kg^{-1} KH_2PO_4 and Na_2HPO_4) and a dilute hydrogen carbonate standard (7.0×10^{-5} mol kg^{-1} $NaHCO_3$ and 1.25×10^{-4} mol kg^{-1} KCl), measured at three laboratories during a 6 month period

	pH					
	Dilute phosphate standard			Dilute hydrogen carbonate standard		
Source of variation	DF	Variance	Per cent. of total	DF	Variance	Per cent. of total
Among laboratory	2	0.0006	22	2	0.0281	49
Among day (within laboratory)	143	0.0017	63	68	0.0202	35
Within day (error)	216	0.0004	15	85	0.0087	16
Total	361	0.0027	100	155	0.0570	100
	ANC/10^{-6} equiv dm^{-3}					
Source of variation	DF	Variance	Per cent. of total	DF	Variance	Per cent. of total
Among laboratory	2	6.543	30	2	2.635	25
Among day (within laboratory)	111	8.684	40	76	2.371	22
Within day (error)	180	6.339	30	93	5.608	53
Total	293	21.566	100	171	10.614	100
	Conductivity/10^{-4} S m^{-1} at 25 °C					
Source of variation	DF	Variance	Per cent. of total	DF	Variance	Per cent. of total
Among laboratory	2	0.054	1	2	0	0
Among day (within laboratory)	117	6.489	94	114	1.096	87
Within day (error)	188	0.331	5	145	0.169	13
Total	307	6.874	100	261	1.265	100

phosphate standard, mean values for all laboratories were within 3×10^{-6} equiv dm^{-3} (2%) of the predicted ANC. For all laboratories, precision estimates for the dilute hydrogen carbonate standard (Table 6) were less than ±10% of both the mean value and the predicted ANC. For the dilute phosphate standard, precision estimates for all laboratories were within ±8% of both the mean value and the predicted ANC (Table 5).

The conductivity of the dilute hydrogen carbonate standard could be measured more precisely by the laboratories than could the dilute phosphate standard. Mean values for all laboratories (Table 6) were within 0.2×10^{-4} S m^{-1} of the predicted conductivity of the dilute hydrogen carbonate standard. For the dilute phosphate standard, mean values for all laboratories were within 0.5×10^{-4} S m^{-1} of the predicted conductivity (Table 5). It should be noted that because of the higher valence states, ion pairs, and possible triple ions[24] associated with the phosphoric acid equilibria, the Onsager equation is expected to produce theoretical conductivity values larger than those actually measured[6,28] for the dilute phosphate standard. Precision estimates for the dilute hydrogen carbonate standard (Table 6) ranged between $\pm 0.72 \times 10^{-4}$ and $\pm 3.20 \times 10^{-4}$ S m^{-1} for the individual laboratories. For the dilute phosphate standard, only two laboratories had precision estimates between $\pm 3 \times 10^{-4}$ and $\pm 4 \times 10^{-4}$ S m^{-1} (Table 5). The conductivity of the dilute phosphate standard is influenced to a small extent by changes in atmospheric CO_2 concentrations [1×10^{-4} S m^{-1} at 25 °C between 170 and 680 vppm (Table 4)]. The conductivity of the dilute hydrogen carbonate standard is unaffected by changes in atmospheric CO_2 concentrations over this same range.

Components of Variation in Measurements of Two Dilute Standards

A standard solution to be used as a daily check on analytical accuracy should provide reproducible results over time both within and among laboratories. The contribution of various sources of variation to measurements of the dilute phosphate and dilute hydrogen carbonate standards was evaluated. The total variance associated with measurements of both types of standard was analysed using a nested (hierarchical) design,[31] which identified and quantified three sources of variation of interest: among-laboratory variation, among-day variation within a laboratory (which included preparation error) and within-day variation (measurement error). Variance components for each source of error were computed using the PROC VARCOMP procedure of the Statistical Analysis System (PC-SAS).[32]

Variance component estimates are presented in Table 7. For the pH of the dilute phosphate standard, the magnitude of all variance components is reduced substantially over those for the dilute hydrogen carbonate standard (Table 7). For the dilute phosphate standard, the major source of variation is among-day (within-laboratory), which contributes 63% to the total variance. For the hydrogen carbonate standard, the major source of variation is among-laboratory, which contributes 49% to the total variance. This is believed to be evidence for the confounding effect that different ambient CO_2 levels in different laboratories have on determining possible measurement differences among laboratories. This conclusion is strengthened by the observation that dilute acid standards, measured as quality control samples in the same batches, have more accurate and precise pH values than those of the hydrogen carbonate standard. Conclusive evidence awaits simultaneous measurements of CO_2 concentration in the laboratory air.

The null hypothesis, that the precision associated with pH measurements of the dilute phosphate standard is equal to or greater than the precision associated with the dilute hydrogen carbonate standard, was tested using an F-test on the total variances. The results of the F-test indicate that the null hypothesis is rejected [$F = 21.1$, with 155 and 361 degrees of freedom (DF), $p < 0.0001$], and the total variance associated with the dilute phosphate standard is significantly smaller than the total variance associated with the dilute hydrogen carbonate standard. Some of the difference in the magnitude of the observed variances may be attributable to differences in the theoretical pH values of the two standards. In order to

evaluate such potential concentration-dependent effects on variance, the variances of the dilute hydrogen carbonate and dilute phosphate standards were compared with those estimated for a large number of pH measurements of a dilute sulphuric acid standard (1×10^{-4} equiv dm^{-3}, pH = 4.01) by Metcalf.[30] Total variance of the sulphuric acid standard was smaller than that of the dilute phosphate standard (0.0005 *versus* 0.0027), indicating there is some concentration-dependent effect. However, this effect is over a range of H^+ concentration spanning almost three orders of magnitude. The magnitude of the concentration-dependent effect is smaller than the difference in total variance observed for the two dilute standards (Table 7). Therefore, one can be confident that the significant difference in the variance in pH of the dilute hydrogen carbonate and dilute phosphate standards is not the result of differences in H^+ concentration.

For ANC, both types of standards are comparable in terms of the contributions from different sources of variation to the total measurement variance. Comparable results of the variance components analysis of the two types of standards for ANC are expected because ANC is not affected by changes in CO_2 concentrations. Larger variance component estimates (approximately 2–4 times larger) were observed for the dilute phosphate standard (due to the higher theoretical ANC value). In relative terms, total variances observed for the two standards were almost identical (within ±4%). Among-laboratory variation was about equal for both standards [30 *versus* 25% (Table 7)]. Within-day variation for the dilute hydrogen carbonate standard contributed much more to the total variation of the dilute hydrogen carbonate standard (53%) than to the dilute phosphate standard (30%).

For conductivity, the magnitudes of the various components for the dilute phosphate standard were larger than those for the dilute hydrogen carbonate standard (Table 7). However, the relative contributions from different sources of variation were similar for both standards (Table 7). In both instances, among-laboratory variation was not an important source of variation. For the dilute phosphate standard, 94% of the observed total variation was due to among-day (within-laboratory) effects. For the dilute hydrogen carbonate standard, 87% of the total variation observed was due to among-day (within-laboratory) effects. This pattern suggests that for conductivity, differences in daily measurement conditions (*e.g.*, solution temperatures, temperature correction, changes in ambient CO_2 levels, calibration graphs or cell constants) are more influential in measurement error than are measurement differences among different laboratories.

Table 8 Dilute aqueous standards for pH, conductivity and ANC, based on additions of HCl to a 1.25×10^{-4} mol kg^{-1} KH_2PO_4 and Na_2HPO_4 standard. (Theoretical values calculated using MINTEQA2 program, assuming an atmosphere of 340 vppm CO_2 and 25 °C)

ANC/ 10^{-6} equiv kg^{-1}	pH	Conductivity/ 10^{-4} S m^{-1}*	Ionic strength/ 10^{-4} mol kg^{-1}	Concentration of HCl/ 10^{-4} mol kg^{-1}
125	6.89	37.6	4.60	0.000
105	6.79	37.8	4.48	0.200
85	6.68	38.5	4.36	0.400
45	6.37	38.5	4.09	0.800
25	6.10	38.8	3.95	1.000
0	5.34	40.5	3.83	1.250
−15	4.80	45.5	3.92	1.400
−35	4.46	53.7	4.11	1.600
−75	4.13	70.4	4.50	2.000
−115	3.95	87.3	4.90	2.400
−160	3.81	106.2	5.35	2.850

* Based on limiting equivalent conductivity values at infinite dilution from reference 24, and corrected for ionic concentration using the Onsager equation (references 27 and 28).

Discussion and Conclusions

This study has demonstrated that the MINTEQA2 computer program can be used to design standard solutions appropriate for a particular type of water sample composition. In this instance, a standard that could be used for concurrent measurements of pH, ANC and conductivity was of interest. Advantages of the proposed approach are: (*i*) preparation time is reduced, because one solution can be used for three different measurements; and (*ii*) concurrent measurements of pH, ANC and conductivity can serve as a cross-check to identify measurement problems as opposed to preparation errors. The stock standard can be prepared in bulk amounts at fairly low cost, and should remain stable in composition for at least 6 months if kept sealed and refrigerated. This satisfies properties (*a*) and (*c*) of an ideal quality control sample for determining pH in low ionic strength water, (*a*) that the solution should be of known pH and (*c*) that the solution should be stable over several batches of analysis, or it should be possible to prepare fresh identical aliquots for each batch of analysis, as specified by Gardner *et al.*[33] Analysts at the laboratories who conducted the test measurements of the dilute phosphate standard have reported that individual preparations are stable for up to 1 week if kept refrigerated between daily use.

As described earlier, the theoretical ANC of the dilute phosphate standard was calculated using the MINTEQA2 program to simulate a 'titration' with HCl. In Table 8, the exact solution composition, ionic strength, ANC, pH and conductivity (at 25 °C in equilibrium with an atmosphere containing 340 vppm CO_2) for each of the 'titration points' are

Table 9 Ionic strength of some common pH standards at 25 °C, assuming an atmosphere containing 340 vppm CO_2

Number	Composition	Ionic strength/ mol kg^{-1}	pH
1	0.025 mol kg^{-1} Na_2HPO_4 + 0.025 mol kg^{-1} KH_2PO_4	9.75×10^{-2}	6.87
2	0.0025 mol kg^{-1} Na_2HPO_4 + 0.0025 mol kg^{-1} KH_2PO_4	9.89×10^{-3}	7.05
3	0.003043 mol kg^{-1} Na_2HPO_4 + 0.0008659 mol kg^{-1} KH_2PO_4	9.78×10^{-3}	7.51
4	0.05 mol kg^{-1} $KC_8H_5O_4$	5.34×10^{-2}	4.00
5	0.01 mol kg^{-1} $KC_8H_5O_4$	1.07×10^{-2}	4.11
6	0.0001 mol kg^{-1} HCl	1.00×10^{-4}	4.00
7	0.00005 mol kg^{-1} H_2SO_4	1.49×10^{-4}	4.01
8	0.00001 mol kg^{-1} HCl	1.05×10^{-5}	4.98
9	0.000125 mol kg^{-1} Na_2HPO_4 + 0.000125 mol kg^{-1} KH_2PO_4	4.60×10^{-4}	6.89
10	0.000070 mol kg^{-1} $NaHCO_3$ + 0.000175 mol kg^{-1} KCl	2.45×10^{-4}	7.14
11	0.00100 mol dm^{-3} $NaHCO_3$*	1.01×10^{-3}	8.28

* See reference 34.

Table 10 Theoretical pH values for a 200-fold dilution (by mass) of an NBS phosphate buffer standard for changing future atmospheric CO_2 concentrations, assuming the same rate of change (1.15 vppm CO_2 per year) observed from 1958 to 1984 (see reference 35)

Year	Potential CO_2 concentration (vppm)	Theoretical pH at 25 °C
—*	340	6.888
1990	352	6.882
2000	364	6.876
2010	375	6.870
2020	387	6.864
2030	398	6.859
2040	410	6.853
2050	421	6.848

* Values used as normal atmospheric CO_2 concentration throughout this study.

given in detail. The concentration of HCl titrant varies in order to achieve the HCl concentration in solution stated in Table 8. The 'titrated volume' of the dilute standard is constant for all practical purposes, and effectively large enough to render any dilution corrections negligible. This is achieved by preparing each solution (data point) shown in Fig. 2 (or Table 8) separately, rather than by incremental additions of a titrant of constant concentration to a changing volume of solution, as is usually the situation. This information gives a wide range of ANC (125×10^{-6} to -160×10^{-6} equiv kg^{-1}), pH (6.89–3.81) and conductivity (37.6×10^{-4}–106.2×10^{-4} S m^{-1} at 25 °C) reference values at ionic strengths much lower than most pH standards. These standards may prove useful to many analysts requiring quality control standards or synthetic audit samples during studies of acidic precipitation that are more appropriate to the determinand levels of interest. One advantage of these proposed standards over previous low ionic strength, low ANC standards is that they have a more complex matrix than pure mineral acids.

The dilute phosphate and dilute hydrogen carbonate standards presented in this study are the only near neutral pH standards that have an ionic strength of 10^{-4} mol kg^{-1} (Table 9) and a conductivity of less than 150×10^{-4} S m^{-1} at 25 °C, as recommended by Gardner *et al.*[33] This is an important advance in monitoring pH reference junction potential errors of neutral pH, low ionic strength waters. However, for almost a decade, Smith, D., Macaskill, B., and Bryers, G., [Department of Scientific and Industrial Research (DSIR), Water Quality Centre, Hamilton, New Zealand] have used a 1×10^{-3} mol dm^{-3} $NaHCO_3$ solution (pH = 8.28 at 25 °C) as a fairly dilute standard for neutral pH water analyses.[34] Laboratory CO_2 partial pressures also influenced their pH measurements, but rather than designing new standards (as was carried out in the present study) they steadily improved procedures in order to make their hydrogen carbonate-based standards effective. They used a 2 dm^3, wide mouth (approximately 0.10 m diameter) polyethylene bottle, rinsed then filled with about 0.15 dm^3 of standard. The bottle was vigorously agitated for several minutes while open to the air outside of their laboratory. Normally, this yields a quality control standard very near to pH 8.28 at 25 °C. This approach is very useful in laboratories with ambient CO_2 concentrations greater than atmospheric. The DSIR pH group has noticed in some large urban areas, under relatively stagnant conditions, that pH measurements of the 1×10^{-3} mol dm^{-3} $NaHCO_3$ standard are too acidic (below pH 8.20), indicative of local atmospheric CO_2 concentrations which are greater than the global mean value.

The DSIR pH group has also used 1×10^{-4} mol dm^{-3} $NaHCO_3$ standards, but found them to be too unstable with respect to CO_2 in practice to avoid confounding measurement and actual sample variability errors. This agrees well with experiences using the dilute hydrogen carbonate standard (2.45×10^{-4} mol kg^{-1} ionic strength) described in this paper. One additional variable for analysts trying to equilibrate dilute neutral pH standards (such as the dilute phosphate standard used here) with atmospheric CO_2 values outside their laboratory is that the mean global CO_2 concentrations are definitely increasing (from 315 vppm in 1958 to 345 vppm in 1984 at Hawaii).[35] Crudely assuming this linear increase of 1.15 vppm of CO_2 per year, a decrease in the theoretical pH of the dilute phosphate standard of 0.04 pH units over the next 60 years (Table 10) is estimated. It is recognized that the instantaneous CO_2 values in air will vary as a function of time of day, time of year and geographic location,[36] according to biological respiration, photosynthesis and the burning of fossil fuels. Any pH measurement of the dilute phosphate standard may be affected by these variables. However, we believe that the long-term mean pH values could have the relative differences shown in Table 10. The pH values in Table 10 are given to three decimal places because the relative differences caused by mean global CO_2 concentration differences at 25 °C may be reproducible with good equipment in the middle of the next century.

The MINTEQA2 program can also be used to test the sensitivity of a proposed or existing standard to external influences such as temperature or ambient atmospheric composition (Tables 3 and 10). Such simulations provide an estimate of the expected variation in composition to assist in the interpretation of confirmatory analyses. This helps to satisfy property (*d*) of an ideal quality control sample specified by Gardner *et al.*[33] for pH measurements, *i.e.*, that the solution should be of similar pH and ionic strength as unknown samples and should be of a composition that minimizes pH changes from p_{CO_2} or temperature.

The dilute phosphate standard permits an assessment of measurement precision and bias at levels of pH, ANC and conductivity that are more relevant to acid-sensitive waters than dilute acid standards. Previous studies implicitly assumed that the sign and magnitude of pH combination electrode error measured in a dilute acid standard are equal to, and directly applicable as estimates for, pH errors in natural waters (of neutral pH) measured at nearly the same time (within s to min) with the same electrode. In numerous field and laboratory studies, evidence that this assumption is incorrect has been noted by our pH research group.

In order to illustrate this point, quality control checks were conducted over a period of 4 d in the field on a pH electrode using a dilute acid standard ($5.00 \pm 0.05 \times 10^{-5}$ mol dm^{-3} H_2SO_4, 4.01 pH units with an activity correction but without correcting for the residual liquid junction potential) and well characterized natural audit samples of filtered lake water [FN-09 (Seventh Lake, NY), 6.84 pH units; FN-10 (Big Moose Lake, NY), 5.15 pH units]. The results of these checks (Fig. 5) illustrate that the magnitude and sign of error in pH measurements of the dilute acid standard is not always the same as that predicted from the natural audit samples, which have H^+ activities 30–680 times less than the mineral acid standard.

The critical point in evaluating Fig. 5 is that twice the 95% confidence interval for the within-batch pH measurements is 0.01 pH units (at pH 4 based on 1×10^{-4} mol dm^{-3} HCl) and 0.02 pH units (near pH 7, based on the dilute phosphate standard, Table 7). Usually, it is expected that differing pH

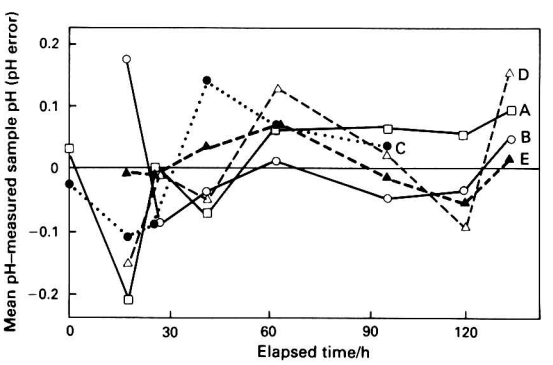

Fig. 5 Plot of difference between mean pH and measured sample pH for four natural audit samples (filtered lake water). A, 5.00×10^{-5} mol dm^{-3} H_2SO_4 standard solution (theoretical pH = 4.01, theoretical ANC = -100×10^{-6} equiv dm^{-3} and theoretical conductivity = 42.1×10^{-4} S m^{-1} at 25 °C); B and C, two samples of audit sample lot FN-09 (target pH = 6.84, target ANC = 152×10^{-6} equiv dm^{-3} and target conductivity = 52×10^{-4} S m^{-1} at 25 °C); D and E, two samples of audit sample lot FN-10 (target pH = 5.15, target ANC = -1×10^{-6} equiv dm^{-3}, and target conductivity = 24×10^{-4} S m^{-1} at 25 °C)

combination electrode errors from daily variation in the condition of the reference electrode liquid junction during field work will be observed. However, if the dilute acid pH measurement error was representative of the pH measurement errors of the natural audit samples, the daily reference junction errors could be offset (Fig. 5), but the magnitude and sign of the pH error for the within-batch measurements of the natural audits should not differ by more than ±0.02 pH units (lines connecting pH errors for the standards should be approximately parallel). Fig. 5 shows that the pH measurement errors of the natural audits are generally greater than ±0.02 pH units from the pH errors of the dilute acid standard. Therefore, the pH measurement errors of the dilute acid are not representative of the pH measurement errors of the natural water samples in this instance. To summarize, in most current studies, the implicit assumption is made that pH errors measured with dilute acid standards are equal to the errors which should be measured in waters of low solute content and of near neutral pH. Fig. 5 shows this assumption is incorrect, and that dilute standards in the same pH and conductivity range as the water samples should be employed.

In contrast to Gardner *et al.*[33] it has been found in previous studies at this laboratory that natural water samples filtered and stored at 4 °C can be stable with respect to pH, ANC, conductivity, major cations and anions, dissolved organic carbon, silica and aluminium species.[37,38] Operationally, the usefulness of natural audit samples is limited by the cost of searching for the appropriate sample matrix, transporting, preparing, and storing large volumes of water, and the required cost of confirmatory analyses.

It has been shown that the major improvement of the dilute phosphate standard over the dilute hydrogen carbonate standard is in the measurement of pH. The phosphate standard is designed for use in monitoring and evaluating the precision and accuracy of pH measurements in dilute neutral pH solutions. Because it is less sensitive to changes in pH due to changes in ambient atmospheric CO_2 levels, it will not detect CO_2-induced changes in the sample between collection and measurement. Such changes are important, as they may compromise the assumption that the measured result is representative of actual conditions at the time of collection. Use of the dilute phosphate standard can separate error due to measurement (*e.g.*, meter/electrode performance or procedural errors) from changes in sample pH due to external influences. In this respect, we differ from Gardner *et al.*,[33] by specifying two different quality control samples to minimize pH changes due to CO_2 [property (*d*)[33]] and to evaluate the effect of CO_2-induced pH changes on natural samples [property (*b*), *i.e.*, that the solution should behave in the same way as real samples with respect to likely sources of error[33]]. In order to control or evaluate such external influences, the sample must be protected from such changes (*e.g.*, by collecting it in a sealed syringe and using a closed-system measurement technique),[39] by rigorously specifying the ambient measurement conditions in terms of temperature and atmospheric p_{CO_2}, or by periodically subjecting natural or synthetic audit material (such as the dilute hydrogen carbonate standard) to the entire collection and measurement process (which still may not be representative of the natural sample if it is not at equilibrium with p_{CO_2} under *in situ* conditions). Careful use of the two low ionic strength pH standards presented in this study may help in separating instrumental errors from errors caused by changes in the carbonate equilibria of a sample prior to measurement.

Additional application of chemical equilibrium speciation programs to solving design problems for quality control and quality assurance samples appears promising and justified. The dilute phosphate standard represents a simple example of such an application. It is believed that chemical speciation computer programs can also be utilized in developing more complex standards and inexpensive reference materials appropriate for addressing a wide variety of water quality issues.

We must give much of the credit for our solving this particular problem with MINTEQA2 to J. Allison and to J. Westall. We thank B. Macaskill and J. Westall for useful discussions and M. Stapanian and R. Gerlach for statistical advice; M. Stapanian also helped with the collection of data. J. Baker, J. Pollard, D. Heggem, G. Pearson, R. Schonbrod, R. Snelling, J. Wigington, M. McDowell, D. DeWalle, W. Kretser, P. Murdoch, D. Hillman, S. Pia, C. Monaco, D. Waltman, K. Kohorst, and many other colleagues in the Episodic Response Project team including, D. Horan-Ross, L. Lorenz and M. Olson also supported us in our work. We also thank two anonymous referees whose comments and suggestions significantly improved the final draft and A. Hendricks, B. Freet, M. Brock, R. Wilson, M. Nicklas and G. Arundell for their cooperation during the field work. K. Nordstrom and J. Ball have given us much information about the WATEQ thermodynamic database.

References

1 Peden, M. E., Bachman, S. R., Brennan, C. R., Demir, B., James, K. O., Kaiser, B. W., Lockard, J. M., Rothert, J. E., Sauer, J., Skowron, L. M., and Slater, M. J., *Development of Standard Methods for the Collection and Analysis of Precipitation*, ISWS Contract Report 381, Illinois State Water Survey, Champaign, IL, 1986, pp. 150.6-11 and 150.6-17.
2 Metcalf, R. C., in *Shorter Technical Methods*, ed. Burt, T., British Geomorphological Research Group Technical Bulletin, No. 36, Geo Books, Norwich, 1987, vol. VI, p. 28.
3 Morris, F. A., Peck, D. V., Bonoff, M. B., Cabble, K. J., and Pierett, S. L., *National Surface Water Survey, Eastern Lake Survey (Phase I-Synoptic Chemistry) Field Operations Report*, EPA 600/4-86/010, US Environmental Protection Agency, Las Vegas, NV, 1986, pp. 11 and 12.
4 Engels, J. L., Mitchell-Hall, T. J., Drousé, S. K., Best, M. D., and MacDonald, D. C., *National Surface Water Survey, Eastern Lake Survey (Phase II-Temporal Variability) Quality Assurance Plan*, EPA 600/8-88/083, US Environmental Protection Agency, Las Vegas, NV, 1988, Section 10, p. 2.
5 Peck, D. V., Engels, J. L., Howe, K. M., and Pollard, J. E., *Aquatic Effects Research Program: Episodic Response Project Integrated Quality Assurance Plan*, EPA 600/X-88/274, US Environmental Protection Agency, Las Vegas, NV, 1988, Revision 1, Section 7, pp. 12 and 13.
6 Robinson, R. A., and Stokes, R. H., *Electrolyte Solutions*, Butterworths, London, 2nd edn., 1959, pp. 143–149, 463 and 464, and 520.
7 Truesdell, A. H., and Jones, B. F., *J. Res. U.S. Geol. Surv.*, 1974, **2**, 233.
8 Brown, D. S., and Allison, J. D., *MINTEQA1, An Equilibrium Metal Speciation Model: User's Manual*, EPA 600/3-87/012, US Environmental Protection Agency, Athens, GA, 1987, p. 75.
9 Bates, R. G., *Determination of pH: Theory and Practice*, Wiley, New York, 1973, pp. 73–79, and 95.
10 Metcalf, R. C., Peck, D. V., and Arent, L. J., *Geochim. Cosmochim. Acta*, 1989, **53**, 773.
11 Felmy, A. R., Girvin, D. C., and Jenne, E. A., *MINTEQ, A Computer Program for Calculating Aqueous Geochemical Equilibria*, EPA 600/3-84/032, US Environmental Protection Agency, Athens, GA, 1984, pp. 1–15.
12 Westall, J. C., Zachary, J. L., and Morel, F. M. M., *MINEQL, A Computer Program for the Calculation of Chemical Equilibrium Composition of Aqueous Systems*, Dept. Civil Eng. Tech. Note 18, Massachusetts Institute of Technology, Cambridge, MA, 1976, pp. 91.
13 Ball, J. W., Jenne, E. A., and Cantrell, M. W., *WATEQ3, A Geochemical Model with Uranium Added*, Open-File Report 81-1183, US Geological Survey, Menlo Park, CA, 1981.
14 Covington, A. K., Whalley, P. D., and Davison, W., *Analyst*, 1983, **108**, 1528.
15 Hamer, W. J., Pinching, G. D., and Acree, S. F., *J. Res. Natl. Bur. Stand.*, 1946, **36**, 47.
16 Picknett, R. G., *Trans. Faraday Soc.*, 1968, **64**, 1059.

17 Kramer, J. R., in *Water Analysis: Volume I, Inorganic Species*, eds. Minear, R. A., and Keith, L. H., Academic Press, New York, 1982, part 1, p. 122.
18 Driscoll, C. T., and Bisogni, J. J., in *Modeling of Total Acid Precipitation Impacts*, ed. Schnoor, J. L., Butterworth, Boston, 1984, *Acid Precipitation Series*, vol. 9, p. 53.
19 Rossum, J. R., *Anal. Chem.*, 1949, **21**, 631.
20 Dobos, D., *Electrochemical Data*, Elsevier, Amsterdam, 1975, pp. 28, 87 and 88.
21 Dean, J. A., *Lange's Handbook of Chemistry*, McGraw-Hill, New York, 11th edn., 1973, pp. 6-30 and 6-31.
22 Stumm, W., and Morgan, J. J., *Aquatic Chemistry*, Wiley, New York, 2nd edn., 1981, pp. 138, 139 and 163–165.
23 Avery, H. E., and Shaw, D. J., *Basic Physical Chemistry Calculations*, Butterworths, London, 2nd edn., 1980, pp. 114 and 115.
24 Selvaratnam, M., and Spiro, M., *Trans. Faraday Soc.*, 1965, **61**, 360.
25 Marx, G., and Fischer, L., *Z. Phys. Chem. (Frankfurt)*, 1964, **41**, 315.
26 Conway, B. E., *Electrochemical Data*, Greenwood Press, Westport, CT, 1969, pp. 145 and 146.
27 Bockris, J. O'M., and Reddy, A. K. N., *Modern Electrochemistry*, Plenum, New York, 1970, vol. 1, pp. 434–440.
28 Crow, D. R., *Principles and Applications of Electrochemistry*, Chapman and Hall, London, 3rd edn., 1988, pp. 59–65.
29 US Environmental Protection Agency, *Handbook of Methods for Acid Deposition Studies: Laboratory Analyses for Surface Water Chemistry*, EPA 600/4-87/026, US Environmental Protection Agency, Office of Research and Development, Washington, DC, 1987, Sections 5, 20 and 23.
30 Metcalf, R. C., *Analyst*, 1987, **112**, 1573.
31 Miller, J. C., and Miller, J. N., *Statistics for Analytical Chemistry*, Ellis Horwood, Chichester, 1984, p. 146.
32 SAS Institute, *SAS/STAT Guide for Personal Computers, Version 6 Edition*, SAS Institute, Cary, NC, 1987, ch. 35, pp. 967–978.
33 Gardner, M. J., Gill, R., and Ravenscroft, J. G., *Analyst*, 1990, **115**, 371.
34 Smith, D. G., Macaskill, J. B., Stevenson, C. D., and Edgerley, W. H. L., *Physical and Chemical Methods for Water Quality Analyses*, Water and Soil Miscellaneous Pub. 38, Water and Soil Division, Ministry of Works and Development, Wellington, New Zealand, 1982, pp. pH1–pH10.
35 Neftel, A., Moor, E., Oeschger, H., and Stauffer, B., *Nature (London)*, 1985, **315**, 45.
36 Post, W. M., Peng, T.-H., Emanuel, W. R., King, A. W., Dale, V. H., and DeAngelis, D. L., *Am. Sci.*, 1990, **78**, 310.
37 Arent, L. A., and Lewis, T. E., in *Environmental Chemistry and Toxicology of Aluminium*, ed. Lewis, T. E., Lewis Publishers, Chelsea, MI, 1989, pp. 41–57.
38 Cougan, K. A., Sutton, D. W., Peck, D. V., Miller, V. J., and Pollard, J. E., *National Stream Survey-Phase I: Quality Assurance Report*, EPA 600/4-88/018, US Environmental Protection Agency, Las Vegas, NV, 1988, pp. 101–110.
39 Peck, D. V., Baker, J. R., and Hillman, D. C., *Verh. Int. Ver. Theor. Angew. Limnol.*, 1988, **23**, 903.

Paper 0/03668D
Received August 9th, 1990
Accepted October 24th, 1990

Use of Ion-selective Electrodes in Kinetic Flow Injection: Determination of Phenolic and Hydrazino Drugs With 1-Fluoro-2,4-dinitrobenzene Using a Fluoride-selective Electrode

John C. Apostolakis, Constantinos A. Georgiou and Michael A. Koupparis*
Laboratory of Analytical Chemistry, Department of Chemistry, University of Athens, Panepistimiopolis, Kouponia, Athens 15771, Greece

A flow injection (FI) kinetic potentiometric method for the determination of phenolic (acetaminophen and isoxsuprine) and hydrazino (isoniazid) drugs is described. This work shows the usefulness of ion-selective electrodes as detectors in FI systems, not only for direct ion determination but also in routine kinetic analysis. The method is based on the reaction of 1-fluoro-2,4-dinitrobenzene (FDNB) with the analytes in a weakly alkaline medium, which proceeds through the liberation of fluoride from the reagent. The slow reactions with phenols are catalysed by micelles of cetyltrimethylammonium bromide. The reaction rate is monitored with a fluoride-selective electrode in a wall-jet configuration and is used to construct a calibration graph of antilog($\Delta E/S$)-1 *versus* c (where E = potential, s = slope of the electrode and c = concentration), using the fixed-time approach. The response time and the long-term stability of the electrode were found to be adequate for such kinetic determinations. The proposed method overcomes problems associated with end-point spectrophotometric methods using FDNB and allows measurements in highly coloured or turbid solutions. The optimized method has a linear concentration range of 1×10^{-4}–50×10^{-4} mol dm^{-3}, a measurement throughput of 20 or 40 per hour and the precision ranges from 1.8 to 3.6% relative standard deviation (n = 3). Results obtained for commercial pharmaceutical formulations compare favourably with those given by reference methods.

Keywords: *Flow injection kinetic potentiometric determination; fluoride-selective electrode; acetaminophen; isoxsuprine; isoniazid*

Ion-selective electrodes (ISEs) have been widely used as detectors in air-segmented continuous-flow and flow injection (FI) systems, mainly for the direct determination of the corresponding ions. Such automated methods have been adopted as accepted or recommended routine methods in clinical and environmental laboratories.

The combination of ISEs with kinetic (reaction-rate) methods of analysis has proved to be a very attractive analytical technique.[1] The selectivity of ISEs combined with the selectivity, rapidity and flexibility of kinetic methods provides selective analytical methods having increased measurement throughput. The manual performance of routine batch kinetic methods using ISEs suffers from the increased effort required to ensure the reproducible performance of the procedural steps, *i.e.*, addition of the various reagent solutions, usually in a fixed order, mixing, waiting for a stable and reproducible initial value of the potential, starting the reaction by the rapid addition of a reagent, recording the potential (E) *versus* time (t), emptying and washing the reaction cell and measuring a reaction-rate parameter ($\Delta E/\Delta t$) or ΔE in a fixed time interval. The laborious performance of manual kinetic potentiometric methods leads to decreased measurement throughput, which discourages the wide use of the technique in routine analysis.

Automated FI is a suitable technique for the manipulation of samples and reagents, signal processing and data treatment. Flow-through ISEs with suitable response-time characteristics can be very useful detectors in reaction-rate methods. Various configurations (dip-type, with flow-through cap, tubular, wall-jet, *etc.*) have been designed for flow-through ISEs.[2–9] Peroxidase has been determined with a fluoride ISE, using a carrier stream containing H_2O_2 and *p*-fluoroaniline as substrate in an FI manifold.[10]

In this paper, the applicability of ISEs as detectors in automated FI potentiometric reaction-rate techniques is shown by the development of a method for the determination of two phenolic drugs [acetaminophen (paracetamol) and isoxsuprine] and one hydrazino drug (isoniazid) based on monitoring the liberation of fluoride during the reaction of these drugs with 1-fluoro-2,4-dinitrobenzene (FDNB). This reagent is selective for various organic functional groups (*i.e.*, amines, amino acids, phenols, thiols, hydrazines, hydrazides and azides). Several manual end-point spectrophotometric[11–17] and kinetic potentiometric[18–21] methods using FDNB have been described for the determination of these types of substances, including several drugs. The end-point spectrophotometric methods suffer from several disadvantages such as the long time required to complete the reaction, the necessity to heat the reacting mixture and the required additional steps for the hydrolysis of the excess of FDNB and the extraction of the DNB product for measurement. Reactions involving FDNB were found to be accelerated by micellar catalysis, leading to a marked decrease in the analysis time.[21–24] The automated FI kinetic potentiometric method described here permits the determination of phenols that form insoluble DNB products, rendering their spectrophotometric detection impossible. Other benefits expected from this method are increased precision, reduction of steps before measurement, increased measurement throughput and the ability to analyse coloured or turbid sample solutions.

Experimental

Apparatus

The FI analyser used was a laboratory-built automated system consisting of a multi-channel peristaltic pump with remote control (Ismatec MPN-8), a Rheodyne 5001 injection valve equipped with a pneumatic actuator (Rheodyne 5003) controlled by a microcomputer through solenoid valves, mixing and reaction coils made from PTFE tubing (0.8 mm i.d.), an AIM 65 microcomputer associated with the necessary laboratory-built control interface and an analogue to digital converter card for data acquisition (Rockwell RM65-5302E) and a Heath-Schlumberger electrometer–recorder system (units

* To whom correspondence should be addressed.

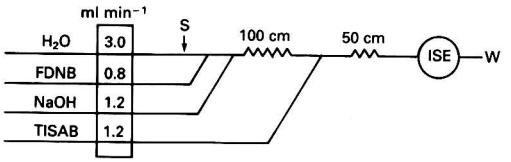

Fig. 1 Flow injection manifold designed for kinetic potentiometric determinations using a fluoride-selective flow-through electrode: S, sample introduction; and W, waste

EU-200-30, EU-200-01, EU-200-02 and EU-205-11) capable of recording the ISE potential. The potentiometric flow-through cell was of the wall-jet type and was constructed using a glass syringe body (15 mm i.d.) according to Douglas[9] in which a combination fluoride electrode (Orion 96-09) was suitably fitted so that a flow cell with an approximate volume of 0.3 ml was obtained. The FI manifold optimized for this application is depicted in Fig. 1. The combination electrode was connected to the pH/pion electrometer unit of the electrometer–recorder system (EU-200-30) and then the electrode potential (in the range from −400 to 0 mV) was fed to the recorder (optional) and the 12-bit analogue to digital converter after a ×12.5 amplification. After digitization, using a suitable Assembly language sub-routine featuring sampling rates up to 7.5 kHz, the potential readings were stored in the microcomputers random access memory (RAM).

Reagents

All reagents were of analytical-reagent grade and distilled, de-ionized water was used throughout. The FDNB stock solution [4.00% m/v (0.215 mol dm^{-3})] was prepared by dissolving 4.00 g of FDNB (Sigma) in 100.0 ml of acetone. This solution was stored in a sealed amber coloured glass vial in the refrigerator and was opened only when used. This reagent should be handled with care as it is vesicatory. The FDNB working solution (4.3×10^{-3} mol dm^{-3}) was prepared daily by dilution of the stock solution with water containing ethanol and was acidified using HCl. This solution contains 10% v/v ethanol to keep the reagent dissolved and 5.0×10^{-4} mol dm^{-3} HCl to prevent solvolysis of the reagent. Total ionic strength (and pH) adjustment buffer (TISAB) of pH 5.5 was prepared according to Frant and Ross[25] and diluted 1 + 1 with water prior to use.

The pH for the reaction was adjusted by pumping a 1.3×10^{-2} mol dm^{-3} NaOH solution, for the determination of isoniazid, and a 1.5×10^{-2} mol dm^{-3} NaOH solution containing 5.0×10^{-4} mol dm^{-3} cetyltrimethylammonium bromide (CTAB, Aldrich) for the determination of acetaminophen and isoxsuprine.

Stock solutions (1.000×10^{-2} mol dm^{-3}) of isoniazid (Sigma), acetaminophen (Serva) and isoxsuprine (Sigma) were prepared from the pure substances. The purity of these substances was determined using the current United States Pharmacopeia (USP) XXI–National Formulary XVI methods. Working standard solutions in the range 1×10^{-4}–50×10^{-4} mol dm^{-3} were prepared by appropriate dilution of the stock solutions.

Procedures

Measurements using the FI analyser

The manifold shown in Fig. 1 was constructed and the analyser pump was started. After stabilization of the baseline to within ±0.2 mV, the program for the routine measurements was run. The program prompts the user to input the number of standards, samples and runs per standard and sample. Immediately after each 100 µl injection of the measured solution the analyser evaluated the baseline voltage by taking 20 voltage readings for 4 s and calculated the standard deviation. Afterwards, 60 voltage readings were taken during a pre-set time span, overlapping the residence time (18 s), and the peak height (ΔE) was calculated as the difference between the baseline and the peak voltage. This method of peak-height measurement compensates for baseline drift between measurements, a common problem when using ISEs. Smoothing the voltage readings taken during peak-height evaluation by using the Savitzky–Golay technique[26,27] had no significant effect on precision and accuracy. After measuring the standards, the calibration graph was constructed by linear regression of $(10^{\Delta E/S}-1)$ *versus* concentration (c),[19] where ΔE is the peak height and S the slope of the fluoride electrode, which is periodically determined by injecting a series of standard fluoride solutions in the concentration range 1×10^{-5}–1×10^{-2} mol dm^{-3} (FI is a fixed-time technique with a Δt value controlled by the reaction time in the FI manifold). The samples were then measured in the same way and their concentrations calculated from the constructed calibration graphs, displayed and printed by the microcomputer. Washing the manifold of the analyser between samples was the most time consuming step taking 3 min when not using the surfactant CTAB (determination of isoniazid) or 1.5 min when using CTAB which also acts as a detergent (determination of acetaminophen and isoxsuprine), leading to measurement rates of 20 or 40 per hour, respectively.

Sample preparation

For solid formulations, the official USP sampling procedures were followed. From the final fine powder an accurately weighed portion was dissolved in water, so that the concentration of the drug was in the linear range of the calibration graphs (1×10^{-4}–50×10^{-4} mol dm^{-3}). By using an ultrasonic bath or a mechanical shaker, the powder was completely disintegrated and the solution was either allowed to settle or filtered or centrifuged. For elixirs and injection solutions, a suitable dilution was the only step required.

All measurements were performed in an air-conditioned laboratory maintained at a nominal temperature of about 25 °C.

Results and Discussion

Design and Optimization of the FI Manifold

In order to automate a kinetic potentiometric determination using FDNB as a reagent and the fluoride-selective electrode as a detector, the following points must be taken into account.[18] Firstly, the reaction with the analytes is subject to base catalysis and therefore is favoured in alkaline solutions; secondly, the FDNB reagent undergoes hydrolysis, accelerated in alkaline solutions, producing fluoride ions and 2,4-dinitrophenol; and thirdly, the optimum pH range for measurements with the fluoride ISE is 5–5.5, the hydroxide ions being the main interferent with a potentiometric selectivity coefficient of 0.04.[19] Hence, the FI manifold (Fig. 1) was constructed in such a way that the reaction takes place in the first coil (100 cm) in an alkaline environment prepared *in situ* by on-line mixing of the acidified FDNB reagent solution with the basifying NaOH solution, and then the pH is adjusted on-line (second coil, 50 cm) to the optimum pH for the electrode operation (pH 5.5). This design shows the great flexibility of the FI technique when designing analytical schemes which require different experimental conditions during the various steps.

The characteristics of the fluoride electrode in the TISAB buffer were studied under both batch and FI conditions. The slope was found to be 55.2 and 55.6 mV $decade^{-1}$ under batch and flow conditions, respectively, and the lower linear concentration limit 2×10^{-5} and 5×10^{-5} mol dm^{-3}, respectively. The slope remained constant to within ±0.4 mV over 8 months of use in the FI system.

As kinetic methods of analysis can be performed using various approaches, *viz.*, initial slope, fixed time and reciprocal time, the first two were tested. An FI–stopped flow mode was initially tested and the reacting mixture at pH 9.0 was stopped in the cell, the electrode potential being monitored *versus* time. Although linear E *versus* t recordings were obtained, the procedure suffered from the slow response time of the fluoride electrode when used in weakly alkaline solutions and the poor reproducibility of the measurements (because the reacting mixture was not stirred before measurement). Hence the fixed-time approach, using the wall-jet type electrode configuration, was used.

The residence time in the FI system for a fixed-time approach can be increased either by stopping the reaction mixture (at pH 9.0) in a short reaction coil for an adjustable time interval before proceeding to the detector for measurement or by increasing the length of the reaction coil in a continuous-flow mode. In the first mode, the reaction time in the kinetic procedure increases without a subsequent increase in the dispersion. The results obtained for the determination of isoniazid using the first kinetic mode are shown in Table 1. The slope of the calibration graph increased with the stop time (reaction time) but the blank value (due to hydrolysis of FDNB at pH 9.0 during the stop time) also increased considerably. Therefore, this mode was not exploited further in routine assays. In the scheme finally chosen, a continuous flow was used to provide an 18 s residence time in the specified length of the reaction coil (Fig. 1). In this mode, the blank value is included in the baseline. In order to increase the precision and improve the electrode response time, the pH of the flowing mixture was adjusted to 5.5 immediately before measurement.

The concentration of the basifying NaOH solution was optimized for each determination. As shown in Fig. 2, the slope of the calibration graph for isoniazid increases with the concentration of NaOH, up to an optimum for [NaOH] = 1.3×10^{-2} mol dm^{-3}. Further increase in the concentration decreases the slope, owing to the acceleration in the hydrolysis of FDNB which increases the baseline value (thereby decreasing ΔE). For the two phenols, the reactions of which are slow, the surfactant CTAB was added in order to accelerate the reaction by micellar catalysis, thus improving the sensitivity of the determinations. As the hydrolysis of FDNB is also subject to micellar catalysis by CTAB, an optimization study was carried out and the optimum concentrations of NaOH (1.5×10^{-2} mol dm^{-3}) and CTAB (5.0×10^{-4} mol dm^{-3}) were selected as a compromise between increased sensitivity and a low blank value.

Table 1 Effect of stop time on the characteristics of the calibration graph ($10^{\Delta E/S}-1$ *versus* c) for isoniazid. Analytical range 1×10^{-4}–50×10^{-4} mol dm^{-3}

Stop time/s	Slope/ ($10^{\Delta E/S}-1$) dm^3 mol^{-1}	Intercept/ ($10^{\Delta E/S}-1$)	Correlation coefficient	Blank value/ ($10^{\Delta E/S}-1$)
0	538.4 ± 6.4	0.019 ± 0.015	0.9998	0.044
5	903.8 ± 9.9	0.186 ± 0.023	0.9998	0.225
10	1273 ± 33	0.351 ± 0.075	0.9990	0.426
15	1629 ± 10	0.638 ± 0.023	0.9999	0.688
20	1910.8 ± 5.0	0.847 ± 0.011	0.9999	1.04
25	2414 ± 36	1.036 ± 0.082	0.9997	1.15

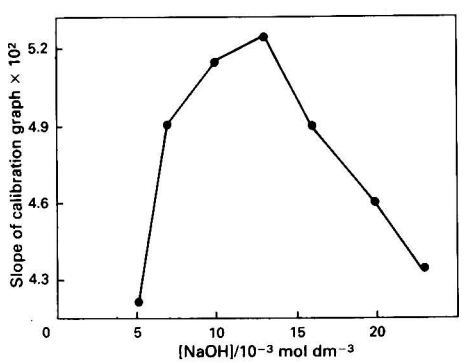

Fig. 2 Effect of NaOH concentration on the slope of the calibration graph for isoniazid

Table 2 Data for typical calibration graphs for isoniazid, acetaminophen and isoxsuprine (range 1×10^{-4}–50×10^{-4} mol dm^{-3})

Drug	Slope/ ($10^{\Delta E/S}-1$) dm^3 mol^{-1}	Intercept/ ($10^{\Delta E/S}-1$)	Correlation coefficient
Isoniazid	525 ± 10	−0.023 ± 0.016	0.9997
Acetaminophen	95.6 ± 3.7	0.0135 ± 0.0025	0.9990
Isoxsuprine	4033 ± 34	0.114 ± 0.078	0.9999

Table 3 Recovery of isoniazid from synthetic mixed solutions containing excipients and rifamycin

Interferent	Interferent: isoniazid concentration ratio* (m : m)	Recovery (%)
Gelatin	10	101.2
Cellulose acetate hydrogen phthalate	10	99.9
Lactose	10	101.4
Polyethylene glycol 4000 (Carbowax)	10	99.8
Magnesium stearate	10	99.9
Starch	10	102.3
Sodium lauryl sulphate	10	98.0
Sugar	10	98.8
Glucose	10	99.6
Carboxypolymethylene (Carbopol)	10	91.0
	5	92.4
Galactose	10	99.6
Rifamycin	10	94.8
	5	97.7

* [Isoniazid] = 1.000×10^{-4} mol dm^{-3} (13.72 mg l^{-1})

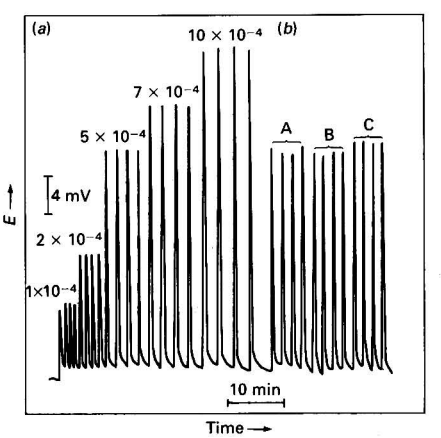

Fig. 3 Typical recordings for the determination of isoxsuprine with the proposed method. (*a*) Calibration graph (values above each set of peaks are isoxsuprine concentrations in mol dm^{-3}); and (*b*) unknown samples A, B and C

Table 4 Determination of acetaminophen, isoniazid and isoxsuprine in commercial formulations by using FI and reference methods

	Drug content/mg per unit or mg per 5 ml			
		Found ± standard deviation (n = 3)*		
Formulation	Claimed	FI	Reference method†	t-test‡
Acetaminophen—				
Panadol§	500	494 ± 12	496 ± 10	0.222
Norgesic§	450	450 ± 15	447 ± 16	0.237
Lonarid§	400	391.2 ± 7.1	396.1 ± 5.4	0.951
Medamol§	500	485 ± 11	489 ± 10	0.466
Depon§	500	495 ± 12	493 ± 14	0.188
Panadol¶	160	164.3 ± 4.6	167.7 ± 3.5	1.019
Depon¶	120	114.8 ± 4.1	114.3 ± 1.5	0.198
Isoniazid—				
Dianicotyl§	100	98.3 ± 2.8	102.0 ± 1.0	2.155
Rifinah§,‖	150	142.2 ± 4.3	148.2 ± 2.3	2.131
Isoxsuprine—				
Duvadilan**	10	10.2 ± 0.2	10.2 ± 0.2	0.000

* Average of three samples measured in triplicate.

† Isoniazid, bipotentiometric titration with bromine in strongly acidic solution after extraction of rifamycin (USP XXI); acetaminophen, spectrophotometric method based on nitrosation[28]; and isoxsuprine, high-performance liquid chromatographic method.[29]

‡ Theoretical t-value for 95% confidence level and 3 + 3 measurements = 2.776.

§ Tablets.

¶ Elixirs. Formulations coloured owing to the presence of colouring agents.

‖ Contains 300 mg of rifamycin.

** Injection.

Evaluation of the Method

Data for typical calibration graphs for isoniazid, acetaminophen and isoxsuprine are shown in Table 2. The linearity was good and the analytical range suitable for drug analysis. In order to examine the applicability of the proposed FI method to routine pharmaceutical analyses, the effect of various excipients and the antibiotic rifamycin, which coexists in combined formulations with isoniazid, was studied. Recovery results from synthetic mixed solutions of isoniazid and the substances studied are shown in Table 3. Common excipients do not interfere except for carboxypolymethylene (Carbopol), which gave negative errors. This might be due to the formation of mixed micellar solutions or partial saturation of the surfactant micelles, changing their catalytic action. The analysis of pharmaceutical formulations is possible when this excipient is absent or removed by using an ion-exchange column. Typical FI recordings for the determination of isoxsuprine are shown in Fig. 3.

Applications

The proposed FI kinetic method was applied to the determination of isoniazid, acetaminophen and isoxsuprine in commercial formulations. The results (Table 4) are in good agreement with those given by reference methods. Elixirs containing acetaminophen, and the isoniazid formulation containing the antibiotic rifamycin, were coloured. These formulations can be analysed by using the proposed FI method, as the potentiometric measurements are not affected by coloured solutions. The proposed method offers both good accuracy and precision [1.8–3.6% relative standard deviation (n = 3)].

Conclusions

The proposed kinetic method overcomes problems associated with: (*a*) the incompleteness of analytical reactions requiring high temperatures and long reaction times in end-point spectrophotometric methods; and (*b*) the need to hydrolyse the unreacted reagent and subsequently extract the reaction product from the reaction mixture. This kinetic method permits the determination of substances forming insoluble products with FDNB (phenols), is applicable to the analysis of highly coloured samples and has a measurement throughput of 20–40 per hour.

We gratefully acknowledge support from the Ministry of Industry, Energy and Technology, General Secretariat of Research and Technology of Greece, and the Greek National Drug Organization.

References

1 Efstathiou, C. E., Koupparis, M. A., and Hadjiioannou, T. P., *Ion-Sel. Electrode Rev.*, 1985, **7**, 203.
2 Thomson, H., and Rechnitz, G. A., *Chem. Instrum.*, 1972, **4**, 239.
3 Papastathopoulos, D. S., Diamandis, E. P., and Hadjiioannou, T. P., *Anal. Chem.*, 1980, **52**, 2100.
4 Meyerhoff, M. E., and Kovach, P. M., *J. Chem. Educ.*, 1983, **60**, 766.
5 Alegret, S. Alonso, J., Bartroli, J., Paulis, J. M., Lima, J. L. F. C., and Machado, A. A. S. C., *Anal. Chim. Acta*, 1984, **164**, 147.
6 van Staden, J. F., *Anal. Chim. Acta*, 1986, **179**, 407.
7 Stulik, K., and Pacakova, V., *Electroanalytical Measurements in Flowing Liquids*, Ellis Horwood, Chichester, 1987.
8 Christopoulos, T. K., and Diamandis, E. P., *Analyst*, 1987, **112**, 1293.
9 Douglas, J. G., *Anal. Chem.*, 1989, **61**, 922.
10 Alexander, P. W., and Maitra, C., *Anal. Chim. Acta*, 1988, **208**, 173.
11 McIntire, F. C., Clements, L. M., and Sprouli, M., *Anal. Chem.*, 1953, **25**, 1757.
12 Kolbezen, M. J., Eckert, J. W., and Bretschneider, B. F., *Anal. Chem.*, 1962, **34**, 583.
13 Goodwin, J. F., *Clin. Chem.*, 1968, **14**, 1080.
14 Lehmann, P. A., *Anal. Chim. Acta*, 1971, **54**, 321.
15 Couch, R., *J. Assoc. Off. Anal. Chem.*, 1975, **58**, 599.
16 Weber, J. D., *J. Pharm. Sci.*, 1976, **65**, 105.
17 Ryan, J. A., *J. Pharm. Sci.*, 1984, **73**, 1301.
18 Athanasiou-Malaki, E., and Koupparis, M. A., *Analyst*, 1987, **112**, 757.

19 Athanasiou-Malaki, E., Koupparis, M. A., and Hadjiioannou, T. P., *Anal. Chem.*, 1989, **61**, 1358.
20 Athanasiou-Malaki, E., and Koupparis, M. A., *Talanta*, 1989, **36**, 431.
21 Archontaki, H. A., Koupparis, M. A., and Efstathiou, C. E., *Analyst*, 1989, **114**, 591.
22 Connors, K. A., and Wong, M. P., *J. Pharm. Sci.*, 1979, **68**, 1470.
23 Wong, M. P., and Connors, K. A., *J. Pharm. Sci.*, 1983, **72**, 146.
24 Athanasiou-Malaki, E., and Koupparis, M. A., *Anal. Chim. Acta*, 1989, **219**, 295.
25 Frant, M. S., and Ross, J. W., *Anal. Chem.*, 1968, **40**, 1169.
26 Savitzky, A., and Golay, M. J. E., *Anal. Chem.*, 1964, **36**, 1627.
27 Madden, H. H., *Anal. Chem.*, 1978, **50**, 1383.
28 Belal, S. F., Elsayed, M. A., Elwalily, A., and Abdine, H., *Analyst*, 1979, **104**, 919.
29 Volpe, F., Zintel, J., and Spiegel, D., *J. Pharm. Sci.*, 1979, **68**, 1264.

Paper 0/04477F
Received October 4th, 1990
Accepted October 31st, 1990

Amitriptyline-selective Plastic Membrane Sensors and Their Pharmaceutical Applications

Andrei A. Bunaciu, Mariana S. Ionescu, Cornelia Pălivan and Vasile V. Coşofreţ*
Institute of Chemical and Pharmaceutical Research Bucharest, 74351-Sos. Vitan 112, Bucharest-3, Romania

The construction and general performance characteristics of potentiometric amitriptyline–plastic membrane sensors, based on ion-pair complexes with triphenylstilbenylborate and tetra(2-chlorophenyl)borate, respectively, are described. Both electrodes show near-Nernstian responses over the range 1×10^{-2}–7×10^{-6} mol dm^{-3} with a detection limit of about 5×10^{-6} mol dm^{-3}. The electrodes proved useful in the determination of amitriptyline hydrochloride in pure drug substances and pharmaceutical preparations. They were also applied to the determination of content uniformity and dissolution rate of sugar-coated amitriptyline tablets. The physical processes were numerically simulated by typical equations.

Keywords: *Amitriptyline–plastic membrane sensor; drug analysis; content uniformity; dissolution rate; release profile*

Developments in pharmaceutical analysis with ion-selective membrane electrodes[1–6] have enabled the activity of various organic cations or anions of pharmaceutical interest to be measured directly and selectively and, in most instances, without prior separation of the active substance from the formulation matrix. It is usually possible to develop methods for the determination of drug substances in pharmaceutical preparations that would need only a pre-dilution step (*e.g.*, injection preparations) or dissolution of tablets in the measuring solvent.

This paper describes the preparation and characterization of two amitriptyline-selective membrane electrodes based on ion-pair complexes embedded in a poly(vinyl chloride) (PVC) matrix. In one of them, triphenylstilbenylborate (TPSB) is used as the counter ion (electrode A) and in the other, tetra(2-chlorophenyl)borate (ClTPB) is used as the counter ion (electrode B). Both electrodes show near-Nernstian responses over the range 1×10^{-2}–7×10^{-6} mol dm^{-3} with a detection limit of about 5×10^{-6} mol dm^{-3}. The electrodes have been used successfully for the determination of amitriptyline hydrochloride in pure drug substances and pharmaceuticals by a potentiometric titration technique. They were also applied to the determination of content uniformity and dissolution rate of sugar-coated amitriptyline tablets. In order to investigate all the important physical processes during the dissolution period, the release profiles of the active principle were numerically simulated by typical equations.

Amitriptyline hydrochloride {3-(10,11-dihydro-5*H*-dibenzo[*a*,*d*]cyclohepten-5-ylidene)propyldimethylamine hydrochloride} (**I**) is a tricyclic antidepressant showing sedative effects on anxious nervousness and on psychomotor nervousness. It also shows anticholinergic, antihistaminic and antiserotonimic effects.[7]

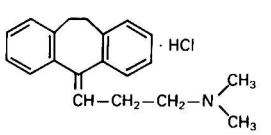

(I)

The official standard methods for the assay of amitriptyline in pharmaceutical preparations are based on extraction of the drug followed by determination by spectrophotometry, at 239 nm,[8] or liquid chromatography.[9] Analytical methods based on potentiometry,[10] including the use of ion-selective membrane electrodes sensitive to the amitriptyline cation,[11,12] have been developed for the determination. In this paper, a method for the determination of amitriptyline hydrochloride in pharmaceuticals is proposed, which is rapid and shows good reproducibility.

Experimental

Apparatus

A Prăcitronic digital pH/millivolt meter, Model 870 MV, was used for all direct potentiometric measurements. The electrodes were used in conjunction with a Radiometer K 401 calomel electrode. The titration curves were obtained by using an automatic titration assembly consisting of an ABU 12 autoburette and a TTT 2 titration and SBR 2c recorder (Radiometer). The pH measurements were performed with a Radiometer G 202B glass electrode in combination with a Radiometer K 401 calomel electrode. The dissolution test was performed in a basket-stirrer United States Pharmacopeia (USP)-type apparatus. The ultraviolet (UV) determinations were performed on a Pye Unicam SP-1800 spectrophotometer. The statistical approach and simulation of the experimental data were performed on a 4021 Coral computer (PDP-11/44 compatible).

Reagents and Materials

Amitriptyline hydrochloride was supplied by Terapia (Cluj-Napoca) and other materials and reagents [potassium triphenylstilbenylborate (KTPSB), potassium tetra(2-chlorophenyl)borate (KClTPB), dinonyl phthalate (DNP), 2-nitrophenyl octyl ether (2-NPOE), PVC of high relative molecular mass and tetrahydrofuran (THF)] were of analytical-reagent grade. The pharmaceutical preparations were purchased from a pharmacy.

Solutions of amitriptyline hydrochloride were prepared by serial dilution, while keeping both pH and ionic strength constant.

A standard solution of sodium tetraphenylborate (5×10^{-2} mol dm^{-3}) was prepared by dissolving 17.122 g of the compound in distilled water and diluting to 1 l.

Construction of the Electrodes

The PVC membranes and the electrodes, based on association of amitriptyline ion-pair complexes (electrodes A and B), were constructed according to the method of Moody and

* To whom correspondence should be addressed.

Thomas.[13] Powdered PVC, the ion exchanger and plasticizer–mediator were dissolved in a volatile solvent such as THF. The solution was poured onto a glass sheet, and the membrane was formed as the solvent evaporated. Punched circular membranes were attached to a 10 mm Tygon tube. The other end of the Tygon tube was fitted onto a glass tube to form the electrode body (compositions are given in a later section). In both instances the electrode body was filled with a 1×10^{-3} mol dm^{-3} amitriptyline hydrochloride solution. The electrodes were pre-conditioned for 1 h by soaking them in a 1×10^{-2} mol dm^{-3} amitriptyline hydrochloride solution.

Electrode Characteristics

The performance of the electrodes was investigated by measuring the e.m.f. values of 1×10^{-2}–1×10^{-6} mol dm^{-3} amitriptyline hydrochloride solutions. Potentials were recorded when stable readings had been obtained.

Recommended Procedure

Direct potentiometry

Standard solutions (in 0.1 mol dm^{-3} HCl) of 1×10^{-3}, 3×10^{-4}, 7×10^{-4}, 1×10^{-4}, 3×10^{-5}, 7×10^{-5} and 1×10^{-5} mol dm^{-3} concentrations are prepared by serial dilution of a 1×10^{-2} mol dm^{-3} amitriptyline hydrochloride solution. The electrodes are placed in the stirred standard solution in the order 1×10^{-5}–1×10^{-3} mol dm^{-3}; E (mV) *versus* log concentration (c) is plotted. The unknown concentration is determined from the calibration graph.

Potentiometric titration

The electrodes are placed in the sample solution (30–40 ml, concentration approximately 1×10^{-2} mol dm^{-3}), and the solution is titrated with 5×10^{-2} mol dm^{-3} sodium tetraphenylborate. The end-point corresponds to the maximum slope on the E (mV) *versus* volume of titrant curve (1 ml of 5×10^{-2} mol dm^{-3} tetraphenylborate is equivalent to 15.695 mg of amitriptyline hydrochloride).

Content uniformity assay of sugar-coated amitriptyline tablets

Ten individual tablets are placed in separate 100 ml calibrated flasks and dissolved by shaking with distilled water. The solutions are titrated potentiometrically, as described above.

Dissolution test

The test is carried out according to the USP XXII method,[9] with use of the equipment shown in Fig. 1.

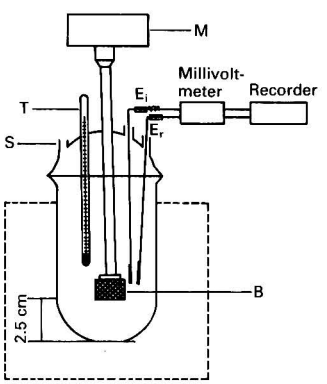

Fig. 1 Modified USP basket-stirrer dissolution apparatus: T, thermometer; S, sampling device; M, motor; B, basket-stirrer; E_i, amitriptyline membrane electrode; and E_r, SCE connected to the dissolution medium by a saturated KNO_3 agar–agar bridge

One sugar-coated tablet is placed in the basket, and the dissolution medium (250 ml of 0.1 mol dm^{-3} HCl) is maintained at 37 ± 0.5 °C. The basket is rotated at 50 rev min^{-1}. For the potentiometric determination, after an appropriate time interval, the potential values are recorded, and the amount of amitriptyline hydrochloride is calculated from the calibration graph. For the UV determination, after an appropriate time interval, 5 ml aliquots are withdrawn, filtered and diluted with the dissolution medium, and the absorbance of the solution at 239 nm is measured against the dissolution medium. The amount of amitriptyline hydrochloride released in the dissolution medium is calculated from the calibration graph. In order to investigate all the important physical processes during the dissolution period, the release profiles of the active principle of the sugar-coated amitriptyline tablets were numerically simulated by typical equations.[14,15]

Results and Discussion

Membrane Materials

Amitriptyline hydrochloride and other organic amines are well known for reacting with KTPSB and KClTPB, respectively, to form stable ion-pair complexes. The complexes are obtained *in situ*, by soaking the PVC membranes in 1×10^{-2} mol dm^{-3} amitriptyline hydrochloride solution. Dinonyl phthalate and 2-NPOE exhibited good behaviour regarding response time and reproducibility of e.m.f. values of the electrodes. The membrane compositions were: 4.0% m/m KTPSB, 64.0% m/m 2-NPOE and 32.0% m/m PVC (electrode A); and 4.0% m/m KClTPB, 64.0% m/m DNP and 32.0% m/m PVC (electrode B).

Electrode Response

Typical calibration graphs for the amitriptyline membrane sensors in amitriptyline hydrochloride solution of two different pH values show that the electrode responses are linear in the range 1×10^{-2}–1×10^{-4} mol dm^{-3} for acetate buffered solution (pH 5.0) and 1×10^{-2}–7×10^{-6} mol dm^{-3} for HCl (0.1 mol dm^{-3}) medium. The calibration graphs are presented in Fig. 2.

The critical response characteristics of the electrodes in 0.1 mol dm^{-3} HCl (simulated gastric fluid) are summarized in Table 1.

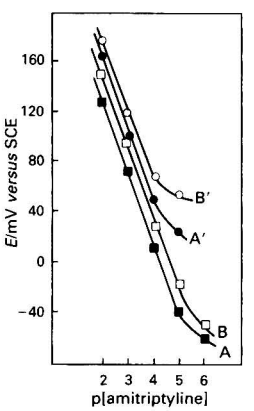

Fig. 2 Electrode functions for the amitriptyline membrane sensors in different solutions: A, electrode A (TPSB membrane type) in 0.1 mol dm^{-3} HCl; B, electrode B (ClTPB membrane type) in 0.1 mol dm^{-3} HCl; A′, electrode A (TPSB membrane type) in acetate buffer (pH 5.0); and B′, electrode B (ClTPB membrane type) in acetate buffer (pH 5.0)

Table 1 Response characteristics for amitriptyline membrane sensors

Parameter	KTPSB membrane	KClTPB membrane
Slope/mV per log a*	56.68 ± 1.83	56.72 ± 1.42
Intercept/mV†	245 ± 1.63	260 ± 3.39
Linear range/mol dm^{-3}‡	1×10^{-2}–7×10^{-6}	1×10^{-2}–6×10^{-6}
Detection limit/mol dm^{-3}	5×10^{-6}	3.5×10^{-6}
Detection limit/μg ml^{-1}	1.57	1.10

* Standard deviation of average slope value for multiple calibration.
† Standard deviation of values recorded over a period of 1 month.
‡ Region of Nernstian response.

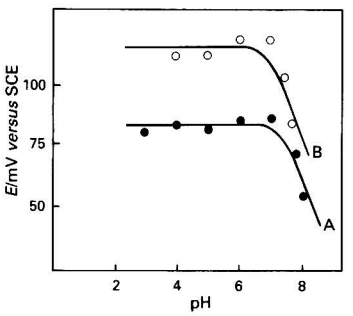

Fig. 3 Effect of pH on the response of the amitriptyline electrodes: A, electrode A (TPSB membrane type); and B, electrode B (ClTPB membrane type)

The calibration graphs for the electrodes were found to be reproducible from day to day; the electrodes were stored in air between measurements.

Effect of pH

The effect of pH on the potential readings of the amitriptyline membrane sensors was checked by recording the e.m.f. of a cell of the type: Ag–AgCl | 1×10^{-3} mol dm^{-3} amitriptyline hydrochloride (inner solution) || plastic membrane || 1×10^{-3} mol dm^{-3} amitriptyline hydrochloride (outer solution) | SCE, and varying the acidity by the addition of very small volumes of hydrochloric acid and/or sodium hydroxide solution (1.0 mol dm^{-3} of each). The graphs presented in Fig. 3 show that the linearity of the potential E (mV) *versus* pH function, in the range 2–7, is independent of the nature of the counter ion used. In both instances, at higher pH values, free base precipitates in the aqueous test solution, and consequently, the concentration of unprotonated species gradually increases. As a result, lower e.m.f. readings are recorded.

Response Time

The response time of the electrodes was tested for 1×10^{-2}–1×10^{-6} mol dm^{-3} amitriptyline hydrochloride solutions; the sequence of measurements was from low to high concentration. For both electrodes, response times were relatively fast and were almost instantaneous at higher concentrations. Only 1 min was required for solutions of 1×10^{-5}–1×10^{-6} mol dm^{-3}.

Selectivity of the Electrodes

Amitriptyline hydrochloride very often has to be determined in pharmaceuticals, which also contain various inorganic and organic substances. The effect of some of these matrices on the response of the electrodes was studied by the mixed solution method and the respective selectivity coefficients, $k^{pot}_{Ami,j}$, were calculated from the equation:

$$k^{pot}_{Ami,j} = (10^{\Delta E/S} - 1)\,[Ami^+]/[j^{z+}]^{1/z} \quad (1)$$

where ΔE is the change in potential in the presence of the interfering ion, j^{z+}, S is the slope of the calibration graph for the amitriptyline ion, and $[Ami^+]$ and $[j^{z+}]$ are the concentrations of the amitriptyline and interfering ions, respectively. The selectivity coefficients, presented in Table 2, indicate that the response of the proposed electrodes is not affected by the presence of the interfering ions studied. Excipients such as corn starch, gelatine, sugar and lactose also do not interfere.

Table 2 Selectivity coefficients for the amitriptyline electrodes. $[Ami^+]/[j^{z+}] = 1 \times 10^{-4}/1 \times 10^{-2}$

Interfering species (j^{z+})	Selectivity coefficient	
	Electrode A	Electrode B
DL-Histidine	$<1 \times 10^{-4}$	$<1 \times 10^{-4}$
Glycine	$<1 \times 10^{-4}$	$<1 \times 10^{-4}$
Vitamin B_1	7×10^{-4}	8.5×10^{-4}
Vitamin B_6	4×10^{-4}	4×10^{-4}
Mianserin	5.3×10^{-4}	5×10^{-4}
Ephedrine	$<1 \times 10^{-4}$	$<1 \times 10^{-4}$
Timolol	$<1 \times 10^{-4}$	$<1 \times 10^{-4}$
Imipramine	0.2	0.17

Table 3 Determination of amitriptyline hydrochloride in pharmaceutical formulations with the amitriptyline–TPSB membrane sensor

Product	Sample	Recovery (% of nominal value)*	Relative standard deviation (%)
Amitriptyline tablets, 25 mg (Terapia, Cluj-Napoca)	1	100.1	1.87
	2	99.7	
	3	100.8	
Amitriptyline vials, 50 mg (ICCF, Bucharest)	1	100.7	0.95
	2	100.8	
	3	100.6	

* All values are the average of four determinations.

Table 4 Results of content uniformity assay of amitriptyline hydrochloride tablets (Batch 002)* with the amitriptyline–TPSB membrane electrode

Tablet	Found		Relative standard deviation (%)
	mg per tablet	Percentage of nominal value	
1	24.8	99.1	5.88
2	26.5	105.9	
3	27.1	108.3	
4	23.5	94.2	
5	26.9	107.7	
6	26.1	104.5	
7	24.1	96.6	
8	25.4	101.6	
9	23.9	95.5	
10	22.9	91.9	

* Label amount: 0.025 g per tablet.

Analytical Applications

The electrodes proved useful for the assay of the amitriptyline content of pharmaceutical formulations by using the potentiometric titration method.

The results of the amitriptyline assay with electrode A, applied to two pharmaceutical formulations, are given in Table 3.

As can be seen in Table 3, a high precision [relative standard deviation (RSD) <2.0%] was attainable. Usually, the potentiometric assay could be accomplished within 15 min, in contrast to the 1 h required for the assay by the official standard methods.[8,9] Similar results were obtained by using the spectrophotometric method.[8] The present procedure offered the advantages of high selectivity and greater precision. Similar results were obtained with electrode B.

Other immediate fields of application of the electrodes would appear to be in the determination of tablet content uniformity and in dissolution-profile studies.

In many instances the content-uniformity test is preferred to the assay of a composite sample, as both preparation of the sample and measurements can be carried out more rapidly than those of the assay of a composite sample. If the accuracy of the assay is satisfactory, the mean value of the content-uniformity test can be used as the assay result.

Table 4 presents the results obtained for the determination of the content uniformity of sugar-coated amitriptyline tablets and indicates the suitability of the electrode method for this purpose.

The tested batch was considered acceptable as each of the individual units tested was found to be between 85 and 115% of the label amount and the RSD was less than 6.0%.

The desirability of an *in vitro* test that adequately reflects the physiological availability of solid dosage forms of drugs is now recognized. The measurement of a parameter that is related to the rate of dissolution of a solid has been suggested as a more realistic variable and this has led to numerous papers describing different methods and equipment for monitoring dissolution tests.[16–19]

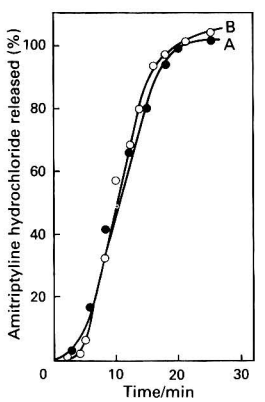

Fig. 4 Dissolution profiles of sugar-coated amitriptyline tablets: A, potentiometric method; and B, UV spectrophotometric method

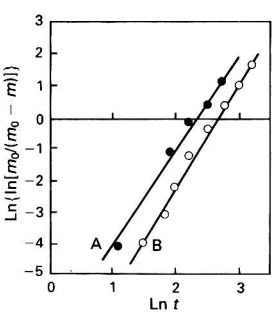

Fig. 5 Simulation of the experimental data according to the Langenbucher model for: A, potentiometric method; and B, UV spectrophotometric method

The advantage of the electrode technique for carrying out such a test is that the selective electrode can monitor continuously the concentration of the active ingredient in the standardized dissolution cells.

The dissolution test was performed with a basket-stirrer USP-type apparatus operated at 50 rev min^{-1} in 250 ml of 0.1 mol dm^{-3} hydrochloric acid (simulated gastric fluid), with the use of both a potentiometric amitriptyline membrane sensor method and a UV assay. For the former method, after an appropriate time interval (1 min), the potential values were recorded and the amount of amitriptyline hydrochloride released was determined from the calibration graph. For the UV determination, after an appropriate time interval (5 min), fixed volumes of the dissolution medium (5 ml) were withdrawn and subsequently diluted with the dissolution medium for measurement of the absorbance at λ_{max} = 239 nm, in comparison with that of a standard solution of amitriptyline hydrochloride (reference substance) in the same medium. The volumes withdrawn were replaced with 5 ml of simulated gastric fluid kept at 37 ± 0.5 °C.

Fig. 4 shows the dissolution profiles of sugar-coated amitriptyline tablets obtained by both methods. As can be seen, there are no significant differences between the two profiles.

Taking into account the S-shape of both curves, there are some possibilities for the simulation of physical processes involved in the dissolution steps.

Both methods proved that the release of the active principle of the sugar-coated amitriptyline tablets in simulated gastric fluid follows the Langenbucher model;[15] *i.e.*, the dissolution process involves two main steps: an initial step, of about 4 min, while the coated layer is removed, followed by a rapid process of active principle dissolution.

As can be seen from Fig. 5, the experimental data fit the Langenbucher model well.

All other simulation possibilities tested were found to be inadequate for the sugar-coated amitriptyline tablets.

Conclusions

The amitriptyline-selective plastic membrane sensors, based on amitriptyline–triphenylstilbenylborate and amitriptyline–tetra(2-chlorophenyl)borate ion-pair complexes in a PVC matrix, exhibit useful analytical characteristics for the determination of amitriptyline hydrochloride in pharmaceutical preparations (sugar-coated tablets and injectable aqueous solutions). The sensors can be successfully used in establishing dissolution profiles for sugar-coated amitriptyline tablets.

References

1 Coşofreţ, V. V., *Ion-Sel. Electrode Rev.*, 1980, **2**, 159.
2 Pinkerton, T. C., and Lawson, B. L., *Clin. Chem. (Winston-Salem, NC)*, 1980, **52**, 562.
3 Pungor, E., Feher, Z., Nagy, G., and Tóth, K., *Anal. Proc.*, 1982, **19**, 79.
4 Coşofreţ, V. V., *Membrane Electrodes in Drug-Substances Analysis*, Pergamon Press, Oxford, 1982, pp. 127–343.
5 Coşofreţ, V. V., and Buck, R. P., *Ion-Sel. Electrode Rev.*, 1984, **6**, 59.
6 Zang, Z.-r., and Coşofreţ, V. V., *Ion-Sel. Electrode Rev.*, 1990, **12**, 35.
7 *Martindale, The Extra Pharmacopoeia*, The Pharmaceutical Press, London, 26th edn., 1972, p. 1438.
8 *The British Pharmacopoeia 1980*, HM Stationery Office, London, 1980, p. 732.
9 *The United States Pharmacopeia XXII*, US Convention Inc., Rockville, MD, 1990, p. 74.
10 Christopoulos, T. K., Diamandis, E. P., and Hadjiioannou, T. P., *Anal. Chim. Acta*, 1982, **143**, 143.
11 Mitsana-Papazoglu, A., Christopoulos, T. K., Diamandis, E. P., and Hadjiioannou, T. P., *Analyst*, 1985, **110**, 1091.

12 Leng, Z.-z., and Hu, X.-y., *Fenxi Huaxue*, 1989, **17**, 139.
13 Moody, G. J., and Thomas, J. D. R., in *Ion Selective Electrodes in Analytical Chemistry*, ed. Freiser, H., Plenum Press, New York, 1978, ch. 4, pp. 287–309.
14 Leeson, L. J., and Carstensen, J. T., *Dissolution Technology*, Whitlock Press, Washington, DC, 1974, p. 189.
15 Langenbucher, F., *J. Pharm. Pharmacol.*, 1972, **24**, 979.
16 Wagner, J. C., *Biopharmaceutics and Relevant Pharmacokinetics*, Drug Intelligence Publications, Hamilton, IL, 1971, pp. 65–71.
17 Heilmann, K., *Therapeutic Systems; Rate-Controlled Drug Delivery: Concept and Development*, Verlag, Stuttgart, 2nd edn., 1984, pp. 24–33.
18 Cooper, J., and Rees, J. E., *J. Pharm. Sci.*, 1972, **61**, 1511.
19 Hersey, J. A., *Manuf. Chem. Aerosol News*, 1969, **40**, 32.

Paper 0/03676E
Received August 10th, 1990
Accepted October 22nd, 1990

Ion-selective Electrodes in Organic Analysis: Determination of Amides *Via* Hydrolysis to Carboxylates

Wing Hong Chan,* Albert Wai Ming Lee,* Po Lin Tong and Kwok Yin Tsang
Department of Chemistry, Hong Kong Baptist College, 224 Waterloo Road, Kowloon, Hong Kong

An indirect ion-selective electrode system for the determination of aromatic amides has been developed. In the presence of an excess of sodium peroxide, both primary and secondary amides were converted quantitatively into the corresponding carboxylates. Subsequently, the carboxylates obtained were determined, without further purification, using a tetraheptylammonium benzoate–poly(vinyl chloride) matrix membrane electrode. The electrode exhibited a Nernstian response in the concentration range 1×10^{-1}–7×10^{-3} mol dm^{-3} benzoate with an average slope of −47.2 mV per concentration decade. It has a working pH range of 7.0–9.5, a rapid response time (less than 3 min) and a stable response for at least 2 months.

Keywords: *Benzoate-selective electrode; amide determination; hydrolysis to carboxylate; organic analysis*

Amides are important intermediates in organic synthesis, and some aromatic amides are essential in the manufacture of medicines and pesticides.[1] Numerous chemical and instrumental methods have been reported in the literature; however, owing to the inertness of amides, most of these methods either require tedious treatment procedures or have a limited scope of application.[2–5] In order to expand the use of ion-selective electrodes (ISEs) in organic analysis, we have developed a strategy that involves converting covalent organic functional groups such as esters,[6] alcohols,[7] aldehydes[8] and amines[9] into water-soluble ionic derivatives that are amenable to potential measurement. Such an approach could be extended to the determination of amides after hydrolysis to the corresponding ionic carboxylates. In the presence of an excess of sodium peroxide, both primary and secondary aromatic amides can be hydrolysed quantitatively to the corresponding carboxylates[10] with an isolated yield of greater than 80%.

$$\begin{matrix}\mathrm{RCONH_2}\\ \text{or}\\ \mathrm{RCONHR'}\end{matrix} + \mathrm{Na_2O_2} \rightarrow \mathrm{RCOO^-Na^+} + \begin{matrix}\mathrm{NH_3}\\ \text{or}\\ \mathrm{R'NH_2}\end{matrix}$$

The carboxylates generated from the aromatic amides are then determined, without isolation, using an aromatic carboxylate selective poly(vinyl chloride) (PVC) membrane electrode.

Experimental

Apparatus

Potentiometric measurements were made at a constant temperature in the range 20–25 °C with an Orion pH/ISE meter (Model SA720). A tetraheptylammonium benzoate–PVC matrix membrane electrode in conjunction with an internal Ag–AgCl reference electrode, with 0.1 mol dm^{-3} sodium benzoate and 0.1 mol dm^{-3} sodium chloride as the reference solution, was used. A saturated calomel electrode (SCE) from Cole-Parmer (Model N-05990-52) was used as an external reference electrode. The pH of the solution was measured with a combined pH electrode from Broadley–James (Model 119115-03). Proton nuclear magnetic resonance (^{1}H NMR) spectra were recorded on a Jeol NMR (60 MHz) spectrometer (Model PMX 60SI) in order to confirm the structure of the sensor.

* To whom correspondence should be addressed.

Reagents

All solutions were prepared with distilled, de-ionized water and analytical-reagent grade reagents, unless stated otherwise. The organic solvents were also of analytical-reagent grade. Tetrahydrofuran (THF) obtained from Ajax Chemicals was distilled before use. Tetraheptylammonium bromide and PVC powder were obtained from Aldrich. Bis(2-ethylhexyl) phthalate (DEHP) was from Fluka. The amides were prepared according to a procedure described in the literature,[11] except for benzamide, which was obtained from BDH.

Tetraheptylammonium Benzoate–PVC Matrix Membrane Electrode

Preparation of the sensor (tetraheptylammonium benzoate ion pair)

One equivalent of sodium benzoate (about 0.01 mol) in 30 ml of distilled, de-ionized water and 0.95 equiv of tetraheptylammonium bromide in 30 ml of chloroform were stirred overnight. The organic layer was then separated in a separating funnel and the aqueous layer was extracted with three 20 ml portions of chloroform. The organic layers obtained were combined, dried over anhydrous magnesium sulphate and the solvent was evaporated using a rotary evaporator. The viscous, yellow fluid that remained was the sensor, tetraheptylammonium benzoate.

Preparation of the sensing material (tetraheptylammonium benzoate–PVC matrix membrane)

A mixture of tetraheptylammonium benzoate (0.40 g), PVC powder (0.40 g) and plasticizer (DEHP, 0.20 g) was stirred thoroughly with 25 ml of dried THF until dissolved. The solution was poured into a Petri dish and covered with a piece of filter-paper. After all the THF had evaporated (usually after about 2 d), a sheet of the tetraheptylammonium benzoate–PVC matrix membrane was obtained.

Assembly of electrode

The electrode body was made from a screw-cap adaptor. A portion of the sensor membrane (1.5 cm in diameter) was cut and placed in the space between the plastic screw-cap and the glass adaptor. With the help of an O-ring, the membrane was held tightly at the bottom of the electrode so that there was no leakage of the reference solution, which was composed of 0.1 mol dm^{-3} solutions of sodium chloride and sodium benzoate. An Ag–AgCl electrode was used as the internal reference electrode.

Pre-conditioning and storage procedure

The assembled electrode was pre-conditioned by soaking it in 0.1 mol dm^{-3} sodium benzoate solution for 1 d after preparation. Prior to use, the electrode was soaked in distilled, de-ionized water for at least 2 h. The electrode was stored in 0.1 mol dm^{-3} sodium benzoate solution when not in use.

Construction of the ISE system

The assembled electrode, immersed in a solution of sodium benzoate, acted as a half-cell. The other half-cell was formed by inserting an SCE into a saturated KCl solution. The ISE system was completed by connecting the two half-cells with a potassium nitrate salt bridge. The structure of the ISE system can be represented as follows:

Internal reference electrode (Ag–AgCl)	NaCl (0.1 mol dm^{-3})–sodium benzoate (0.1 mol dm^{-3})	PVC matrix membrane with tetraheptylammonium benzoate
Sample or standard solution at pH 9	Saturated KCl solution	External reference electrode (SCE)

Calibration

A 1.00 mol dm^{-3} sodium benzoate solution was prepared by dissolving 0.10 mol of benzoic acid and 1.1 equiv of sodium hydroxide solution in 100 ml of distilled, de-ionized water. By appropriate dilution, a series of standard solutions with different concentrations were obtained. A 75 ml volume of the standard solutions was taken and the pH adjusted to 9 by the addition of a few drops of sodium hydroxide solution or hydrochloric acid (about 1×10^{-2} mol dm^{-3}). Then the electrochemical cell was set up and the measured potential readings (in mV) were plotted as a function of the logarithm of the concentration of the standard solution.

Determination of Amides

The amide was suspended in 50 ml of de-ionized water in a 100 ml round-bottomed flask and 2.5 equiv of sodium peroxide were added in portions with care. The mixture was refluxed for 2–8 h and the resulting solution containing the carboxylate was diluted to 100 ml. The concentration of carboxylate in the resulting solution was determined by interpolation of a typical calibration graph.

Results and Discussion

Sensing Membrane

Tetraheptylammonium bromide reacts with sodium benzoate to form a stable 1 : 1 ion pair, the composition of which was verified by ^1H NMR spectroscopy. The integration ratio and the multiplicity of the various proton signals of the NMR spectrum agree well with the proposed structure (Fig. 1). In the fabrication of the PVC matrix sensing membrane, a suitable amount of plasticizer was added to improve the plasticity of the membrane.

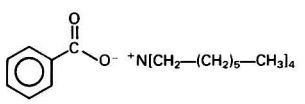

Fig. 1 Structure of the sensor (sensing membrane)

Characteristics of the Electrode

A typical calibration graph for the tetraheptylammonium benzoate–PVC membrane electrode showed a Nernstian response in the range 1×10^{-1}–7×10^{-3} mol dm^{-3} benzoate. The response characteristics of the electrode are summarized in Table 1. The influence of pH on the response of the tetraheptylammonium benzoate–PVC matrix membrane electrode was evaluated by performing potential measurements on the standard sodium benzoate solutions at different pH values. Because the potential difference of the solutions varied by less than ±1 mV within the pH range 7.0–9.5, subsequent potential measurements of the carboxylate solutions were therefore made at pH 9. On the other hand, the response of the membrane electrode was sufficiently rapid. Stable and constant readings (±1 mV) were obtained within 3 min for benzoate solutions with concentrations between 1×10^{-1} and 3×10^{-3} mol dm^{-3} (Fig. 2). The linearity and the Nernstian response of the electrode were reproducible for at least 2 months.

Hydrolysis of Amides to Carboxylates

The hydrolysis of each of the amides was monitored with the tetraheptylammonium benzoate–PVC membrane electrode. After a period of time, a fixed portion of the hydrolysed reaction mixture was removed from the reaction vessel and subjected to potential measurement. A constant potential reading was observed on completion of the reaction. This reading coincided with the potential reading of the corresponding carboxylate solution at the same concentration level. For primary and secondary aromatic amides, in the presence of an excess of sodium peroxide, the corresponding carboxylates were obtained quantitatively after refluxing for a specific period of time in water (Table 2).

Table 1 Response characteristics of the tetraheptylammonium benzoate–PVC matrix membrane electrode

Slope/mV (log [benzoate])$^{-1}$	−47.2
Standard deviation/mV	1.48*
Correlation coefficient	0.9994
Detection limit	4.55×10^{-3} mol dm^{-3}

* Average of nine calibration graphs.

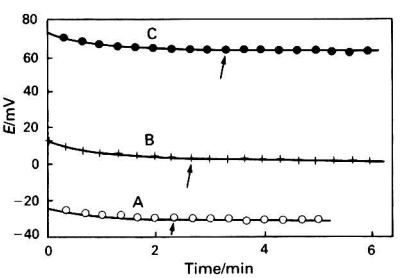

Fig. 2 Response time of the tetraheptylammonium benzoate–PVC matrix membrane electrode for different concentrations of sodium benzoate at pH 9. Benzoate concentration: A, 1.0×10^{-1}; B, 3.0×10^{-2}; and C, 3.0×10^{-3} mol dm^{-3}. The arrows indicate when the readings were taken after stabilization

Table 2 Reaction time for the hydrolysis of various amides to the corresponding carboxylates

Amide	Time/h
Benzamide	2.5
N-Butylbenzamide	8
p-Nitrobenzamide	5
N-Butyl-*p*-nitrobenzamide	8
p-Bromobenzamide	6

Table 3 Determination of amides using the tetraheptylammonium benzoate–PVC membrane electrode

Amide	Concentration taken/ mol dm^{-3}	Concentration found with the electrode/ mol dm^{-3}	Recovery (%)
Benzamide	4.996×10^{-2}	5.052×10^{-2}	101.1
	9.009×10^{-2}	9.088×10^{-2}	100.9
	0.900×10^{-2}	0.899×10^{-2}	99.9
	1.043×10^{-2}	1.022×10^{-2}	98.0
N-Butylbenzamide	1.115×10^{-2}	1.192×10^{-2}	106.9
	1.215×10^{-2}	1.318×10^{-2}	108.5
	0.607×10^{-2}	0.650×10^{-2}	107.1
p-Nitrobenzamide	5.959×10^{-3}	6.185×10^{-3}	103.8
	5.959×10^{-3}	6.010×10^{-3}	100.9
	5.959×10^{-3}	5.998×10^{-3}	100.6
N-Butyl-*p*-nitrobenzamide	0.415×10^{-2}	0.426×10^{-2}	102.6
	1.971×10^{-2}	1.928×10^{-2}	97.8
	1.021×10^{-2}	1.048×10^{-2}	102.6
p-Bromobenzamide	0.626×10^{-2}	0.660×10^{-2}	105.4
	0.548×10^{-2}	0.556×10^{-2}	101.4

Table 4 Selectivity coefficients, $k^{pot}_{A,B}$, and effect of foreign compounds on the detection limit and slope of the calibration graph for the tetraheptylammonium benzoate–PVC matrix membrane electrode

Interfering compound (B)	Concentration of interfering compound/ mol dm^{-3}	$k^{pot}_{A,B}$	Detection limit/ mol dm^{-3}	Slope/mV (log[benzoate])$^{-1}$
Potassium carbonate	1.00×10^{-2}	0.063	6.30×10^{-3}	−40.30
Phenol	1.00×10^{-2}	0.52	5.25×10^{-3}	−48.27
Sodium acetate	1.00×10^{-2}	0.19	1.91×10^{-3}	−48.31
Ammonium nitrate	1.00×10^{-2}	2.19	2.20×10^{-2}	−17.49
Ammonium chloride	1.00×10^{-2}	0.83	8.32×10^{-3}	−42.68
	5.00×10^{-2}	0.25	1.30×10^{-2}	−37.67

Determination of Amides

Initially, it was anticipated that the sensing material of the electrode could be used to detect both primary and secondary amides. In practice, when the electrode was used to determine the different concentrations of the hydrolysed products of benzamide, *p*-nitrobenzamide, *p*-bromobenzamide, *N*-butylbenzamide and *N*-butyl-*p*-nitrobenzamide, the results obtained were found to be fairly accurate (Table 3). However, the absolute potentials recorded with the electrode for various amides at the same concentration level were slightly different; hence the concentration of each amide had to be determined by the interpolation of the calibration graph using standard solutions of the respective carboxylate.

Effect of Foreign Compounds

In order to demonstrate the selectivity of the electrode, the electrode was examined in the presence of various foreign ions. The potentials of solutions containing 1×10^{-2} mol dm^{-3} of the foreign compound (B) with various benzoate (A) concentrations in the range 1×10^{-1}–1×10^{-3} mol dm^{-3} were measured. The selectivity coefficients ($k^{pot}_{A,B}$) were calculated using the fixed interference method (Table 4).[12] A comparison of the absolute potential readings, the values of the detection limit and the slope of the calibration graph in the presence of the foreign compounds showed that ammonium nitrate seriously interfered with the determination of amides. However, ammonium chloride was found to interfere only slightly, and no significant interference was caused by potassium carbonate, sodium acetate and phenol.

Conclusion

An indirect ISE system for the determination of primary and secondary aromatic amides has been developed. It is believed that, with some modifications, this simple and selective method could be extended to the determination of aliphatic amides.

References

1 Gessner, G. N., *The Condensed Chemical Dictionary*, Van Nostrand Reinhold, New York, 8th edn., 1971.
2 Siggia, S., and Hanna, J. G., *Quantitative Organic Analysis via Functional Groups*, Wiley, New York, 4th edn., 1979, pp. 183–223.
3 Scoggins, M. W., and Miller, J. W., *Anal. Chem.*, 1975, **47**, 152.
4 Ellis, J., and Holland, A. M., *Analyst*, 1976, **101**, 996.
5 D'Alonzo, R. P., and Siggia, S., *Anal. Chem.*, 1977, **49**, 262.
6 Chan, W. H., Lee, W. M., Wong, C. W., and Lam, K. S., *Analyst*, 1988, **113**, 1415.
7 Chan, W. H., Lee, A. W. M., Lam, K. S., and Tse, C. L., *Analyst*, 1989, **114**, 233.
8 Chan, W. H., Lee, A. W. M., and Ng, A. C. W., *Analyst*, 1990, **115**, 205.
9 Chan, W. H., Lee, A. W. M., and Chan, L. K., *Analyst*, 1990, **115**, 201.
10 Vanghu, H. L., and Robbins, M. D., *J. Org. Chem.*, 1975, **40**, 1187.
11 Vogel, A. I., *A Textbook of Practical Organic Chemistry Including Qualitative Organic Analysis*, English Language Book Society, London, 3rd edn., 1956.
12 Guilbault, G. G., *Ion-Sel. Electrode Rev.*, 1979, **1**, 139.

Paper 0/04131I
Received September 10th, 1990
Accepted October 29th, 1990

Differential-pulse Adsorptive Stripping Voltammetric Determination of Tyrosine and Histidine at a Hanging Mercury Drop Electrode After Coupling With Diazotized Sulphanilic Acid

Josino C. Moreira and Arnold G. Fogg
Department of Chemistry, Loughborough University of Technology, Loughborough, Leicestershire LE11 3TU, UK

Tyrosine and histidine can be determined in the range between 5.0×10^{-8} and 1.0×10^{-6} mol dm^{-3} by differential-pulse adsorptive stripping voltammetry after derivatization with diazotized sulphanilic acid (DSA) at pH 9.2 for 1 h. The amount of DSA added has to be controlled as, in large excess, DSA competes with the derivatives for adsorption on the electrode surface. The relative standard deviation (six determinations at the 2.5×10^{-7} mol dm^{-3} level) was typically 5%.

Keywords: *Adsorptive stripping voltammetry; tyrosine; histidine; diazotized sulphanilic acid derivative*

The use of derivatization reactions in analytical chemistry to improve the characteristics of determinands has been widely reported.[1–4] The possibility of using derivatization reactions prior to making determinations by adsorptive stripping voltammetry has extended the advantages of this technique to a range of electro-inactive or poorly adsorbed compounds and permits the differentiation of the analyte from the interferents by providing signals at different potentials from those of unmodified molecules. An increase in the sensitivity has been reported even for electro-active molecules after derivatization.[5–8]

The coupling reactions between diazonium salts and amino acids and proteins in alkaline solution are of wide interest in protein chemistry, physiology, immunology and immunochemistry. This type of reaction has been employed in order to modify proteins, study their composition and structure, their relationship to the function of enzymes and produce specific antigenic determinands.[9–14] Diazonium salts are produced by the reaction of aromatic amines with an equivalent amount of nitrous acid. Coupling occurs mainly with the histidyl, tyrosyl and lysyl residues of proteins. Tyrosine and histidine can be mono- or bi-substituted, depending on the ratio of diazonium salt to amino acid or protein. The reaction with tyrosine takes place at the position *ortho* to the hydroxyl group and with histidine at the carbon 2 and 4 positions in the imidazole ring. The pentadiazine derivatives formed by diazotization of lysine are not very stable.[14]

The diazo coupling reactions with histidine and tyrosine form the basis of several colorimetric methods for determining these compounds.[15–18] There is restricted interest in their use as site-specific reagents for spectrophotometric determinations of these amino acid residues in proteins, because of both the lack of specificity and the degradation of the diazo derivatives in alkaline solution.[18,19]

Among electro-analytical methods, polarography has been applied to study the reduction of diazotized compounds at the dropping mercury electrode[20,21] and azo-labelled antigen–antibody reactions.[22] Adsorptive stripping voltammetry has been used in the determination of aromatic amines after diazotization and coupling with 1-naphthol.[5]

Diazotized sulphanilic acid (DSA) is relatively stable and reactions with this compound can be carried out at room temperatures.[23,24] The DSA couples with tyrosine and histidine quantitatively giving diazo derivatives and this serves as the basis of a method for the determination of these amino acids. In the present study the diazo derivatives of tyrosine and histidine were found to be adsorbed at the surface of a hanging mercury drop electrode (HMDE) and a method for their determination using differential-pulse adsorptive stripping voltammetry is described.

Experimental

Adsorptive stripping voltammetry was carried out using a Metrohm 626 Polarecord with a 663 VA Stand, or a Metrohm 646 with a 647 Stand in conjunction with a multi-mode electrode in the HMDE mode. The three-electrode system was completed by means of a glassy carbon auxiliary electrode and a silver–silver chloride (Ag–AgCl) reference electrode. All potentials given are relative to this Ag–AgCl electrode. A pulse amplitude of 50 mV was used with a scan rate of 10 mV s^{-1} and a pulse interval of 1 s. A Metrohm 646 VA Processor in conjunction with a VA 647 Stand was used for cyclic voltammetry; a drop with a surface area of 0.40 mm^2 and a medium stirrer speed (1920 rev min^{-1}) were used. pH measurements were made with a Corning combined pH/reference electrode using a Radiometer PHM 64 pH meter, standardized with phosphate buffer (pH 7.00) and borate buffer (pH 9.18). The amino acids were obtained from Sigma and were used without further purification.

A 1.0×10^{-3} mol dm^{-3} solution of tyrosine was prepared by dissolving 181.2 mg of L-tyrosine in 1000 ml of water containing 2–3 drops of 6 mol dm^{-3} sodium hydroxide solution. Solutions for voltammetry were prepared from these by dilution with de-ionized water from a LiquiPure system. A 0.1 mol dm^{-3} stock solution of sulphanilic acid was prepared by dissolving 8.65 g of the acid in an aliquot of water containing 5 ml of concentrated ammonia solution. This was diluted to 500 ml.

Coupling of DSA with tyrosine or histidine was carried out as follows: to 10 ml of a standard solution of 0.1 mol dm^{-3} sulphanilic acid were added 5.0 ml of a 0.6 mol dm^{-3} hydrochloric acid solution. The mixture was cooled in an ice-bath for 10 min, and 5.0 ml of a 0.2 mol dm^{-3} solution of sodium nitrite solution were added dropwise with stirring. The diazotization was permitted to continue in the ice-bath for 10 min. Then 80 ml of water were added making the solution 0.01 mol dm^{-3} in diazonium ion. A 10 μl aliquot of this solution was added to a tyrosine or histidine solution in a 50 ml calibrated flask, giving a solution that was 2×10^{-6} mol dm^{-3} in diazonium ion. The pH was 9.2 (0.01 mol dm^{-3} borate buffer) and the reaction was permitted to proceed for 60 min at room temperature (22 °C). In some instances, sodium azide was used to stop the reaction after 60 min. A blank assay was carried out in parallel with each determination.

Procedure

The general procedure used to obtain adsorptive stripping voltammograms was as follows. A 15 ml aliquot of the derivatized amino acid solution was placed in a voltammetric cell. The stirrer was switched on and the solution was purged with nitrogen for 6 min. Subsequently, a 15 s de-oxygenation procedure was carried out between adsorptive stripping cycles. After forming a new HMDE, a 2 min accumulation was effected at the required potential whilst stirring the solution. At the end of the accumulation period the stirrer was switched off, and after 20 s had elapsed in order to allow the solution to become quiescent, a negative potential scan was initiated between the accumulation potential and −1.00 V.

Results and Discussion

Voltammetric Behaviour

The DSA is adsorbed at the HMDE from a pH 9.2 borate solution giving peaks at −0.27 and −0.75 V *versus* Ag–AgCl. These peaks occur at approximately the same potential as the half-wave potential observed in d.c. polarography. In the polarographic work,[21,25] the first wave was reported to correspond to a one-electron reduction of the diazonium salt itself according to the following equation:

$$ArN_2^+ + e^- \rightarrow ArN_2 \quad (1)$$

and the second wave to a two-electron reduction of the undissociated diazo hydroxide formed in an alkaline medium, as follows:

$$Ar\text{–}N{=}N\text{–}OH + 2H^+ + 2e^- \rightarrow 2ArH + N_2 + H_2O \quad (2)$$

In the presence of derivatized tyrosine or histidine, *i.e.*, after the coupling reaction had taken place, new peaks were observed at −0.52 V for tyrosine, as shown in Fig. 1, and −0.49 V *versus* Ag–AgCl for histidine in the differential-pulse adsorptive stripping voltammogram. This peak is due to the reduction of the azo derivative formed by coupling of the diazotized sulphanilic acid and the amino acids. The height of this peak depends on the tyrosine and DSA concentrations, pH, reaction time, accumulation time and the accumulation potential. The effect of these parameters was studied in order to optimize conditions for the determination of tyrosine and histidine.

Influence of Reaction Time and pH

The influence of the reaction time on the peak height, studied at pH values varying from 8 to 9.2 is shown in Fig. 2. No reaction was observed at a pH <8.0, as is expected for coupling reactions of phenols with diazonium salts.[26] At pH values >9.3, high values for the blank were obtained even at short reaction times. In this instance, the solution became yellowish owing to the degradation of the DSA and the coupling of the non-degraded molecules with themselves or with the phenol formed in the decomposition of the diazonium compound.[19] Good results were obtained between pH 8.8 and 9.2 but, owing to the better sensitivity, pH 9.2 was chosen as the optimum pH and 60 min as the preferred reaction time. At reaction times longer than 60 min, increases in the blank current signal were observed indicating that some degradation and coupling was occurring with the DSA.

Pyridine was used as a catalyst for the coupling reaction[23] but the results obtained showed no increase in the reaction rate under the conditions used.

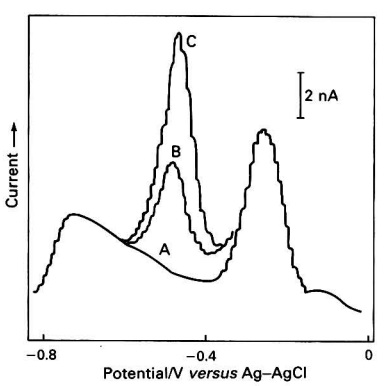

Fig. 1 Differential-pulse adsorptive stripping voltammograms of a 2 μmol dm^{-3} solution of A, DSA alone and in the presence of B, a 1.0×10^{-7}; and C, a 2.0×10^{-7} mol dm^{-3} solution of tyrosine, after 60 min of reaction. Accumulation step, 120 s at 0 V

Influence of Accumulation Potential

The influence of the accumulation potential on the peak current of a 5×10^{-7} mol dm^{-3} solution of tyrosine at pH 9.2 (0.01 mol dm^{-3} borate buffer) is shown in Table 1. Accumulation potentials in the range between 0.0 and −0.1 V gave the highest current. At potentials more negative than −0.1 V, a decrease in the peak current was observed as the peak potential was approached.

Other Coupling Reagents

In order to study the possibility of improving the rate of the diazo coupling reaction, diazo-1*H*-tetrazole, diazotized sulphanilamide and diazotized *p*-nitroaniline were used as coupling reagents.[24] High blank values were obtained with *p*-nitroaniline due to the reduction of the nitro group[25] and no advantages were observed with the use of diazo-1*H*-tetrazole or sulphanilamide compared with the diazotized sulphanilic acid.

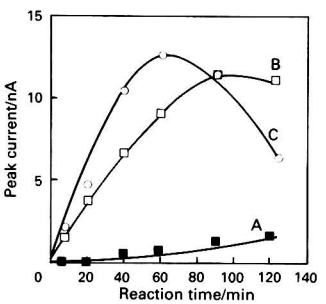

Fig. 2 Influence of the reaction time on the peak height of the DSA–tyrosine at various pH values: A, pH 8.0; B, pH 8.8; and C, pH 9.2. Accumulation step, 120 s at 0 V

Table 1 Influence of the accumulation potential on the peak current (i_p) of a 5×10^{-7} mol dm^{-3} solution of tyrosine after coupling with a 2×10^{-6} mol dm^{-3} solution of DSA for 60 min at room temperature, in 0.01 mol dm^{-3} borate buffer, pH 9.2. Accumulation time, 120 s

Accumulation potential/V *versus* Ag–AgCl	i_p/nA
0.0	14.8
−0.1	14.3
−0.2	11.2
−0.3	9.6

Table 2 Effect of the DSA concentration on the peak height due to the reduction of the azo derivative formed after reaction with tyrosine in 0.01 mol dm^{-3} borate solution, pH 9.2. (A, 1.0×10^{-7}; B, 7.5×10^{-7} mol dm^{-3}; and accumulation step, 120 s at 0.0 V)

[DSA]/10^{-6} mol dm^{-3}	i_p/nA	
	A	B
1.0	3.1	8.1
2.0	5.4	33.4
4.0	2.1	39.2
8.0	1.0	24.6
20.0	—	8.2

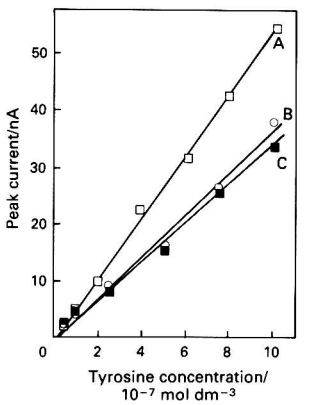

Fig. 3 Calibration graphs for DSA–tyrosine in 0.01 mol dm^{-3} borate buffer pH 9.2 using the time controlled technique and in the presence of added sodium azide (1×10^{-5} mol dm^{-3}). A, time controlled experiment; B, addition of sodium azide immediately after 60 min; C, same as B but 5 h after the addition of sodium azide. Reaction time, 60 min at room temperature; and accumulation step, 120 s at 0 V

Effect of Temperature

The optimum temperature for the coupling reaction was shown to be 20–30 °C. At temperatures higher than 30 °C higher blank values were obtained caused by degradation of the DSA.

Effect of Addition of Sodium Azide

As the reaction continues after the selected derivatization time, strict control of the reaction time, or the use of a reagent capable of reacting with the excess of DSA, thereby stopping the process, is necessary. The addition of sodium azide stopped the reaction after 60 min and no decomposition of the azo compound was observed even 24 h after the addition.[27] In these instances, no significant differences were observed when calibration graphs were prepared immediately after the addition of sodium azide or 5 h later. Although the linearity between peak current and tyrosine concentration persisted, higher blank values were obtained compared with the time-controlled procedure.

Influence of DSA Concentration

The influence of the DSA concentration on the peak heights for two different concentrations of tyrosine is shown in Table 2. In both instances the peak current reaches a maximum value at about 2×10^{-6}–4×10^{-6} mol dm^{-3} and at higher concentrations a modification of the baseline and a decrease of the peak current were observed. This is due to competition between the excess of DSA and the diazotized amino acid for adsorption sites on the electrode surface. In order to obtain better sensitivity 2×10^{-6} mol dm^{-3} was considered as the optimum DSA concentration.

Calibration Graphs

The peak current for the reduction of a 2.5×10^{-7} mol dm^{-3} solution of the diazotized tyrosine increased rectilinearly with the accumulation time up to 4 min ($r = 0.9993$). At longer accumulation times, rectilinearity was lost, probably due to saturation of the electrode surface.

Calibration graphs for the determination of tyrosine under time-controlled conditions and after the addition of sodium azide are shown in Fig. 3. The time-controlled graph was obtained using the Metrohm 646 and the Metrohm 626 after the addition of sodium azide. When using the same equipment the signal size was similar. Similar behaviour was observed for *N*-acetyltyrosine ethyl ether ($r = 0.998$) and histidine ($r = 0.9976$). Six determinations of tyrosine at the 5.0×10^{-7} mol dm^{-3} level gave a relative standard deviation of 5.2%.

Interferences

Of the amino acids, tryptophan, phenylalanine, arginine, glycine and lysine were shown not to interfere at the 1×10^{-6} mol dm^{-3} level. Cysteine adsorbs at the electrode surface giving a peak at −0.6 V which partially overlaps and interferes with the azo tyrosine–azo histidine peaks. Surfactants (sodium dodecylbenzenesulphonate, Triton X-100 and benzyldimethylhexadecylammonium chloride) at a concentration of 0.5 mg l^{-1} reduce the azo amino acid peaks by 20%.

J. C. M. thanks the Conselho Nacional de Desenvolvimento Cientifico e Technologico (CNPq-Brazil) for financial support.

References

1 *Chemical Derivatisation in Analytical Chemistry*, eds. Frei, R. W., and Lawrence, J. F., Plenum Press, NY, 1982, vols. 1 and 2.
2 Radzik, D. M., and Lunte, S. M., *Crit. Rev. Anal. Chem.*, 1989, **20**, 317.
3 *Fluorescent Protein Tracing*, ed. Nairns, R. C., E & S Livingstone, London, 1964.
4 Maeda, H., Ishida, N., Kawauchi, H., and Tuzimura, K., *J. Biochem.*, 1969, **65**, 777.
5 Fogg, A. G., and Lewis, J. M., *Analyst*, 1986, **111**, 1443.
6 Tocksteinova, Z., and Kopanica, M., *Anal. Chim. Acta*, 1987, **191**, 77.
7 Palecek, E., *Bioelectrochem. Bioenerg.*, 1986, **15**, 275.
8 Moreira, J. C., and Fogg, A. G., *Analyst*, 1990, **115**, 41.
9 Howard, A. N., and Wild, F., *Biochem. J.*, 1957, **65**, 651.
10 Gundlach, G., Kohne, C., and Turba, F., *Biochem. Z.*, 1962, **336**, 215.
11 Landsteiner, K., and van der Sheer, J., *J. Exp. Med.*, 1932, **56**, 399.
12 Landsteiner, K., *The Specificity of Serological Reactions*, Harvard University Press, Cambridge, MA, 1945.
13 Nisonoff, A., in *Methods in Immunology and Immunochemistry*, eds. William, C. A., and Chase, M. W. Academic Press, New York, 1967, vol. 1, p. 120.
14 Tabachnick, M., and Sobotka, H., *J. Biol. Chem.*, 1959, **234**, 1726.
15 Macpherson, H. T., *Biochem. J.*, 1942, **36**, 59.
16 Pauly, H. Z., *Z. Physiol. Chem.*, 1915, **94**, 284.
17 Pauly, H. Z., *Z. Physiol. Chem.*, 1904, **42**, 508.
18 Sokolovsky, M., and Vallee, B. L., *Biochemistry*, 1966, **5**, 3574.
19 Horinishi, H., Hachimori, Y., Kurihara, K., and Shibata, K., *Biochim. Biophys. Acta*, 1964, **86**, 477.
20 Elofson, R. M., Edsberg, R. L., and Mecherly, P. A., *J. Electrochem. Soc.*, 1950, **97**, 166.

21 Atkinson, E. R., Garland, C. E., and Butler, A. F., *J. Am. Chem. Soc.*, 1953, **75**, 983.
22 Breyer, B., and Radclif, F. J., *Aust. J. Exp. Biol.*, 1953, **31**, 167.
23 Zollinger, H., *Azo and Diazo Chemistry*, Interscience, London, 1961.
24 Fox, J. B., *Anal. Chem.*, 1979, **51**, 1493.
25 Kochi, J. K., *J. Am. Chem. Soc.*, 1955, **77**, 3208.
26 Hazzard, B. J., *Organicum*, Addison–Wesley Edn., 1973.
27 Nourbakhsh, M., and Baumgarten, A., *Experientia*, 1972, **28**, 1419.

Paper 0/04283H
Received September 21st, 1990
Accepted October 19th, 1990

Determination of Free Sulphur Dioxide in Red Wine by Alternating Current Voltammetry

Terence J. Cardwell, Robert W. Cattrall and Guo Nan Chen
Analytical Chemistry Laboratories, Chemistry Department, La Trobe University, Melbourne, Victoria 3083, Australia

Geoffrey R. Scollary
Institute of Education, University of Melbourne, Parkville, Victoria 3052, Australia

Ian C. Hamilton
BHP Central Research Laboratories, Newcastle, New South Wales 2287, Australia

Anthocyanins and oxygen interfere in the determination of 'free SO_2' in red wine by d.c. and differential-pulse voltammetry. However, the a.c. voltammetric behaviour of anthocyanins extracted from red wine shows that there is no interference in the determination of SO_2. Furthermore, there is minimal interference from oxygen which overcomes the need for de-oxygenation and its associated loss of SO_2. A phase-selective second harmonic a.c. voltammetric procedure is described for the determination of free SO_2 in red wine. The results of the analyses of several red wine samples are compared with those given by the spectrophotometric method accepted by the Australian wine industry.

Keywords: *Alternating current voltammetry; red wine analysis; free sulphur dioxide determination; anthocyanin interference*

Sulphur dioxide is traditionally used as a preservative in winemaking to prevent oxidation and bacterial growth. Dissolved SO_2 in wine always coexists with 'free SO_2' and 'bound SO_2'. Free SO_2 is an equilibrium mixture of S^{IV} species consisting of SO_2, hydrogen sulphite and sulphite, and the relative concentration of each species is a function of the pH of the medium. Bound SO_2, which occurs in many different forms, is mainly divided into carbonyl-bound (*e.g.*, with acetaldehyde) and pigment-bound (*e.g.*, with anthocyanin), the latter existing in red wine. Several methods have been recommended for the determination of free SO_2 in white wines.[1–8] However, there is still no satisfactory method for the determination of free SO_2 in red wines, not only because of the low actual level of free SO_2, which can be tolerated in red wines, but also because of the interference of anthocyanins. An aspiration–oxidation method, which was recommended for adoption by the Association of Official Analytical Chemists,[6] has been widely used for the determination of free and total SO_2 in the Australian wine industry.[9] This method has the major advantage that free SO_2 can be determined accurately in white wines; however, it is still very difficult to determine the real free SO_2 in red wines. In this method, the free SO_2 measured in red wines is actually the sum of free and pigment-bound SO_2. A spectrophotometric method is accepted by the Australian wine industry for the determination of free SO_2 in red wines.[10,11]

Several procedures for the determination of SO_2 have been based on electrochemical reduction at a dropping mercury electrode.[12–23] In this work, the reduction of SO_2 and other wine constituents has been carried out at a glassy carbon electrode using d.c., a.c. and differential-pulse (DP) voltammetric techniques. A phase-selective second harmonic a.c. voltammetric procedure is recommended for the determination of free SO_2 in red wine and the results of these analyses are compared with those given by the spectrophotometric method accepted by the Australian wine industry.

Experimental

Instrumentation

The polarograph used was a Metrohm E506 Polarecord with a three-electrode cell consisting of a saturated calomel reference electrode (SCE), a platinum auxiliary electrode and a glassy carbon working electrode. Spectrophotometric analysis of the red wine samples was carried out using a Shimadzu UV-240 recording spectrophotometer.

Reagents and Solutions

A stock solution of SO_2 (1000 mg l^{-1}) was prepared daily from analytical-reagent grade sodium hydrogen sulphite (metabisulphite) and then standardized against a standard iodine solution. The supporting electrolyte for all the voltammetric measurements was prepared by adding 0.2 mol dm^{-3} HCl to 0.2 mol dm^{-3} KCl solution until the pH was 1.8.

An anthocyanin concentrate from red wine was prepared by solvent extraction[10] of 650 ml of red wine successively with four 200 ml portions of isopentyl alcohol, previously equilibrated with 10% v/v ethanol–water saturated with potassium hydrogen tartrate. The combined extracts (800 ml) were shaken with 400 ml of light petroleum (boiling range 60–80 °C) plus 1 ml of 1 mol dm^{-3} HCl, and the lower aqueous phase, containing most of the anthocyanin, was separated. This was evaporated at 30 °C in order to remove trace amounts of solvent and finally diluted to 40 ml. Analysis of the concentrate was carried out by two-dimensional paper chromatography using a two-phase solvent system consisting of butanol–acetic acid–water (4 + 1 + 5).[24] Matching of retention factor (R_f) values showed that the extract contained chiefly malvidin-3-glucoside pigments with only trace amounts of other monomeric anthocyanins.[10,24]

Procedures

Voltammetric procedure for standards

A 20 ml aliquot of an SO_2 standard solution was added to the electrochemical cell, 2.0 ml of the KCl–HCl electrolyte solution (pH 1.8) were added and the solution was mixed. The surface of the working electrode was freshly polished with alumina powder before each scan. Phase-selective second harmonic a.c. voltammograms were recorded by scanning the potential from −0.1 to −1.4 V (*versus* SCE) at a scan rate of 16 mV s^{-1}, with an amplitude of 20 mV and a phase angle of zero. Peak heights were measured and a standard calibration graph was plotted.

Voltammetric procedure for wine samples

After the addition of the electrolyte to 20 ml of the wine sample, the pH was adjusted to 1.8 by the dropwise addition of 3 mol dm^{-3} HCl, with allowance being made for the volume change in the final calculation. Peak heights were measured under the same conditions as the standards and the concentration of SO_2 in the wine sample was evaluated from the calibration graph. A blank wine sample was obtained from a wine containing added electrolyte, by bubbling nitrogen through it in order to remove the SO_2.

Spectrophotometric procedure

The wine spectrum was recorded in the region from 400 to 550 nm using a cell with a path length of 1 mm and a volume of 0.33 ml, according to the procedure described in references 10 and 11. The absorbance (A_0) was measured at 520 nm. Sodium hydrogen sulphite solution (5 μl) was added to the above sample (giving approximately 2000 mg l^{-1} SO_2), mixed thoroughly by inversion and the spectrum was recorded again after 1 min. The absorbance (A_1) of this solution was measured at 520 nm. Acetaldehyde solution (20 μl) was added to 2.0 ml of a fresh wine sample. After about 45 min at 25 °C, the absorbance (A_2) was measured at 520 nm in a 1 mm cell.

Free SO_2 (mg l^{-1}) in the wine sample was calculated as follows:

$$\text{Free } SO_2 = 3.84\,(A_2 - A_0)/(A_0 - A_1)$$

Results and Discussion

Voltammetric Behaviour of Anthocyanins

The anthocyanins are red pigments widely distributed in red wine and they are known to exist as the mono- and di-glucosides of common anthocyanidins such as cyanidin, peonidin, delphinidin, petunidin and malvidin.[24] The sample of anthocyanin used was extracted from a red wine and has been confirmed by paper chromatographic examination to contain chiefly malvidin 3-glucoside.[10,24]

Several chemical properties of anthocyanins influence their structure and consequently their coloration which in turn affects the colour of red wine. Under the weakly acidic conditions in wines, anthocyanins exist in a red oxonium form which is in reversible equilibrium with a colourless pseudo-base, the position of the equilibrium being dependent on the pH as represented by the general equation

$$\underset{\text{red}}{[AnO]^+} + OH^- \rightleftharpoons \underset{\text{colourless}}{[AnO]OH}$$

where AnO^+ designates the oxonium form of anthocyanins.

The reaction of anthocyanins with SO_2 probably involves the combination of the hydrogen sulphite anion (which predominates at the pH of wine) with the oxonium cation to form an anthocyanin–hydrogen sulphite addition complex. The general equation is

$$\underset{\text{red}}{[AnO]^+} + SO_3H^- \rightleftharpoons \underset{\text{colourless}}{[AnO]SO_3H}$$

which again decreases the colour by forming a colourless compound. This reaction is the basis of the spectrophotometric procedure for the determination of free SO_2 in red wines.

The d.c. and DP voltammetric scans at a glassy carbon electrode show that SO_2 and anthocyanin give overlapping peaks at −0.60 and −0.46 V (*versus* SCE), respectively. When SO_2 is added to an anthocyanin solution, the SO_2 peak potential shifts to −0.56 V after about 30 min, which is very close to the peak potential for free SO_2. Hence, both anthocyanin and pigment-bound SO_2 are readily detected at a glassy carbon electrode and would interfere with the determination of SO_2 using the d.c. or DP voltammetric procedure.

The phase-selective fundamental harmonic and phase-selective second harmonic a.c. voltammograms of SO_2 and anthocyanin are shown in Figs. 1 and 2, respectively. In both scans, SO_2 gives a peak at −0.60 V and anthocyanin a peak at −0.52 V. Moreover, the reduction current of anthocyanin is much smaller than that observed for SO_2, even though the concentration of anthocyanin used in these scans is of the order of 2100 mg l^{-1} (measured spectrophotometrically[11]), which is 2–10 times higher than the normal concentration of anthocyanins in red wine (200–1000 mg l^{-1}).[25] It should be noted that the anthocyanin-bound SO_2 also gives a low reduction current compared with the free SO_2 and its peak potential is slightly more positive than the anthocyanin peak. Therefore, neither anthocyanin nor anthocyanin-bound SO_2 would interfere in the determination of SO_2 by phase-selective a.c. voltammetric techniques as the total concentration of the anthocyanin species in wines would be much lower than those used in the anthocyanin samples that were studied (Figs. 1 and 2).

Interference From Oxygen

It is known that dissolved oxygen is reduced during cathodic voltammetric scans and it is normal practice to remove the oxygen by passing nitrogen through the solution for about 10 min before the run. The electrochemical reduction of SO_2 at a glassy carbon electrode is dependent on the pH of the

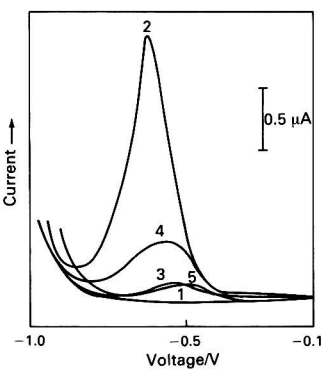

Fig. 1 First harmonic a.c. voltammograms of anthocyanin and SO_2 at a glassy carbon electrode. Conditions: electrolyte KCl–HCl (pH 1.8); scan rate, 16 mV s^{-1}; amplitude, 20 mV; phase angle, 0°; frequency, 75 Hz. 1, Background; 2, 10 mg l^{-1} SO_2 solution; 3, anthocyanin solution; 4, anthocyanin plus added SO_2 (10 mg l^{-1}); and 5, solution 4 run after 30 min

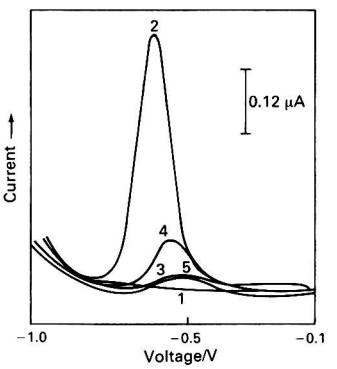

Fig. 2 Second harmonic a.c. voltammograms of anthocyanin and SO_2 solutions. Frequency, 37.5 Hz, all other conditions and solution identities as for Fig. 1

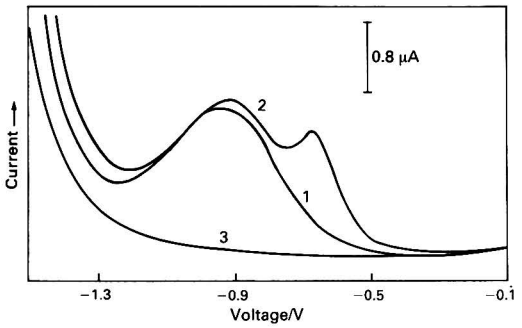

Fig. 3 Differential-pulse voltammogram of SO_2 in the presence of oxygen at a glassy carbon electrode. Electrolyte, as in Fig. 1; scan rate, 16 mV s^{-1}; and pulse amplitude, 30 mV. 1, Background electrolyte without de-oxygenation; 2, SO_2 solution (10 mg l^{-1}) without de-oxygenation; and 3, background electrolyte after de-gassing for 10 min

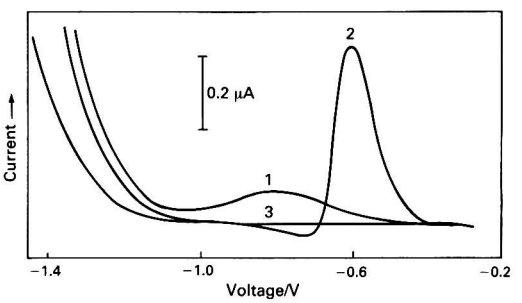

Fig. 4 Second harmonic a.c. voltammogram of SO_2 at a glassy carbon electrode in the presence of oxygen. Conditions as in Fig. 2 and solution identities as in Fig. 3

solution, the most sensitive signal being given at about pH 2. At this pH, calculations show that molecular SO_2 represents about 50% of the total S^{IV} species present in solution. As nitrogen is bubbled through the solution to remove oxygen, molecular SO_2 is easily removed from solution at low pH values. If the pH of the solution is higher than 3, at which pH the molecular SO_2 represents about 5% of the total, the signal will decrease after de-oxygenation, but not to the same extent as at pH 2 or lower. Fig. 3 shows that oxygen interferes in the determination of SO_2 when using DP voltammetry at a glassy carbon electrode and a similar result is obtained using d.c. voltammetry.

The electrochemical reduction of oxygen is a slow charge-transfer process, hence a.c. voltammetry might be suitable for the determination of SO_2 in the presence of oxygen. The phase-selective second harmonic a.c. voltammograms presented in Fig. 4 show that there is negligible interference from oxygen in the determination of SO_2 in solutions where their concentrations are similar. As the levels of oxygen in bottled wines are much lower than those displayed in Fig. 4,[26] it is possible to determine SO_2 in wine samples by this method without interference from oxygen. Furthermore, one avoids the loss of SO_2 from solution which would accompany the normal de-oxygenation step, as there is no need to de-oxygenate the solution before carrying out the scan.

Optimization of Experimental Parameters

Condition of the electrode surface

In the determination of SO_2 in wine samples, the repeatability of the method is very dependent on the condition of the surface of the glassy carbon electrode. In repeated

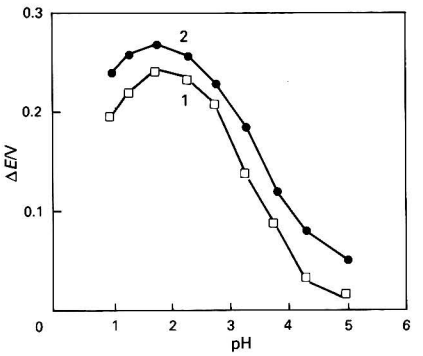

Fig. 5 Effect of pH on the peak potential difference (ΔE) of the SO_2 and oxygen a.c. voltammetric peaks. 1, First harmonic a.c. data; 2, second harmonic a.c. data

voltammetric scans, the height of the SO_2 peak was found to decrease unless the electrode surface was polished before each scan. Electrochemical pre-treatment of the electrode was found to be ineffective for the conditioning of the surface before each scan. In general, precision was of the order of 5% relative standard deviation (RSD) ($n = 5$), by using a polished electrode, for levels of SO_2 below 4 mg l^{-1}.

Effects of pH

As with mercury electrodes in polarography,[14,17–19] the electrochemical reduction of SO_2 at a glassy carbon electrode is dependent on the pH of the solution. No reduction wave is observed in neutral or alkaline solutions, but a well defined wave is recorded at pH <5. The most sensitive measurements can be made in the pH range 1.0–2.3 with the maximum signal being achieved at pH 1.8.

It is interesting to note that the pH of the electrolyte not only affects the peak height but also the difference in the potentials of the SO_2 and oxygen peaks, mainly because of a shift in the SO_2 peak to more negative potentials in the pH range 2.0–5.0. Fig. 5 indicates that the largest peak potential difference is achieved at pH 1.8 for both techniques and that the pH of natural wine (3.0–3.5) is not ideal for performing the voltammetric analysis. Therefore, it was considered to be essential to adjust the wine to pH 1.8 for all subsequent experiments.

Amplitude effects

In the presence of oxygen, the ideal amplitudes were found to be 15–20 mV as the peak height ratio and the peak to peak separation of the oxygen and SO_2 peaks were optimal for these values. At amplitudes above 20 mV, the resolution of the two peaks was inferior. Hence, an amplitude of 20 mV was chosen for all subsequent work.

Selection of phase angle

In phase-sensitive a.c. techniques, it should be possible to discriminate against the charging current by careful choice of the phase angle. For a fast electron transfer a.c. electrode process, the charging current will be theoretically zero, if measurements are carried out at a phase angle of 0° relative to the applied voltage. As expected, voltammograms for the SO_2 system, at phase angles greater than 0°, tended to be less sensitive. Hence, a phase angle of 0° was chosen for all subsequent wine analyses.

Interference of Other Components in Wine

The voltammetric behaviour of some of the more commonly occurring compounds in wine such as glucose, malic acid, benzoic acid, glycerol, proline, 2-oxoglutaric acid, ascorbic

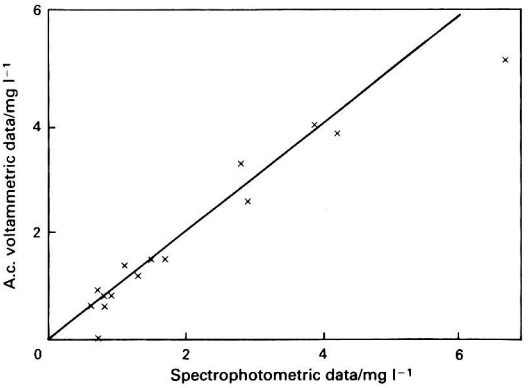

Fig. 6 Correlation of a.c. voltammetric and spectrophotometric data for free SO_2 in 15 red wines

acid, succinic acid, acetaldehyde, fructose, gallic acid, pyruvic acid and arabinose was examined in the reduction mode. None of these constituents gave reduction waves in the potential range 0.0 to −1.2 V.

Ascorbic acid and gallic acid (a natural component and a model phenolic compound) are easily oxidized in solution by oxygen and it is usually considered that these compounds are present in their oxidized forms in wine.[26,27] In order to investigate the possible interference of the oxidized forms of these acids in the determination of SO_2, complete oxidation of the acids was carried out by controlled potential coulometry of individual solutions of ascorbic and gallic acids in a KCl–HCl electrolyte (pH 1.8) using a large surface area carbon felt electrode maintained at +1.00 V (*versus* SCE) for 20 min in a stirred solution. The current was recorded during the electrolysis in order to determine when the oxidation was essentially 99% complete. No reduction waves were detected in the range 0 to −1.4 V for the voltammetric scans of these solutions at a glassy carbon electrode, indicating that the oxidized forms of these two acids would not interfere in the determination of SO_2 by cathodic a.c. voltammetry.

Although some common metal ions are known to be reduced in the potential range used in the voltammetric scans described here, there is no interference from Cu^{2+}, Fe^{2+} and Fe^{3+} up to 5 mg l^{-1} or from Cd^{2+} and Pb^{2+} up to 1 mg l^{-1}.

Analysis of Red Wine Samples

In principle, the fundamental and the second harmonic a.c. techniques could be used for the determination of free SO_2 in wine samples. Only the results of the second harmonic procedure are presented here because of better discrimination against oxygen.

Using this procedure under the specified conditions, the calibration graph for SO_2 is linear in the concentration range 0–20 mg l^{-1}. The analyses of 15 red wine samples were performed and a comparison of these results with those given by the spectrophotometric method (Fig. 6) gave a correlation coefficient of 0.97.

The a.c. voltammetric procedure is recommended as an alternative to the spectrophotometric procedure because of the time saved in performing an analysis. On average, 5–6 samples h^{-1} can be analysed by a.c. voltammetry including the time required to polish the electrode, whereas 1 h is required to perform each analysis by spectrophotometry. At concentrations of SO_2 below 4 mg l^{-1}, the precision in the a.c. technique (about 5%) is better than that achieved in the spectrophotometric method and the correlation between the data from the two methods is acceptable. Furthermore, the spectrophotometric procedure is subject to significant error because the calculations rely on the use of absorbance differences, which are experimentally small owing to the low levels of free SO_2 in red wines.

We thank the Australian Grape and Wine Research Council for financial support and G. N. C. thanks La Trobe University for the award of a postgraduate scholarship.

References

1 Monier-Williams, G. W., *Analyst*, 1927, **52**, 415.
2 Tanner, H., *Mitt. Geb Lebensmittelunters Hyg.*, 1963, **54**, 158.
3 Jennings, N., Bunton, N. G., Crosby, N. T., and Alliston, T. G., *J. Assoc. Public Anal.*, 1978, **16**, 59.
4 Rankine, B. C., *Aust. Wine Brew. Spirit Rev.*, 1962, **80**, 14.
5 Fujita, K., Ikuzawa, M., Izumi, T., Hamano, T., Mitsuhashi, Y., Matsuki, Y., Adachi, T., Nonogi, H., Fuke, T., Suzuki, H., Toyoda, M., Ito, Y., and Iwaida, M., *Z. Lebensm. Unters. Forsch.*, 1979, **168**, 206.
6 *Official Methods of Analysis of the Association of Official Analytical Chemists*, ed. Horwitz, W., Association of Official Analytical Chemists, Washington, DC, 14th edn., 1984, pp 229, 391 and 392.
7 Ripper, M., *J. Prakt. Chem.*, 1892, **46**, 428.
8 Vahl, J. M., and Converse, J. E., *J. Assoc. Off. Anal. Chem.*, 1980, **63**, 194.
9 Rankine, B. C., and Pocock, K. F., *Aust. Wine Brew. Spirit Rev.*, 1970, **88**, 40.
10 Burroughs, L. F., *Am. J. Enol. Vitic.*, 1975, **26**, 25.
11 Somers, T. C., and Evans, M. E., *J. Sci. Food Agric.*, 1977, **28**, 279.
12 Kolthoff, I. M., and Miller, C. S., *J. Am. Chem. Soc.*, 1941, **63**, 2818.
13 Diemair, W., Koch, J., and Hess, D., *Fresenius Z. Anal. Chem.*, 1961, **178**, 321.
14 Bruno, P., Caselli, M., Di Fano, A., and Traini, A., *Analyst*, 1979, **104**, 1083.
15 Bruno, P., Caselli, M., Della Monica, M., and Di Fano, A., *Talanta*, 1979, **26**, 1011.
16 Gossman, B., *Collect. Czech. Chem. Commun.*, 1930, **2**, 185.
17 Cermak, V., *Collect. Czech. Chem. Commun.*, 1958, **23**, 1471.
18 Cermak, V., *Collect. Czech. Chem. Commun.*, 1958, **23**, 1871.
19 Jacobsen, E., and Sawyer, D. T., *J. Electroanal. Chem.*, 1967, **15**, 181.
20 Reynolds, W. L., and Yuan, Yu., *Polyhedron*, 1986, **5**, 1467.
21 Ciaccio, L. L., and Cotsis, T., *Anal. Chem.*, 1967, **39**, 260.
22 Humphrey, R. E., and Laird, C. E., *Anal. Chem.*, 1971, **43**, 1895.
23 Garber, R. W., and Wilson, C. E., *Anal. Chem.*, 1972, **44**, 1357.
24 Ribereau-Gayon, P., in *Chemistry of Winemaking*, ed. Webb, A. D., *Advances in Chemistry Series No.* 137, American Chemical Society, Washington, DC, 1974, p. 50.
25 Singleton, V. L., in *Wine Analysis*, eds. Linskens, H. F., and Jackson, J. F., Springer-Verlag, Berlin, 1988, p. 189.
26 Singleton, V. L., *Am. J. Enol. Vitic.*, 1987, **38**, 69.
27 Ough, C. S., in *Wine Analysis*, eds. Linskens, H. F., and Jackson, J. F., Springer-Verlag, Berlin, 1988, p. 111.

Paper 0/03798B
Received August 21st, 1990
Accepted October 30th, 1990

Differential-pulse Polarographic Determination of Copper and Iron in Biological and River-water Samples as Their *N*-Phenylbenzohydroxamic Acid Complexes by Gas-stirred Solvent Extraction With Ethyl Acetate

Y. Nagaosa and T. Menjyo
Faculty of Engineering, Fukui University, Bunkyo 3-9-1, Fukui 910, Japan
A. M. Bond
Division of Chemical and Physical Sciences, Deakin University, Geelong 3217, Victoria, Australia

A simple and rapid method for the simultaneous determination of Cu^{II} and Fe^{III} in biological and river-water samples has been developed. The method utilizes the extraction of metal–*N*-phenylbenzohydroxamic acid complexes into ethyl acetate, followed by direct determination by differential-pulse polarography (DPP) in the organic medium (1.5 ml). Two well defined DPP peaks appear at −0.17 and −0.59 V *versus* the Ag–AgCl reference electrode for Cu^{II} and Fe^{III}, respectively. Both the extraction and oxygen-removal steps in the analytical scheme can be performed by passing nitrogen through the two phases. This feature enhances the time efficiency and simplifies the method of solvent extraction with polarographic detection. Detection limits (signal to noise ratio = 3) are 20 ng ml^{-1} for Cu^{II} and 10 ng ml^{-1} for Fe^{III} in the original aqueous phase, and both DPP peak heights are directly proportional to metal concentrations in the aqueous phase of up to 10 μg ml^{-1}. Except for V^{V}, common metal ions examined do not interfere with the simultaneous determination of the two metal ions.

Keywords: *Differential-pulse polarography; copper; iron; solvent extraction; ethyl acetate*

Solvent extraction has been used extensively for both enrichment and, if required, separation of a desired analyte from an aqueous sample containing foreign substances[1,2] prior to subsequent instrumental analysis, by techniques such as atomic absorption spectrometry,[3] spectrophotometry[4,5] and voltammetry.[6] Unfortunately, solvent extraction normally requires the inherently tedious and time consuming procedures of stirring of the aqueous and organic phases and removal of the organic extract from the aqueous layer for the instrumental determination of the analytes of interest.

In order to improve analytical methods that utilize liquid–liquid extraction procedures, complete automation has been achieved by combining the flow-injection technique with continuous-flow extraction.[7–13] In this approach, in which solutions are transported by use of a pump, a segmented stream is introduced into an extraction coil, followed by a phase separation. The mixing of the two phases can be achieved by incorporating a magnetic stirrer in the continuous-batch extraction system. After phase separation, part of the organic phase is transferred into a flow cell for spectrophotometry or other instrumental method of determination.[14–16]

To date, various polarographic methods have been used as a detection method, following solvent extraction.[17–26] Unfortunately, electrochemical methods for the determination of reducible substances usually require the additional step of bubbling an inert gas through the test solution to eliminate interference from dissolved oxygen[27,28] In the course of our studies on extraction–polarography, we observed that the aqueous and organic phases can be stirred by use of a vigorous flow of nitrogen. With ethyl acetate as the organic solvent, both solvent extraction of analytes and de-oxygenation of the organic extract can be performed simultaneously in a single cell. Hence, the need to remove oxygen, normally considered to be a disadvantage, can actually be employed as part of the automated procedure. The proposed method of gas-stirred extraction followed by direct differential-pulse polarography (DPP) has some additional advantages: there is no need for removal of the organic extract (ethyl acetate) from the aqueous solution, and the volume of the two phases can be reduced to less than 10 ml. In this study, 2.0 ml of ethyl acetate and 4.0 ml of aqueous sample solution have been used in each experiment. Evaporative loss of organic solvent by the flow of nitrogen, which is a potential disadvantage, has been minimized by using solvent-saturated gas. Finally, the application of the method to the simultaneous determination of Cu^{II} and Fe^{III} in biological and river-water samples as their *N*-phenylbenzohydroxamic acid (PBA) complexes is presented.

Experimental

Apparatus

Differential-pulse and direct current (d.c.) polarograms were obtained with a Yanako (Kyoto, Japan) Y-1100 polarograph and recorded on a Rika-Denki (Tokyo, Japan) RW-11 *x–y* recorder. The DPP settings were as follows: drop time, 1 s; scan rate, 5 mV s^{-1}; modulation amplitude, −50 mV; sweep potential range, 0.0 to −1.0 V *versus* Ag–AgCl. The three-electrode system consisted of a dropping mercury working electrode with a mercury head height (h) of 65 cm, a platinum counter electrode and an Ag–AgCl (saturated KCl) reference electrode (Bioanalytical Systems, West Lafayette, IN, USA). The dropping mercury electrode had the characteristics of drop time (t) 7.72 s and flow-rate of mercury (m) 1.19 mg s^{-1} at h = 65 cm. Viscosity and conductivity measurements were effected with a TOP Model G-1790 (Tokyo, Japan) Ostwald viscosimeter and a Toa Denpa (Tokyo, Japan) Model CM-15A digital conductimeter. The laboratory-built cell for solvent extraction and polarographic determination is shown in Fig. 1.

Reagents

All the reagents used were of analytical-reagent grade. The water used was obtained from a Millipore (Bedford, MA, USA) water-purification system.

The Cu^{II} and Fe^{III} standard solutions (10 μg ml^{-1}) were prepared by diluting a certified 1000 μg ml^{-1} stock solution

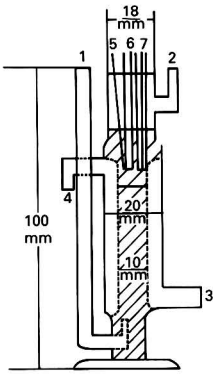

Fig. 1 Schematic diagram of the glass voltammetric cell used: 1, nitrogen inlet for gas-stirred extraction; 2, nitrogen inlet for protection from dissolution of oxygen; 3 and 4, water inlet and outlet for keeping the cell at 20 °C; 5, platinum counter electrode; 6, Ag–AgCl reference electrode; and 7, dropping mercury working electrode

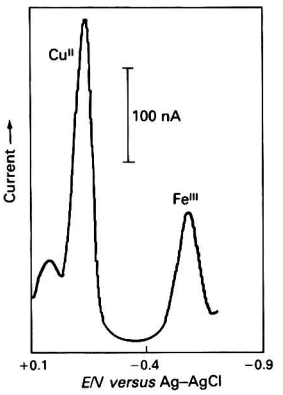

Fig. 2 Differential-pulse polarograms for reduction of Cu^{II}–PBA and Fe^{III}–PBA complexes in the ethyl acetate phase (0.1 mol dm^{-3} TBAP). Original Cu^{II} and Fe^{III} concentrations were each 1.0 μg ml^{-1} in the aqueous phase prior to extraction. Pulse amplitude, −50 mV; drop time, 1.0 s; for other parameters, see text

(Wako Chemicals, Tokyo, Japan) with the appropriate amount of water.

Acetate buffer solution (pH 5.9), 0.1 mol dm^{-3}, was prepared by mixing 0.1 mol dm^{-3} acetic acid and 0.1 mol dm^{-3} sodium acetate in a volume ratio of 1 : 4.

The extractant solution was prepared by dissolving 0.1 mol dm^{-3} tetrabutylammonium perchlorate (TBAP) (Fluka, Buchs, Switzerland) and 0.05 mol dm^{-3} PBA (Dojindo, Kumamoto, Japan) in ethyl acetate.

General Procedure for the Determination of Cu^{II} and Fe^{III}

The Cu^{II} and Fe^{III} standard solutions were made up in 2.0 ml of the acetate buffer solution and 2.0 ml of water. The 4.0 ml total volume of aqueous solution was placed in the polarographic cell (Fig. 1). A 2.0 ml portion of the extractant solution was then added to the aqueous solution in the cell. In order to complete the complex formation, the two phases were stirred with organic solvent-saturated nitrogen at a flow-rate of 60 ml min^{-1} for 30 s, and then the cell was allowed to stand for 5 min at 40 °C in a water-bath. After cooling, the temperature of the cell was maintained at 20 ± 0.1 °C by a thermostated water-circulating system (Fig. 1). Solvent-saturated nitrogen was passed through the two phases at a flow-rate of 60 ml min^{-1} for 5 min to remove oxygen, after which the differential-pulse polarogram was recorded in the organic phase.

Pre-treatment of Biological Samples

Each sample was analysed at least five times. Approximately 0.4 g of bovine liver or oyster tissue was weighed precisely and placed in a 250 ml beaker. An acid mixture, containing 10 ml of concentrated nitric acid, 5 ml of concentrated sulphuric acid and 10 ml of concentrated perchloric acid, was then added. The sample was decomposed with the acid mixture on a sand-bath at about 250 °C, by evaporating almost to dryness. After cooling, the residue was dissolved in 0.1 mol dm^{-3} acetate buffer, and the solution was transferred into a 100 ml calibrated flask and diluted with distilled water. A 4.0 ml portion of this solution was transferred with a pipette into the polarographic cell, together with 2 ml of ethyl acetate, for the determination. The above pre-treatment method ensures that all the Fe^{II} is oxidized to Fe^{III}, so that total iron is determined.

Pre-treatment of River-water Samples

The river water was filtered through a 0.45 μm Millipore filter immediately after sampling, then 100 ml of the filtrate were transferred with a pipette into a 250 ml beaker, and 1.0 ml of concentrated nitric acid was added. Any metal-bonded organics were decomposed by heating the solution at 100 °C until it was evaporated almost to dryness. The residue was dissolved in 0.1 mol dm^{-3} acetate buffer, and the solution was transferred into a 25 ml calibrated flask and diluted with distilled water. A 4.0 ml portion of this solution was transferred into the polarographic cell and the determination was undertaken as described above. As for the pre-treatment method for biological samples, total iron is determined when this pre-treatment is used on water samples.

Results and Discussion

Organic Solvents for Gas-stirred Extraction and Polarography

A range of organic solvents were investigated for liquid–liquid extraction, *via* a flow of nitrogen, followed by polarographic analysis of the extract. Slightly water-soluble solvents, such as ethyl acetate, propylene carbonate and nitromethane, lead to a moderate degree of emulsion being formed between water and the solvent when stirring takes place by means of a flow of nitrogen. Rapid phase separation takes place when the gas flow is stopped. This technique is referred to as 'gas-stirred solvent extraction'. Organic solvents, except highly non-polar ones, were polarographically usable when the organic solution contained a high concentration of supporting electrolyte. Ethyl acetate containing 0.1 mol dm^{-3} TBAP was chosen as the organic solvent in this work, because it afforded the greatest sensitivity for the polarographic determination of Cu^{II} and Fe^{III}, as their PBA complexes, after the gas-stirred solvent extraction. The organic solution containing 0.1 mol dm^{-3} TBAP had a specific conductivity of 0.25 mΩ^{-1} and a viscosity coefficient of 5.05 mP.

Polarograms of Metal–PBA Complexes in Ethyl Acetate

A number of metal ions, as their PBA complexes, were extracted into ethyl acetate, and the DPP measurement was carried out under the conditions described under Experimental. Of the metal species investigated, V^{V}, Cu^{II}, Fe^{III} and Mo^{VI} gave well defined DPP peaks at −0.05, −0.17, −0.59 and −0.98 V, respectively, *versus* Ag–AgCl (saturated KCl).

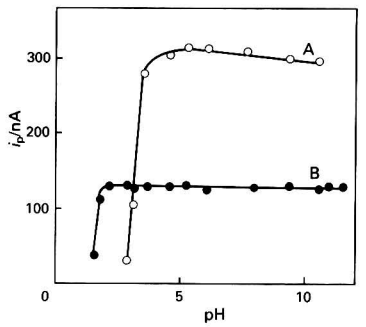

Fig. 3 Effect of pH on differential-pulse polarographic peaks for reduction of Cu^{II}–PBA and Fe^{III}–PBA complexes in the ethyl acetate phase. Experimental conditions as for Fig. 2. A, Cu^{II}; and B, Fe^{III}

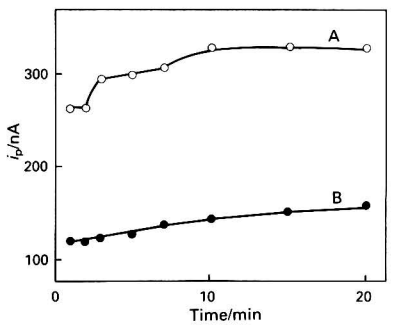

Fig. 4 Effect of the nitrogen flow-time on differential-pulse polarographic peaks for reduction of Cu^{II}–PBA and Fe^{III}–PBA complexes in the ethyl acetate phase. Experimental conditions as for Fig. 2. A, Cu^{II}; and B, Fe^{III}

Fig. 2 shows typical differential-pulse polarograms for the Cu^{II} and Fe^{III} complexes in the organic medium, indicating that the two peaks are sufficiently separated to allow determination of both metal ions simultaneously. Further, the background current is negligibly low over the relevant potential range from −0.10 to −0.95 V *versus* Ag–AgCl. The V^{V}–PBA complex showed one DPP reduction peak at −0.05 V *versus* Ag–AgCl, which partly overlapped the oxidation wave of the ligand. The Mo^{VI} complex also gave a sharp polarographic peak at −0.98 V *versus* Ag–AgCl when extracted from acidic solutions. Accordingly, the above four metal ions can be determined simultaneously by the proposed method. It was found that the limiting current of the reduction d.c. polarographic waves of the Cu^{II} and Fe^{III} complexes exhibited diffusion-controlled behaviour. The apparent diffusion-current constants (I), $I = id/cm^{\frac{2}{3}}t^{\frac{1}{6}}$, where id is the diffusion current and c is the concentration of the metal, were 6.34 and 3.65 μA $mg^{-\frac{2}{3}}$ $s^{-\frac{1}{2}}$ dm^3 $mmol^{-1}$ for Cu^{II} and Fe^{III}, respectively, which suggests that the reduction of Cu^{II} is a two-electron process producing Cu(amalgam), whereas the reduction of Fe^{III} is a one-electron process generating Fe^{II}. However, the slopes of a plot of $\log[i/(id - i)]$ *versus* E, where i denotes the measured value of d.c. for an applied potential E, were 53 and 82 mV for Cu^{II} and Fe^{III}, respectively, indicating that the processes are not reversible.

Effect of the Experimental Variables

The effects of changing the pH of the aqueous phase, the standing time for complex formation, and the flow time of nitrogen gas were examined in order to optimize the polarographic determination of Cu^{II} and Fe^{III} after extraction with ethyl acetate.

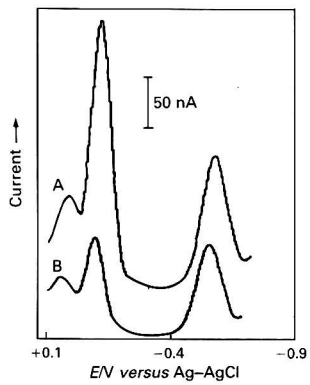

Fig. 5 Simultaneous determination of Cu and Fe in A, NIST SRM 1577 Bovine Liver; and B, NIST SRM 1566 Oyster Tissue. Sample pre-treatment and experimental conditions are as described under Experimental

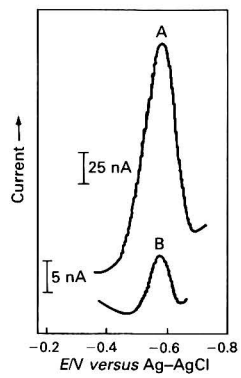

Fig. 6 Determination of Fe in a river-water sample. A, Sample was treated with nitric acid without filtration; B, sample was filtered through a 0.45 μm membrane filter and treated with nitric acid. Other conditions are as described under Experimental

The DPP peak currents for the reduction of Cu^{II} and Fe^{III} in the ethyl acetate phase were found to be almost constant over the pH ranges 4.5–10.5 and 2.0–11.0, respectively, as shown in Fig. 3. From these results, a pH of 5.0 was chosen to be a suitable pH for the aqueous phase. It was observed that DPP peak potentials (E_p) were shifted to a more negative direction when the pH was increased, but a plot of E_p *versus* pH was not linear.

The metal–PBA complexes must be formed completely in the aqueous phase, prior to extraction. The standing time of the solution prior to extraction was varied from 1 to 30 min at 40 °C. Data indicate that the DPP peak currents obtained at this temperature were almost constant for both metal ions at any standing times longer than 1 min. In contrast, complex formation at the lower temperature of 20 °C was incomplete, particularly in the presence of large amounts of foreign ions, for standing times up to 30 min. It is, therefore, recommended that the two phases be allowed to stand for 5 min at 40 °C, after which time they are allowed to cool to 20 °C prior to the polarographic determination.

The effect of nitrogen flow time on peak currents of the cooled 20 °C solution was investigated at a constant nitrogen flow-rate of 60 ml min^{-1}. A moderate degree of emulsion of the two phases was observed to occur during this stage of the experiment. It is clear from the data shown in Fig. 4 that both the quantitative extraction of the PBA complexes and removal of dissolved oxygen in the ethyl acetate phase were simultaneously achieved with a nitrogen flow time of 3–5 min. After

this time interval, reproducible differential-pulse polarograms could be recorded. As ethyl acetate has a relatively large vapour pressure of 92 Torr at 25 °C,[29] the DPP peak current gradually increases at excessively long flow times as evaporation takes place (see Fig. 4). The nitrogen flow time was restricted to 5 min in order to avoid loss of the organic phase, with the knowledge that, after this period, an apparently higher result will be obtained.

On the basis of the above experimental results, the conditions for the determination of Cu^{II} and Fe^{III} were fixed as described under Experimental.

Calibration Graphs

Calibration graphs for the determination of Cu^{II} and Fe^{III} were prepared according to the general procedure described under Experimental. Linearity was obtained between DPP peak current and each metal concentration up to 10 μg ml^{-1} (aqueous phase), with the correlation coefficients being 0.9996 for Cu^{II} and 0.9999 for Fe^{III}. The detection limits (signal to noise ratio = 3) were 20 ng ml^{-1} for Cu^{II} and 10 ng ml^{-1} for Fe^{III}.

Effect of Foreign Ions

The selectivity of the method was tested by studying the effect of foreign ions on the determination of 5 μg of both Cu^{II} and Fe^{III}. Calcium(II), Al^{III}, Ni^{II}, Pb^{II}, Bi^{III}, Mn^{II}, Sn^{IV}, Sb^{III}, Ti^{IV}, Se^{IV}, Zn^{II}, Co^{II}, As^{III}, U^{VI} and Mo^{VI} did not interfere with the simultaneous determination of the two metal ions when added at the 500 μg level. Vanadium(v) interfered, *via* overlap with the Cu response, even when present at the 0.5 μg level. Magnesium nitrate, sodium chloride, ammonium chloride, sodium bromide, ammonium sulphate and ammonium acetate (10 mg of each) had no effect on the determination. It is, therefore, concluded that the method can be applied to biological and river-water samples when Cu and Fe are known to be major components and the vanadium concentration is relatively low.

Analytical Applications

The applicability of the proposed method was evaluated by the determination of Cu and Fe in two samples of biological origin. Fig. 5 shows the differential-pulse polarograms obtained for the determination of Cu and Fe in National Institute of Standards and Technology (NIST), Standard Reference Materials (SRMs) 1577 Bovine Liver (curve A) and 1566 Oyster Tissue (curve B). The results were: Cu, 184 ± 6 ppm (certified value, 193 ± 10 ppm); and Fe, 257 ± 5 ppm (268 ± 8 ppm) for SRM 1577; and Cu, 63.7 ± 4.9 ppm (63 ± 3.5 ppm); and Fe, 193 ± 16 ppm (195 ± 34 ppm) for SRM 1566. It is concluded that, from comparison of the certified values shown in parentheses, the two biological samples could be successfully analysed for Cu and Fe by the proposed method.

Sokobami river water (Fukui city, Japan) was pre-treated and analysed for Fe according to the procedure described under Experimental. When the river-water sample was filtered through a 0.45 μm membrane filter, the Fe concentration was determined to be 18.6 ± 0.8 ng ml^{-1} after ten replicate analyses (see Fig. 6B). This value is considered to correspond to the dissolved Fe concentration in the river-water sample. On the other hand, the Fe concentration was found to be 265 ± 29 ng ml^{-1} when the sample was examined immediately after collection, but without filtration (see Fig. 6A). This difference between the two determinations indicates that the Fe in the river-water sample was mostly present in components larger in size than 0.45 μm. In the proposed method, the total Fe is determined because the Fe^{II} in the water sample solution is oxidized to Fe^{III} through the pre-treatment procedure. The concentration ratio of Fe^{III} to Fe^{II} in the water sample solution is, therefore, not known. The Cu concentration could not be determined by the method because it was too low.

References

1 Morrison, G. H., and Freiser, H., *Solvent Extraction in Analytical Chemistry*, Wiley, New York, 1957.
2 Minczewski, J., Chwastowska, J., and Dybczynski, R., *Separation and Preconcentration Methods in Inorganic Trace Analysis*, Ellis Horwood, Chichester, 1982.
3 Cresser, M. S., *Solvent Extraction in Flame Spectroscopic Analysis*, Butterworth, London, 1978.
4 Charlot, G., *Colorimetric Determination of Elements*, Elsevier, New York, 1964.
5 Sandell, E. S., and Onishi, H., *Photometric Determination of Traces of Metals. General Aspects*, Wiley, New York, 1978.
6 Zagorski, Z., and Cyrankowska, M., in *Advances in Polarography*, eds. Zuman, P., and Kolthoff, I. M., Pergamon Press, London, 1960, p. 584.
7 Foreman, J. K., and Stockwell, P. B., *Automatic Chemical Analysis*, Ellis Horwood, Chichester, 1975.
8 Furman, J. K., *Continuous Flow Analysis Theory and Practice*, Marcel Dekker, New York, 1976.
9 Růžička, J., and Hansen, E. H., *Flow Injection Analysis*, Wiley, New York, 1981.
10 Karlberg, B., and Thelander, S., *Anal. Chim. Acta*, 1978, **98**, 1.
11 Castro, M. D., *J. Autom. Chem.*, 1986, **8**, 56.
12 Shelly, D. C., Roassi, T. M., and Warner, I. M., *Anal. Chem.*, 1982, **54**, 87.
13 Bengtsson, M., and Johansson, G., *Anal. Chim. Acta*, 1984, **158**, 147.
14 Atallah, R. H., Růžička, J., and Christian, G. D., *Anal. Chem.*, 1987, **59**, 2909.
15 Dietz, M. L., and Freiser, H., *Anal. Chem.*, 1987, **59**, 2444.
16 Miyazaki, A., Tao, H., Kimura, A., and Bansho, K., *Anal. Sci.*, 1987, **3**, 583.
17 Fujinaga, T., Brodowsky, H., Nagai, T., and Yamashita, K., *Rev. Polarogr. (Kyoto)*, 1963, **11**, 217.
18 Kambara, T., and Hasebe, K., *Bunseki Kagaku*, 1965, **14**, 491.
19 Afghan, B. K., Dagnall, R. M., and Thompson, K. C., *Talanta*, 1966, **13**, 1097.
20 Kitagawa, T., and Ichimura, A., *Bunseki Kagaku*, 1973, **22**, 120.
21 Fujinaga, T., and Puri, B. K., *Talanta*, 1975, **22**, 71.
22 Fujinaga, T., and Nagaosa, Y., *Chem. Lett.*, 1978, 587.
23 Nagaosa, Y., *Talanta*, 1979, **26**, 987.
24 Nagaosa, Y., *Anal. Chim. Acta*, 1980, **120**, 279.
25 Nagaosa, Y., *Fresenius Z. Anal. Chem.*, 1983, **316**, 794.
26 Nagaosa, Y., and Kobayashi, K., *Talanta*, 1984, **31**, 593.
27 Kolthoff, I. M., and Lingane, J. J., *Polarography*, Interscience, New York, 2nd edn., 1952.
28 Bond, A. M., *Modern Polarographic Methods in Analytical Chemistry*, Marcel Dekker, New York, 1980.
29 Riddick, J. A., and Bunger, W. B., in *Organic Solvents*, ed. Weissberger, A., Wiley, New York, 3rd edn., 1970, pp. 279–280.

Paper 0/00748J
Received February 19th, 1990
Accepted October 24th, 1990

Fractional Determination of Ionizable and Stable Forms of Inorganic Mercury in Animal Tissue Using Atomic Absorption Spectrometry

Katsutoshi Suetomi and Hitoshi Takahashi
Department of Pharmacology, Institute for Medical Immunology, Kumamoto University Medical School, Kumamoto 860, Japan

Tetsuro Konishi
Kumamoto Municipal Institute of Public Health, 269 Tainoshima, Tamukaemachi, Kumamoto 862, Japan

A method for the determination of ionizable inorganic mercury in animal tissue has been developed. The method can be used to determine the amounts of both ionizable (toxic) and stable (non-toxic) inorganic mercury in tissue, when used in combination with a previous method for the direct determination of total inorganic mercury. The release of ionizable inorganic mercury from tissue proteins using sodium chloride in a solution of high ionic strength was followed by vaporization, amalgamation and atomic absorption spectrometry. The limit of detection is 0.6 ng of Hg and the relative standard deviation for 50 ng of Hg in the form of $HgCl_2$ is 0.9%. The application of the proposed method to the determination of mercury in tissue is also described.

Keywords: *Ionizable inorganic mercury determination; stable inorganic mercury; mercury–sulphur complex; mercury–selenium complex; mercury in tissue*

The existence of a stable form of inorganic mercury is evident in the tissues of animals some time after exposure to inorganic and organic mercury compounds. However, no method has been available to determine the amounts of such a stable form of inorganic mercury in tissue. A previously published method,[1] which determines directly all the inorganic mercury in biological materials, regardless of the presence of organic mercury, is used. Thus, it was thought that it should be possible to measure the stable form of inorganic mercury if a method for the determination of only the ionizable form of inorganic mercury could be developed. Such a method should be useful in providing an understanding of the toxicity of inorganic mercury remaining for a long period of time in the body of the animal after exposure to mercury compounds.

It is known that the administration of selenium with mercury(II) chloride delays the excretion of mercury from the body of an animal,[2,3] suggesting the interaction of selenium and mercury. As rats injected with a large amount of mercury(II) sulphide or mercury(II) selenide survived for a long period of time without developing toxicity symptoms, it was tentatively decided that HgS and HgSe were the stable inorganic mercury compounds in tissue.

In the present paper a method for the determination of only ionizable inorganic mercury in tissue without the decomposition of HgS, HgSe or methylmercury is described. By using this method in combination with the previous method,[1] by which all the inorganic mercury in tissue is determined, it is possible to estimate the stable portion of inorganic mercury such as HgS, HgSe or other similar mercury compounds. In order to demonstrate the reliability of the method, it is applied to a study of the formation of stable inorganic mercury in animals and to the mechanism of its formation.

Experimental

Apparatus

A similar apparatus to that used in the method of Konishi and Takahashi[1] was used except for the cooling system of the reaction flask.

Reagents

Sodium chloride (Wako Pure Chemical, Japan).
Sulphuric acid (Wako Pure Chemical).
Mercury(II) chloride (Katayama Chemical, Japan).
Methylmercury chloride (Merck, Darmstadt, Germany).

All other chemicals used were of analytical-reagent grade and glass-distilled, de-ionized water was used for preparing the solutions.

Gold-coated Celite for amalgamation. Gold(III) chloride (2 g) was added to 15 g of acid-washed Celite-545 (30–60 mesh) (Johns–Mansville, Denver, CO, USA) with sufficient water to make a slurry. The mixture was dried and ignited in a muffle furnace at 600 °C for 1 h.

Mercury(II) standard solution (1 μg ml^{-1} of Hg). Prepared by a 500-fold dilution of a stock solution of mercury(II) chloride (0.5 mg ml^{-1} of Hg) before use.

Mercury(II) sulphide solution (1 μg ml^{-1} of Hg). Prepared by passing pure hydrogen sulphide gas through the working mercury(II) standard solution in the reaction flask.

Mercury(II) selenide solution (1 μg ml^{-1} of Hg). Prepared by passing hydrogen selenide gas, which was prepared from aluminium selenide (Kojundo Chemical Laboratory, Saitama, Japan) according to the method described,[4] through the working mercury(II) standard solution.

All the gas, H_2S or H_2Se, was completely driven out by flushing with N_2 gas.

Methylmercury standard solution (1 μg ml^{-1} of Hg). Prepared by a 500-fold dilution of a stock solution of methylmercury chloride (0.5 mg ml^{-1} of Hg) before use.

Procedures

Procedure I for the determination of total mercury

Total mercury determination was carried out using electrothermal atomic absorption spectrometry in combination with gold amalgamation after digestion with H_2SO_4, HNO_3 and V_2O_5 and then reduction with $SnCl_2$.

Procedure II for the determination of total inorganic mercury

The determination was carried out according to the method of Konishi and Takahashi[1] using H_2O_2 as the reducing agent, except that the concentration of the potassium cyanide solution was increased to 1% m/v.

Procedure III for the determination of ionizable inorganic mercury

Ionizable inorganic mercury was released from tissue proteins as follows: 50 ml of 0.30 mol dm^{-3} H_2SO_4 and 50 ml of 5

mol dm^{-3} NaCl were added to an aliquot of the tissue homogenate previously placed in a 200 ml flask and mixed thoroughly. Then, 10 ml of 50% v/v H_2SO_4 and 1–3 drops of silicone antifoam emulsion were added. After careful addition of 10 ml of 10% m/v $SnCl_2$ (dissolved in approximately 2 mol dm^{-3} H_2SO_4) to the mixture, the reaction flask was immediately connected to the apparatus and purged under a continuous stream of nitrogen in order to vaporize the mercury. After 30 min, all of the vaporized mercury was amalgamated on a gold trap and the mercury was then released from the trap by rapid heating to 700 °C in the furnace; the furnace was usually air-cooled rapidly for the next application. The vaporized mercury was determined by electrothermal atomic absorption spectrometry at 253.7 nm.

Addition of 50 ml of 0.30 mol dm^{-3} sulphuric acid was used to facilitate the release of ionizable inorganic mercury from tissue proteins by sodium chloride and also to avoid the adsorption of released mercury onto the wall of the flask. The peak height of the mercury reached a maximum within 30 s and a very sharp peak was obtained by preconcentration on the gold trap. Loss of mercury owing to its adsorption on the new silicone–rubber stopper and Tygon tubing was noticeable on initial use, but was negligible after several assays. The relationship between the three procedures is shown in Fig. 1.

Animal Treatment and the Preparation of Tissue Homogenates for a Test

Animal treatment I

Nine Wistar male rats were fed on the ordinary diet Labo MR Stock (Nihon Nosan Kogyo K. K., Yokohama, Japan) during the experiment starting from 7 weeks old. All the rats were treated with a subcutaneous injection of 1 mg kg^{-1} of Hg in the form of $HgCl_2$ for two successive days, and divided into three groups. Each group of three rats was sacrificed 1, 7 or 14 d after the last $HgCl_2$ injection.

Animal treatment II

In order to study the effect of dietary sulphur and selenium on the formation of stable inorganic mercury, three groups of 3 week old rats ($n = 12$) were fed on each of three different experimental diets (Nihon Nosan Kogyo K. K., Yokohama, Japan) for 5 weeks. The diets were prepared using Torula yeast (Oriental Yeast, Tokyo, Japan) as the protein source, which contained low concentrations of sulphur and selenium. As shown in Table 1, the control diet (CD) was supplemented with selenium as Na_2SeO_3 in preparing the selenium supplemented diet (SeSD) or with L-methionine to prepare the sulphur supplemented diet (SSD). At 8 weeks old, the rats were injected subcutaneously with 1 mg kg^{-1} of Hg in the form of $HgCl_2$ for two successive days. Half of the rats in every three groups were sacrificed by deep ether anesthesia on the first day and the remainder 14 d after the last injection of $HgCl_2$.

Animal treatment III

In an additional experiment to show the effect of supplementation of sulphur on the formation of stable inorganic mercury, the rats being fed the CD were treated with parenteral rather than dietary supplementation of sulphur, using cysteine instead of methionine. The 3 week old rats were fed the CD for 5 weeks. At 8 weeks old these rats were given supplementary sulphur by an intraperitoneal injection of L-cysteine (250 mg kg^{-1}) daily for 15 d, starting from the first day of $HgCl_2$ injection until the day before the animal was sacrificed.

As soon as the rats expired, they were immediately perfused through the heart with a cold 0.9% m/v saline solution in order to flush out blood from the body. Then, the brain, liver and kidneys were removed. Homogenates of the organs at concentrations from 0.2 to 10% were prepared with distilled, de-ionized water using a polytetrafluoroethylene homogenizer. The sample volume was chosen so that each sample contained less than 100 ng of the total inorganic mercury.

Statistical Analysis

All data are reported as the mean ± standard deviation (SD). Significance between two groups was calculated using the Student's *t*-test. For the investigation of significance among three groups, the data were analysed by a one-way analysis of variance. When the analysis indicated that a significant difference existed, the groups of rats sacrificed 7 or 14 d after the last $HgCl_2$ injection were compared with the group of rats sacrificed 1 d after the last $HgCl_2$ injection by Duncan's multiple range test.[5] As there were unequal variances in some of the data, it was necessary to use the non-parametric Kruskal–Wallis test[6] followed by the appropriate multiple comparison test.

Results

Test Studies on the Determination of Ionizable Inorganic Mercury

In Fig. 2, the curves A and B show the time courses of mercury vaporization by the proposed method from sample solutions containing 50 ng of Hg in the form of $HgCl_2$ with and without 1.0 ml of 10% rat liver homogenate, respectively. The vaporization with and without liver homogenate appeared to be complete within 20 and 7 min, respectively. Therefore, in order to ensure complete vaporization a time of 30 min was chosen for the passage of nitrogen.

When sample solutions containing 0–100 ng of Hg as $HgCl_2$ were analysed by the proposed method, a good linear relationship was obtained. The blank value which is the amount of mercury present in the carrier gas and the reagents used in the analysis was 0.9 ± 0.2 ng. Assuming that the limit of detection is three times the value of the SD of the blank

Table 1 Compositions of three different diets (CD, SeSD and SSD)

Ingredient	CD (%)	SeSD (%)	SSD (%)
Torula yeast	30.0	30.0	30.0
Sucrose (fine granule)	50.0	50.0	48.8
Corn starch	8.2	8.2	8.2
Lard	5.0	5.0	5.0
Cod-liver oil	2.0	2.0	2.0
Vitamin mixture	1.0	1.0	1.0
Mineral mixture*	3.5	3.5	3.5
L-Methionine	0.3	0.3	1.5

* The final selenium concentrations of three diets were adjusted to be 0.04, 0.40 and 0.04 μg g^{-1} by adding Na_2SeO_3 to the mineral mixtures.

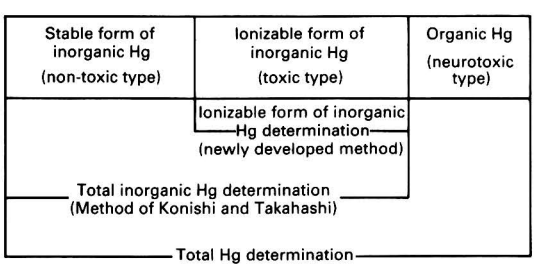

Fig. 1 Analyses for different forms of mercury in tissue

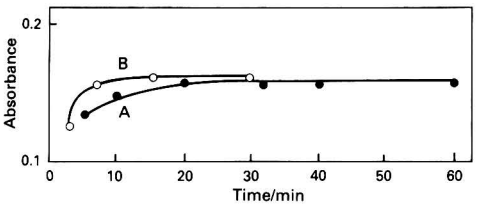

Fig. 2 Time courses for the vaporization of mercury from $HgCl_2$ with or without liver homogenate. A, 50 ng of Hg from $HgCl_2$ with 1 ml of 10% liver homogenate; and B, 50 ng of Hg from $HgCl_2$ without liver homogenate. Each point represents the mean of duplicate determinations

Table 2 Recoveries of ionizable inorganic Hg by the proposed method from four liver samples (0.3 g)* with the addition of $HgCl_2$, HgS, HgSe or MeHgCl

Form of Hg added	Hg content/ ng	Hg found†/ ng	Recovery (%)
$HgCl_2$	50	49.9	99.8
HgS	1000	13.6	1.4
HgSe	1000	0.7	0.1
MeHgCl	1000	5.6	0.6

* Ionizable inorganic Hg found in 0.3 g of liver was 0.01 ng.
† Mean of three determinations.

value, it is considered to be 0.6 ng. A good reproducibility of the recovery of ionizable inorganic mercury from the sample solutions was also obtained and the relative standard deviation was 0.9%.

Recovery of Known Amounts of Mercury Added in Various Forms to the Tissue Homogenate

The recovery of Hg from the tissue homogenates after the addition of 50 ng of Hg as mercury(II) chloride, 1000 ng of Hg as mercury(II) sulphide, 1000 ng of Hg as mercury(II) selenide or 1000 ng of Hg as methylmercury chloride was determined. Almost 100% of ionizable inorganic mercury from mercury(II) chloride could be recovered, but only negligible amounts of the other three mercury compounds, as shown in Table 2.

The maximum amount of tissue that could be tested using the present apparatus was about 0.5 g.

Demonstration of the Reliability of the Method for the Determination of Ionizable Inorganic Mercury in Rat Tissues Treated With Mercury(II) Chloride

As shown in Fig. 3, the ratio of stable inorganic to total inorganic Hg, expressed as a percentage, in all of the three tissues taken from the rats, described under Animal treatment I, was almost 0% 1 d after the last injection of mercury(II) chloride. This indicated that the ionizable inorganic mercury in the rat tissues investigated was determined completely using this method. However, this percentage increased in the liver and tended to increase further with time. Only a very small increase was observed in the brain and there was no evident increase in the kidney 14 d later.

The ratio of stable inorganic Hg to total inorganic Hg, as a percentage, in the three rat tissues described under Animal treatment II, is shown in Fig. 4. Almost no increase in this percentage was observed in the tissues of the rats fed on CD and no significant increase in those of rats fed on SSD after 2 weeks. On the contrary, stable inorganic mercury showed a tendency to increase in the rats fed on SeSD, especially in the liver. The parenteral administration of sulphur as L-cysteine facilitated the formation of stable inorganic mercury in the liver of the rats fed on CD.

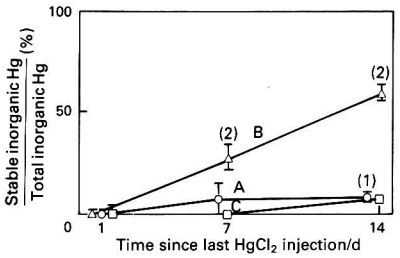

Fig. 3 Stable form of inorganic Hg found in the organs of rats ($n = 3$) fed on a stock diet. The $HgCl_2$ (1 mg kg^{-1} of Hg) was subcutaneously injected for two successive days. (Each point = duplicate determinations ± SD.) A, Brain; B, liver; and C, kidney. Numbers indicate significant differences, by using the multiple range test of Duncan, from the values found in the rats sacrificed 1 d after the last $HgCl_2$ injection. (1), $p < 0.05$ and (2), $p < 0.01$

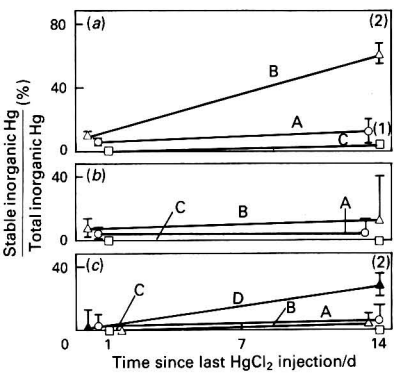

Fig. 4 Effect of supplementation of either S or Se on the formation of stable inorganic Hg in the rat organs ($n = 6$). The $HgCl_2$ was subcutaneously injected for two successive days. (Each point = duplicate determinations ± SD.) (*a*), Se supplemented diet (SeSD); (*b*), sulphur supplemented diet (SSD); and (*c*), control diet (CD). A, Brain; B, liver; C, kidney; and D, liver of rats fed CD and supplemented S by an intraperitoneal injection of L-cysteine (250 mg kg^{-1}) daily for 15 d, starting from the first day of $HgCl_2$ injection to the day before sacrifice. Numbers indicate significant differences, by the Student's *t*-test, from the values found in the rats sacrificed 1 d after the last $HgCl_2$ injection. (1), $p < 0.01$ and (2), $p < 0.001$

The results for the amount of total mercury agreed well with those obtained for the determination of total inorganic mercury in the tissue, by the method of Konishi and Takahashi,[1] indicating that no organic mercury was present.

Discussion

Several workers[7–9] showed that selenium reduced the toxicity of mercury in the simultaneous administration of selenium and mercury, although the retention of both elements increased in the organs. This suggested that the stable form of inorganic mercury might be formed by the interaction of mercury and selenium. There have been reports[1,10] concerning the direct determination of inorganic mercury in biological samples regardless of the presence of organic mercury, but to date no method has been available for the fractional determination of ionizable and stable forms of inorganic mercury in biological specimens. Therefore, a method for the determination of ionizable inorganic mercury in animal tissues without decomposing stable inorganic mercury or organic mercury has been developed.

Strong acid hydrolysis or alkali digestion, used to release mercury from tissue proteins, resulted in the decomposition of the stable form of inorganic mercury such as HgS or HgSe into the ionic form. Thus, another method for the release of

ionizable inorganic mercury from tissue proteins was investigated. A sodium chloride solution of high ionic strength was used to release the ionizable inorganic mercury from tissue proteins, especially under acidic conditions and proved to be satisfactory. As shown, ionizable inorganic mercury was recovered completely from the $HgCl_2$ added, but negligible amounts were recovered from HgS, HgSe or CH_3HgCl. This shows that ionizable inorganic mercury can be determined separately from stable inorganic mercury and alkyl mercury. It appears that both HgS and HgSe are stable forms of inorganic mercury in tissues; the reasons are as follows. Firstly, when this method was applied to the tissues of the rats fed on a stock diet, almost all the inorganic mercury in the organs was in the ionizable form for a while after $HgCl_2$ treatment. However, the forms resistant to ionization increased in the organs, particularly in the liver, over a period of time after $HgCl_2$ injection. Secondly, the appearance of this form of mercury occurred much more slowly in the rats fed on CD containing the minimum requirement of S and Se, but it was hastened remarkably by the supplementation of the diet with Se but not remarkably with S. However the injection of L-cysteine accelerated the formation of stable inorganic mercury in the rats fed on CD. This result suggested that sulphur might be another factor influencing the formation of stable inorganic mercury.

Satake *et al.*[11] found the accumulation of particles which were likely to be HgS, in liverwort collected from a stream in Aomori, Northern Japan. The presence of an Hg–Se complex with a molar ratio of 1 : 1 was suggested in the organs of the animals administered mercury and selenium simultaneously,[12–14] and the presence of a similar complex was suggested in the organs of mercury miners.[15] The method may be applicable to these studies.

In summary, the proposed method, which determines the ionizable form of inorganic mercury in animal tissue, can be used to determine stable coexisiting forms of inorganic mercury, by combining it with the previous method[1] for the measurement of total inorganic mercury. These methods may be useful for studying the mechanism of detoxification of mercury in animals and plants.

We thank Professor F. Kai and Dr. M. Nakamura, Faculty of Science, Kumamoto University, for their kind guidance in the preparation of hydrogen selenide.

References

1 Konishi, T., and Takahashi, H., *Analyst*, 1983, **108**, 827.
2 Eybl, V., Sykora, J., and Mertl, F., *Arch. Toxikol.*, 1969, **25**, 296.
3 Kristensen, P., and Hansen, J. C., *Toxicology*, 1979, **12**, 101.
4 *Inorganic Syntheses*, eds. Fernelius, W. C., Audrieth, L. F., Bailar, J. C., Jr., Booth, H. S., Johnson, W. C., Kirk, R. E., and Schumb, W. C., McGraw-Hill, New York, 1946, vol. II, p. 184.
5 Bliss, C. I., *Statistics in Biology*, McGraw-Hill, New York, 1970, pp. 365 and 580.
6 Campbell, R. C., *Statistics for Biologists*, Cambridge University Press, Cambridge, 1974, pp. 61–63.
7 Parizek, J., Ostadalova, I., Kalouskova, J., Babicky, A., and Benes, J., in *Newer Trace Elements in Nutrition*, eds. Mertz, W., and Cornatzer, W. E., Marcel Dekker, New York, 1971, p. 85.
8 Potter, S., and Matrone, G., *J. Nutr.*, 1974, **104**, 638.
9 Fang, S. C., *Chem. Biol. Interact.*, 1977, **17**, 25.
10 Magos, L., *Analyst*, 1971, **96**, 847.
11 Satake, K., Soma, M., Seyama, H., and Uchiro, T., *Arch. Hydrobiol.*, 1983, **99**, 80.
12 Burk, R. F., Foster, K. A., Greenfield, P. M., and Kiker, K. W., *Proc. Soc. Exp. Biol. Med.*, 1974, **145**, 782.
13 Wada, O., Yamaguchi, N., Ono, T., Nagahashi, M., and Morimura, T., *Environ. Res.*, 1976, **12**, 75.
14 Komiya, K., Koike, I., and Kawauchi, S., *Eisei Kagaku*, 1977, **23**, 244.
15 Kosta, L., Byrne, A. R., and Zelenko, V., *Nature (London)*, 1975, **254**, 238.

Paper 0/04363J
Received September 27th, 1990
Accepted November 14th, 1990

Facile Detection of Anatoxin-a in Algal Material by Thin-layer Chromatography With Fast Black K Salt

Ilkka Ojanperä and Erkki Vuori
Department of Forensic Medicine, University of Helsinki, Kytösuontie 11, SF-00300 Helsinki, Finland
Kimmo Himberg
Technical Research Centre of Finland, Food Research Laboratory, Biologinkuja 1, SF-02150 Espoo, Finland
Matti Waris
General Headquarters of the Finnish Defence Forces, Helsinki, Finland
Kauko Niinivaara
Department of Water Economy, University of Oulu, Oulu, Finland

A method for facile high-capacity screening of algal samples for anatoxin-a (ANTX-a), a potent neurotoxin of *Anabaena flos-aquae*, is presented. The method is based on *in situ* colour reaction of algal extracts containing ANTX-a on a thin-layer chromatographic plate with the diazonium reagent Fast Black K salt, and subsequent separation of the orange–red product. The product, shown to be a stable 3,3-dialkyltriazene, is derived from a reaction involving the aliphatic secondary amino group of ANTX-a. The detection limit for ANTX-a is 10 μg g^{-1} of lyophilized algal material, which is comparable to earlier methods using more complex instrumentation.

Keywords: *Anatoxin-a detection; Fast Black K salt; thin-layer chromatography; triazene;* Anabaena flos-aquae

Cyanobacteria or blue–green algae are able to produce several toxins that have caused animal poisonings world-wide and are also a risk to human health. The exotoxins excreted by some strains of cyanobacteria are either neurotoxins, hepatotoxins or dermatotoxins.[1] Anatoxin-a (ANTX-a) [see Fig. 1 (**1**)] is a neurotoxin, a depolarizing neuromuscular blocking agent produced mainly by *Anabaena flos-aquae*.[2,3] It is among the more potent of the natural toxins, having an acute intraperitoneal lethal dose (median) (LD_{50}) in many species of about 0.25 mg kg^{-1} and an oral LD_{50} from 1 to 10 mg kg^{-1}.[4]

Anatoxin-a is a bicyclic aliphatic secondary amine with an α,β-enone structure,[5,6] and a pK_a of 9.4.[7] Natural (+)-ANTX-a, with the seven-membered ring in the twisted-chair conformation and the conjugated enone part in the *S-cis* conformation,[7] fits the nicotinic acetylcholine receptor, being a more potent agonist than the (−)-enantiomer or acetylcholine.[8–10] Anatoxin-a is not susceptible to enzymic hydrolysis as it possesses no ester function.

Before the elucidation of the structure of the toxin, the only way of testing the toxicity of the suspected algal material was by mouse bioassay. Chemical analysis of ANTX-a has been performed by high-performance liquid chromatography,[11–13] thin-layer chromatography (TLC),[13] gas chromatography with electron-capture detection,[14] gas chromatography–mass spectrometry,[15–17] and mass spectrometry.[17] Many of these methods are specific and sensitive but not suited to routine screening for toxic blooms. However, fast, high-capacity screening of blooms is of vital importance particularly as the same bloom can be either toxic or non-toxic, depending on the location of sampling.

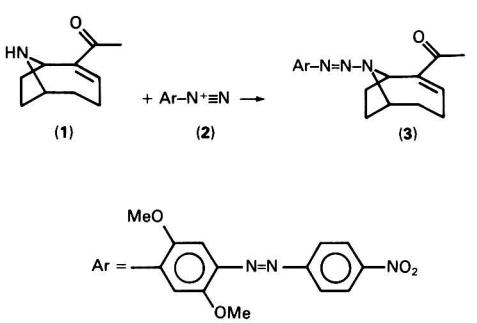

Fig. 1 Reaction between anatoxin-a (**1**) and Fast Black K salt (**2**) yielding a 3,3-dialkyltriazene (**3**)

In this paper, a facile method for the high-capacity screening of ANTX-a in algal material is described, based on a liquid–liquid extraction of sonicated cells, derivatization with Fast Black K salt (FBK) [Fig. 1 (**2**)],[18] and thin-layer chromatographic separation of the coloured product. The structure of the dye has been determined and spectroscopic data are given.

Experimental

Materials

The algal materials used in this study have been characterized earlier.[16] The algal standards were prepared by diluting lyophilized *Anabaena* containing 4.4 mg g^{-1} of ANTX-a with lyophilized *Aphanizomenon*, which was used also as a blank sample.

The FBK and *N*-methyl-2-phenylethylamine were obtained from Aldrich (Milwaukee, WI, USA). The other chemicals were Merck analytical-reagent grade (Darmstadt, Germany). The thin-layer chromatographic plates were silica gel 60 F_{254} glass plates, with a layer thickness of 0.25 mm, also from Merck. A size of 20 × 10 cm was used. The developments were carried out in a twin-trough chamber for 20 × 10 cm plates from Camag (Muttenz, Switzerland).

Apparatus

The centrifugal evaporator was a Howe Gyrovap GV 2 (London, UK) equipped with a Vacuubrand ME 2C diaphragm pump (Wertheim, Germany).

Ultraviolet–visible spectra, in methanol, were recorded with a Hitachi (Tokyo, Japan) U-2000 spectrophotometer using 1 cm quartz cuvettes.

Proton nuclear magnetic resonance (^1H NMR) spectra, in $CDCl_3$, were recorded with a Varian (Palo Alto, CA, USA) Gemini-200 Fourier transform NMR spectrometer, using a standard ^1H–^{13}C dual probe.

Mass spectra and high-resolution mass spectra were recorded with a Jeol (Tokyo, Japan) JMS SX102 spectrometer, using a direct inlet probe and an electron energy of 70 eV. The sample temperature was about 250 °C.

Sample Preparation

For the investigation of the derivatization reaction, methanolic solutions containing 0.01–1 mg ml^{-1} of *N*-methyl-2-phenylethylamine were prepared and 1 μl volumes were applied to the plate.

For the extraction of ANTX-a, a 100 mg amount of lyophilized algae was suspended in 5 ml of purified water and, after adjusting the pH to 2.5 with dilute hydrochloric acid, the suspension was sonicated for 0.5 h. After centrifuging at 4000 *g* for 10 min, the clear blue–green supernatant was separated off and adjusted to pH 11–11.5 with dilute sodium hydroxide. The solution was extracted by gently shaking with 10 ml of dichloromethane–isopropyl alcohol (95 + 5) for 0.5 h and, after centrifuging at 4000 *g* for 10 min, the aqueous supernatant was aspirated to waste and the organic phase transferred into a conical test-tube. After evaporating to dryness in a centrifugal evaporator at 60 mbar and at 35 °C, the residue was reconstituted with 15 μl of chloroform and the whole volume applied to the TLC plate.

Detection

The extracts were overspotted with 2 μl of 0.5 mol dm^{-3} $NaHCO_3$ and, after drying, with 3 μl of a 1% aqueous solution of FBK. The plate was dried with a hot-air blower and developed for 5 cm with 20 ml of a toluene–methanol solution (90 + 10). Before development the chamber was allowed to saturate, whilst containing a piece of filter-paper, for 0.5 h.

Structure Determination

Sample preparation

The isolation of ANTX-a from 1.0 g of lyophilized *Anabaena* (ANTX-a, 4.4 mg g^{-1}) was performed as described above, but using 20 ml of purified water and 20 ml of the extraction solvent. The dry residue was dissolved in 200 μl of 0.5 mol dm^{-3} $NaHCO_3$, and 2 ml of 1% FBK were added. The mixture was shaken until precipitation ceased and the suspension extracted with 4 ml of dichloromethane. The organic phase was separated, washed with 2 ml of water, and evaporated to dryness. The procedure yielded 6 mg of a black solid material which, by TLC, was identified as fairly pure and identical with that obtained by derivatization on the plate.

Spectroscopic determinations

(1*R*)-2-Acetyl-9-({2,5-dimethoxy-4-[(*p*-nitrophenyl)azo]-phenyl}azo)-9-azabicyclo[4.2.1]non-2-ene [Fig. 1 (**3**)]. Ultraviolet: λ_{max} 476 nm (ε 18500). Proton NMR: δ (ppm) 1.45–2.65 (8H, m), 2.37 (3H, s), 3.89 (3H, s), 4.03 (3H, s), 4.75–4.95 (1H, broad s), 5.65 (1H, d), 6.65–6.80 (1H, broad s), 7.14 (1H, s), 7.41 (1H, s), 8.00 (2H, d), 8.35 (2H, d). Mass spectra: *m/z* 478 (78%) (M^+), 450 (45), 314 (83), 302 (33), 286 (22), 258 (100), 151 (58), 122 (87). High-resolution mass spectra: elemental composition $C_{24}H_{26}N_6O_5$ requires 478.1965, found 478.1959.

Results and Discussion

Detection of Anatoxin-a

The FBK derivative of ANTX-a appeared as an orange–red spot at R_f 0.42 on the developed TLC plate. The intensity of the spot was fairly linear within the concentration range tested, 10–100 μg g^{-1} of lyophilized algal material, the detection limit being 10 μg g^{-1}. There were no clear interfering spots in the vicinity of ANTX-a, but an intensive orange–red spot originating from *Aphanizomenon* appeared at R_f 0.25. The structure of this compound remained undetermined but was assumed to be a secondary aliphatic or aromatic amine.

The sensitivity of the method is comparable to the mass spectrometric assay by Himberg[16] who, starting with 20 mg of lyophilized algae, reported a limit of detection of 5 μg g^{-1}. Whereas in the current method the chromatographic background did not interfere at the R_f region of the ANTX-a derivative, an improvement in the detection limit could apparently be obtained by using a larger sample size or a more effective extraction method. The ANTX-a concentration of the natural blooms in Finland has been found to vary from 12 μg g^{-1} to 4.4 mg g^{-1} of lyophilized material.[19]

The post-chromatography derivatization technique can also be employed for the visualization of ANTX-a. The chromatographic plate was developed with an ethyl acetate–methanol–ammonia solution (85 + 10 + 5),[20] without chamber saturation. After spraying the plate with a 0.5% aqueous solution of FBK, ANTX-a appeared as an orange–red spot at R_f 0.27. The detection limit was 20 μg g^{-1} of lyophilized algal material. Spraying with the appropriate base did not improve the detection of ANTX-a owing to the visibility of the interfering background.

Derivatization Reaction

Fast Black K salt has been shown to be a sensitive TLC visualization reagent especially for aliphatic primary and secondary amines, producing a violet colour with primary and an orange–red or red colour with secondary amines when sprayed over the plate.[18] As the reaction with aliphatic secondary amines gives stable, defined products, pre-chromatographic derivatization can be used to improve the detection characteristics of this type of compound.

Spectroscopic determinations revealed the spot at R_f 0.42 to be the expected 3,3-dialkyltriazene [Fig. 1 (**3**)]. The mass spectrum (Fig. 2) shows the M^+ ion at *m/z* 478 and also shows the same type of fragmentation as has been observed earlier for triazenes derived from FBK:[18] the ions at *m/z* 450, 314, 286 and 258 probably correspond to $[M^+ - N_2]$, $[M^+ - RR'N]$, $[M^+ - RR'N_3]$ and $[M^+ - RR'N_5]$, respectively, the RR'N referring to the ANTX-a moiety. The ^1H NMR spectrum shows features characteristic to both FBK derivatives[18] and ANTX-a:[7] these include the two methoxy singlets at δ 3.89 and 4.03 ppm and the aromatic pattern at δ 7.14–8.35 ppm from FBK, and the acetyl singlet at δ 2.37 ppm from ANTX-a. The resonances at δ 4.75–4.95 and 5.65 ppm obviously correspond to the methine protons adjacent to a nitrogen in the ANTX-a moiety. They experience a downfield shift of about Δδ 1 ppm compared with the ANTX-a base,[7] whereas such a shift is not observed with the olefinic proton at δ 6.65–6.80 ppm.

The derivatization reaction was developed using *N*-methyl-2-phenylethylamine. The main factors governing the reaction on the chromatographic plate were the type and concentration of the added base and the order in which the reagents were applied. Without a base the yield was lower. Organic bases could not be used because of their reactivity with FBK. Sodium hydroxide and sodium carbonate were found to produce by-products even when used in low concentrations, whereas sodium acetate gave only a moderate yield even at a concentration of 5 mol dm^{-3}. Sodium hydrogen carbonate and disodium phosphate gave good yields. The optimum concentration of $NaHCO_3$ in relation to yield and by-products was 0.5 mol dm^{-3}.

The yield was improved when the base was applied before FBK. Heating the chromatographic plate on a hot-plate at 65 °C did not improve the yield, suggesting a rapid reaction.

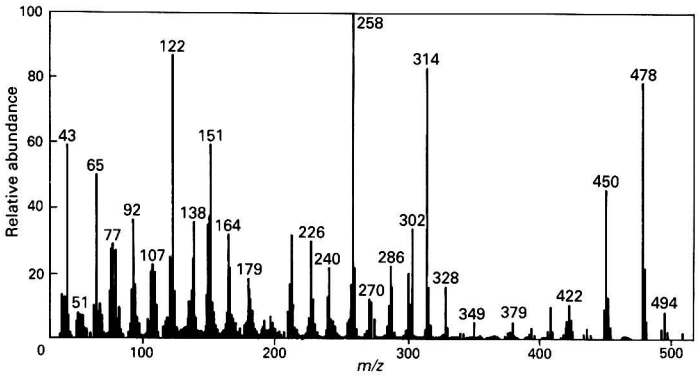

Fig. 2 Mass spectrum of the 3,3-dialkyltriazene (**3**)

The FBK was used in excess of the amine, and a 5-fold increase of the concentration did not significantly improve the yield but increased the background. The detection limit for *N*-methyl-2-phenylethylamine (R_f 0.6) was 0.02 μg.

Screening of Algal Blooms

In order to test the method with fresh algal material, samples were taken from a suspected algal bloom at Lake Tuusulanjärvi in southern Finland on August 20th, 1990. The samples were taken radially from the centre of the bloom towards clear water, and the amount of algal material in the most concentrated sample was approximately the same as that in the experiments with lyophilized algae. No pre-treatment was carried out but the 5 ml samples were prepared as described above. Because of the formation of an emulsion, probably owing to other algae, the most concentrated samples were not sonicated. The bloom was found to contain significant amounts of ANTX-a, with the concentration of the toxin decreasing going outwards from the centre of the bloom and falling below the detection limit in clear water.

Conclusions

The detection method presented for ANTX-a appears to be a good alternative to more laborious and expensive instrumental methods of analysis. It provides a means for fast, simultaneous, semi-quantitative screening of a multitude of algal samples in the investigation of suspected blooms. The pre-chromatographic derivatization with FBK is novel and this sensitive detection technique seems to be applicable to aliphatic secondary amines in general.

The authors thank K. Wähälä for cooperation and for running the NMR spectra, J. Matikainen for running the mass spectra and J. Vartiovaara who organized the screening of the fresh algal bloom for ANTX-a. This work was supported by a grant from the foundation Maa- ja vesitekniikan tuki r.y.

References

1 Carmichael, W. W., Jones, C. L. A., Mahmood, N. A., and Theiss, W. C., *CRC Crit. Rev. Environ. Control*, 1985, **15**, 275.
2 Carmichael, W. W., Biggs, D. F., and Gorham, P. R., *Science*, 1975, **187**, 542.
3 Carmichael, W. W., Biggs, D. F., and Peterson, M. A., *Toxicon*, 1979, **17**, 229.
4 Astrachan, N. B., Archer, B. G., and Hilbelink, D. R., *Toxicon*, 1980, **18**, 684.
5 Devlin, J. P., Edwards, O. E., Gorham, P. R., Hunter, N. R., Pike, R. K., and Stavric, B., *Can. J. Chem.*, 1977, **55**, 1367.
6 Huber, C. S., *Acta Crystallogr., Sect. B, Struct. Crystallogr. Cryst. Chem.*, 1972, **28**, 2577.
7 Koskinen, A. M. P., and Rapoport, H., *J. Med. Chem.*, 1985, **28**, 1301.
8 Spivak, C. E., Witkop, B., and Albuquerque, E. X., *Mol. Pharmacol.*, 1980, **18**, 384.
9 Swanson, K. L., Allen, C. N., Aronstam, R. S., Rapoport, H., and Albuquerque, E. X., *Mol. Pharmacol.*, 1986, **29**, 250.
10 Kofuji, P., Aracava, Y., Swanson, K. L., Aronstam, R. S., Rapoport, H., and Albuquerque, E. X., *J. Pharmacol. Exp. Ther.*, 1990, **252**, 517.
11 Astrachan, N. B., and Archer, B. G., in *The Water Environment: Algal Toxins and Health*, ed. Carmichael, W. W., Plenum Press, New York, 1981, p. 437.
12 Wong, S. H., and Hindin, E., *J. Am. Water Works Assoc.*, 1982, **74**, 528.
13 Harada, K.-I., Kimura, Y., Ogawa, K., Suzuki, M., Dahlem, A. M., Beasley, V. R., and Carmichael, W. W., *Toxicon*, 1989, **27**, 1289.
14 Stevens, D. K., and Krieger, R. I., *J. Anal. Toxicol.*, 1988, **12**, 126.
15 Smith, R. A., and Lewis, D., *Vet. Hum. Toxicol.*, 1987, **29**, 153.
16 Himberg, K., *J. Chromatogr.*, 1989, **481**, 358.
17 Ross, M. M., Kidwell, D. A., and Callahan, J. H., *J. Anal. Toxicol.*, 1989, **13**, 317.
18 Ojanperä, I., Wähälä, K., and Hase, T. A., *Analyst*, 1990, **115**, 263.
19 Sivonen, K., Himberg, K., Luukkainen, R., Niemelä, S. I., Poon, G. K., and Codd, G. A., *Toxic. Assess.*, 1989, **4**, 339.
20 Davidow, B., Li Petri, N., and Quame, B., *Am. J. Clin. Pathol.*, 1968, **50**, 714.

Paper 0/04516K
Received October 8th, 1990
Accepted November 9th, 1990

Simplified Method for the Determination of Organochlorine Pesticides in Honey

Miguel A. Fernández Muíño and Jesús Simal Lozano
Departamento de Química Analítica, Nutrición y Bromatología, Area de Nutrición y Bromatología, Facultad de Farmacia, Universidad de Santiago de Compostela, 15706 Santiago de Compostela, Spain

A method is described for the detection and quantitative determination of organochlorine pesticides in honey. After extraction with hexane, the pesticides were cleaned-up by adsorption chromatography on a Florisil Sep-Pak cartridge and eluted with 15% diethyl ether in hexane. The detection of organochlorine pesticides was performed by capillary gas chromatography with electron-capture detection. The quantification limit obtained for different pesticides ranged from 0.56 to 2.78 μg kg^{-1} and recoveries from fortified honey samples averaged 89.6%.

Keywords: *Organochlorine pesticide; honey; extraction; clean-up; capillary gas chromatography*

In recent years many methods have been utilized in order to detect residues of acaricides used for treatment against varroatosis[1–7] and other substances used for the treatment of diseases suffered by bees.[8–14] However, only a few methods have been published for the determination of organochlorine pesticides in honey although their presence has been demonstrated in several studies.[15–24]

Mueller[25] proposed a semi-quantitative method without a clean-up step for the determination of pesticide residues by use of thin-layer chromatography. Ogata and Bevenue,[15] Estep *et al.*[16] and Serra Bonvehí[22] used a classical method for determining pesticides in non-fatty foods involving extraction of organochlorine pesticides with an organic solvent, a clean-up step by liquid–liquid partitioning [NaCl(aq)–organic solvent], clean-up on a column (Florisil or silica), elution with two solvents of different polarity and analysis by gas chromatography (GC). Finally, Trevisani *et al.*[26] proposed a gas chromatographic multi-residue method for the study of residues from several groups of pesticides in agricultural products including honey. This method involves complicated clean-up steps that make it extremely slow.

This paper describes a method for the determination of organochlorine pesticides in honey which is much simpler and more rapid than those previously reported, as clean-up procedures were reduced to a minimum by eliminating the first clean-up step and using a Florisil Sep-Pak cartridge for the clean-up.

Experimental

Reagents and Solvents

Distilled water was purified by treating 1 l of water with 50 ml of hexane of pesticide residue analysis grade (Sharlau) in order to extract any organics present. Analytical-reagent grade diethyl ether was obtained from Probus and then distilled in an all-glass system. Anhydrous granular Na_2SO_4 for residue analysis was obtained from Merck. The solid-phase extraction column and Florisil Sep-Pak cartridge were obtained from Waters. Organochlorine pesticide standards (99% purity) were purchased from Alltech Associates. Stock solutions were prepared by dissolving the following organochlorine pesticides in hexane: lindane (5.5 μg ml^{-1}); heptachlor (11.4 μg ml^{-1}); aldrin (8.7 μg ml^{-1}); heptachlor epoxide (11.4 μg ml^{-1}); dieldrin (15 μg ml^{-1}); endrin (11.7 μg ml^{-1}); *p,p'*-DDT (4.5 μg ml^{-1}) and methoxychlor (14.5 μg ml^{-1}). All pesticide standards were weighed by using an analytical balance which could be read to within ±1 μg (Sartorius 2405 digital microbalance). Working solutions were prepared by mixing or diluting the stock solutions as required.

Apparatus

A Heraeus Christ Model Labofuge I centrifuge with speeds from 0 to 4700 rev min^{-1}, a Kuderna–Danish evaporator (500 ml capacity) fitted with a 5 ml calibrated glass tube, a Perkin-Elmer Series 8500 gas chromatograph equipped with a ^{63}Ni electron-capture detector, a split/splitless injector, a BP-1 capillary column (12 m × 0.22 mm i.d., 0.25 μm film thickness) and a Spectra-Physics 4270 integrator were used.

Procedures

Extraction

Honey (25 g) was dissolved in 50 ml of distilled water, which had been treated with hexane, in a 100 ml beaker and then extracted with 50 ml of hexane. A magnetic stirrer was used at low speed (200 rev min^{-1}) for 15 min. The contents of the beaker were transferred into a 250 ml separating funnel and the phases allowed to separate, centrifuging at 3000 rev min^{-1} for 10 min if necessary. The aqueous layer was transferred into a beaker and extracted with two further 25 ml portions of hexane. The combined organic extracts were dried over anhydrous sodium sulphate and evaporated to 1 ml in a Kuderna–Danish evaporator fitted with a 5 ml calibrated glass tube.

Clean-up

The concentrated extract was loaded onto a Florisil Sep-Pak cartridge, pre-rinsed with 10 ml of hexane, and the calibrated tube was washed with hexane (2 × 1 ml) which was also loaded onto the cartridge. The hexane effluent from the cartridge was discarded during rinsing and loading.

Pesticides were eluted from the cartridge with 15% diethyl ether in hexane, collecting the eluate (4 ml) in a calibrated test-tube after which it was ready for gas chromatographic analysis.

Gas chromatographic analysis and quantification

A 1 μl volume of eluate was chromatographed under the following conditions: injector, 250 °C; detector, 250 °C; initial temperature of the column, 50 °C held for 1 min and programmed at 20 °C min^{-1} from 60 to 175 °C and at 3 °C min^{-1} from 175 to 240 °C; carrier gas, nitrogen at 0.5 ml min^{-1}; split valve, 22 ml min^{-1}; purge valve, 2 ml min^{-1}; make-up gas, nitrogen at 60 ml min^{-1}; and splitless valve on for 1 min.

For quantification, a Spectra-Physics 4270 integrator which compared peak areas in samples and standard solutions was used.

Table 1 Parameters for the calibration graphs constructed from six points ($y = a + bx$) and estimated quantification limits

Pesticide	Concentration range of standards used for calibration graphs/ μg l^{-1}	Correlation coefficients of calibration graphs	Slope, b	Intercept, a	Quantification limit of pesticide standard solution/ μg l^{-1}	Quantification limit of a real sample/ μg l^{-1}
Lindane	4.27–136.50	0.9991	−1510.64	846.71	14.28	0.56
Heptachlor	8.75–280.00	0.9976	−2916.53	1030.96	22.64	0.92
Aldrin	6.80–217.50	0.9988	−1924.81	1251.24	12.32	0.48
Heptachlor epoxide	8.90–284.75	0.9994	−1455.16	1020.35	11.40	0.48
Dieldrin	11.67–373.50	0.9989	−10400.84	1210.61	68.72	2.76
Endrin	9.05–289.50	0.9994	801.23	718.34	8.33	0.91
p,p'-DDT	3.55–113.50	0.9994	−537.32	383.26	11.20	1.06
Methoxychlor	11.35–363.25	0.9997	−579.11	152.31	30.40	2.78

Table 2 Recoveries obtained for pesticides at various spiking levels

Pesticide	Fortification level/μg kg^{-1}	Recovery (%)	Relative standard deviation (%)
Lindane	3	83	11.1
	5	92	5.7
	11	101	2.8
Heptachlor	6	97	3.3
	11	84	7.9
	22	84	7.1
Aldrin	4	105	2.5
	9	78	9.9
	17	79	10.2
Heptachlor epoxide	6	83	8.0
	11	90	7.4
	23	94	8.6
Dieldrin	7	89	1.2
	15	90	6.1
	30	84	6.7
Endrin	6	87	2.8
	12	93	6.5
	24	94	3.5
p,p'-DDT	2	91	2.5
	5	89	6.9
	9	95	7.2
Methoxychlor	7	81	13.6
	15	93	3.3
	29	96	5.9

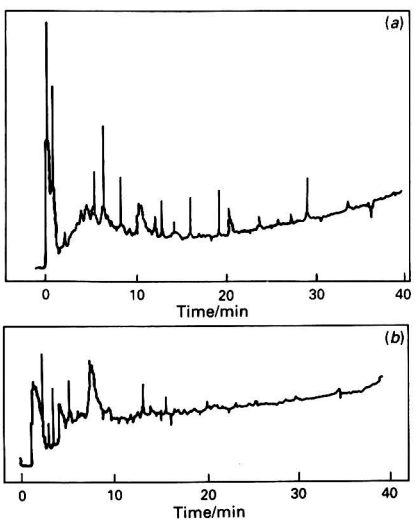

Fig. 1 Chromatograms of an unspiked sample (*a*) before and (*b*) after clean-up on a Florisil Sep-Pak cartridge. Chart speed, 2 mm min^{-1}

Construction of calibration graph

Solutions of the pesticide standards were prepared at five concentration levels and chromatographed. A calibration graph was constructed by plotting the peak area on the ordinate of a Cartesian coordinate system and the corresponding concentrations on the abscissa. The concentration range for each pesticide is shown in Table 1.

Quantification limits

Quantification limits for each pesticide were determined according to Knoll's definition:[27] the analyte concentration that produces a chromatographic peak equal to five times the standard deviation of the baseline noise, and considering the values of the intercept, a, and the slope, b, in the calibration equation, in order to ensure that any pesticide detection limit is greater than twice the amount of pesticide giving an area count of zero in this equation. Quantification limits in real samples were determined in the same manner but using the baseline noise obtained for a honey blank with no pesticide content.

Recovery studies

The recovery of organochlorine pesticides was investigated by adding known volumes of mixed standard solutions in hexane to 25 g samples of honey. After allowing the solvent to evaporate, samples were treated as described under Procedures. Recoveries of each pesticide were determined at three fortification levels in triplicate and a blank was analysed at the same time.

Results

Table 2 summarizes the recoveries obtained for pesticides at various spiking levels. The recoveries ranged from 78 to 105% and averaged 89.6 ± 6.7%.

Calibration data obtained for different organochlorine pesticides and detection limits are shown in Table 1. The large numerical values of a and b are derived from area counts produced by the integrator, *e.g.*, integrator area counts for lindane at 136.5 μg l^{-1} = 115716.

Fig. 1 shows chromatograms of an unspiked sample (*a*) before and (*b*) after clean-up on a Florisil Sep-Pak cartridge. As can be seen most of the interfering compounds have been removed.

Fig. 2 shows the chromatogram of a pesticide standard solution and Fig. 3 shows a chromatogram of a honey sample spiked with the same pesticide standard solution; the pesticides are effectively separated and the recoveries are satisfactory.

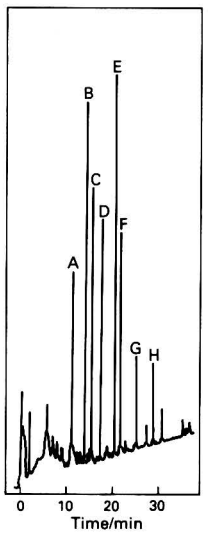

Fig. 2 Chromatograms of organochlorine pesticides: A, lindane (68 pg); B, heptachlor (140 pg); C, aldrin (109 pg); D, heptachlor epoxide (142 pg); E, dieldrin (187 pg); F, endrin (145 pg); G, *p,p'*-DDT (57 pg); and H, methoxychlor (182 pg). Chart speed, 2 mm min^{-1}

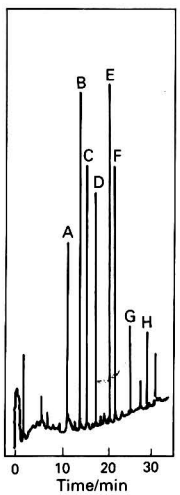

Fig. 3 Chromatogram of a spiked honey sample: A, lindane (68 pg); B, heptachlor (140 pg); C, aldrin (109 pg); D, heptachlor epoxide (142 pg); E, dieldrin (187 pg); F, endrin (145 pg); G, *p,p'*-DDT (57 pg); and H, methoxychlor (182 pg). Chart speed, 2 mm min^{-1}

Discussion and Conclusions

The proposed method allows the reliable determination of organochlorine pesticide residues in honey without the need for a complicated clean-up operation. A Florisil Sep-Pak cartridge separates organochlorine pesticides adequately from interfering co-extractives and also allows a small elution volume to be used, thus eliminating the need for a concentration step.

The linearity of the response to the organochlorine pesticides was good for the concentration ranges used (Table 1).

Recoveries reached almost 90% and were therefore extremely satisfactory (Table 2). Two factors were important in obtaining these good recoveries: firstly, the extraction method (using a magnetic stirrer instead of liquid–liquid extraction in a separating funnel) avoids the formation of a whitish gel which is difficult to separate and gives recoveries below 60%; and secondly, the concentration step prior to gas chromatographic analysis could be eliminated as better recoveries could be achieved without concentration of the 4 ml of eluate.

Further alternative techniques [determination of p-values (partition values), chemical reactions, GC–mass spectrometry] can be used to confirm the identities of the organochlorine pesticides detected by the proposed GC method.

References

1 Formica, G., *J. Assoc. Off. Anal. Chem.*, 1984, **67**, 896.
2 Calcagno, C., Evangelisti, P., and Zunin, P., *Riv. Soc. Ital. Sci. Aliment.*, 1985, **6**, 441.
3 Bachvarova, D., Demirev, P., Mollova, N., and Blagoeva, Y., *Dokl. Bolg. Akad. Nauk*, 1988, **41**, 75.
4 Barbina Taccheo, M., de Paoli, M., and Spessoto, C., *Pestic. Sci.*, 1988, **23**, 59.
5 Fabbris, F., Rogledi, R., Cantoni, C., and Palma, R., *Ind. Aliment. (Pinerolo, Italy)*, 1988, **27**, 551.
6 Thrasyvoulou, A. T., and Pappas, N., *J. Api. Res.*, 1988, **27**, 55.
7 Barbina Taccheo, M., de Paoli, M., and Spessoto, C., *Pestic. Sci.*, 1989, **25**, 11.
8 Grandi, A., *Apidologie*, 1975, **6**, 91.
9 Petukhov, R. D., *Veterinariya, Moscow*, 1976, **7**, 101.
10 Sporns, P., *J. Assoc. Off. Anal. Chem.*, 1981, **64**, 337.
11 Barry, C. P., and McEachern, M., *J. Assoc. Off. Anal. Chem.*, 1983, **66**, 4.
12 Neidert, E., Baraniak, Z., and Sauve, A., *J. Assoc. Off. Anal. Chem.*, 1986, **69**, 641.
13 Oka, H., Ikay, Y., Kawamura, N., Uno, K., Yamada, M., Harada, K., Uchiyama, M., Asukabe, H., Mon, Y., and Suzuki, M., *J. Chromatogr.*, 1987, **389**, 417.
14 Sherma, J., Bretsneider, W., Dittamo, M., DiBiase, N., Huh, D., and Schwartz, D. P., *J. Chromatogr.*, 1989, **463**, 229.
15 Ogata, J., and Bevenue, A., *Bull. Environ. Contam. Toxicol.*, 1973, **9**, 143.
16 Estep, C. B., Menon, N., Williams, H. E., and Cole, A. C., *Bull. Environ. Contam. Toxicol.*, 1977, **17**, 168.
17 Bentler, W., and Frese, E., *Arch. Lebensmittelhyg.*, 1981, **32**, 130.
18 Tsvetkova, T. S., Peneva, V., and Grigorova, D., *Vet. Med. Nauki*, 1981, **18**, 93.
19 Bigazzi Grasso, C., and Capei, R., *Ig. Mod.*, 1983, **80**, 975; *Chem. Abstr.*, 1984, **100**, 208010u.
20 Rexilius, L., *Nachrichtenbl. Dtsch. Pflanzenschutzdienstes (Braunschweig)*, 1986, **38**, 49.
21 Gayger, J., and Dustmann, J. H., *Arch. Lebensmittelhyg.*, 1985, **36**, 93.
22 Serra Bonvehí, J., *Alimentaria*, 1985, **166**, 55.
23 Moilanen, R., Kumpulainen, J., and Pyysalo, H., *Ann. Agric. Fenn.*, 1986, **25**, 177; *Chem. Abstr.*, 1987, **107**, 76292v.
24 Orbaek, K., *Chem. Abstr.*, 1988, **109**, 169103r.
25 Mueller, B., *Nahrung*, 1973, **17**, 381.
26 Trevisani, G. R., Michelini, F., and Baldi, M., *Boll. Chim. Unione Ital. Lab. Prov., Parte Sci.*, 1982, **33**, 69.
27 Knoll, J. E., *J. Chromatogr. Sci.*, 1985, **23**, 422.

Paper 0/02829K
Received June 25th, 1990
Accepted October 3rd, 1990

Analysis of Fluazifop-butyl and Fluazifop Residues in Soil and Crops by Gas Chromatography

Weiping Liu, Zeweng Chen, Qiongyan Lu and Yingyo Shi
Department of Chemistry, Zhejiang University, Hangzhou 310027, People's Republic of China

A method is described for the determination of fluazifop-butyl and fluazifop residues in soil, leaves, cotton seed and peanuts. The residues were extracted with acetone and the extracts concentrated and derivatized, fluazifop-butyl to its bromo derivative and fluazifop to its pentafluorobenzyl derivative. The products were then purified on a chromatographic column containing Al_2O_3 and Florisil and quantified by gas chromatography with electron-capture detection. The determination limits of fluazifop-butyl and fluazifop were between 0.04 and 0.05 mg kg^{-1}. The average recoveries ranged from 73.7 to 110.0% and 77.8 to 105.7%, respectively, making the method suitable for statutory residue testing purposes.

Keywords: *Fluazifop-butyl; fluazifop; derivatization; residue; gas chromatography*

Fluazifop-butyl(**I**), butyl 2-[4-(5-trifluoromethyl-2-pyridyloxy)phenoxy]propionate, is the active ingredient of the selective grass herbicide product Onecide. In the environment, it is rapidly hydrolysed to the corresponding acid, fluazifop(**II**), 2-[4-(5-trifluoromethyl-2-pyridyloxy)phenoxy]-propionic acid.[1,2]

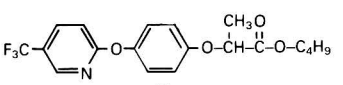

(I)

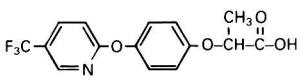

(II)

Most of the published methods for the determination of fluazifop-butyl and fluazifop have used either gas–liquid chromatography (GLC) or high-performance liquid chromatography (HPLC). Fluazifop-butyl in formulations can be determined by GLC with flame-ionization detection.[3] Procedures have been developed for the HPLC determination of fluazifop-butyl[4,5] or fluazifop-butyl and fluazifop[6,7] with ultraviolet detection. Although these procedures do not require derivatization and additional clean-up steps, they are not suitable for the determination of residues in plants or their fruits, *e.g.*, in leaves, cotton seed and peanuts.

The procedure proposed here for the determination of fluazifop-butyl and fluazifop residues in soil, leaves, cotton seed and peanuts involves: (*a*) acetone extraction; (*b*) filtration and concentration; (*c*) derivatization[8–10] of fluazifop-butyl to its bromo derivative and of fluazifop to its pentafluorobenzyl derivative; (*d*) clean-up on a chromatographic column containing Al_2O_3 and Florisil; and (*e*) gas chromatography (GC) with electron-capture detection. This work is part of a wider study on the movement and degradation of fluazifop-butyl and fluazifop in the agrosystem.[11]

Experimental

Reagents and Materials

Light petroleum (boiling-point range 68–70 °C) and other solvents used were of analytical-reagent grade (Hangzhou Oil Refining Plant and Shanghai Chemical Reagent Plant). Standards of fluazifop-butyl (99.0%), brominated fluazifop-butyl (98.1%), fluazifop (99.2%) and the pentafluorobenzyl ester of fluazifop (98.8%), were kindly supplied by Ishihara Sangyo Kaisha. Pentafluorobenzyl bromide was of guaranteed-reagent grade (PCR Research Chemicals).

Neutral Al_2O_3 (200–300 mesh) (Shanghai Wu Si Chemical Reagent Plant) was heated at 500 °C for 3 h, cooled to 50 °C, mixed with 9 g of water per 100 g of Al_2O_3 and stored in air-tight containers overnight. Florisil (120–160 mesh)(Floridin) was heated at 650 °C for 3 h, cooled to 50 °C, mixed with 2 g of water per 100 g of Florisil and stored in a desiccator overnight.

The samples of soil, leaves, cotton seed and peanuts were obtained from the Zhejiang Agricultural University.

Apparatus

A chopper, ultrasonic bath, shaker, water-bath, vacuum pump, 500 ml separating funnels, Kuderna–Danish evaporators and chromatographic columns (15 × 1 cm i.d.) for clean-up were used for sample pre-treatment. The GC system consisted of a Shimadzu Model GC-9A chromatograph, an ECD-7 ^{63}Ni electron-capture detector and a C-R3A integration system.

Standard Solutions

Stock solutions (0.1 g l^{-1}) of fluazifop-butyl, brominated fluazifop-butyl, fluazifop and the pentafluorobenzyl ester of fluazifop in light petroleum were prepared. Working standards were obtained by suitable dilutions of the stock solutions with light petroleum and were stored at 0 °C. Fresh solutions were prepared every 4 months.

Procedures

Pre-treatment, extraction and filtration

After chopping, weigh a representative sample (10 g) into a 250 ml conical flask. For the extraction of fluazifop-butyl, add 10 ml of distilled water and 40 ml of acetone. Place the flask in an ultrasonic bath filled with sufficient water and sonicate for 30 min. For the extraction of fluazifop, add 10 ml of 6 mol dm^{-3} HCl and 40 ml of acetone. Place the flask in an ultrasonic bath filled with sufficient water and sonicate for 30 min.

Filter the extract through a Büchner funnel fitted with a filter-paper (pre-wash the filter-paper with 20 ml of acetone) and transfer the filtrate into a 500 ml separating funnel. Add 100 ml of 2% Na_2SO_4 solution and 60 ml of light petroleum (for the extraction of fluazifop, add 80 ml of chloroform) and shake. Discard the aqueous layer and wash the organic layer with 60 ml of 2% Na_2SO_4 solution. Dry the organic layer by filtration through 10 g of anhydrous Na_2SO_4 into a Kuderna–Danish evaporator and evaporate the extract to dryness at 40 °C.

Derivatization

Bromination of fluazifop-butyl. Add 1 ml of 2% soybean oil in acetone to the dry residue obtained as described above and evaporate to dryness with a gentle stream of air at room

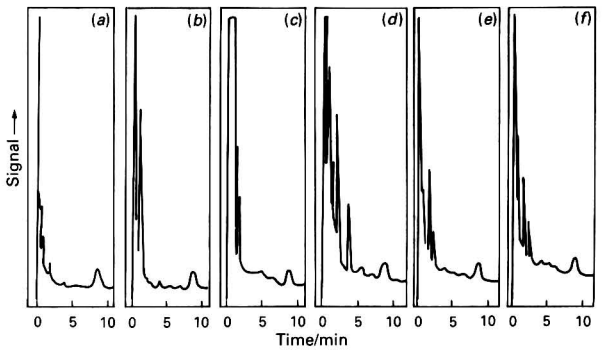

Fig. 1 Chromatograms of fluazifop-butyl (brominated fluazifop-butyl) residues in various samples. Residual level in samples, 0.05 mg kg^{-1}; final volume, 20 ml; injection volume, 1 μl; range, 10; detector current 2.0 nA; and attenuation, 4. (*a*) Standard; (*b*) soil; (*c*) cotton leaf; (*d*) peanut leaf; (*e*) cotton seed; and (*f*) peanuts

Table 1 Column components and eluting solvents for clean-up of brominated fluazifop-butyl

Sample	Column components	Eluting solvents	Volume of eluate collected*/ml
Soil	Anhydrous Na_2SO_4 (2 g), Florisil	Acetone–light petroleum (1.5 + 98.5) (70 ml)	60
Peanut leaf, cotton leaf	Anhydrous Na_2SO_4 (2 g), neutral Al_2O_3 (10 g), Florisil (5 g)	Acetone–light petroleum (1 + 99) (100 ml), acetone–light petroleum (1.5 + 98.5) (100 ml)	100
Cotton seed, peanuts	Anhydrous Na_2SO_4 (4 g), neutral Al_2O_3 (2 g), Florisil (5 g)	Acetone–light petroleum (2 + 98) (130 ml)	80

* The last fraction of the total volume eluted was collected in each instance.

Table 2 Column components and eluting solvents for clean-up of the pentafluorobenzyl ester of fluazifop

Sample	Column components	Eluting solvents	Volume of eluate collected*/ml
Soil	Anhydrous Na_2SO_4 (4 g), Florisil (8 g)	Light petroleum (20 ml), acetone–light petroleum (1 + 99) (60 ml)	70
Cotton leaf, peanut leaf	Anhydrous Na_2SO_4 (4 g), neutral Al_2O_3 (2 g), Florisil (8 g)	Acetone–light petroleum (2 + 98) (30 ml), acetone–light petroleum (0.5 + 99.5) (80 ml)	70
Cotton seed, peanuts	Anhydrous Na_2SO_4 (2 g), neutral Al_2O_3 (3 g), Florisil (10 g)	Acetone–light petroleum (1 + 99) (160 ml)	60

* The last fraction of the total volume eluted was collected in each instance.

Table 3 Determination limits of fluazifop-butyl and fluazifop in various samples

	Determination limit/mg kg^{-1}	
Sample	Fluazifop-butyl	Fluazifop
Soil	0.04	0.04
Cotton leaf	0.04	0.05
Peanut leaf	0.04	0.05
Cotton seed	0.05	0.05
Peanuts	0.04	0.05

temperature (the addition of the soybean oil avoids dibromination of the benzene ring of fluazifop-butyl and ensures that the substitution of a single bromine atom in the benzene ring is quantitative). Add 0.3 ml of liquid bromine, stopper the flask and heat at 40 °C in a water-bath for 30 min in the dark. The reaction is as follows:

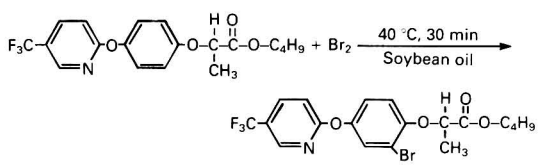

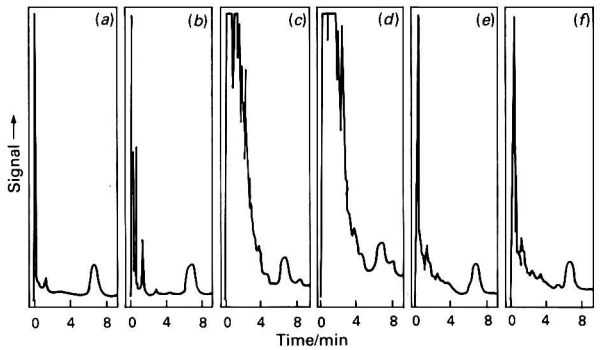

Fig. 2 Chromatograms of fluazifop (fluazifop, pentafluorobenzyl ester) residues in various samples. Residual level in samples, 0.05 mg kg^{-1}; final volume, 20 ml; injection volume, 1 μl; range, 10; detector current, 2.0 nA; and attenuation, 8. (*a*) Standard; (*b*) soil; (*c*) cotton leaf; (*d*) peanut leaf; (*e*) cotton seed; and (*f*) peanuts

Table 4 Recoveries of fluazifop-butyl and fluazifop from various samples using the method of standard additions

Sample	Amount added/mg kg^{-1}	Recovery ± standard deviation*(%) Fluazifop-butyl	Fluazifop
Soil	0.96	73.9 ± 9.8	81.2 ± 7.6
	0.48	87.4 ± 6.2	83.5 ± 14.4
	0.10	90.5 ± 9.2	84.3 ± 9.3
Cotton leaf	0.96	80.1 ± 10.7	92.8 ± 8.6
	0.48	78.1 ± 7.0	94.0 ± 8.3
	0.10	91.7 ± 9.0	101.0 ± 6.9
Peanut leaf	0.96	76.9 ± 6.9	77.8 ± 10.3
	0.48	93.3 ± 8.5	81.4 ± 6.9
	0.10	84.9 ± 7.9	89.9 ± 9.8
Cotton seed	0.96	110.0 ± 11.8	80.1 ± 8.7
	0.48	81.1 ± 14.3	97.4 ± 9.6
	0.10	73.7 ± 9.1	86.0 ± 11.2
Peanuts	0.96	86.9 ± 7.8	105.7 ± 9.9
	0.48	97.9 ± 14.8	78.7 ± 10.8
	0.10	73.7 ± 9.1	94.3 ± 7.6

* Values obtained from five measurements.

After cooling, remove the excess of bromine by passing a stream of air over the mixture and add 10 ml of acetone. Transfer the solution into a 500 ml separating funnel, add 60 ml of light petroleum and wash the mixture with 60 ml of 2% Na_2SO_4 solution and 40 ml of 2% Na_2CO_3 solution. Transfer the organic phase into a Kuderna–Danish evaporator and concentrate it to 5 ml at 40 °C.

Pentafluorobenzylation of fluazifop. Add 2 ml of 2% pentafluorobenzyl bromide in acetone and 2 drops of triethylamine to the dry residue obtained as described above. Mix and heat at 30 °C in a water-bath for 1 h in the dark. The reaction is as follows:

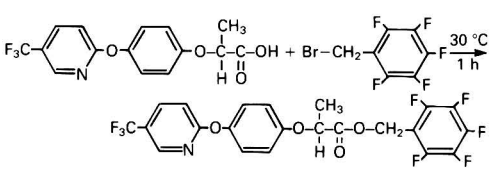

After cooling in ice, add 50 ml of light petroleum and transfer the solution into a 500 ml separating funnel. Wash the product with 50 ml of 1% HCl and 80 ml of Na_2SO_4 solution in turn. Transfer the organic phase into a Kuderna–Danish evaporator and concentrate it to 50 ml at 40 °C.

Clean-up

Pre-pack a chromatographic column as described in Tables 1 and 2 and pre-wash the column with 10 ml of light petroleum. Add the sample extract and allow the solvent to settle and run off at the rate of 90–100 drops min^{-1}. Elute the products from the column using the solvents and collecting volumes listed in Tables 1 and 2. Then concentrate the collected liquid to 20 ml using a Kuderna–Danish evaporator at 40 °C.

Determination by GC with electron-capture detection

The following conditions were used for the determination of the derivative products: column, glass, 1.6 m × 3.2 mm i.d. (7.0 mm o.d.), packed with 2% OV-17 Chromosorb HP W, 60–80 mesh; oven temperature 220 °C; injector and detector temperatures, 260 °C; carrier gas, nitrogen (60 ml min^{-1}); and injection volume, 1 μl.

Results and Discussion

Under the chromatographic conditions described above the chromatograms shown in Figs. 1 and 2 were obtained. Calibration graphs of peak area *versus* amount of brominated fluazifop-butyl or pentafluorobenzylated fluazifop injected were linear in the ranges 0–0.15 and 0–0.08 ng, respectively. The determination limit was calculated using the following equation:

$$\text{Determination limit (mg kg}^{-1}) = \frac{\text{minimum detectable amount (ng)}}{\text{injection volume (μl)}} \times \frac{\text{final volume (ml)}}{\text{sample mass (g)}}$$

The results for various samples are shown in Table 3. The recoveries of fluazifop-butyl and fluazifop from various samples were found to be satisfactory (Table 4).

The method described has high sensitivity and gives high recoveries. It is used routinely in this laboratory for studies on the movement and degradation of fluazifop-butyl and fluazifop in the agrosystem and for the statutory chemical confirmation of their residues in cotton seed and peanuts. The method is also suitable, however, for other vegetable samples.

The authors gratefully acknowledge financial support from Ishihara Sangyo Kaisha Ltd.

References

1 Horellou, A., Painparay, G., and Morand, P., *Def. Veg.*, 1981, **36**, 251.
2 Wheeler, A. F., in *Proceedings, British Technical Week*, ICI, Bratislava, 1980, Fusilade (Abstract pp-009).

3 Bland, P. D., *J. Assoc. Off. Anal. Chem.*, 1984, **67**, 499.
4 Parker, N. Y., Monaco, T. J., Leidy, R. B., and Shets, T. J., *Weed Sci.*, 1985, **33**, 405.
5 Hajslova, J., Pudil, F., Jehickova, Z., Viden, I., and Davidek, J. J., *J. Chromatogr.*, 1988, **438**, 55.
6 Neger, M., Gennari, M., and Cigentti, A., *J. Chromatogr.*, 1987, **387**, 541.
7 Patumi, M., Marucchini, C., Businelli, M., and Vischetti, C., *Pestic. Sci.*, 1987, **21**, 193.
8 Attreye, N. C., and Dick, J. P., Analytical Method No. 52, ICI Plant Protection Division, Bracknell, 1980.
9 *The Determination of Residues of Fluazifop-butyl and Fluazifop in Soybeans*, Ishihara Sangyo Kaisha, Tokyo, 1983.
10 Liu, W. P., Chen, Z. W., and Lu, Q. Y., *Fenxi Huaxue.*, 1990, **1**, 57.
11 Liu W. P., Chen, Z. W., Lu, Q. Y., and Yu, K. N., *Huanjing Kexue Xuebao*, in the press.

Paper 0/00235F
Received January 16th, 1990
Accepted May 30th, 1990

Determination of Iron, Cobalt and Nickel as Chelates With 4-(2-Thiazolylazo)resorcinol by Reversed-phase High-performance Liquid Chromatography

Chang-shan Lin, Xiao-song Zhang and Xue-zhu Liu
Department of Applied Chemistry, University of Science and Technology of China, Hefei, Anhui 230026, China

The chelates of iron, cobalt and nickel with 4-(2-thiazolylazo)resorcinol were separated on a column (250 × 4.6 mm i.d.) of Zorbax ODS (6 μm) with a mobile phase (0.75 ml min^{-1}) of methanol–water (40 + 60, v/v) containing 0.01 mol dm^{-3} KH_2PO_4–Na_2HPO_4 buffer (pH 7.0) and were detected at 580 nm. The calibration graphs were rectilinear from 0.1 to 5 ppm for both cobalt and nickel, and from 1 to 5 ppm for iron. The detection limits were 2.0, 0.2 and 0.6 ng for iron, cobalt and nickel, respectively. The method has been applied to the analysis of real samples.

Keywords: *Iron, cobalt and nickel determination; 4-(2-thiazolylazo)resorcinol; high-performance liquid chromatography; ore sample; anode mud sample*

The separation and simultaneous determination of mixtures of metal ions as their chelates with organic reagents by high-performance liquid chromatography (HPLC) has received increasing attention and has been used in inorganic analysis in recent years. Several reviews on the separation of metal chelates using HPLC have been published.[1–3] A wide variety of organic reagents have been used to complex metal ions prior to separation by HPLC. The most popular complexing agents such as dithiocarbamates,[4,5] 8-hydroxy-quinoline,[6,7] 4-(2-pyridylazo)resorcinol (PAR),[8–13] and other highly sensitive azo dyes[14–16] have been investigated. These reagents form either neutral or ionic chelates with a large number of metal ions, and the chelates in the eluate can be detected spectrophotometrically.

4-(2-Thiazolylazo)resorcinol (TAR) is similar in chemical structure to PAR and has been used extensively for the spectrophotometric determination of numerous metal ions.[17] Although the two reagents have the same chelating system with metal ions, both TAR and its chelates with metal ions are insoluble in water. However, they are readily soluble in solvents that are miscible with water and they can be extracted into solvents that are immiscible with water. As might be expected from these properties, most metal chelates with TAR can be separated by HPLC and detected spectrophotometrically. To date, no reports on the separation and determination of metal ions as chelates with TAR using HPLC have been reported.

In this work, the conditions for pre-column derivatization and for the separation and simultaneous determination of iron, cobalt and nickel as chelates with TAR by reversed-phase (RP) HPLC have been investigated.

Experimental

Apparatus

Liquid chromatography was performed by use of a Shimadzu Model LC-4A HPLC instrument equipped with a Model SPD-1 spectrophotometric detector and a Chromatopac Model C-R2A data processor. A Zorbax ODS column (Du Pont, 250 × 4.6 mm i.d.) with a particle size of 6 μm was used for all experiments. A Shimadzu Model UV-240 recording spectrophotometer was used for spectral measurements. A Shanghai Model pH S-2 pH meter was also used.

Reagents and Solutions

A standard solution of Fe^{II} was prepared by dissolving ammonium iron(II) sulphate in water with a slightly acidic pH. Standard solutions of Co^{II} and Ni^{II} were prepared by dissolving cobalt metal (99.99%) and nickel metal (99.99%), respectively, in concentrated hydrochloric–nitric acid (2 + 1) on a hotplate, evaporating to near dryness and then diluting with water.

4-(2-Thiazolylazo)resorcinol (purity, 97%) was purchased from Aldrich and dissolved in methanol to give a concentration of 5×10^{-3} mol dm^{-3}.

The mobile phase was methanol–water (40 + 60, v/v) containing 0.01 mol dm^{-3} KH_2PO_4–Na_2HPO_4 buffer (pH 7.0). All other chemicals used were of analytical-reagent grade.

Procedure

To a slightly acidic solution containing 5–50 μg of Fe^{II}, and 0.5–50 μg each of Co^{II} and Ni^{II} in a 10 ml calibrated flask, add 1.0 ml of 0.1 mol dm^{-3} KH_2PO_4–Na_2HPO_4 buffer solution (pH 7.0) and 2.0 ml of 5×10^{-3} mol dm^{-3} TAR solution, and heat the mixture in a boiling water-bath for about 10 min. After cooling, add 5 ml of methanol and dilute to volume with water. Filter the solution through a 0.3 μm membrane and inject a 20 μl aliquot of the filtered solution onto the column. Elute the TAR chelates with the methanol–water mobile phase at a flow rate of 0.75 ml min^{-1} and detect the chelates in the eluate at 580 nm. Determine the amount of each metal by measuring the peak areas.

Results and Discussion

Selection of Conditions for Pre-column Derivatization and Detection Wavelength of the Metal–TAR Chelates

In a solution in the pH range 7.0–8.5, buffered with KH_2PO_4–Na_2HPO_4, Fe^{II}, Co^{II} and Ni^{II} form red chelates with TAR, and have absorption maxima at 505, 555 and 550 nm, respectively. These findings were consistent with measurements made by stopped-pump and wavelength-scanning methods at the respective retention times of the chelates in the mobile phase. Because the peaks of the unreacted reagent and the Ni^{II}–TAR chelate overlapped to some extent, the concentration of the reagent was varied from 1×10^{-3} to 5×10^{-3}

mol dm^{-3} and the detection wavelength was set at 580 nm, where the absorption of the reagent was very slight.

In order to accelerate the colour development of the Fe^{II}–TAR chelate, the sample solution had to be heated in a boiling water-bath for 10–15 min. As the reagent and the metal chelates are insoluble in water, the concentration of methanol in the sample solution should not be less than 40%.

The three chelates formed with TAR under the above-mentioned conditions had stable peak areas for at least 1 week.

Effect of the Concentration of Methanol in the Mobile Phase

Several organic solvents, such as methanol, ethanol, acetonitrile, tetrahydrofuran and isopropyl alcohol, combined with water, were investigated as binary and ternary mobile phases. The methanol–water binary system was found to be satisfactory for the separation of the TAR chelates of Fe^{II}, Co^{II} and Ni^{II}. A simple methanol–water mobile phase, however, gave tailing peaks and low sensitivities; moreover, the unreacted reagent appeared as two peaks which overlapped with the peaks of the Ni^{II}– and Fe^{II}–TAR chelates, respectively. When KH_2PO_4–Na_2HPO_4 buffer was added to the mobile phase, excellent peak shapes and high sensitivities were obtained and only the reagent peak that overlapped with the peak of the Ni^{II}–TAR chelate remained. If detection was carried out at 580 nm, the effect of the unreacted reagent on the Ni^{II}–TAR chelate could be eliminated. The effect of the concentration of methanol in the mobile phase on the retention of the chelates is shown in Fig. 1. The optimum results were obtained with 40% methanol and 60% water (v/v).

Effect of pH of the Buffer Added to the Mobile Phase

Two buffers (0.01 mol dm^{-3}), KH_2PO_4–Na_2HPO_4 and tris-(hydroxymethyl)aminomethane (Tris), were used to determine the optimum pH range of the mobile phase and the former was found to improve the peak shapes and produce higher peak heights for the TAR chelates of Fe^{II}, Co^{II} and Ni^{II}; Tris had no beneficial effect on the separation. The results obtained are shown in Fig. 2. It is evident that the retention of the Ni^{II}–TAR chelate changed very little, but that of the Fe^{II}– and Co^{II}–TAR chelates increased markedly in the pH range 6.0–7.5. A constant peak area for each chelate was obtained in the pH range 6.5–7.5.

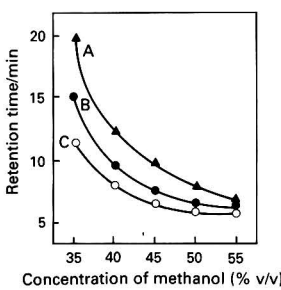

Fig. 1 Effect of concentration of methanol in the mobile phase on the retention times of the TAR chelates of A, Fe^{II}; B, Co^{II}; and C, Ni^{II}. Mobile phase, 0.01 mol dm^{-3} KH_2PO_4–Na_2HPO_4 buffer (pH 7.0). Flow rate, 0.75 ml min^{-1} and column, Zorbax ODS

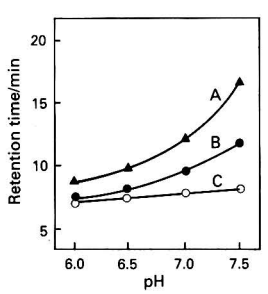

Fig. 2 Effect of pH of KH_2PO_4–Na_2HPO_4 buffer in the methanol–water (40 + 60, v/v) mobile phase on the retention times of the TAR chelates of A, Fe^{II}; B, Co^{II}; and C, Ni^{II}; all other conditions as in Fig. 1

Chromatogram and Calibration Graphs

A typical chromatogram for the separation of the TAR chelates of Fe^{II}, Co^{II} and Ni^{II} is shown in Fig. 3. The TAR chelates were eluted in the order Ni^{II}, Co^{II} and Fe^{II}, and the retention times were 7.9, 9.5 and 12.2 min, respectively, at a flow rate of 0.75 ml min^{-1}. Baseline separation of the three chelates was achieved. The slopes and intercepts of the calibration graphs for the simultaneous determination of iron, cobalt and nickel, calculated by linear regression analysis of the peak area *versus* metal ion concentration (ppm) data, are given in Table 1. The calibration graphs were linear in the range 0.1–5.0 ppm for both Co^{II} and Ni^{II} and in the range 1.0–5.0 ppm for Fe^{II}. The absolute detection limits, calculated as the amount injected that gave a signal that was three times the background noise (*i.e.*, signal to noise ratio of 3 : 1), were 2.0, 0.2 and 0.6 ng, respectively, for iron, cobalt and nickel.

Effect of Foreign Ions

The effect of possible interferences was studied by adding each foreign ion in turn to the sample before pre-column derivatization of the metal–TAR chelates. The maximum level (in μg) of foreign ion, which gives a change of less than ±5% in the peak area of the TAR chelates of Fe^{II}, Co^{II} and Ni^{II}, that could be tolerated in the simultaneous determination of 10 μg each of iron, cobalt and nickel was as follows: Al^{III}, 100; Cd^{II}, Hg^{II} and Pb^{II}, 50; Zn^{II}, 40; Mg^{II} and Ti^{IV}, 20; and Cr^{III}, Cr^{VI}, Cu^{II} and V^{V},

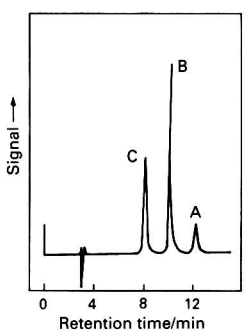

Fig. 3 Chromatogram of Fe^{II}–, Co^{II}– and Ni^{II}–TAR chelates on a Zorbax ODS column with a 20 μl injection of a solution containing 2 ppm of Fe^{II}, 1 ppm each of Co^{II} and Ni^{II}, and 1×10^{-3} mol dm^{-3} TAR using methanol–water (40 + 60, v/v) containing 0.01 mol dm^{-3} KH_2PO_4–Na_2HPO_4 buffer (pH 7.0) as the mobile phase at a flow rate of 0.75 ml min^{-1}. Detection wavelength, 580 nm

Table 1 Coefficients of linear regression analysis for calibration of the chromatographic detector

	Metal ion		
Parameter	Fe^{II}	Co^{II}	Ni^{II}
Concentration (ppm)	1.0–5.0	0.1–5.0	0.1–5.0
Amount injected/ng	20–100	2–100	2–100
Slope/area ml μg^{-1}	657	5516	2768
Intercept (area)	−1468	−1694	2179
Correlation coefficient	0.996	0.9992	0.9995

Table 2 Results for real samples

Sample	Found* (% m/m) Iron	Cobalt	Nickel
Nickel ore	7.84 (0.09†)	0.034 (0.036‡)	1.27 (1.27‡)
Anode mud	—	—	0.61 (0.02†)
Catalyst recovery solution	0.52 (0.016†)	0.79 (0.01†)	2.00 (0.05†)

* Average of five analyses
† Standard deviation
‡ Certified value

10. Of the metal ions tested only Mn^{II} (20 μg) caused a serious interference in the determination of iron but did not interfere in the determination of cobalt and nickel.

Application to the Determination of Iron, Cobalt and Nickel in Real Samples

A nickel ore sample, or an anode mud sample from a copper smelter, was dissolved in concentrated hydrochloric–nitric acid (2 + 1) on a hotplate and evaporated to near dryness. A small amount of water was added and the mixture was heated to dissolve all soluble salts. Iron(III) was reduced with hydroxylamine hydrochloride. The solution was adjusted to a slightly acidic pH with dilute sulphuric acid or sodium hydroxide, then filtered into a 250 ml calibrated flask and diluted to volume with water. A 1 ml aliquot of this solution was taken, and the Fe^{II}–, Co^{II}– and Ni^{II}–TAR chelates were formed by reaction with TAR and determined by HPLC as described above.

The proposed method was also applied to the determination of iron, cobalt and nickel in a catalyst recovery solution. The results for real samples are given in Table 2.

References

1 Willeford, B. R., and Veening, H., *J. Chromatogr.*, 1982, **251**, 61.
2 O'Laughlin, J. W., *J. Liq. Chromatogr.*, 1984, **7**, 127.
3 Nickless, A., *J. Chromatogr.*, 1985, **313**, 129.
4 Schwedt, G., *Chromatographia*, 1978, **11**, 145.
5 King, J. N., and Fritz, J. S., *Anal. Chem.*, 1987, **59**, 703.
6 Berthod, A., Kolosky, M., Rocca, J. L., and Vitori, O., *Analusis*, 1979, **7**, 395.
7 Bond, A. M., and Nagaosa, Y., *Anal. Chim. Acta*, 1985, **178**, 197.
8 Hoshino, H., Yotsuyanagi, T., and Aomura, K., *Bunseki Kagaku*, 1978, **27**, 315.
9 Watanabe, E., Nakajima, H., Ebina, T., Hoshino, H., and Yotsuyanagi, T., *Bunseki Kagaku*, 1983, **32**, 469.
10 Roston, D. A., *Anal. Chem.*, 1984, **56**, 241.
11 Hoshino, H., and Yotsuyanagi, T., *Anal. Chem.*, 1985, **57**, 625.
12 Zhang, X.-s., Zhu, X.-p., and Lin, C.-s., *Talanta*, 1986, **33**, 838.
13 Lin, C.-s., Zhang, X.-s., and Zhu, X.-p., *Fenxi Huaxue*, 1987, **15**, 1000.
14 Shijo, Y., and Sakai, K., *J. Chromatogr.*, 1985, **333**, 133.
15 Lin, C.-s., and Zhang, X.-s., *Analyst*, 1987, **112**, 1659.
16 Zhang, X.-s., and Lin, C.-s., *Fenxi Huaxue*, 1988, **16**, 122.
17 *CRC Handbook of Organic Analytical Reagents*, eds. Cheng, K. L., Ueno, K., and Imamura, T., CRC Press, Boca Raton, FL, 1982, pp. 203–212.

Paper 0/02434A
Received May 31st, 1990
Accepted September 27th, 1990

Adsorption of Chromium(VI) by Titanium(IV) Oxide Coated on a Silica Gel Surface

Lauro T. Kubota and Yoshitaka Gushikem*
Instituto de Química, Unicamp, CP 6154, 13081 Campinas, São Paulo, Brazil
José C. Moreira
Instituto de Química, Unesp-Araraquara, CP 174, 14800 Araraquara, São Paulo, Brazil

Titanium(IV) oxide, coated on the surface of silica gel (surface area, 308 $m^2\ g^{-1}$; amount of Ti^{IV} per gram of modified silica gel, 1.8×10^{-3} mol), was used to adsorb CrO_4^{2-} ions from acidic solutions. The exchange capacity increased at lower pH values and was affected to some extent by the acid used. The material was used to preconcentrate Cr^{VI} from 0.5 ppm solutions of chromate very efficiently and virtually 100% recovery was achieved in every instance.

Keywords: *Titanium(IV) oxide modified silica; silica gel surface coated with titanium(IV) oxide; chromium(VI) determination; preconcentration of chromium(VI)*

Hydrated titanium(IV) oxide (TiO_2) has attracted considerable attention as an ion exchanger owing to its highly selective sorption of certain metal ions.[1,2] In order to improve the utilization of this oxide, it has usually been used dispersed in a silica matrix and the procedure employed for its preparation has been the coprecipitation method.[3,4] However, many problems have been found in establishing reproducible experimental conditions in the preparation of the gel.[5]

Many papers have been published describing the grafting of chemical compounds onto silica gel, and in this respect, the use of $TiCl_4$ as a coupling reagent has received particular attention.[6–8] The Ti^{IV} modified silica gel thus prepared has been used extensively as a catalyst[9–11] but not as an ion exchanger.

This paper describes the preparation and use of TiO_2 coated on silica gel, obtained by careful hydrolysis of previously attached $TiCl_4$. The main objective in obtaining a metal oxide monolayer dispersed in a matrix was to produce a mechanically resistant solid with a high efficiency and rapid rate for the sorption of chemical species. The material prepared in this work was used to adsorb Cr^{VI} from acidic and neutral aqueous solutions.

Experimental

Silica gel having a surface area of 500 $m^2\ g^{-1}$ and a particle size of between 0.025 and 0.2 mm was previously activated at 400 K for 6 h under high vacuum (less than 1×10^{-4} mmHg). About 80 g of this activated silica gel were placed in 400 ml of pure CCl_4 and then 40 ml of $TiCl_4$ were added. The mixture was refluxed for 10 h under a dry nitrogen atmosphere. The resulting solid was filtered in a Schlenk apparatus under a nitrogen atmosphere and then heated at 400 K for 4 h under high vacuum. The modified silica gel was then placed in an atmosphere saturated with water vapour and allowed to hydrolyse very slowly. Finally, the solid was washed with demineralized water until all the Cl^- ions had been removed and then dried in an oven at 423 K.

The amount of metal coated was determined by treating the modified silica gel with hot concentrated HCl. The solid was filtered and the Ti in the solution determined gravimetrically. The amount of Ti^{IV} found was 1.8×10^{-3} mol g^{-1}.

The surface area of the modified silica gel, determined by the method of Brunauer *et al.*[12], was 308 $m^2\ g^{-1}$.

The isotherms for the adsorption of CrO_4^{2-} ions from an aqueous solution by the modified silica gel were obtained at 298 K by using the batch technique. The flasks, containing 50 ml of a solution with acid concentrations ranging from 1×10^{-5} to 1 mol dm^{-3} and a fixed amount of 250 μmol of CrO_4^{2-}, were shaken with 0.2 g of the modified silica gel for 30 min. The amount of Cr^{VI} in the supernatant was determined and the amount of metal sorbed on the silica gel (N_f) calculated from the equation

$$N_f = \frac{N_a - N_s}{m}$$

where N_a is the initial number of moles of Cr^{VI} in the solution, N_s the number of moles of the metal in the solution in equilibrium with the solid phase and m the mass of the modified silica gel (in grams).

The preconcentration of chromate and the recovery experiments were carried out using a small glass column (10×0.2 cm i.d.), which was packed with 0.1 g of the modified silica gel. A dilute solution of chromate (0.5 ppm) was allowed to percolate through the column at a flow-rate of 3.5 ml min^{-1}. The adsorbed chromate was eluted from the column using a 0.5 mol dm^{-3} NaOH solution at a flow-rate of 3.5 ml min^{-1}. The eluted ion was determined spectrophotometrically, using a 0.25% m/v diphenylcarbazide solution in acetone–water (50 + 50).

Results and Discussion

Sorption of CrO_4^{2-} Ions From Solution

Hydrated TiO_2, either in the pure form or coprecipitated on silica gel, is strongly influenced by the pH of the solution in equilibrium with the solid phase in exchange processes.[2–5] In the present work, the metal oxide film lost its activity for

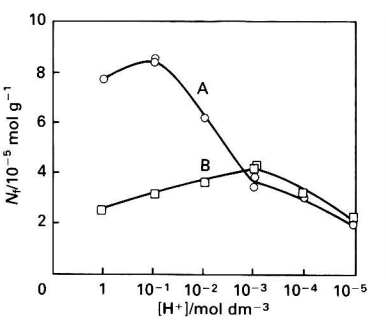

Fig. 1 Isotherms for the adsorption of CrO_4^{2-} from acidic solutions by TiO_2 coated onto silica gel: A, HNO_3 and B, HCl

* To whom correspondence should be addressed.

sorbing metal ions on ageing, even in the favourable pH range between 5 and 6. However, this aged film was shown to adsorb CrO_4^{2-} ions very efficiently from an acidic solution (Fig. 1).

The sorption of Cr^{VI} from such solutions can be explained by the reaction:

$$2\,\text{—TiOH} + Cr_2O_7^{2-} + 2H^+ \rightarrow 2\,\text{—TiOCrO}_3\text{H} + H_2O$$

The enhancement of the adsorption process at lower pH values is therefore associated with a change in the charge on the surface of the modified silica. Presumably, the dissociation of —TiOH groups in an acidic medium involves the following process:[1]

$$\text{—TiOH} + H^+ \rightarrow \text{—Ti}^+ + H_2O$$

The acid used to acidify the solutions might have some significance. The N_f values for solutions with acid concentrations between 1×10^{-5} and 1×10^{-3} mol dm^{-3} were not significantly affected when HNO_3 or HCl was used. However, at higher acid concentrations, *i.e.*, $[H^+] > 1 \times 10^{-3}$ mol dm^{-3}, it was observed that sorption of CrO_4^{2-} from HNO_3 solutions was considerably higher than from HCl solutions. These larger values of N_f, when HNO_3 was used rather than HCl, appear to be due to a competition reaction which becomes significant at $[H^+] > 1 \times 10^{-3}$ mol dm^{-3}. The Cl^- ion competes more effectively with the CrO_4^{2-} ion for the exchanger sites than does the NO_3^- ion.[1]

Effect of Thermal Treatment of the TiO_2 Modified Silica Gel

The adsorption capacity of the modified silica gel was considerably affected by thermal treatment prior to use. Fig. 2 shows the isotherms for the adsorption of CrO_4^{2-} by the solid phase after treatment of the latter at 573 and 673 K compared with treatment at 423 K. The maximum adsorption capacity, which was 9.4×10^{-5} mol g^{-1} for the material dried at 423 K, decreased to 5.3×10^{-5} and 3.4×10^{-5} mol g^{-1} for the material dried at 573 and 673 K, respectively. The loss of water at higher temperatures, which is normally accompanied by a decrease in the surface area, results in the migration of Ti atoms from the surface into the silica matrix where they are inaccessible as adsorption sites for Cr^{VI}.[13]

Chemical Stability and Rate of Sorption

The Ti^{IV} coated onto the surface of the silica gel was also shown to be very stable to treatment with acid. No leaching of the metal from the surface was detected using 6 mol dm^{-3} HNO_3. However, the oxide was completely removed by 3 mol dm^{-3} HCl.

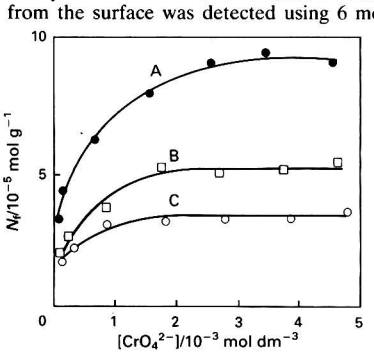

Fig. 2 Isotherms for the adsorption of CrO_4^{2-} from 0.1 mol dm^{-3} HNO_3 by TiO_2 coated onto silica gel treated at temperatures of: A, 423; B, 573; and C, 673 K

A general characteristic of a hydrated oxide obtained using the precipitation method is that this solid, in contact with the solution phase, normally requires a period of 24 h or 10 d for the system to achieve equilibrium conditions. In this work, the minimum time for the system to achieve equilibrium was found to be about 10 min (Fig. 3). The relatively short time required in this instance is presumably due to the distribution of the exchange sites of the resulting modified surface produced by the coating process. In this process, the metal oxide is covalently bound to the surface and forms a monolayer film in which all the metal oxide is exposed.[14]

Preconcentration and Recovery

The results of the preconcentration of CrO_4^{2-} and of the recovery experiments carried out under dynamic conditions are shown in Table 1. A 250 ml volume of a 0.5 ppm solution of CrO_4^{2-} (125 μg of chromate ion) was allowed to percolate through the glass column, packed with the modified silica gel, at a relatively high flow-rate of 3.5 ml min^{-1}. The recovery of the adsorbed species was effected by using a 0.5 mol dm^{-3} NaOH solution as the eluent. The experiment was repeated four times and after each run the packing material was replaced. However, in subsequent experiments, the same packing material was used for five adsorption–desorption cycles and no apparent loss of adsorption capacity was observed (see Table 2).

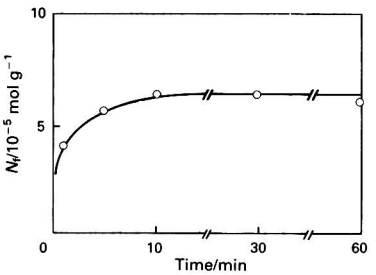

Fig. 3 Adsorption of CrO_4^{2-} from 0.1 mol dm^{-3} HNO_3 by TiO_2 coated onto silica gel as a function of time at 298 K. Initial concentration of chromate ions, $[CrO_4^{2-}] = 5 \times 10^{-3}$ mol dm^{-3}

Table 1 Preconcentration and recovery of Cr^{VI} with TiO_2 modified silica gel

Batch*	Cr^{VI} added/ μg	Cr^{VI} recovered/ μg	Recovery (%)
1	125	123 ± 3	98.4
2	125	125 ± 2	100
3	125	123 ± 3	98.4
4	125	125 ± 2	100

* For each batch, the packing material (0.1 g) was replaced.

Table 2 Chemical stability of TiO_2 modified silica gel after various sorption–desorption cycles

Cycle* No.	Cr^{VI} added/ μg	Cr^{VI} recovered/ μg	Recovery (%)
1	125	123 ± 3	98.4
2	125	125 ± 2	100
3	125	125 ± 2	100
4	125	123 ± 3	98.4
5	125	123 ± 3	98.4

* The same packing material was used in all cycles. After each run, the column was activated with HNO_3.

Conclusion

A comparison between the TiO_2 coated onto the surface of the silica gel and the amorphous hydrated TiO_2 showed that both forms have a similar ability to adsorb CrO_4^{2-} ions from an acidic solution. However, as shown in Fig. 3, the rate at which the equilibrium in the solid–solution interface was achieved was faster for the coated TiO_2. The time required to reach equilibrium in the batch study of the adsorption of CrO_4^{2-} by amorphous hydrated TiO_2 was 24 h.[1]

The material described here is potentially useful in the chemical analysis of CrO_4^{2-} as it also showed relatively high chemical stability towards the action of acidic and alkaline solutions. No loss of exchange capacity was observed for repeated adsorption–desorption cycles.

L. T. K. is indebted to Fundação de Amparo a Pesquisa do Estadode São Paulo (FAPESP) for a fellowship.

References

1 Strelko, V. V., Khainakov, S. A., Kvashenko, A. P., Belyakov, V. N., and Bortun, A. I., *J. Appl. Chem. USSR*, 1988, **61**, 1922.
2 Abe, M., Wang, P., Chitrakar, R., and Tsuji, M., *Analyst*, 1989, **114**, 435.
3 Kaneko, S., and Tsukamoto, K., *Chem. Lett.*, 1983, 1425.
4 Kaneko, S., and Tsukamoto, K., *Chem. Lett.*, 1984, 505.
5 Yamazaki, H., Kanno, Y., and Inoue, Y., *Bull. Chem. Soc. Jpn.*, 1989, **62**, 1837.
6 Riis, T., Dahl, I. M., and Ellestad, O. H., *J. Mol. Catal.*, 1983, **18**, 203.
7 Ellestad, O. H., and Blindheim, U., *J. Mol. Catal.*, 1985, **33**, 275.
8 Sosnov, E. A., Malkov, A. A., and Malygin, A. A., *J. Appl. Chem. USSR*, 1988, **61**, 26.
9 Slotfeldt-Ellingsen, D., Dahl, I. M., and Ellestad, O. H., *J. Mol. Catal.*, 1980, **9**, 423.
10 Ellestad, O. H., *J. Mol. Catal.*, 1985, **33**, 289.
11 Dahl, I. M., Halvorsen, S., and Slotfeldt-Ellingsen, D., *J. Mol. Catal.*, 1986, **35**, 55.
12 Brunauer, S., Emmett, P., and Teller, E., *J. Am. Chem. Soc.*, 1938, **60**, 309.
13 Kubota, L. T., Gushikem, Y., and Castro, S., *Colloids Surf.*, in the press.
14 Bond, G. C., Flamerz, S., and Shukri, R., *Faraday Discuss. Chem. Soc.*, 1989, **87**, 65.

Paper 0/01854F
Received April 26th, 1990
Accepted August 21st, 1990

Electrolytically Generated Manganese(III) Sulphate as a Redox Titrant: Potentiometric Determination of Thiosemicarbazide, Its Metal Complexes and Thiosemicarbazones

Ivan Pinto* and B. S. Sherigara†
Department of Post-Graduate Studies and Research in Chemistry, Mangalore University, Mangalagangothri 574 199, India
H. V. K. Udupa
Chemical Engineering Department, Manipal Institute of Technology, Manipal 576 119, India

Conditions have been established for the electrogeneration of Mn^{III} from Mn^{II} in a sulphuric acid medium. The Mn^{III} formed was identified and characterized by ultraviolet spectra. The stability of standard solutions of manganese(III) sulphate at various concentrations of H^+, Mn^{II} and acetic acid and in the presence of the complexing agents $P_2O_7^{4-}$, Cl^- and F^- was studied and conditions for the potentiometric determination of thiosemicarbazide (TSC), its metal complexes, $M(TSC)_2SO_4$, and its thiosemicarbazone derivatives, propanal thiosemicarbazone (PTSC) and benzaldehyde thiosemicarbazone (BTSC), have been investigated. Thiosemicarbazide in H_2SO_4 underwent a six-electron oxidation. The $M(TSC)_2SO_4$ complex participates in a 12-electron redox process, indicative of the number of TSC ligands present in the complex. The PTSC in an H_2SO_4–HOAc (20% v/v) medium underwent oxidation in two stages, namely, six-electron oxidation of TSC with the regeneration of propionaldehyde and two-electron oxidation of the aldehyde to the corresponding carboxylic acid. The benzaldehyde regenerated from BTSC did not undergo further oxidation. Above 40% HOAc, a reproducible four-electron stoichiometry was achieved thereby showing the selectivity of Mn^{III} as an oxidizing agent. The formal redox potential of the Mn^{III}–Mn^{II} couple with and without the complexing agents and at various concentrations of H^+ was determined. Addition of complexing agents decreased the formal redox potential of the Mn^{III}–Mn^{II} couple, thereby reducing the oxidation rate, but did not alter the over-all stoichiometry of the electron transfer process.

Keywords: *Potentiometric titration; electrolytically generated manganese(III) sulphate; thiosemicarbazide and its derivatives; sulphuric acid–acetic acid medium*

Manganese metal in heptavalent, tetravalent and trivalent states is known to act as a good oxidizing agent. Although Mn^{III} is one of the less stable oxidation states, it is being used increasingly, presumably because of its selectivity, for the oxidation of various compounds.[1–4] The aim of the present work was to establish conditions for the preparation of manganese(III) sulphate by the anodic oxidation of manganese(II) sulphate in an electrolytic cell, to investigate the stability of the electrolytically generated redox species and to use it as a redox titrant.

Thiosemicarbazide (TSC) and its derivatives are of interest because of their biological activities and wide synthetic and analytical applications.[5,6] Their ability to chelate trace metals is thought to be responsible for their microbial activity. The titrants employed so far for the redoximetric determination of TSC include alkali metal hypohalites, lead tetraacetate and halosulphonamides.[7] The number of electrons involved in the above redox processes was dependent on the nature of the redox species and the reaction conditions. In this work, electrolytically generated manganese(III) sulphate was employed for the determination of TSC in the free state, in the metal-bound state and as the thiosemicarbazone.

Experimental

Preparation of manganese(III) sulphate in the form of a paste, a highly concentrated form useful for organic preparation work, using an electrolytic method has been reported previously.[8] The method was suitably modified in the present study.

The electrolytic cell consisted of a 500 cm^3 beaker (Borosil) and spectroscopically pure 1% antimony–lead alloy-strips as electrodes. The ratio of anode to cathode area was maintained at 10 : 1 for higher current efficiency. The electrolyte was a 0.2 mol dm^{-3} solution of manganese(II) sulphate in 5.0 mol dm^{-3} H_2SO_4. A special quality (SQ) sample of $MnSO_4 \cdot H_2O$ (Glaxo) and analytical-reagent grade H_2SO_4 were used. Direct current was passed from a silicon rectifier unit. Electrolysis was carried out at 6 V and at a current density of 2 mA cm^{-2}, while the solution was stirred with a magnetic stirrer. The electrolysis was continued until the concentration of Mn^{III} reached 0.05 mol dm^{-3}. Further electrolysis might have resulted in a turbid suspension of sparingly soluble manganese(III) sulphate and was therefore stopped at the appropriate stage. The clear cherry-red solution contained an excess but known concentration of Mn^{II} (Table 1) to suppress the disproportionation reaction:[9]

$$Mn^{III} + Mn^{III} \rightleftharpoons Mn^{II} + Mn^{IV}$$

The solutions were prepared daily, although they appeared to be stable for at least 1 month at a H^+ concentration of >5.0 mol dm^{-3}. Analysis by atomic absorption spectrometry revealed that the concentration of lead ions in solution (owing to the dissolution of the lead electrodes) was 2.0 ppm, within the tolerance limit.

Thiosemicarbazide (Loba-Chemie, India) was purified by recrystallization from an aqueous solution of the sample. Propanal thiosemicarbazone (PTSC) was prepared by refluxing a mixture of TSC and propionaldehyde in ethanol. On cooling, some of the PTSC crystallized out in a needle-like form, the remainder was precipitated by the addition of water. The sample was recrystallized from aqueous ethanol. The PTSC was characterized by elemental analysis and by its infrared spectrum.

Benzaldehyde thiosemicarbazone (BTSC) was prepared by the same method as described above.

* Present address: St. Aloysius College, Mangalore 575 003, India.
† To whom correspondence should be addressed.

Table 1 Changes in the concentration of a 0.005 mol dm^{-3} solution of manganese(III) sulphate at various concentrations of H_2SO_4 and Mn^{II}

		Mn^{III} found (%)						
		Time/h						
$[H_2SO_4]$/ mol dm^{-3}	$[Mn^{II}]$/ mol dm^{-3}	1.0	2.0	3.0	6.0	12.0	18.0	24.0
2.5	0.102	100	100	100	100	100	100	100
	0.062	100	100	100	100	100	98.0	97.5
1.75	0.162	100	100	100	100	100	100	100
	0.112	100	100	100	100	100	100	98.2
	0.062	98.2	96.3	94.4	91.0	88.0	86.5	83.4
1.5	0.162	100	100	100	100	100	100	100
	0.112	100	100	100	100	100	98.2	91.5
	0.062	98.0	Turbidity appears and solution becomes cloudy					
1.25	0.262	100	100	100	100	100	100	100
	0.162	100	100	100	96.2	91.8	—	—
	0.112	100	100	97.4	90.5	—	—	—
1.0	0.862	100	100	96.6	93.1	88.0	—	—
	0.662	100	96.1	90.8	83.1	—	—	—
	0.262	100	—	—	—	—	—	—
0.5	0.850	Solution becomes cloudy within 15 min.						

The metal complexes, $M(TSC)_2SO_4$ (where M = Ni^{2+}, Zn^{2+} or Cd^{2+}), were obtained by mixing aqueous solutions of TSC and the corresponding salt in a molar ratio of 2 : 1.[10] The resulting solution was slowly evaporated at 60 °C over a water-bath and then cooled in ice, whereupon crystals of the complex appeared. The complexes were always purified by repeated recrystallization from warm water.

The glacial acetic acid employed was obtained from Glaxo (SQ) and was further purified by refluxing with chromium trioxide for 4 h, followed by distillation.

The absorption spectra of the Mn^{III} solutions were recorded using a Hitachi 220 ultraviolet(UV)/visible spectrophotometer with 1 cm quartz cells. Under the experimental conditions, the absorption maximum of the electrolytically generated Mn^{III} species occurred at 490 nm. Absorbance *versus* concentration graphs for manganese(III) sulphate at an H_2SO_4 concentration of 1.5–6.0 mol dm^{-3}, always containing an excess but known concentration of Mn^{II}, showed that Beer's law is obeyed at 490 nm.

Potentiometric Titration

A Digisun (India) Model 801 digital potentiometer equipped with a platinum–calomel electrode assembly was used for the potentiometric studies throughout this work.

A known volume of the reductant [TSC, $M(TSC)_2SO_4$, PTSC or BTSC] of final concentration 0.001 mol dm^{-3} in an H_2SO_4 medium of 1.0–3.0 mol dm^{-3} was placed in a 100 cm^3 beaker into which were placed a platinum indicator electrode and a standard calomel reference electrode (SCE) and the cell electromotive force (E) (V *versus* SCE) was noted. A mixture of aqueous H_2SO_4–HOAc (over-all concentration of H_2SO_4, 2.5 mol dm^{-3}; and HOAc, 20–50% v/v), was employed for the thiosemicarbazones, as these compounds are insoluble in an aqueous medium. Manganese(III) at a concentration of 0.01 mol dm^{-3} in aqueous H_2SO_4 or H_2SO_4–HOAc of appropriate concentration also containing Mn^{II} at a suitable concentration, as required for stability, was added from the micro-burette. The E (V *versus* SCE) value was noted after each addition. The titration produced a sigmoidal curve (Fig. 1). A large potential change was observed at the end-point. The potential jump at the equivalence point ranged from 500 to 600 mV per 0.05 cm^3 of 0.01 mol dm^{-3} Mn^{III}. The reaction with TSC and its metal complexes, $M(TSC)_2SO_4$ (M = Ni^{2+}, Zn^{2+} or Cd^{2+}), in an H_2SO_4 medium was moderately fast, requiring 1 h for the titration. The behaviour was different with the thiosemicarbazones, PTSC and BTSC. Because of the poor solubility of thiosemicarbazones in an aqueous medium, the reaction was carried out in an H_2SO_4–HOAc medium. The reaction was moderately fast at the beginning but as the end-point approached, it was necessary to wait 10–15 min after the addition of the titrant.

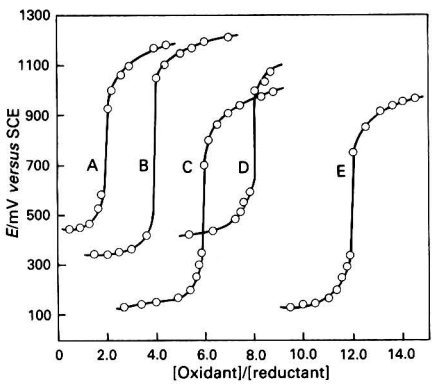

Fig. 1 Potentiometric titration curves of 0.001 mol dm^{-3} solutions of A, propionaldehyde; B, thiosemicarbazide; C, thiosemicarbazide; D, propanol thiosemicarbazone (PTSC); and E, zinc–thiosemicarbazide complex $[Zn(TSC)_2SO_4]$ titrated with a 0.01 mol dm^{-3} solution of Mn^{III}. Medium: C and E, at $[H_2SO_4]$ = 2.5 mol dm^{-3}; A and D, in an H_2SO_4 + HOAc mixture of over-all strength 2.5 mol dm^{-3} and 20% v/v, respectively; B, in an H_2SO_4 + HOAc mixture of over-all concentration 2.5 mol dm^{-3} and 40% v/v, respectively

Back-titration Method

To known amounts of reductant (10.0 cm^3 of a 0.005 mol dm^{-3} solution) in 2.5 mol dm^{-3} H_2SO_4, in an iodine flask, was added a known excess of oxidant (25.0 cm^3 of a 0.02 mol dm^{-3} solution) in 2.5 mol dm^{-3} H_2SO_4 and a known amount of Mn^{II}. The reaction mixture was allowed to stand for different intervals of time at laboratory temperature (30 °C) with occasional shaking. The excess of oxidant was determined both iodimetrically and spectrophotometrically. However, the back-titration method did not give reproducible values, probably because it conforms to a higher stoichiometry under conditions of an excess of oxidant.

Results and Discussion

It has been established[11–14] that manganese(III) sulphate in H_2SO_4 contains $Mn^{3+}(aq)$ and $Mn(OH)^{2+}(aq)$ as the reactive species

$$Mn^{3+}(aq) + H_2O \rightleftharpoons Mn(OH)^{2+}(aq) + H^+$$

Hydrolysis constant (K_h) = 0.93 ± 0.03 (reference 13)

The absorption spectra of both $Mn^{3+}(aq)$ and $Mn(OH)^{2+}(aq)$ have been reported to be similar in both the visible and UV regions.[13] The absorption spectra obtained here were consistent with those reported earlier. Previous work has shown that $MnOH^{2+}(aq)$ is more reactive, in view of the decrease in the rate of oxidation, with an increase in the concentration of H^+.[15] Formation of the dihydroxy species $Mn(OH)_2^+$ produced by further hydrolysis of $MnOH^{2+}$ is another possibility.

$$MnOH^{2+} + H_2O \rightarrow Mn(OH)_2^+ + H^+$$

A fresh solution of manganese(III) sulphate was always prepared and used immediately after the electrolysis had ceased, thereby eliminating any reaction due to $Mn(OH)_2^+$.

The molar absorption coefficient, ε, at 490 nm varied as a function of the H^+ concentration (ε ranged from 131 to 110 $dm^3\ mol^{-1}\ cm^{-1}$ at a H^+ concentration of 1.28–2.98 mol dm^{-3}) (Fig. 2). The high value of ε has been attributed to the presence of the hydrolysed species, $Mn(OH)^{2+}$.[13]

It was observed that solutions with a concentration of Mn^{III} of 0.05 mol dm^{-3} were unstable in 2–6 mol dm^{-3} H_2SO_4, giving rise to a precipitate of MnO_2 after the solution was left to stand for 24 h, as follows:

$$2Mn^{3+} + 2H_2O \rightarrow MnO_2 + Mn^{2+} + 4H^+$$

The concentration of H_2SO_4 was varied from 1.0 to 3.5 mol dm^{-3}, and the optimum value for the concentration of H_2SO_4 and the ratio of the concentrations of Mn^{III}:Mn^{II} for the solution to be stable for at least 24 h was determined. The concentration of Mn^{III} in solution was determined by adding an excess of 2% KI solution and rapidly titrating the liberated iodine against sodium thiosulphate using starch as an indicator. The changes in concentration and absorbance with time were monitored for more than 48 h. Whenever black particles of MnO_2 appeared as a result of the disproportionation reaction, the solution was filtered and the concentration and absorbance of the clear filtrate noted. At a lower concentration of H_2SO_4, manganese(III) deteriorated at a faster rate, but its stability could be increased by adding larger amounts of Mn^{II} (Table 1). Cations such as Ni^{2+}, Zn^{2+} and Cd^{2+} and anions such as HSO_4^-, ClO_4^-, $P_2O_7^{4-}$, Cl^- and F^- did not alter the stability. The oxidant species at a concentration of less than 0.002 mol dm^{-3} was found to be stable in aqueous H_2SO_4–HOAc (over-all concentration of H_2SO_4, 2.5 mol dm^{-3}; and HOAc, 20–60% v/v).

The statistical data obtained are presented in Tables 1 and 2. The redox reactions of Mn^{III} with TSC and its derivatives are stoichiometric and involve six electrons, which may be represented by the equation:

$$H_2NHN\overset{\overset{S}{\|}}{C}NH_2 + 6Mn^{3+} + 5H_2O \rightarrow 6Mn^{2+} + SO_4^{2-} + 2NH_4^+ + CNO^- + 7H^+$$

An attempt to detect CNO^- was not successful, probably because free cyanic acid (HCNO) which was liberated

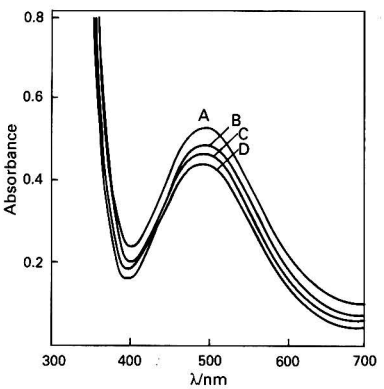

Fig. 2 Absorption spectra of Mn^{III} in H_2SO_4. [H^+]: A, 1.20; B, 1.62; C, 2.04; and D, 2.50 mol dm^{-3}

Table 2 Potentiometric titrations of TSC, its metal complexes [$M(TSC)_2SO_4$] and thiosemicarbazones (PTSC and BTSC) in H_2SO_4 and H_2SO_4–HOAc medium at 30 °C

Compound	No. of trials	Medium: Sulphuric acid/ mol dm^{-3}	Medium: Acetic acid (% v/v)	Electrons participating in redox reaction: Calculated	Electrons participating in redox reaction: Found*	Standard deviation
TSC	8	1.25	—	6.0	6.10	0.02
	8	1.5	—	6.0	6.02	—
	8	2.0	—	6.0	6.01	—
	8	2.5	—	6.0	6.01	0.04
	8	3.0	—	6.0	6.02	—
	6	2.5	20	6.0	6.05	0.03
	6	2.5	30	—	5.20	0.05
	6	2.5	40	4.0	4.00	0.02
	6	2.5	50	4.0	4.00	0.02
	6	2.5	60	4.0	4.00	0.03
$Ni(TSC)_2SO_4$	6	2.5	—	12.0	12.02	0.06
$Zn(TSC)_2SO_4$	6	2.5	—	12.0	11.99	0.05
$Cd(TSC)_2SO_4$	6	2.5	—	12.0	11.99	0.04
Propionaldehyde†	6	2.5	20	2.0	1.98	0.06
Benzaldehyde†	4	2.5	20	0	0	—
PTSC	6	2.5	20	8.0	8.02	0.02
BTSC	6	2.5	20	6.0	5.99	0.02

* Average values.
† At 70 °C.

initially was decomposed into carbon dioxide and ammonia and the latter combined with the H_2SO_4 present to form ammonium sulphate. A little of the cyanic acid, however, was not decomposed and was recognized in the evolved gas by its penetrating odour.

In H_2SO_4–HOAc medium although the reactions were moderately fast in the initial stages, they subsequently became very sluggish. Near the end-point the potential reached a steady value after 10–15 min, each titration taking about 1–2 h at 30 °C. A reproducible six-electron stoichiometry could be observed only when the acetic acid concentration in the mixture was less than 20% v/v. Therefore, the maximum permitted concentration of HOAc in the reaction mixture is 20% for a six-electron stoichiometry. However, above 40% HOAc, a reproducible four-electron stoichiometry was achieved (Table 2), as shown in the following equation:

$$H_2NHN\overset{S}{\overset{\|}{C}}NH_2 + 4Mn^{3+} + H_2O \rightarrow 4Mn^{2+} + COS + NH_4^+ + N_2 + 3H^+$$

The product, carbonyl sulphide (COS) is known to undergo slow hydrolysis[16] in acid medium to give CO_2 and H_2S

$$COS + H_2O \rightarrow CO_2 + H_2S$$

Therefore, the reaction mixture was heated to 70 °C, and the expelled gas turned lead acetate paper black, thus confirming COS as the reaction product. Carbonyl sulphide was not detected in the oxidation of TSC with Mn^{III} when the concentration of HOAc was less than 20%. These results demonstrate the selectivity of manganese(III) as an oxidizing agent, *i.e.*, it reacts differently under different reaction conditions.

Titrations with an aqueous solution of the metal complexes, $M(TSC)_2SO_4$, where M = Ni^{2+}, Zn^{2+} or Cd^{2+}, were very explicit. Twelve-electron stoichiometry conformed to two TSC ligand molecules being present in the complexes as follows:

$$M(H_2NHN\overset{S}{\overset{\|}{C}}NH_2)_2SO_4 + 12Mn^{3+} + 10H_2O \rightarrow 12Mn^{2+} + 3SO_4^{2-} + 4NH_4^+ + 2CNO^- + 14H^+ + M^{2+}$$

Propanal thiosemicarbazone in 20% HOAc medium undergoes oxidation in two stages, namely six-electron oxidation of TSC with the regeneration of propionaldehyde. At elevated temperatures (70 °C) propionaldehyde undergoes further oxidation to propionic acid. However, the rate of oxidation of propionaldehyde is sufficiently slow so that this determination is possible when conditions are adequately controlled. The reaction can be represented as

$$CH_3CH_2CH{=}NNH\overset{S}{\overset{\|}{C}}NH_2 + 6Mn^{3+} + 5H_2O \rightarrow 6Mn^{2+} + SO_4^{2-} + 2NH_4^+ + CNO^- + 7H^+ + CH_3CH_2CHO$$

$$CH_3CH_2CHO + 2Mn^{3+} + H_2O \rightarrow 2Mn^{2+} + CH_3CH_2COOH + 2H^+$$

Benzaldehyde thiosemicarbazone was oxidized in a similar manner. However, the regenerated benzaldehyde did not undergo further oxidation

$$C_6H_5CH{=}NNH\overset{S}{\overset{\|}{C}}NH_2 + 6Mn^{3+} + 5H_2O \rightarrow 6Mn^{2+} + SO_4^{2-} + 2NH_4^+ + CNO^- + 7H^+ + C_6H_5CHO$$

Benzaldehyde was identified in the ether extract of the reaction mixture as its 2,4-dinitrophenylhydrazone and could be isolated giving yields of up to 90%.

The formal redox potential of the Mn^{III}–Mn^{II} couple ($E_0'_{Mn^{III}-Mn^{II}}$) is a measure of the oxidizing power of the oxidant and it generally decreases on complexation. Different

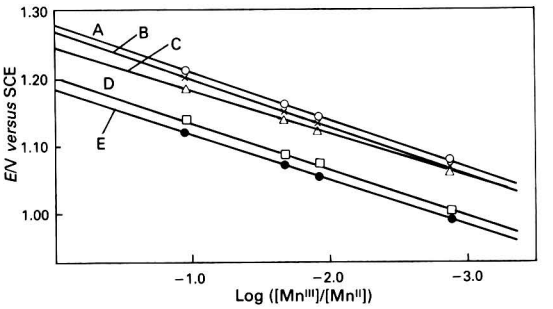

Fig. 3 Plot of E (V *versus* SCE) *versus* log([Mn^{III}]/[Mn^{II}]). Temperature = 298 K; [H_2SO_4] = 2.5 mol dm^{-3}. A, No complexing agent; B, [HSO_4^-] = 0.1 mol dm^{-3}; C, [$P_2O_7^{4-}$] = 0.1 mol dm^{-3}; D, [F^-] = 0.1 mol dm^{-3}; and E, [Cl^-] = 0.1 mol dm^{-3}

known amounts of Mn^{II} were anodically generated in a measured volume of the anolyte and the electrode potentials measured each time. The Nernst equation, in which E (V *versus* SCE) indicates the equilibrium potential of the dynamic equilibrium between the oxidized and reduced forms, which is established rapidly at the platinum indicator electrode surface, can be represented as follows:

$$E\,(\text{V } versus \text{ SCE}) = E_0'_{Mn^{III}-Mn^{II}} + \frac{2.303RT}{nF}\log\frac{[Mn^{III}]}{[Mn^{II}]}$$

where R = 8.314 J mol^{-1}, T = 298 K, n = 1, F = 96 500 C mol^{-1}. A plot of E (V *versus* SCE) against log ([Mn^{III}]/[Mn^{II}]) gave a straight line with an intercept equal to [$E_0'_{Mn^{III}-Mn^{II}} - E_{cal}$] (Fig. 1). Taking E_{cal} (standard potential of the SCE) for saturated KCl at 298 K as 0.241 V, $E_0'_{Mn^{III}-Mn^{II}}$ could be found. The measurements were carried out at different concentrations of H_2SO_4 and in the presence of the anions HSO_4^- and ClO_4^-, and the complexing agents, $P_2O_7^{4-}$, F^- and Cl^-. The formal redox potentials of the Mn^{III}–Mn^{II}couple in the presence of each of these species were calculated to be 1.52, 1.51, 1.48, 1.44 and 1.42 V, respectively (see Fig. 3).

The kinetics of the oxidation of an essential amino acid, L-histidine, by manganese(III) sulphate in H_2SO_4 has recently been studied.[15] Addition of complexing agents such as $P_2O_7^{4-}$, Cl^- and F^- decreased the oxidation rate without affecting the over-all mechanism of the reaction. A similar interpretation can be extended to the reaction between Mn^{III} and TSC, and its derivatives. In the presence of complexing agents the reaction became slightly sluggish but the over-all stoichiometry of the redox process remained the same.

Conclusions

A detailed investigation of the oxidation of TSC and its derivatives with manganese(III) sulphate under highly acidic conditions was carried out. A simple and safe method for the preparation of manganese(III) sulphate in H_2SO_4 for use as a redox titrant was developed. It was observed that reductants such as TSC and its derivatives can be titrated potentiometrically with manganese(III) sulphate in H_2SO_4 media. The reaction was moderately fast when carried out in H_2SO_4, however, the course of the reaction differed when it was performed in an H_2SO_4–HOAc medium containing more than 20% v/v HOAc. It was also noted that the addition of complexing agents reduced the formal redox potential of the Mn^{III}–Mn^{II} couple but did not alter the over-all stoichiometry of the electron transfer process.

References

1 Davies, G., *Coord. Chem. Rev.*, 1969, **4**, 199.
2 Berka, A., Vulterin, J., and Zyka, J., *Newer Redox Titrants*, Pergamon Press, London, 1965.
3 Pastor, T. J., and Antonijević, M. M., *Analyst*, 1984, **109**, 235.
4 Krishnamurthy, N., Upendra Prasad, G., and Rama Rao, K., *Talanta*, 1979, **26**, 1049.
5 Ali, M. A., and Livingstone, S. E., *Coord. Chem. Rev.*, 1974, **13**, 101.
6 Campbell, M. J. M., *Coord. Chem. Rev.*, 1975, **15**, 279, and references cited therein.
7 Gowda, B. T., and Mahadevappa, D. S., *J. Indian Chem. Soc.*, 1978, **55**, 342, and references cited therein.
8 Venkatachalapathy, R. R., and Udupa, H. V. K., *Proceedings of the Symposium on Electrolytic Cells*, Central Electrochemical Research Institute, Karaikudi, India, 1961, p. 147.
9 Selim, R. G., and Lingane, J. J., *Anal. Chim. Acta*, 1959, **21**, 536.
10 Mahadevappa, D. S., and Ananda Murthy, A. S., *Aust. J. Chem.*, 1972, **25**, 1565.
11 Diebler, H., and Sutin, N., *J. Phys. Chem.*, 1964, **68**, 174.
12 Fackler, J. P., and Chawla, I. D., *Inorg. Chem.*, 1964, **3**, 1130.
13 Wells, C. F., and Davies, G., *J. Chem. Soc. A*, 1967, 1858.
14 Rambabu, R., Vasu, P., and Dikshitalu, L. S. A., *Indian J. Chem., Sect. A*, 1987, **26**, 1027.
15 Pinto, I., Sherigara, B. S., and Udupa, H. V. K., *Bull. Chem. Soc. Jpn.*, in the press.
16 Sanderson, R. T., *Inorganic Chemistry*, Affiliated East–West Press, New Delhi, 1971, p. 233.

Paper 0/03482G
Received July 31st, 1990
Accepted October 11th, 1990

Analysis of Mixtures of Oxytetracycline and Riboflavine by First-derivative Synchronous Spectrofluorimetry

Francisco Salinas, Arsenio Muñoz de la Peña and María Soledad Durán
Department of Analytical Chemistry, University of Extremadura, 06071 Badajoz, Spain

The simultaneous determination of oxytetracycline and riboflavine in mixtures by first-derivative synchronous spectrofluorimetry is described. The proposed method is based on the formation of a fluorescent complex between aluminium and oxytetracycline, and on the native fluorescence of riboflavine. The constant wavelength difference between the excitation and emission wavelengths in a synchronous scan has been optimized by analysing the multi-dimensional information obtained on the excitation–emission matrices. The combination of synchronous scanning spectrofluorimetry and differentiation of the spectra allows for the complete resolution of the mixture. The method has been applied to the determination of these drugs in pharmaceutical preparations.

Keywords: *First-derivative synchronous spectrofluorimetry; oxytetracyline; riboflavine*

Despite the possibility of selection of both the excitation and emission wavelengths, conventional spectrofluorimetric methods have limited applicability to the analysis of complex mixtures, because the spectra are often overlapped. Hence, new approaches have been developed for multi-component analysis by spectrofluorimetry. The utilization of multi-channel detectors has been proposed,[1] but the commercially available spectrofluorimeters incorporating these detectors are not yet widely accessible. Other approaches to improve the spectral resolution are least-squares deconvolution,[2] spectra differentiation[3] and matrix-isolation spectroscopy.[4] In addition, synchronous scanning,[5] constant-energy synchronous scanning[6] and variable-angle synchronous scanning spectrofluorimetry[7] have been proposed to improve the selectivity of fluorescence methods. In order to perform multi-component analysis, it is useful to develop simple methods, which can be used on a routine basis without resorting to separation techniques that are expensive or excessively time consuming. The determination of oxytetracycline and riboflavine in mixtures, using variable-angle synchronous spectrofluorimetry, has been proposed.[8]

In the present paper, an alternative method for the analysis of pharmaceutical preparations by first-derivative synchronous spectrofluorimetry is proposed. The combination of synchronous scanning and differentiation of the spectra is a more common technique and is easier to use than variable-angle synchronous spectrofluorimetry.

Variable-angle synchronous scanning involves the use of a more sophisticated approach, hence, the technique is fairly uncommon. Three different approaches have been proposed. (*i*) In order to manipulate the speed of the monochromators, two independent motors are used. To scan, the motors are run at different rates. This has been accomplished by modifying commercially available analogue instruments.[7] (*ii*) The excitation–emission matrices are acquired and the data stored on an interfaced microcomputer. The desired angle (*viz.*, trajectory) is cut by the software.[9] (*iii*) There can also be digital control of the scanning system, controlling the speeds of the monochromator in digital-computerized instruments, by means of suitable software.[8,10]

Synchronous spectrofluorimetry does not require highly specialized equipment, as it can be performed with any commercially available spectrometer in which the excitation and emission monochromators can be interlocked. Analogue commercial apparatus are generally fitted with a synchronous-scan mode, intended originally for absorption measurements. Modern digital spectrofluorimeters all have the facility for synchronous scanning.

In order to combine synchronous spectrofluorimetry with derivative spectrometry, the equipment required is inexpensive, as the derivative technique requires only the incorporation of a simple 'outboard' circuit.[11] An alternative is to interface to a microcomputer and perform the differentiation of the spectra digitally.[12,13] Modern commercially available instrumentation allows for this possibility.

Synchronous-scanning spectrofluorimetry, in combination with derivative techniques, has been applied to the analysis of mixtures of compounds of clinical and pharmacological interest. The technique has been applied to these analyses in order to minimize the interference of bilirubin in the determination of fluorescein,[12] and it has also been used to analyse mixtures of tyrosine and tryptophan,[14] epinephrine and norepinephrine,[15] serotonin and melatonin,[16] pyridoxal, pyridoxal 5′-phosphate and pyridoxic acid,[17] histidine and histamine,[11] thiabendazole and 2-benzimidazol-2-ylcarbamic acid methyl ester,[18] mixtures of indol-3-ylacetic acid, indol-3-ylbutyric acid and indol-3-ylpropanoic acid,[19] salicylic and salicyluric acids,[13] and binary and ternary mixtures of salicylic, salicyluric and gentisic acids.[20]

The following mixtures of inorganic ions have been resolved by synchronous derivative spectrofluorimetry: binary and ternary mixtures of titanium, zirconium and hafnium;[21] gallium in the presence of aluminium;[22] gallium and zinc;[22,23] aluminium and zinc;[24] beryllium and aluminium;[25] and molybdenum and tungsten.[26]

Experimental

Apparatus

All the spectrometric measurements were recorded with a Perkin-Elmer MPF-43 fluorescence spectrophotometer, equipped with an Osram BO 150 W xenon lamp as the excitation light source and a Hamamatsu R-508 photomultiplier tube as the detector. The instrument sensitivity was adjusted daily, by using a Rhodamine B bar as a reference standard. A thermostatic water-bath circulator, Selecta 382, was used for temperature control. For synchronous measurements, both the excitation and emission monochromators were locked together and scanned simultaneously.

The spectrofluorimeter was interfaced to an IBM XT-286 microcomputer, *via* a 12-bit analogue to digital conversion card. The sampling rate was synchronized with a start-up signal from the spectrofluorimeter and with the scan rate of the monochromators. Synchronization was achieved through the closure of two micro-switches when the excitation or the

emission monochromators were scanned. The software program used was written in BASIC, and was based on previous software developed for a Commodore 64 microcomputer.[27]

The program provided a graphic display of the data on the screen, and a cursor allowed the wavelength and the relative fluorescence intensity at any point of the spectrum to be requested. Spectra could be subtracted from each other, stored on a disk file, output to a printer and subsequently recalled from the disk for further manipulation. Smoothing is achieved and derivatives are calculated by the Savitzky–Golay procedure.[28,29] The program also allows for the collection of three-dimensional spectra by successively scanning the emission monochromator at different excitation wavelengths. The spectra can be represented as a pseudo-isometric three-dimensional plot. In the plot, the spectra are superimposed with the aid of a 'hidden line removal' routine in order to clarify them. The program has the capability of generating contour plots. In this representation the two normal axes represent the emission and excitation wavelengths, while the intensities are expressed as a series of contours. Contours are produced by connecting points of equal fluorescence, using contour lines. These equifluorescence lines are calculated by linear interpolation between neighbouring points in the excitation–emission matrix to find the (λ_{ex}, λ_{em}) pair corresponding to the fluorescence of the contours.

The three-dimensional data files can also be converted for use as the input data of a commercial program, SURFER (from Golden Software),[30] in order to obtain isometric projections or contour maps.

Reagents

All the experiments were performed with analytical-reagent grade chemicals and pure solvents. Doubly distilled, demineralized water was used throughout.

Oxytetracycline was obtained from Sigma. A stock solution was prepared in a 100 ml calibrated flask by dissolving 0.05 g of the drug in water. Riboflavine was obtained from Sigma. A stock solution was prepared in a 500 ml calibrated flask by dissolving 0.01 g of the drug in water. These stock solutions were used to prepare standard solutions by suitable dilutions.

Sodium hydroxide–potassium hydrogen phosphate (0.05 mol dm^{-3}) of pH 5, acetic acid–sodium acetate (1 mol dm^{-3}) of pH 5 and aluminium chloride (0.05 mol dm^{-3}), in water, were also used.

Procedure

To an aliquot of the sample solution, containing between 0.05 and 0.33 μmol of oxytetracycline and between 0.001 and 0.02 μmol of riboflavine, add 3 ml of 0.05 mol dm^{-3} aluminium chloride and 3 ml of 1 mol dm^{-3} acetic acid–sodium acetate buffer of pH 5, and dilute to 25 ml with distilled water. Record the synchronous spectra, by using the following fixed instrumental parameters: $\Delta\lambda = \lambda_{em} - \lambda_{ex} = 60$ nm; scan speed, 240 nm min^{-1}; and spectrofluorimeter response time, 1.5 s. Record the spectra on a disk file and calculate the first-derivative spectra by the Savitzky–Golay method,[28,29] with a bandwidth of 15 nm. Take first-derivative measurements as the vertical distance from the first-derivative synchronous spectrum at $\lambda_{ex}/\lambda_{em} = 373/433$ nm to the baseline for oxytetracycline and from $\lambda_{ex}/\lambda_{em} = 471/531$ nm to the baseline for riboflavine. In order to construct the calibration graphs, record first-derivative synchronous spectra of known amounts of oxytetracycline and riboflavine under the conditions given above.

Results and Discussion

The objective of this work was to resolve mixtures of oxytetracycline and riboflavine, by using first-derivative synchronous spectrofluorimetry. The optimum chemical conditions for the resolution of these compounds in their mixtures were established.

Riboflavine shows remarkably intense native fluorescence, whereas oxytetracycline shows only weak fluorescence in aqueous solution. The spectrofluorimetric determination of oxytetracycline has been enhanced by the formation of fluorescent complexes with aluminium,[31,32] calcium,[33–36] magnesium[37,38] and beryllium.[39]

In this paper, aluminium was utilized as the complexing agent, because of the higher emission intensity of the complex formed with oxytetracycline, compared with that of other ions. This is consistent with Clark *et al.*,[8] who used aluminium for the resolution of oxytetracycline and riboflavine mixtures by variable-angle synchronous spectrofluorimetry.

Spectral Characteristics and Effect of Experimental Variables

The excitation and emission fluorescence spectra of oxytetracycline in the presence of aluminium, and riboflavine are shown in Fig. 1. Aluminium has no influence on the fluorescence of riboflavine. The fluorescence intensity of oxytetracycline is enhanced about 8-fold in the presence of aluminium. Excitation and emission maxima for oxytetracycline are at 392 and 460 nm, respectively, while the corresponding maxima for riboflavine are centred at 378 and 465 nm for excitation and at 525 nm for emission. With excitation at 465 nm, oxytetracycline shows a negligible fluorescence and under these conditions it is possible to determine riboflavine, by measuring its emission at 525 nm, in the presence of oxytetracycline. However, oxytetracycline cannot be determined in the presence of riboflavine owing to overlapping of the spectra. It is not possible to use conventional spectrofluorimetry to determine both compounds simultaneously, although by appropriate selection of the excitation and emission wavelengths, riboflavine can be determined without interference from oxytetracycline.

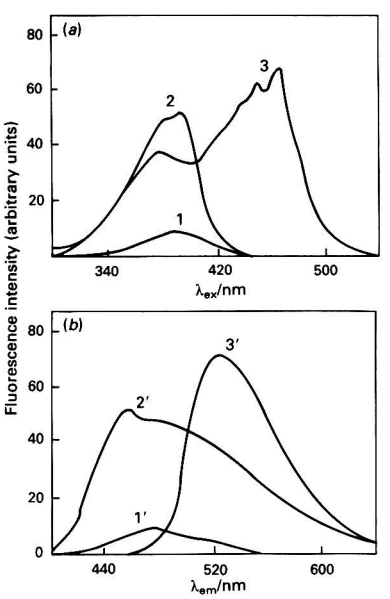

Fig. 1 (*a*) Excitation and (*b*) emission spectra of: 1 and 1′, oxytetracycline; 2 and 2′, oxytetracycline–aluminium complex; and 3 and 3′, riboflavine at pH 5. [Oxytetracycline] = 11 μmol dm^{-3}; [riboflavine] = 0.53 μmol dm^{-3}; and [aluminium] = 0.2 mol dm^{-3}

Studies of the effect of acidity on the fluorescence intensity showed that the fluorescence emission increases with pH, up to pH 2 for the oxytetracycline–aluminium complex, and up to pH 4 for riboflavine. The fluorescence intensity reaches a maximum and levels off at pH 10.6 for the oxytetracycline–aluminium complex and at pH 8.5 for riboflavine, decreasing at higher pH values. Consequently, pH 5 was selected as the optimum for the determination of both species.

Initial experiments were performed using 0.05 mol dm^{-3} sodium hydroxide–sodium hydrogen phosphate buffer of pH 5 to control the pH. However, under these conditions, the buffer did not function satisfactorily, probably because of the high aluminium concentration in the solutions. Consequently, an acetic acid–sodium acetate (1 mol dm^{-3}) solution of pH 5, which has a superior buffering capacity, was tested. By assaying different concentrations of the buffer solution, it was found that the intensity of the fluorescence of riboflavine is not affected by the buffer solution concentration, whereas the emission of the complex of oxytetracycline with aluminium decreases slightly with an increase in the buffer concentration. A 0.12 mol dm^{-3} buffer concentration was selected as the optimum.

A study of the stability of the solutions (at 20 °C) showed that the compounds were stable for at least 1 h (Table 1). The complex of oxytetracycline with aluminium is not formed immediately, requiring about 15 min to reach maximum fluorescence, it is then stable during the first hour, with the fluorescence decreasing slowly thereafter. The fluorescence of riboflavine develops immediately after sample preparation and is also constant during the first hour, decreasing over longer periods of time. Consequently, the measurements were performed 15 min after the preparation of the samples.

The dependence of the fluorescence intensity on temperature is critical, the fluorescence emission decreasing when the temperature increases. Therefore, it is recommended that a thermostatically controlled water-bath be used, choosing a measurement temperature of 20 °C. The fluorescence intensity of both compounds is not affected by the order of addition of the reagents. Also, the effect of the concentration of aluminium in the medium was studied. The presence of this species does not affect the fluorescence of riboflavine. For 11 μmol dm^{-3} oxytetracycline solutions, the fluorescence intensity increases with increasing aluminium concentrations of up to 2×10^{-3} mol dm^{-3}, remaining constant for higher aluminium concentrations. A 6×10^{-3} mol dm^{-3} aluminium concentration was selected to ensure an excess of aluminium.

Selection of the Optimum Δλ for Synchronous Scanning

As has been stated above, the analysis of mixtures of riboflavine and oxytetracycline is not possible by conventional spectrofluorimetry because of the overlapping of the emission spectra. Previously, in order to record synchronous scans, it was necessary to optimize the difference between the excitation and emission wavelengths. Hence, the three-dimensional spectra of riboflavine, of the oxytetracycline–aluminium complex and of a mixture of both have been obtained. The spectra were acquired by scanning the emission wavelength between 400 and 640 nm by varying the excitation spectra at 8 nm increments from 300 to 540 nm.

The pseudo-isometric three-dimensional projections of the excitation–emission matrices of riboflavine, of the oxytetracycline–aluminium complex, and of a mixture of both compounds are shown in Fig. 2. The wavelength scanning interval, Δλ, must be optimized in order to minimize the spectral interference caused by each compound in the mixture, with the minimum loss of sensitivity. In order to perform the optimization graphically, the three-dimensional data matrix was transferred to two dimensions by using the cartographic technique of contour plotting. In this method, iso-emissive contours plotted in the (λ_{ex}, λ_{em}) plane map the (F, λ_{ex}, λ_{em}) surface at stepped intervals. In principle, the data set is viewed from a point vertically above the (λ_{ex}, λ_{em}) plane, the fluorescence levels being represented by contours in this plane. In this representation, all the information is displayed in a single plane, so that small peaks are not 'hidden' by larger foreground peaks as in the isometric presentation. The contour representation is shown in Fig. 3. From the contour plots of riboflavine, of the oxytetracycline–aluminium complex and of the mixture, it can be inferred that a Δλ of 60 nm appears to be the optimum for synchronous scanning as this passes around the maximum for both compounds. It is also evident that variable-angle synchronous scanning at 64.3°, as proposed by Clark *et al.*[8] would permit the determination of oxytetracycline without interference from riboflavine.

Table 1 Stability of oxytetracycline (11 μmol dm^{-3}) ($\lambda_{ex}/\lambda_{em}$ = 392/460 nm) and riboflavine (0.53 μmol dm^{-3}) ($\lambda_{ex}/\lambda_{em}$ = 465/525 nm) solutions, in the presence of aluminium, at pH = 5. (The values given are for fluorescence intensity in arbitrary units)

	Time/min						
Compound	0	15	30	45	60	90	120
Oxytetracycline	48.0	54.0	54.0	54.0	53.5	40.0	30.5
Riboflavine	69.0	69.0	68.5	69.0	69.0	62.0	59.0

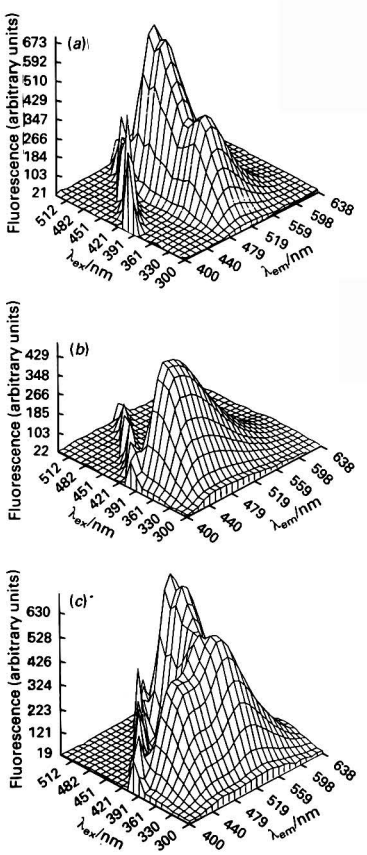

Fig. 2 Pseudo-isometric three-dimensional projections of the excitation–emission matrix of (*a*) riboflavine (1 μmol dm^{-3}); (*b*) oxytetracycline–aluminium complex (22 μmol dm^{-3}); and (*c*) a mixture of both compounds

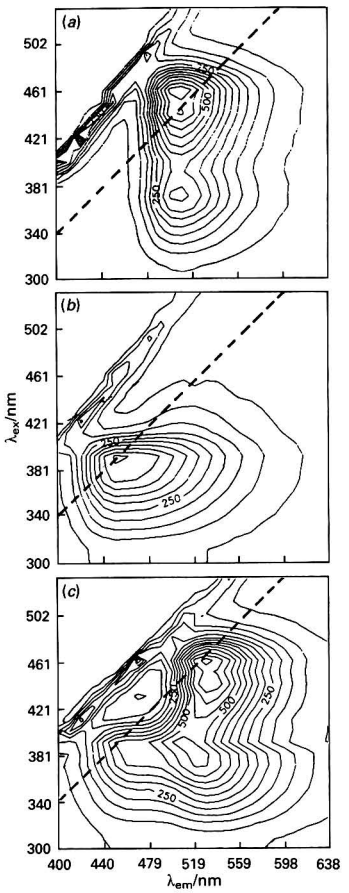

Fig. 3 Contour plots of the excitation–emission matrix of (*a*) riboflavine (1 μmol dm^{-3}); (*b*) oxytetracycline–aluminium complex (22 μmol dm^{-3}); and (*c*) a mixture of both compounds. The diagonal broken line slices the data matrix at an angle of 45°, maintaining a constant $\Delta\lambda = \lambda_{em} - \lambda_{ex} = 60$ nm

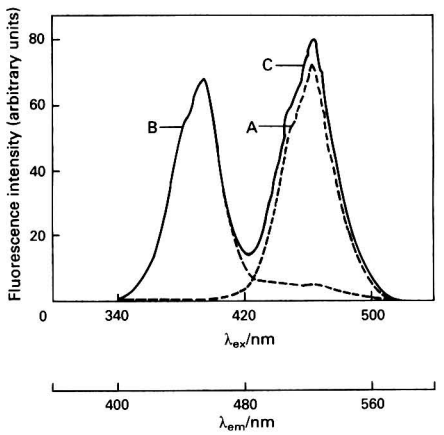

Fig. 4 Synchronous spectra ($\Delta\lambda$ = 60 nm) of A, riboflavine (1 μmol dm^{-3}); B, oxytetracycline–aluminium complex (22 μmol dm^{-3}); and C, a mixture of both compounds

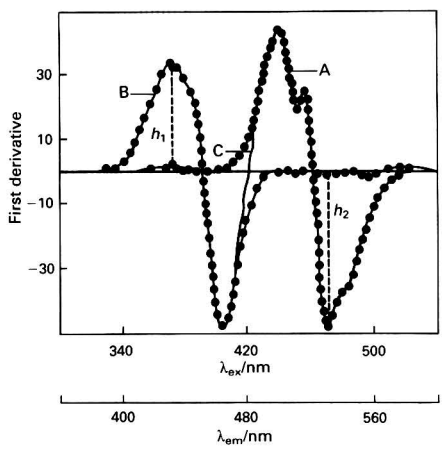

Fig. 5 First-derivative synchronous spectra ($\Delta\lambda$ = 60 nm) of A, riboflavine (1 μmol dm^{-3}); B, oxytetracycline–aluminium complex (22 μmol dm^{-3}); and C, a mixture of both compounds

Fig. 4 shows the synchronous spectra of riboflavine, of the oxytetracycline–aluminium complex and of a mixture of both compounds, while maintaining a constant interval between the emission and excitation wavelengths ($\Delta\lambda = \lambda_{em} - \lambda_{ex} = 60$ nm). From Fig. 4, it can be concluded that oxytetracycline can be determined in the presence of riboflavine at $\lambda_{ex}/\lambda_{em}$ = 392/460 nm, the maximum of the emission of the complex of oxytetracycline with aluminium.

The determination of riboflavine, however, would be interfered with by the oxytetracycline contribution at $\lambda_{ex}/\lambda_{em}$ = 465/525 nm, where the fluorescence of riboflavine is at a maximum. In order to resolve this overlapping, differentiation of the spectra was used. The variables to be optimized when applying the derivative technique to these synchronous spectra are the bandwidth used to calculate the first-derivative spectra by the Savitzky–Golay method,[28,29] the speed of the monochromators, the spectrofluorimeter response time and the wavelengths of measurement for the correct determination of both analytes.

The available bandwidths for the calculation of the derivative spectra obtained by the Savitzky–Golay method[28,29] are 5, 9, 15, 21 and 25 nm, corresponding to 5-, 9-, 15-, 21- and 25-point calculations, respectively. A bandwidth of 15 nm was selected as yielding the best signal to noise ratio. A scan speed of 240 nm min^{-1} and a spectrofluorimeter response time of 1.5 s were selected after verifying that these parameters did not affect the derivative signal obtained, as the differentiation is obtained numerically and not electronically.

The first-derivative synchronous spectra of riboflavine, the oxytetracycline–aluminium complex and a mixture of both compounds are shown in Fig. 5. In order to discriminate between the overlapping bands, it is necessary that a linear relationship be maintained between the analyte concentration and the fluorescence signal in the over-all concentration range studied. It has been shown that the height h_1 ($\lambda_{ex}/\lambda_{em}$ = 373/433 nm) is proportional to the oxytetracycline concentration, whereas h_2 ($\lambda_{ex}/\lambda_{em}$ = 471/531 nm) is proportional to the riboflavine concentration (Fig. 5).

Analytical Parameters

In order to test the mutual independence of the analytical signals for oxytetracycline and riboflavine, *i.e.*, to show that h_1 and h_2 are independent of riboflavine and oxytetracycline concentrations, respectively, three calibration graphs were obtained from height (*h*) measurements for oxytetracycline standards between 2.2 and 13.2 μmol dm^{-3} in the absence of

Table 2 Statistical analysis of the determination of oxytetracycline (2.2–13.2 μmol dm^{-3}) and riboflavine (0.042–0.85 μmol dm^{-3}) in mixtures by first-derivative synchronous spectrofluorimetry

	Other compound present				
Compound determined	Compound	Concentration/ μmol dm^{-3}	Slope	Intercept	Regression coefficient
Oxytetracycline	Riboflavine	—	4.92	2.95	0.998
		0.21	5.01	2.63	0.998
		0.64	4.90	3.08	0.998
Riboflavine	Oxytetracycline	—	146.08	0.76	0.999
		4.4	145.72	0.56	0.999
		11.0	145.64	0.13	0.999

Table 3 Determination of oxytetracycline and riboflavine in binary mixtures (E = relative error)

Riboflavine : oxytetracycline ratio	[Riboflavine]/ μmol dm^{-3}			[Oxytetracycline]/ μmol dm^{-3}		
	Taken	Found	E(%)	Taken	Found	E(%)
1:4	0.425	0.420	1.2	1.76	1.78	1.1
1:8	0.798	0.774	3.0	6.61	6.52	1.4
1:17	0.106	0.103	2.8	1.76	1.72	2.3
1:21	0.106	0.103	2.8	2.20	2.22	0.9
1:50	0.106	0.103	2.8	5.29	5.24	1.0
1:100	0.106	0.103	2.8	10.57	10.51	0.6

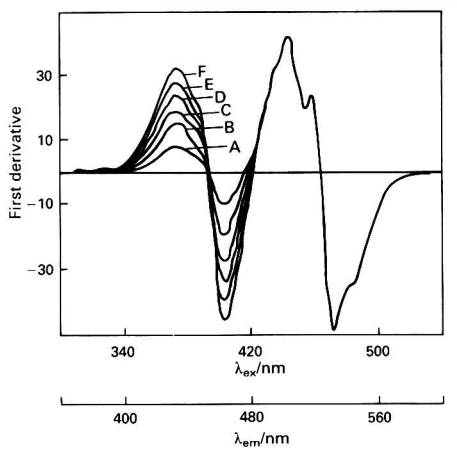

Fig. 6 Calibration graph for the determination of oxytetracycline in the presence of 0.64 μmol dm^{-3} riboflavine. Measurement of the first-derivative signal at $\lambda_{ex}/\lambda_{em}$ = 373/433 nm (zero-crossing of the riboflavine contribution). Oxytetracycline concentration: A, 2.2; B, 4.4; C, 6.6; D, 8.8; E, 11.0; and F, 13.2 μmol dm^{-3}

riboflavine and in the presence of 0.21 and 0.64 μmol dm^{-3} riboflavine. The results obtained in the presence of 0.64 μmol dm^{-3} riboflavine are shown in Fig. 6, and the analytical parameters for the three calibration graphs are summarized in Table 2.

Following the same procedure, three calibration graphs were constructed for riboflavine standards containing between 0.042 and 0.85 μmol dm^{-3} riboflavine in the absence of oxytetracycline and in the presence of 4.4 and 11 μmol dm^{-3} oxytetracycline. The results obtained in the presence of 11 μmol dm^{-3} oxytetracycline are shown in Fig. 7, and the analytical parameters for the three calibration graphs are also summarized in Table 2.

The relative standard deviations (p = 0.05, n = 10) are 2.2% for 8.8 μmol dm^{-3} oxytetracycline and 8.8% for 0.21 μmol dm^{-3} riboflavine.

The first-derivative synchronous-scanning method was applied to the analysis of several synthetic mixtures of oxytetracycline and riboflavine in different ratios. Table 3 summarizes the results calculated from the calibration graphs.

Table 4 Results of the determination of oxytetracycline and riboflavine in terramycin capsules (composition: 250 mg of oxytetracycline and 2.5 mg of riboflavine per capsule)

	Oxytetracycline		Riboflavine	
Sample	Found/mg	Recovery (%)	Found/mg	Recovery (%)
1	252.4	101.0	2.49	99.6
2	250.0	100.0	2.51	100.4
3	251.5	100.6	2.50	100.0

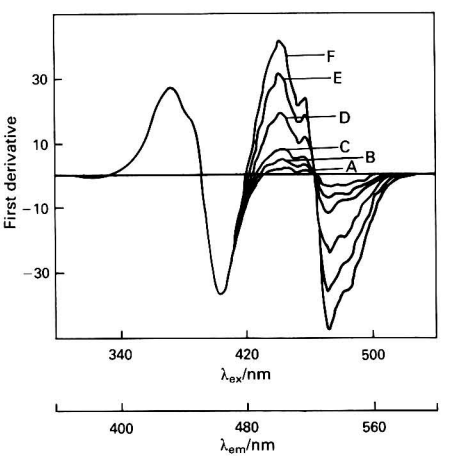

Fig. 7 Calibration graph for the determination of riboflavine in the presence of 11 μmol dm^{-3} oxytetracycline. Measurement of the first-derivative signal at $\lambda_{ex}/\lambda_{em}$ = 471/531 nm (zero-crossing of the oxytetracycline contribution). Riboflavine concentration: A, 0.042; B, 0.127; C, 0.213; D, 0.420; E, 0.640; and F, 0.850 μmol dm^{-3}

Analysis of Oxytetracycline and Riboflavine Mixtures in Pharmaceuticals

Tetracyclines are frequently administered in combination with vitamin complexes. In one of several commercially available dosage forms, oxytetracycline is formulated with vitamin C and with the B complex vitamins (thiamine, nicotinamide and

riboflavine). The proposed method was applied to the determination of these compounds in terramycin capsules. Working samples were prepared by dissolving appropriate amounts of the pharmaceuticals in water. The assay was completed as described under Procedure.

Table 4 shows the results of three replicate analyses of terramycin capsules. The accuracy and precision are satisfactory, and the results conform satisfactorily to the label claims.

Conclusions

The above findings substantiate the usefulness of first-derivative synchronous spectrofluorimetry for the analysis of mixtures of the two compounds tested. The first-derivative technique enables reproducible and accurate measurements to be made, as demonstrated by the statistical analysis of the results.

The proposed method is simpler to perform than the variable-angle synchronous-scanning method, allowing the simultaneous resolution of a mixture in a single scan.

The authors gratefully acknowledge financial support from the Central Nuclear de Almaraz.

References

1 Warner, I. M., Patonay, G., and Thomas, M. P., *Anal. Chem.*, 1985, **57**, 463A.
2 Lindberg, W., Persson, J. A., and Wood, S., *Anal. Chem.*, 1983, **55**, 643.
3 Green, G. L., and O'Haver, T. C., *Anal. Chem.*, 1974, **46**, 2191.
4 O'Haver, T. C., and Parks, W. M., *Anal. Chem.*, 1974, **46**, 1886.
5 Vo-Dinh, T., *Anal. Chem.*, 1978, **50**, 396.
6 Inman, E. L., and Winefordner, J. D., *Anal. Chem.*, 1982, **54**, 2018.
7 Miller, J. N., *Analyst*, 1984, **109**, 191.
8 Clark, B. J., Fell, A. F., Milne, K. T., Pattie, D. G., and Williams, M. H., *Anal. Chim. Acta*, 1985, **170**, 35.
9 Clark, B. J., Fell, A. F., Aitchison, I. E., Pattie, D. M. G., Williams, M. H., and Miller, J. N., *Spectrochim. Acta, Part B*, 1983, **38**, 61.
10 Oms, M. T., Cerdá, V., García Sánchez, F., and Ramos, A. L., *Talanta*, 1988, **35**, 671.
11 Gutiérrez, M. C., Rubio, S., Gómez-Hens, A., and Valcárcel, M., *Talanta*, 1987, **34**, 325.
12 Bright, F. V., and McGown, L. B., *Analyst*, 1986, **111**, 205.
13 Muñoz de la Peña, A., Salinas, F., and Durán-Merás, I., *Anal. Chem.*, 1988, **60**, 2493.
14 Miller, J. N., Fell, A. F., and Ahmad, T. A., *Anal. Proc.*, 1982, **19**, 37.
15 Valcárcel, M., Gómez-Hens, A., and Rubio, S., *Clin. Chem.*, 1985, **31**, 1790.
16 Ortega, M. C., Reyes, A., Morell, M., and Laserna, J. J., *Anal. Lett.*, 1986, **19**, 1097.
17 Petidier, A., Rubio, S., Gómez-Hens, A., and Valcárcel, M., *Anal. Biochem.*, 1986, **157**, 212.
18 García Sánchez, F., and Cruces Blanco, C., *Anal. Chem.*, 1988, **60**, 323.
19 García Sánchez, F., Cruces Blanco, C., Ramos Rubio, A. L., Hernández López, M., Márquez Gómez, J. C., and Carnero, C., *Anal. Chim. Acta*, 1988, **205**, 149.
20 Salinas, F., Muñoz de la Peña, A., Durán-Merás, I., and Durán, M. S., *Analyst*, 1990, **115**, 1007.
21 Rubio, S., Gómez-Hens, A., and Valcárcel, M., *Anal. Chem.*, 1985, **57**, 1101.
22 Salgado, M., Ureña, M. E., García de Torres, A., and Cano Pavón, J. M., *J. Mol. Struct.*, 1986, **143**, 477.
23 Ureña, M. E., García de Torres, A., and Cano Pavón, J. M., *Anal. Chem.*, 1987, **59**, 1129.
24 Muñoz de la Peña, A., Salinas, F., Sánchez, M. E., and Murillo, J. A., *Analyst*, 1988, **113**, 1435.
25 García Sánchez, F., Márquez Gómez, J. C., and Hernández López, M., *Analyst*, 1987, **112**, 649.
26 Salinas, F., Muñoz de la Peña, A., Capitán-Vallvey, L. F., and Navalón, A., *Analyst*, 1989, **114**, 1297.
27 Muñoz de la Peña, A., Murillo, J. A., Vega, J. M., and Baringo, F., *Comput. Chem.*, 1988, **12**, 213.
28 Savitzky, A., and Golay, M. J. E., *Anal. Chem.*, 1964, **36**, 1627.
29 Steinier, J., Termonia, Y., and Deltour, J., *Anal. Chem.*, 1972, **44**, 1906.
30 Golden Software Inc., P.O. Box 281, Golden, CO, USA.
31 Hall, D., *J. Pharm. Pharmacol.*, 1976, **28**, 420.
32 Hall, D., *Br. J. Clin. Pharmacol.*, 1977, **4**, 57.
33 Kohn, K. W., *Anal. Chem.*, 1961, **33**, 862.
34 Poiger, H., and Schlatter, C., *Analyst*, 1976, **101**, 808.
35 Day, S. T., Crouthamel, W. G., Martinelli, L. C., and Ma, J. K. H., *J. Pharm. Sci.*, 1978, **67**, 1518.
36 van der Bogert, C., and Kroon, A. M., *J. Pharm. Sci.*, 1981, **70**, 186.
37 Ibsen, K. H., Saunders, R. L., and Urist, M. R., *Anal. Biochem.*, 1963, **5**, 505.
38 Lever, M., *Biochem. Med.*, 1972, **6**, 216.
39 Alykova, T. V., *Antibiotiki (Moscow)*, 1972, **17**, 353.

Paper 0/02446E
Received June 1st, 1990
Accepted October 24th, 1990

Inhibition of the Peroxidase-like Activity of Manganese Tetrakis(sulphophenyl)porphyrin by Pyridine and Other Substances

Fang Wang and Yun-Xiang Ci*
Department of Chemistry, Peking University, Beijing 100871, People's Republic of China

The inhibition of the peroxidase-like activity of manganese tetrakis(sulphophenyl)porphyrin (Mn-$TPPS_4$) by pyridine and other substances has been studied. The inhibition by spin-trapping species is non-reversible. The constants for the competitively linear reversible inhibitors pyridine and *p*-chlorophenol have been determined from the Michaelis–Menten equation by using H_2O_2 as substrate. The mechanism of the peroxidase-like activity of Mn-$TPPS_4$ is discussed.

Keywords: *Inhibition; pyridine; peroxidase mimesis; manganese porphyrin; fluorescence reaction*

Enzymes have been widely used in biochemistry, chemical engineering and clinical chemistry. However, enzymes are expensive and their solutions are not stable; hence the study of potential enzyme-mimicking compounds is of increasing interest in analytical biochemistry. It has been found that peroxidase-like metalloporphyrins can catalyse the formation of fluorescent dimers.[1–4] Trace amounts of hydrogen peroxide and glucose can be determined by using peroxidase-like metalloporphyrin systems. The catalytic activities of those compounds that mimic peroxidase were measured by using a kinetic method. Recently, evidence was presented[5] that the peroxidase-like activity of manganese tetrakis[4-(*N,N,N*-trimethylamino)]porphyrin [Mn-T(4-TAP)P] proceeds *via* the following reaction mechanism:

$$MP + H_2O_2 \underset{k_2}{\overset{k_1}{\rightleftharpoons}} (MP)S + H_2O \quad (1)$$

$$(MP)S + AH \overset{k_3}{\rightleftharpoons} (MP)S' + A^{\cdot} \quad (2)$$

$$(MP)S' + AH \overset{k_5}{\rightleftharpoons} MP + H_2O + A^{\cdot} \quad (3)$$

$$A^{\cdot} + A^{\cdot} \overset{k_7}{\longrightarrow} A\text{–}A \quad (4)$$

where MP is a peroxidase-like metalloporphyrin such as Mn-T(4-TAP)P, AH is a substrate such as chavicol and (MP)S and (MP)S′ are the enzyme–substrate complexes formed in the reaction. In this paper, the inhibition of the peroxidase-like activity of manganese tetrakis(sulphophenyl)porphyrin (Mn-$TPPS_4$), by pyridine and other substances, has been studied in the fluorescence reaction of homovanillic acid (HVA) with H_2O_2, which proceeds as follows (HRP = horseradish peroxidase):[6]

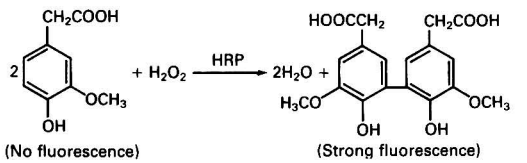

(No fluorescence) (Strong fluorescence)

From the inhibition of the peroxidase-like activity of the metalloporphyrin, the above mechanism has been confirmed.

* To whom correspondence should be addressed.

Experimental

Apparatus

The fluorescence spectra and relative fluorescence intensity were measured with a Hitachi Model-850 fluorescence spectrophotometer (with a 10 mm silica cell).

Reagents

All the chemicals used were of analytical-reagent grade, and all aqueous solutions were made up in triply distilled water.

In order to prepare triply distilled water, doubly distilled water was passed through a charcoal column. Potassium permanganate was added to the eluate to kill bacteria. The water was then distilled from a silica flask.

Homovanillic acid (Merck) was dissolved in triply distilled water. Hydrogen peroxide solutions were prepared by dilution of a 30% solution (titrated with a standard solution of potassium permanganate) with triply distilled water. A 0.5 mol dm^{-3} NaOH solution was also used. The Mn-$TPPS_4$ was synthesized as described previously.[1]

Procedure

Solutions of HVA, Mn-$TPPS_4$, inhibitor and 0.5 ml of 0.5 mol dm^{-3} NaOH were placed in a 5.0 ml calibrated flask and diluted to about 4.5 ml. The flask was then immersed in a

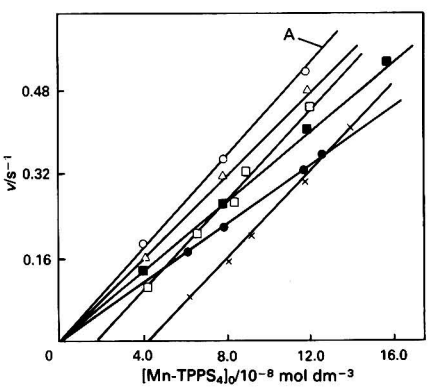

Fig. 1 Inhibition of the peroxidase-like activity of Mn-$TPPS_4$ by △, ■ and ●, reversible inhibitors; and □ and ×, non-reversible inhibitors. △, Diethylenetriamine (1.0×10^{-3} mol dm^{-3}); ■, pyridine (1.0×10^{-2} mol dm^{-3}); ●, *p*-chlorophenol (6.8×10^{-4} mol dm^{-3}); □, DPPH (1.0×10^{-3} mol dm^{-3}); and ×, hydroquinone (1.8×10^{-5} mol dm^{-3}). $[HVA]_0$: 2.0×10^{-3} mol dm^{-3}; $[H_2O_2]_0$: 2.3×10^{-5} mol dm^{-3}. The line marked A shows the result obtained when there is no inhibition

thermostatically controlled water-bath at 30 ± 0.5 °C. After 5 min, slightly less than 0.5 ml of H_2O_2 solution was added and the mixture was diluted to the 5.0 ml mark with triply distilled water. The change in fluorescence intensity with time was measured at an emission maximum of 424 nm with an excitation maximum of 318 nm.

Results and Discussion

Reversible and Non-reversible Inhibition of the Peroxidase-like Activity of Mn-TPPS$_4$

The effect of the concentration of Mn-TPPS$_4$ on the initial rate was studied under conditions where the concentrations of H_2O_2 and HVA were saturated in the test system (shown by line A in Fig. 1).

Inhibitors have effects on the initial rate. From Fig. 1, it can be seen that some inhibitors, such as diethylenetriamine, pyridine and *p*-chlorophenol, have effects only on the slope of line A. The inhibition by these ligands is reversible. The other inhibitors, such as hydroquinone and the 2,2,6,6-tetramethyl-4-hydroxy-1-piperidinyloxy (DPPH) radical, have effects only

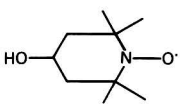

DPPH

on a section of line A rather than on the slope. This type of inhibition is non-reversible. These non-reversible inhibitors are traps to free radicals and can capture those produced in the fluorescence reaction. Therefore, the concentration of peroxidase-like Mn-TPPS$_4$ is sufficiently high to produce more free radicals in the catalysis, so that the fluorescent dimer of HVA can be formed. From the above discussion, it can be seen that the free radicals are produced in the catalysis of the peroxidase-like Mn-TPPS$_4$.

Inhibition of the Peroxidase-like Activity of Mn-TPPS$_4$ by Using H_2O_2 as Substrate

The inhibition of the peroxidase-like activity of Mn-TPPS$_4$ by pyridine and *p*-chlorophenol was studied by using the initial-rate method and assuming steady-state conditions.[7] It was shown that the concentration of HVA was saturated in the test system. The results are shown in Fig. 2, where the slope and the intercept on the ordinate are represented by b_1 and a_1, respectively. The Michaelis–Menten constant, $K_{m(obs)} = a_1/b_1$, and the reaction-rate maximum $V_{max(obs)} = 1/a_1$ were obtained from Lineweaver–Burk plots ($1/v$ *versus* $1/[H_2O_2]_0$) (v = reaction rate),[8] as shown in Fig. 2. From Fig. 2, it can be seen that a_1 remains unchanged, within experimental error.

Fig. 3 shows that $K_{m(obs)}/K_m$ is proportional to the concentration of the inhibitor, within experimental error. The above results indicate that $V_{max(obs)}$ remains unchanged and that $K_{m(obs)}$ increases with an incremental increase in the concentration of the inhibitor.

It is known that the following relationship holds:[9]

$$1/v = K_m(1 + K_I[I])/V_{max}[S]_0 + 1/V_{max}$$

for the first-order enzymic reaction when the reversible inhibition is competitively linear, where K_m is the Michaelis–Menten constant, and V_{max} is the reaction-rate maximum. The inhibitor constant, K_I, is defined by $K_I = [EI]/[E][I]$, where [I] is the concentration of inhibitor, [E] is the concentration of enzyme and $[S]_0$ is the initial concentration of the substrate. From the above equation, it can be seen that if an inhibition

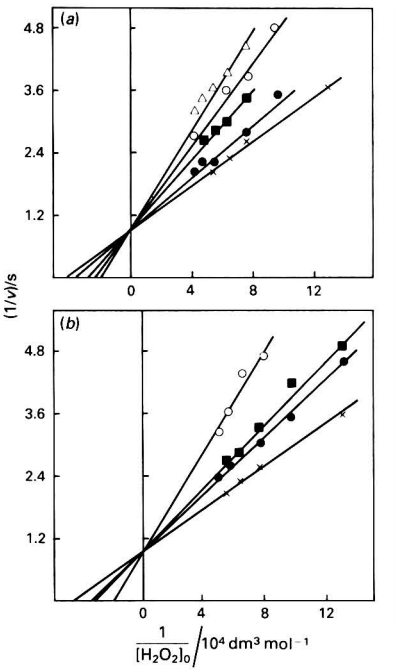

Fig. 2 Variation of $1/v$ with $1/[H_2O_2]_0$ in the presence of inhibitors. Mn-TPPS$_4$: 9.44×10^{-8} mol dm^{-3}; HVA: 1.92×10^{-3} mol dm^{-3}. (*a*) Pyridine: ×, 0; ●, 0.08; ■, 1.60×10^{-2}; ○, 2.40×10^{-2}; and △, 3.20×10^{-2} mol dm^{-3}. (*b*) *p*-Chlorophenol: ×, 0; ●, 2.74×10^{-4}; ■, 4.08×10^{-4}; and ○, 6.80×10^{-4} mol dm^{-3}

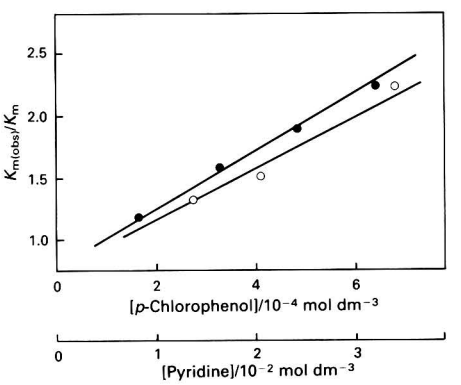

Fig. 3 Variation of $K_{m(obs)}/K_m$ with the concentration of inhibitor. ●, Pyridine; and ○, *p*-chlorophenol

proceeds competitively, the reaction-rate maximum, V_{max}, remains unchanged. The competitive inhibition manifests itself in the Michaelis–Menten constant, $K_{m(obs)} = K_m(1 + K_I[I])$, where $K_{m(obs)}$ is the Michaelis–Menten constant when an inhibitor is present in the test system. The value of K_I can be determined from the equation $K_{m(obs)}/K_m = 1 + K_I[I]$. If $K_{m(obs)}/K_m$ is plotted *versus* [I] the inhibitor constant, K_I, is obtained from the slope of the straight line.

The above discussion confirms the assumption that the reversible inhibition of the peroxidase-like activity of Mn-TPPS$_4$ by pyridine and *p*-chlorophenol is competitively linear when using H_2O_2 as substrate. From Fig. 3, it can be demonstrated that the constants of the inhibitors pyridine and *p*-chlorophenol are 79 and 3300 mol^{-1} dm^3, respectively. The competitively linear reversible inhibition by *p*-chlorophenol is much greater than the inhibition by pyridine for the peroxidase-like activity of Mn-TPPS$_4$ when using H_2O_2 as substrate.

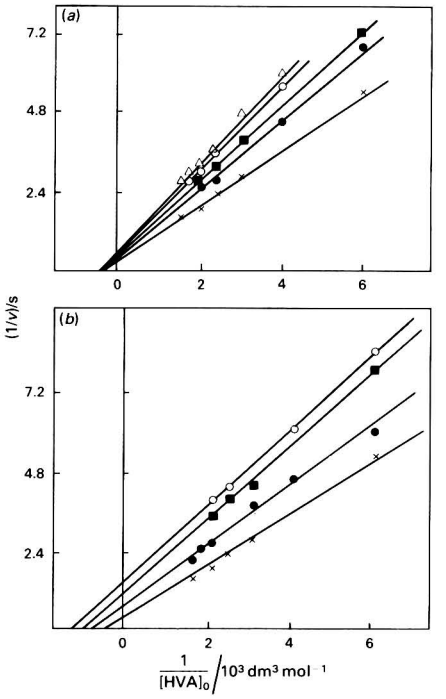

Fig. 4 Variation of $1/v$ with $1/[HVA]_0$ in the presence of inhibitors. Mn-TPPS$_4$: 9.44×10^{-8} mol dm^{-3}; H_2O_2: 5.22×10^{-5} mol dm^{-3}. (*a*) Pyridine: ×, 0; ●, 0.08; ■, 1.60×10^{-2}; ○, 2.40×10^{-2}; and △, 3.20×10^{-2} mol dm^{-3}. (*b*) *p*-Chlorophenol: ×, 0; ●, 4.80×10^{-4}; ■, 5.44×10^{-4}; and ○, 6.80×10^{-4} mol dm^{-3}

Inhibition of the Peroxidase-like Activity of Mn-TPPS$_4$ by Using HVA as Substrate

The inhibition of the peroxidase-like activity of Mn-TPPS$_4$ by pyridine was studied by using the initial-rate method and assuming steady-state conditions, when the concentration of H_2O_2 was saturated in the test system. The results are shown in Fig. 4. It can be seen that $K_{m(obs)} = a_1/b_1$ remains unchanged within experimental error and that the reaction-rate maximum $V_{max(obs)} = 1/a_1$ decreases with an incremental increase in the concentration of pyridine. It is known that if an inhibition proceeds non-competitively, the Michaelis–Menten constant, $K_{m(obs)}$, remains unchanged[9] and that non-competitive inhibition manifests itself in $V_{max(obs)}$.[9] Therefore, the inhibition of the peroxidase-like activity of Mn-TPPS$_4$ by pyridine is non-competitively reversible when using HVA as substrate.

The inhibition of the peroxidase-like activity of Mn-TPPS$_4$ by *p*-chlorophenol, with HVA as substrate, has also been studied. From Fig. 4, it can be seen that both the $K_{m(obs)} = a_1/b_1$ and $V_{max(obs)} = 1/a_1$ decrease with an incremental increase in the concentration of *p*-chlorophenol. The inhibition by *p*-chlorophenol, with HVA as substrate, was complicated, due to the complexity of the three types of reversible inhibition.

Mechanism of the Fluorescence Reaction of HVA With H_2O_2 Catalysed by Mn-TPPS$_4$

From the results obtained, it can be demonstrated that the inhibition of the peroxidase-like activity of Mn-TPPS$_4$ by pyridine and *p*-chlorophenol is competitively linear when using H_2O_2 as substrate. The value of $K_{m(obs)}$ increased with increasing concentrations of pyridine, which means that the affinity of the peroxidase-like Mn-TPPS$_4$ for H_2O_2 decreased when there were competitively linear reversible inhibitors present in the test system. These inhibitors compete with H_2O_2 for the axial position of the peroxidase-like Mn-TPPS$_4$. Therefore, it can be concluded that a complex is formed between Mn-TPPS$_4$ and H_2O_2 in the catalysis, as shown in reaction (1).

The catalytic activity of vitamin B_{12} for the formation of the fluorescent dimer of HVA was studied. The experimental results showed that vitamin B_{12} was unable to catalyse the formation of this fluorescent dimer. It is known that two axial positions of cobalt porphyrin in vitamin B_{12} are occupied by the ligands, which have a strong affinity for the metal. The metalloporphyrin–H_2O_2 complex cannot be formed in the vitamin B_{12} catalysed system. This result further verifies that Mn-TPPS$_4$ complexes H_2O_2 in the catalysis of the formation of the fluorescent dimer.

The experimental results showed that inhibition of the peroxidase-like activity of Mn-TPPS$_4$ by spin-trapping species, such as hydroquinone and DPPH, was non-reversible. This result confirms the assumption that the free radicals were produced in the catalysis of the formation of the fluorescent dimer by metalloporphyrin, as shown in reactions (2) and (3).

From the above, it has been shown that the mechanism for the fluorescence reaction of HVA with H_2O_2, catalysed by Mn-TPPS$_4$, is the same as the mechanism of the reaction of chavicol with H_2O_2 catalysed by Mn-T(4-TAP)P, which is shown in reactions (1)–(4).

This work was supported by the National Natural Science Foundation of China.

References

1 Ci, Y.-X., and Wang, F., *Anal. Chim. Acta*, 1990, **233**, 299.
2 Ci, Y.-X., and Wang, F., *Mikrochim. Acta, Part I*, 1990, 63.
3 Ci, Y.-X., and Wang, F., *Talanta*, in the press.
4 Ci, Y.-X., Chen, L., and Wei, S., *Fresenius Z. Anal. Chem.*, 1989, **334**, 34.
5 Ci, Y.-X., and Chen, L., *Chin. Sci. Bull.*, 1989, **23**, 1788.
6 Guilbault, G. G., Brignace, P. G., Jr., and Zimmer, M., *Anal. Chem.* 1968, **40**, 190.
7 Briggs, G. E., and Haldane, J. B. S., *Biochem. J.*, 1925, **19**, 338.
8 Lineweaver, H., and Burk, D., *J. Am. Chem. Soc.*, 1934, **56**, 658.
9 Roberts, D. V., *Enzyme Kinetics*, Cambridge University Press, Cambridge, 1977, pp. 26–36.

Paper 0/03741I
Received August 14th, 1990
Accepted October 23rd, 1990

Spectrofluorimetric Determination of 5-Hydroxyindoles With Benzylamine or 3,4-Dimethoxybenzylamine as a Selective Fluorogenic Reagent

Junichi Ishida, Masatoshi Yamaguchi* and Masaru Nakamura
Faculty of Pharmaceutical Sciences, Fukuoka University, Nanakuma, Johnan-ku, Fukuoka 814-01, Japan

A spectrofluorimetric method has been developed for the sensitive and selective determination of 5-hydroxyindoles; the method is based on the reaction of 5-hydroxyindoles in a weakly alkaline solution (pH 9.0) with aromatic methylamines in the presence of potassium hexacyanoferrate(III) and dimethyl sulphoxide; the compounds produced fluoresce intensely in an alkaline solution (pH 11–12). Of the eight aromatic methylamines tested, benzylamine and 3,4-dimethoxybenzylamine were found to be the most favourable fluorogenic reagents in terms of sensitivity and reactivity. The methods with benzylamine and 3,4-dimethoxybenzylamine permit the determination of 5-hydroxyindoles at concentrations as low as 22–72 pmol ml^{-1} and 1.0–2.4 nmol ml^{-1}, respectively.

Keywords: *Spectrofluorimetric determination; 5-hydroxyindole; aromatic methylamine; benzylamine; 3,4-dimethoxybenzylamine*

5-Hydroxyindoles are widely distributed in biological materials and play physiologically important roles in the body. Hence, measurement of 5-hydroxyindoles in biological samples has been actively investigated in many laboratories.

Several spectrofluorimetric methods have been proposed for the quantitative analysis of 5-hydroxyindoles. The methods based on native fluorescence[1] and the fluorescence reaction with ninhydrin[2] or *o*-phthalaldehyde[3] are not always selective for 5-hydroxyindoles. Indoles substituted at the 5-position have been determined by measuring the fluorescence produced in hydrochloric acid.[4–8] Another spectrofluorimetric method, which was based on the reaction with perchloric acid,[9] was reported for the determination of 3- and/or 5-substituted indoles. However, no specific method for 5-hydroxyindoles has been developed.

In the present work it was found that several aromatic methylamines (AMAs) react selectively with 5-hydroxyindoles in weakly alkaline medium (pH 9.0); in the presence of potassium hexacyanoferrate(III) and dimethyl sulphoxide, these compounds gave an intense fluorescence in alkaline medium (pH 11–12) (Fig. 1).

In this work, we have investigated the reactivity of eight AMAs with 5-hydroxyindoles and further discussed optimum reaction conditions for the determination of 5-hydroxyindoles with benzylamine (BA) or 3,4-dimethoxybenzylamine (3,4-DBA), which gave good results as fluorogenic reagents. 5-Hydroxytryptophan was used as a model compound to establish suitable reaction conditions for a more general analytical method.

Experimental

Reagents, Solutions and Apparatus

5-Hydroxytryptophan (5-OHTrp), 5-hydroxytryptamine, 5-hydroxyindol-3-ylacetic acid, 5-hydroxytryptophol and *N*-acetyl-5-hydroxytryptamine were purchased from Sigma (St. Louis, MO, USA). Other chemicals were of the highest purity available and were used as received. Distilled water, purified with a Milli-Q II system, was used for all aqueous solutions. The 20 mmol dm^{-3} solutions of BA, 3,4-DBA and other AMAs were prepared by dissolving the reagents in dimethyl sulphoxide; these reagent solutions were stable for at least 1 week, even at room temperature.

* To whom correspondence should be addressed.

Uncorrected fluorescence spectra and intensities were measured by means of a Hitachi 650–60 spectrofluorimeter with silica cells (10 × 10 mm); spectral bandwidths of 5 nm were used for both the excitation and emission monochromators.

Procedure

To 1.0 ml of an aqueous test solution in a 10 ml test-tube, 0.5 ml of 1.0 mmol dm^{-3} borate buffer (pH 9.0), 1.0 ml of the reagent (AMA) solution and 0.5 ml of 15 mmol dm^{-3} potassium hexacyanoferrate(III) were added successively. The mixture was warmed at 37 °C for 20 min. After the reaction, 1.0 ml of 9.0 mmol dm^{-3} sodium hydroxide was added to adjust the reaction mixture to pH 11–12. The reagent blank was prepared in the same way except that the test solution was replaced with water. The fluorescence intensities of the test and blank were measured at the respective excitation and emission maxima (see Table 1).

Results and Discussion

Screening of Aromatic Methylamines as Fluorogenic Reagents

Eight AMAs were screened as fluorogenic reagents by using 5-OHTrp as a representative compound of biological importance. The fluorescence excitation and emission maxima and relative fluorescence intensities are reported in Table 1. Of the AMAs tested, those having electron-donating groups at the 3- and/or 4-position of BA (3,4-DBA, 4-methoxybenzylamine and 4-methylbenzylamine) provided high fluorescence intensities. However, these reagents had a fairly high blank fluorescence. On the other hand, although the fluorescence intensity from BA was slightly lower than that from the above compounds, BA gave an extremely low blank value. Therefore, BA and 3,4-DBA were selected for further investigation, to give the largest signal to noise ratio and the highest fluorescence intensity, respectively, in order to establish suitable reaction conditions for determining 5-hydroxyindoles.

Conditions for the Fluorescence Reaction of 5-OHTrp With BA or 3,4-DBA

The excitation and emission maxima of the fluorescence from BA were 350 and 481 nm, respectively, and those from 3,4-DBA were 351 and 474 nm (Fig. 2). These maxima were

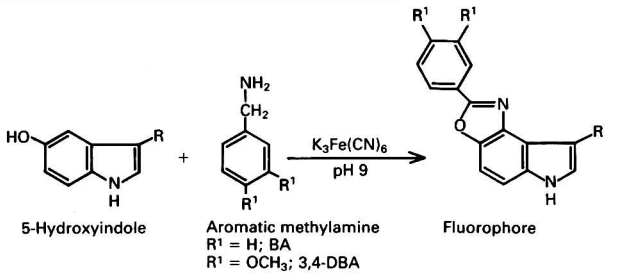

Fig. 1 Fluorescence reaction of 5-hydroxyindoles with aromatic methylamines

Table 1 Excitation and emission maxima and relative fluorescence intensities (RFIs) produced by the reactions of 5-OHTrp with AMAs*

Reagent	Excitation maximum/nm	Emission maximum/nm	RFI† Test	RFI† Blank
BA	350	481	100.0	0.04
3,4-DBA	351	474	205.7	2.52
4-Methoxybenzylamine	346	462	176.0	1.24
4-Methylbenzylamine	347	468	135.5	0.28
4-Aminomethylbenzoic acid	357	509	1.6	0.03
2-Aminomethylpyridine	312	395	4.1	1.33
3-Aminomethylpyridine	311	397	4.0	0.08
1-Naphthylmethylamine	371	519	53.6	2.73

* Portions (1.0 ml) of 50 nmol ml^{-1} of 5-OHTrp (or water for blank) were treated as described under Procedure.
† The intensity obtained by the reaction with BA was taken as 100.

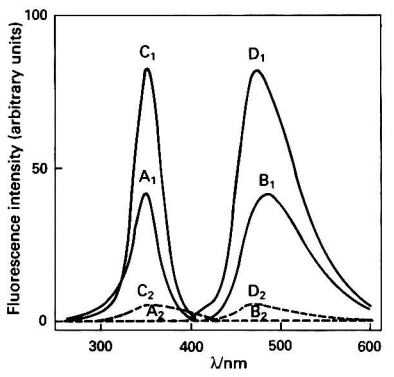

Fig. 2 Excitation and emission spectra of the final reaction mixture obtained from the reaction of 5-OHTrp with BA (A_1 and B_1) and 3,4-DBA (C_1 and D_1). A and C, excitation spectra; B and D, emission spectra. A_1–D_1: portions (1.0 ml) of 5-OHTrp solution (10 nmol ml^{-1}) were treated as described under Procedure. A_2 and B_2: reagent blank corresponding to A_1 and B_1. C_2 and D_2: reagent blank corresponding to C_1 and D_1

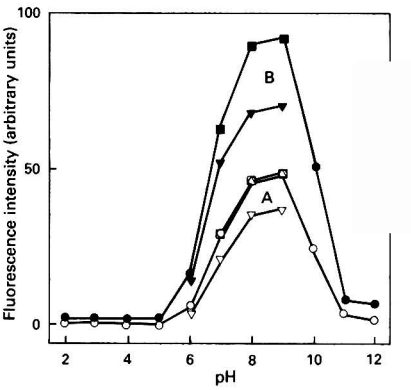

Fig. 3 Effect of pH on the fluorescence reaction. Portions (1.0 ml) of 5-OHTrp solution (5 nmol ml^{-1}) were treated as described under Procedure. The pH values of the reaction mixtures were adjusted with ● or ○, 40 mmol dm^{-3} Britton–Robinson buffer (pH 2–12); ■ or □, 5 mmol dm^{-3} Tris–hydrochloric acid buffer (pH 7–9); ▲ or △, 1 mmol dm^{-3} borate buffer (pH 8–9); and ▼ or ▽, 1 mmol dm^{-3} phosphate buffer (pH 6–9). A, BA; and B, 3,4-DBA

shifted to a longer-wavelength region compared with those of the native fluorescence of 5-OHTrp (λ_{ex} = 280 nm; λ_{em} = 340 nm). Native fluorescence was not observed in the reaction mixture.

The effect of the pH of the reaction mixture on fluorescence development was examined by using borate, tris(hydroxymethyl)aminomethane (Tris)–hydrochloric acid, Britton–Robinson and phosphate buffer solutions (Fig. 3). The optimum pH for the fluorescence reaction was 9.0, and was independent of the buffers used. However, the phosphate buffer afforded an intensity lower than that of the other buffers used; the reason for this is unknown. Therefore, 1.0 mmol dm^{-3} borate buffer (pH 9.0) was used tentatively for the reaction.

The fluorescence reactions with BA and 3,4-DBA proceeded fairly rapidly even at 0 °C (Fig. 4). Higher temperatures allowed the fluorescence to develop more rapidly. The maximum and constant fluorescence intensities were achieved by heating for at least 15 min at 37–80 °C. At 80 °C, the fluorescence intensities reached approximately 70% after 2 min of heating for both the reagents. Hence, a temperature of 37 °C and a reaction time of 20 min were selected for reproducible determinations.

The concentration of potassium hexacyanoferrate(III) had an effect on the fluorescence development (Fig. 5). Maximum fluorescence intensities were obtained at a concentration of 15 mmol dm^{-3} potassium hexacyanoferrate(III) in the solution. Other oxidizing agents such as potassium permanganate and copper nitrate also exhibited fluorescence, but the fluorescence intensities derived from these reagents were lower (47 and 5%, respectively) than that from potassium hexacyanoferrate(III). Even when the oxidizing agents were absent, the

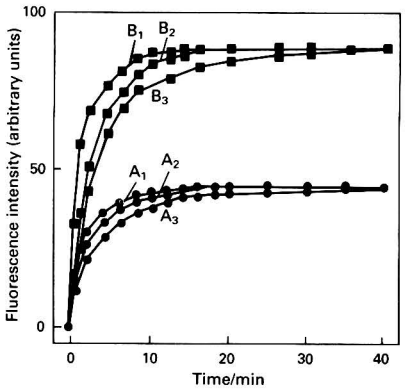

Fig. 4 Effect of reaction temperature and time on the development of fluorescence for BA and 3,4-DBA. Portions (1.0 ml) of 5-OHTrp solution (5 nmol ml^{-1}) were treated as described under Procedure using various reaction temperatures and times. A_1–A_3, BA; B_1–B_3, 3,4-DBA. A_1 and B_1, 80; A_2 and B_2, 37; and A_3 and B_3, 0 °C

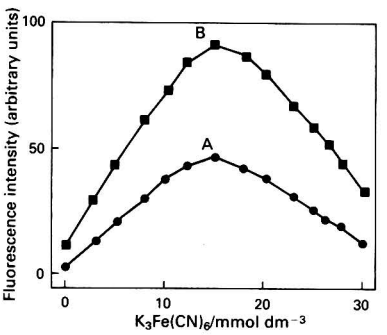

Fig. 5 Effect of potassium hexacyanoferrate(III) concentration on the development of fluorescence. Portions (1.0 ml) of 5-OHTrp solution (5 nmol ml^{-1}) were treated as described under Procedure with various concentrations of potassium hexacyanoferrate(III). A, BA; and B, 3,4-DBA

Table 2 Effect of organic solvents on fluorescence development*

	RFI†	
Solvent	BA	3,4-DBA
Dimethyl sulphoxide	100.0	203.0
N,N-Dimethylformamide	100.0	183.0
Acetonitrile	69.2	127.3
Acetone	81.2	152.4
Methanol	55.9	102.1

* Portions (1.0 ml) of 5 nmol ml^{-1} of 5-OHTrp were treated as described under Procedure, with various organic solvents for dissolving BA or 3,4-DBA.

† The intensity obtained by the reaction with BA in dimethyl sulphoxide was taken as 100.

fluorescence reaction occurred only slightly. This was probably owing to oxygen being dissolved in the reaction mixture. A hexacyanoferrate(III) concentration of 15 mmol dm^{-3} was selected as the optimum.

An organic solvent was required for dissolving BA and 3,4-DBA. Further, acceleration of the fluorescence reaction was observed in the presence of water-soluble organic solvents such as dimethyl sulphoxide, *N,N*-dimethylformamide, acetonitrile, acetone and methanol. Of these solvents, dimethyl sulphoxide was the most effective (Table 2). The effect of the dimethyl sulphoxide concentration is shown in Fig. 6; 33% of

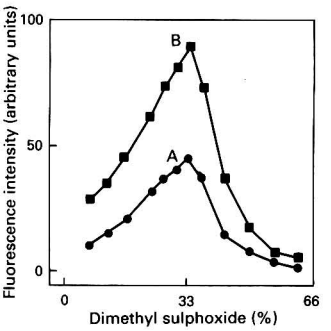

Fig. 6 Effect of dimethyl sulphoxide concentration on the development of fluorescence. Portions (1.0 ml) of 5-OHTrp solution (5 nmol ml^{-1}) were treated as described under Procedure with various volumes of dimethyl sulphoxide. A, BA; and B, 3,4-DBA

dimethyl sulphoxide in the reaction mixture was used to yield maximum fluorescence and dissolve the reagents.

Concentrations of BA (or 3,4-DBA) at 15 mmol dm^{-3} or greater in the reagent solution provided almost maximum and constant fluorescence from 5-OHTrp, but higher concentrations led to increasing values of the reagent blank; a 20 mmol dm^{-3} solution was used in the recommended procedure.

The derivative from BA (or 3,4-DBA) fluoresced most intensely at pH 11–12. Therefore, 1 ml of 9 mmol dm^{-3} sodium hydroxide was added to adjust the pH of the reaction mixture to about 11.5. The fluorescence from BA and 3,4-DBA was stable for at least 5 h, even in daylight at room temperature.

The calibration graphs obtained with BA and 3,4-DBA were linear over the concentration range 0.1–100 nmol ml^{-1} of 5-OHTrp. The precision was established by repeating 15 analyses concurrently on 10 nmol ml^{-1} of 5-OHTrp. The relative standard deviations were 2.9 and 3.3% for BA and 3,4-DBA, respectively.

Fluorescence From Other 5-Hydroxyindoles in the Reaction With BA or 3,4-DHA

All the other 5-hydroxyindoles tested also fluoresced under the reaction conditions described here. The excitation and emission maxima, relative fluorescence intensities and the lower detection limits are listed in Table 3. The excitation and emission spectra of the fluorescence from these 5-hydroxyindoles were very similar in shape and maxima to those from 5-OHTrp, and were not really characteristic of the individual 5-hydroxyindoles, for both BA and 3,4-DBA. In the equimolar reaction, 3,4-DBA gave fluorescence intensities approximately 1.4–2.3 times higher than those obtained with BA for all the 5-hydroxyindoles tested. However, the value of the reagent blank with 3,4-DBA was also 60 times higher than that with BA. In consequence, lower detection limits for the 5-hydroxyindoles, with BA and 3,4-DBA, of 22–72 pmol ml^{-1} and 1.0–2.4 nmol ml^{-1}, respectively, were obtained. These values obtained with BA were at least 3–4 times more sensitive than those obtained with hydrochloric acid[4–8] or perchloric acid.[9]

Reaction of Other Substances

Indoles substituted at the 3-position (tryptamine and indol-3-ylacetic acid) and 3,5-disubstituted indoles other than 5-hydroxyindoles (5-methoxy-L-tryptophan, 5-methoxytryptamine and 5-methoxyindol-3-ylacetic acid) exhibited no fluorescence (except native fluorescence) under the reaction conditions described. Tryptophan exhibited no fluorescence and did not interfere with the determination of 5-hydroxyindoles. It has been reported that quenching of the fluores-

Table 3 Excitation and emission maxima of the fluorescence from 5-hydroxyindoles, their relative fluorescence intensities (RFIs) and limit of detection (LOD)

	BA				3,4-DBA			
5-Hydroxyindole	Excitation maximum*/ nm	Emission maximum*/ nm	RFI†	LOD‡/ pmol ml^{-1}	Excitation maximum*/ nm	Emission maximum*/ nm	RFI†	LOD‡/ nmol ml^{-1}
5-OHTrp	350	481	100.0	31	351	474	202.0	1.2
5-Hydroxyindol-3-ylacetic acid	350	487	42.5	72	352	478	100.9	2.4
5-Hydroxy-tryptophol	350	482	106.3	29	351	473	202.7	1.2
5-Hydroxy-tryptamine	349	482	128.4	24	351	474	178.7	1.4
N-Acetyl-5-hydroxy-tryptamine	350	480	138.1	22	352	473	234.2	1.0

* Portions (1.0 ml) of 5 nmol ml^{-1} solutions of 5-hydroxyindoles were treated as described under Procedure.
† The fluorescence intensity obtained by the reaction of 5-OHTrp with BA was taken as 100.
‡ Defined as the concentration that yields a fluorescence intensity three times that of the blank.

cence from 5-OHTrp was observed in the presence of tryptophan, for the method involving use of hydrochloric acid;[10] a 15% decrease was observed with 1.0 mmol dm^{-3} tryptophan. In the present method, the fluorescence from 5-OHTrp did not decrease even in the presence of 3 mmol dm^{-3} tryptophan in the test solution. 'Kynurenine pathway'[9] compounds such as *N*-formyl-L-kynurenine, L-kynurenine, 3-hydroxy-L-kynurenine and 3-hydroxyanthranilic acid yielded no fluorescence. Several physiologically active compounds, with a phenolic group in the molecule, such as tyrosine, tyramine, β-estradiol, octopamine and epinephrine were examined for their reactivities. However, these compounds did not fluoresce under the conditions of the recommended procedure, even at a concentration of 50 nmol ml^{-1}.

Other biologically important substances examined did not fluoresce at a concentration of 10 nmol ml^{-1}. The compounds tested were 17 different L-α-amino acids, L-ascorbic acid, nicotinamide, vitamin D_3, adenine, guanine, cytosine, thymine, adenosine, guanosine, cytidine, thymidine, lactose, maltose, D-glucose, D-galactose, D-fructose, D-ribose, tryptamine, melatonin, 2-oxoglutaric acid, pyruvic acid, *N*-acetylneuraminic acid, spermine, vanillin, hexadecanoic acid, acetic acid, cholesterol and cortisone. These compounds did not affect the fluorescence development of 5-OHTrp either. This suggests that the proposed method is selective for 5-hydroxyindoles.

The chemical structure of the fluorescent product in the reaction of 5-hydroxyindoles with BA or 3,4-DBA is not known. Sundaramoorthi *et al.*[11] have reported that 1,4-dimethyl-6-hydroxycarbazole, which has a hydroxyindole moiety, reacted with α-monosubstituted primary amines such as propylamine and BA to produce the corresponding oxazole derivatives in the presence of manganese dioxide as an oxidizing agent. Therefore, 2-phenyloxazolo[4,5-*e*]indole derivatives are probably formed in the proposed fluorescence reaction (Fig. 1). The study on the reaction mechanism is still in progress.

The proposed methods permit the selective and sensitive determination of 5-hydroxyindoles. This derivatization method can be applied to an assay of the enzyme activity of tryptophan 5-monooxygenase[12,13] and to the high-performance liquid chromatographic determination of 5-hydroxyindoles in biological materials; further studies are continuing.

The authors are grateful to K. Nagashima and T. Yasunaga for their skilful assistance.

References

1 Duggan, D. E., and Udenfriend, S., *J. Biol. Chem.*, 1956, **223**, 313.
2 Snyder, S. H., Axelrod, J., and Zweig, M., *Biochem. Pharmacol.*, 1965, **14**, 831.
3 Maikel, R. P., and Miller, F. P., *Anal. Chem.*, 1966, **38**, 1937.
4 Udenfriend, S., Weissbach, H., and Bogdanski, D. F., *Science*, 1955, **122**, 972.
5 Bogdanski, D. F., Pletcher, A., Brodie, B. B., and Udenfriend, S., *J. Pharmacol. Exp. Ther.*, 1956, **117**, 82.
6 Adie, P. A., and Hughes, M. R., *Anal. Biochem.*, 1965, **11**, 395.
7 Wise, C. D., *Anal. Biochem.*, 1967, **18**, 94.
8 Wise, C. D., *Anal. Biochem.*, 1967, **20**, 369.
9 Hojo, T., Nakamura, H., and Tamura, Z., *Chem. Pharm. Bull.*, 1982, **30**, 189.
10 Friedman, P. A., Kappelman, A. H., and Kaufman, S., *J. Biol. Chem.*, 1972, **247**, 4165.
11 Sundaramoorthi, R., Kansal, V. K., Das, B. C., and Potier, P., *J. Chem. Soc., Chem. Commun.*, 1986, 371.
12 Nakata, H., and Fujiwara, H., *Eur. J. Biochem.*, 1982, **122**, 41.
13 Cash, C. D., Vayer, P., Mandel, P., and Maitre, M., *Eur. J. Biochem.*, 1985, **149**, 239.

Paper 0/04518G
Received October 8th, 1990
Accepted October 24th, 1990

Spectrofluorimetric Determination of Sulphate in Waters in Normal and Open/Closed Flow Injection Configurations

Beatriz Fernandez-Band,* Pilar Linares, M. D. Luque de Castro and Miguel Valcárcel
Department of Analytical Chemistry, Faculty of Sciences, University of Córdoba, 14004 Córdoba, Spain

A spectrofluorimetric method for the determination of sulphate, based on the formation of a ternary complex with biacetyl monoxime nicotinylhydrazone and zirconium is described. Two flow injection manifolds [normal (nFI) and open/closed] were optimized and used for the determination of sulphate in various water samples with good selectivity. The repeatability and linear range of the calibration graphs was better for the open/closed than for the nFI system (relative standard deviation 2.33% *versus* 3.51%, and linearity 1.5–150 μg ml^{-1} *versus* two linear portions of 2–30 and 30–150 μg ml^{-1}), but the sampling rate using the nFI configuration (30 samples h^{-1}) was at least twice that of the open/closed system.

Keywords: *Sulphate; spectrofluorimetry; flow injection; open/closed system; ternary complex*

There are few reagents available for developing sensitive and selective methods for the determination of anions over the concentration ranges usually required.[1] This accounts for the lack of flow injection (FI) methods for these species compared with cations. Of the approximately 3000 papers on FI published so far, less than 400 describe the determination of anions.[2] More than 20 of the papers deal with the determination of sulphate, usually based on spectrophotometric detection and its competitive reaction with barium chelates such as those of Methylthymol Blue,[3–6] Dimethylsulphonazo-III,[7,8] Nitchromazo[9] and 3-(2-carboxyphenylazo)-6-(2-sulphophenylazo)-4,5-dihydroxynaphthalene-2,7-disulphonic acid[10]; or on turbidimetric detection after precipitation with Ba(II).[3,4,11–19] These methods are scarcely selective because of the universal reactions on which they are based. Occasionally, the use of an on-line ion-exchange separation process overcomes this problem.[19] The limit of detection for most of these methods is >10 μg ml^{-1}.

This work was aimed at filling the gap in FI methods for the determination of sulphate by using a less conventional chemical method and system of detection. The proposed method is based on the formation of a fluorescent ternary complex between the analyte and zirconium–biacetyl monoxime nicotinylhydrazone (BMNH).[20] Two FI manifolds were designed and optimized for this purpose; a conventional three-channel configuration [normal flow injection (nFI)] and an open/closed system,[21] both of which provided good results.

Experimental

Reagents

A 4 × 10^{-3} mol dm^{-3} biacetyl monoxime nicotinylhydrazone solution,[22] an ethanol–water (40% v/v) solution, 0.01 mol dm^{-3} zirconium(IV) in 2.4 mol dm^{-3} HCl and a 1 g l^{-1} sulphate solution were used. More dilute solutions were prepared as required.

Instrumentation

A Perkin-Elmer MPF-44A spectrofluorimeter equipped with a Hellma 176.52-QS flow cell (inner volume, 25 μl) and connected to a Knauer recorder, a Hewlett-Packard 85 microcomputer and an HP-3478A multimeter was used. A Gilson Minipuls-2 peristaltic pump and Rheodyne 5041 injection valves for injection and selection were also used.

* Permanent address: Department of Chemistry and Chemical Engineering, Universidad Nacional del Sur, Bahía Blanca, Argentina.

Manifolds

The two configurations shown in Fig. 1 were designed and optimized for the application of the proposed method. In the nFI system, the sample was injected into a basic carrier which was then merged with the binary complex formed, as a result of the mixing of the BMNH and Zr^{IV} streams, along reactor R_1. After the sample and binary complex had merged, the ternary complex was formed along reactor R_2 and its fluorescence was monitored as it passed through the flow cell. The first part of the open/closed system was identical with that of the nFI configuration. A selecting valve (an injection valve modified for selecting purposes), situated immediately after the point where the sample and the binary complex merged, allowed the sample plug to be trapped within the circuit and

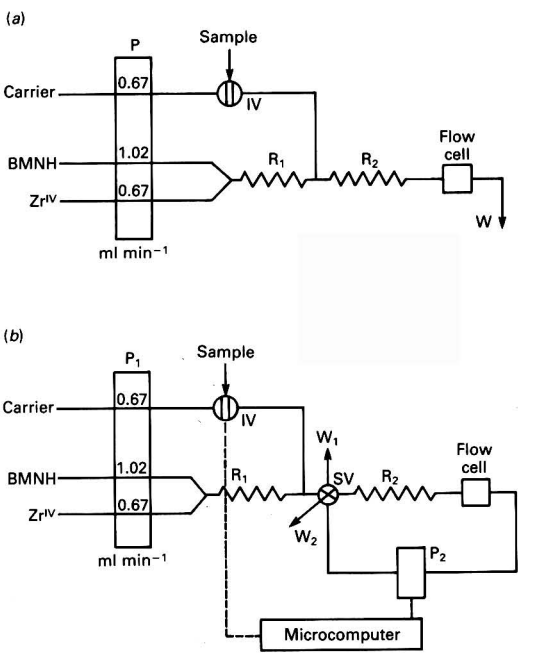

Fig. 1 Flow injection manifolds for the spectrofluorimetric determination of sulphate. (*a*) Normal and (*b*) open/closed configurations. P = Peristaltic pump; R = reactor (R_1 = 415 cm, 0.7 mm diameter; R_2 = 500 cm, 0.5 mm diameter); IV = injection valve; SV = selecting valve; and W = waste

passed through the flow cell as many times as was needed in order to obtain the number of peaks required (one peak per passage through the flow cell was obtained). In both instances, the baseline was adjusted for different values of the binary complex continuously circulated through the system. The recording of a blank solution containing no analyte was essential with the open/closed system, as the evolution of the binary complex between each two peaks influenced the profile of the multi-peak recording. Thus, a correct value for the analyte was obtained by subtracting the contribution to the fluorescence of the kinetics of the binary complex.

Results and Discussion

Chemical System

The BMNH reacts with zirconium(IV) in a mineral acid medium to yield a fluorescent 2:1 BMNH–metal complex. The sulphate ion enhances the fluorescence of this complex through the formation of a hypothetical 2:1:1 BMNH–zirconium(IV)–sulphate ternary complex but causes no changes in the wavelengths of the excitation and emission maxima.[22] The binary complex requires a more acidic medium for its optimal formation than the ternary complex. The wavelengths for maximum excitation and emission (the same values for static and flow working conditions) were 420 and 505 nm, respectively.

Optimization of Variables

Variables were grouped into those common to both configurations and those characteristic of the open/closed system. Table 1 summarizes the optimal values found in this study.

Chemical variables

The acid pH required for the formation of the binary complex was provided by the Zr^{IV} solution, the optimal medium being a 0.24 mol dm^{-3} HCl solution. As the BMNH complex was insoluble in water, an ethanol–water mixture was used as the solvent. A compromise between the increased fluorescence of the binary complex produced by the organic solvent and the solubility of the ligand was made by using an aqueous medium with 40% ethanol in which the solubility of the BMNH complex was 4×10^{-3} mol dm^{-3}. The binary complex had to be formed on-line because of its instability, which gave rise to spurious results with no strict control over the formation time. The optimal pH for the formation of the ternary complex (between 1.70 and 2.00) was obtained by merging the binary complex stream with the sample carrier. These working conditions were achieved in the nFI configuration by using a 0.2 mol dm^{-3} NaOH carrier, and in the open/closed system by using distilled water, which provided a smaller blank signal and a taller multi-peak recording of the analyte, as the time needed to obtain it was much longer than in the normal system.

Table 1 Study of variables

Variable	Optimal value: Normal flow injection system	Optimal value: Open/closed system
[BMNH]/mol dm^{-3}	4×10^{-3}	4×10^{-3}
[Zr^{IV}]/mol dm^{-3}	1×10^{-3}	1×10^{-3}
Carrier	NaOH, 0.20 mol dm^{-3}	Water
pH range	1.7–2.0	1.3–1.5
Injection volume/μl	600	600
$t_{switching}$ t_1/s		62
$t_{switching}$ t_2/min		5
		10

FI variables

Owing to the slow formation kinetics of the binary complex, a length for reactor R_1 of 400 cm (0.7 mm i.d.) was selected, which did not influence the sampling rate or the residence time. As the formation kinetics of the ternary complex was also slow, a length of 500 cm (i.d. 0.5 mm) for R_2 was considered as optimal. The signal increased sharply with an injection volume of up to 200 μl and then more gently up to 600 μl. Above this value, a split peak was obtained. A compromise flow-rate of the different channels was selected because low flow-rates increased the formation of the monitored product and baseline fluorescence, but decreased the sampling rate. The typical variables of the open/closed system were t_1 and t_2 (t_1 being the interval between sample injection and switching of the selecting valve to trap the reacting plug in the circuit, and t_2, the interval during which the reacting plug was kept in the closed circuit). Over the latter interval, the plug was passed through the flow cell once per minute and the fluorescence was monitored at the maximum of the peak. Both t_1 and t_2 were synchronized with the sample injection. A blank was injected under the same working conditions and the resulting data were stored by a treatment program and then subtracted from the data obtained for each sample.

Features of the Proposed Method

Calibration graphs

Standards with concentrations between 1 and 200 μg ml^{-1} were prepared in order to obtain calibration graphs for both manifold configurations. Two linear portions (2–30 and 30–150 μg ml^{-1}) were obtained with the nFI configuration with a precision, expressed as relative standard deviation (RSD), of 3.51% (obtained from 11 samples containing 10 μg ml^{-1} of the analyte and injected in triplicate). The sampling frequency was 30 h^{-1}. A single calibration graph covering the range 1.5–150 μg ml^{-1} of sulphate with an RSD of 2.33% (calculated from 11 samples containing 30 μg ml^{-1} of sulphate and injected in triplicate) was obtained with the open/closed system. The sampling frequency was 12 and 6 h^{-1} for a t_2 value of 5 and 10 min, respectively.

Interference study

A systematic study of the potential interferents in the determination of sulphate in waters was performed by using both configurations. As can be seen from Table 2, the greatest interference was caused by PO_4^{3-} and MoO_4^{2-}. Good tolerance to most of the species commonly found in waters was observed.

Table 2 Interferences from other ions

Ion added	Tolerated foreign ion : analyte ratio: Normal flow injection method	Tolerated foreign ion : analyte ratio: Open/closed method
Cl^-	100	100
Br^-	100	100
I^-	100	100
NO_3^-	100	100
NO_2^-	100	10
CO_3^{2-}	80	80
VO_3^-	5	5
F^-	1	1
PO_4^{3-}	<1	<1
MoO_4^{2-}	<1	<1
K^+	100	100
Ca^{2+}	100	100
Mg^{2+}	100	100
Pb^{2+}	100	100
Cu^{2+}	100	100
Cd^{2+}	100	100
Fe^{3+}	1	1

Table 3 Comparison between methods; (a), t_2 = 5 min and (b), t_2 = 10 min

Sample	Concentration found/μg ml^{-1}			
	Turbidimetric method	Normal flow injection method	Open/closed method (a)	Open/closed method (b)
Bottled waters—				
Cabras	20.6	20.4	18.6	18.3
Lanjarón	19.3	13.4	17.4	16.0
Font-vella	5.8	7.5	8.4	6.5
Unbottled waters—				
Córdoba (urban)	11.0	11.4	12.1	11.1
Well$_1$	20.6	20.4	23.6	22.6
Well$_2$	292.0	292.0	322.0	287.5

Table 4 Recovery study for normal and open/closed flow injection systems

Sample	Sample added/ μg ml^{-1}	Normal flow injection system		Open/closed system	
		Found/ μg ml^{-1}	Recovery (%)	Found/ μg ml^{-1}	Recovery (%)
Bottled waters—					
Cabras	0.0	14.9		14.6	
	10.0	23.4	94.0	24.0	97.6
	16.0	31.0	100.0	31.9	104.0
	20.0	36.0	103.0	36.6	105.0
Lajarón	0.0	13.9		12.8	
	10.0	25.1	105.0	23.6	103.0
	16.0	32.6	109.0	29.9	104.0
	20.0	38.1	112.0	34.7	106.0
Font-vella	0.0	6.7		5.2	
	10.0	15.0	89.8	13.5	88.8
	16.0	21.4	94.3	19.7	92.9
	20.0	25.5	95.5	22.8	90.5
Unbottled waters—					
Córdoba	0.0	10.3		8.9	
(urban)	10.0	17.9	88.2	16.9	89.4
	16.0	23.9	90.9	22.8	91.6
	20.0	28.7	94.7	27.4	94.8
Well$_1$	0.0	12.9		11.5	
	10.0	20.6	90.0	19.6	89.4
	16.0	26.7	92.4	25.7	93.5
	20.0	32.2	97.9	30.5	96.8
Well$_2$	0.0	18.9		18.1	
	10.0	29.6	102.0	28.8	102.0
	16.0	35.5	102.0	34.3	101.0
	20.0	40.6	104.0	38.5	101.0

Determination of sulphate in real samples

The proposed method was applied to the determination of the analyte in various types of water (bottled, tap and well). A comparison of the results obtained using both configurations with those provided by the conventional manual turbidimetric method[23] is shown in Table 3. All three sets of results are fairly consistent. Finally, a recovery study was performed for the open/closed system, by using the same samples and the same t_2 (5 and 10 min) monitoring intervals. Three additions of 10, 16 and 20 μg ml^{-1} of sulphate were made to each type of sample. The concentration of the analyte before the additions, and the recoveries obtained in each instance, are listed in Table 4. The recovery was acceptable in all instances.

Conclusions

Two FI configurations (normal and open/closed) for the spectrofluorimetric determination of sulphate based on the formation of a ternary complex were used for the analysis of real samples and provided very similar results.

The nFI configuration is simpler than its open/closed counterpart and affords a higher sampling frequency. However, the open/closed system uses distilled water rather than an NaOH solution as sample carrier (the pH is less critical than in the nFI configuration) and the calibration graph has a single, wide linear portion.

Comisión Interministerial de Ciencia y Technología (CICyT) is thanked for financial support (Grant No. PA86-0146). One of the authors (B. F. B.) expresses her gratitude to the Consejo Nacional de Investigaciones Científicas y Técnicas de la República Argentina for a grant covering the expenses incurred during her stay in Spain.

References

1 Williams, W. J., *Handbook of Anion Determination*, Butterworths, London, 1979.
2 Chen, D.-h., Luque de Castro, M. D., and Valcárcel, M., *Analyst*, submitted for publication.
3 Moller, J., and Winter, B., *Fresenius Z. Anal. Chem.*, 1985, **320**, 451.
4 Marsden, A. B., and Tyson, J. F., *Anal. Proc.*, 1989, **26**, 157.
5 Madsen, B. C., and Murphy, R. J., *Anal. Chem.*, 1981, **53**, 1924.
6 Koch, B., *Fresenius Z. Anal. Chem.*, 1988, **329**, 707.
7 Kondo, O., Miyata, H., and Toei, K., *Anal. Chim. Acta*, 1982, **134**, 353.
8 Nakashima, S., Yagi, M., Zenki, M., Doi, M., and Toei, K., *Fresenius Z. Anal. Chem.*, 1984, **317**, 29.
9 Kuznetsur, V., and Hangos, M., *Magy. Kem. Foly.*, 1982, **88**, 569.
10 Eremina, I. D., Shpigun, L. K., and Zolotov, Yu. A., *Zh. Anal. Khim.*, 1987, **42**, 1631.
11 Krug, F. J., Bergamin, F°. H., Zagatto, E. A. G., and Jorgensen, S. S., *Analyst*, 1977, **102**, 503.
12 van Staden, J. F., *Fresenius Z. Anal. Chem.*, 1982, **310**, 239.
13 Baban, S., Beetlestone, D., Betteridge, D., and Sweet, P., *Anal. Chim. Acta*, 1980, **114**, 319.
14 Krug, F. J., Zagatto, E. A. G., Reis, B. F., Bahía, F°. O., and Jacintho, A. O., *Anal. Chim. Acta*, 1983, **145**, 179.
15 van Staden, J. F., *Water, SA*, 1986, **12**, 43.
16 Toei, J., *Analyst*, 1987, **112**, 1067.
17 Basson, W. D., and van Staden, J. F., *Water Res.*, 1981, **15**, 333.
18 Xia, B., and Zhang, L., *Fenxi Huaxue*, 1987, **15**, 465.
19 van Staden, J. F., and Bassen, W. D., *Lab. Pract.*, 1980, **29**, 1279.
20 Rubio, S., Gómez-Hens, A., and Valcárcel, M., *Talanta*, 1985, **32**, 203.
21 Ríos, A., Luque de Castro, M. D., and Valcárcel, M., *Anal. Chem.*, 1985, **57**, 1803.
22 Cejas, M. A., Gómez-Hens, A., and Valcárcel, M., *Anal. Chim. Acta*, 1984, **158**, 287.
23 American Public Health Association, American Waterworks Association, Water Pollution Control Federation, *Standard Methods for the Examination of Water and Wastewater*, Washington, DC, 15th edn., 1980.

Paper 0/04705H
Received October 19th, 1990
Accepted November 15th, 1990

Study of the Fluorescence of the Europium–Thenoyltrifluoroacetone–Cetyltrimethylammonium Bromide–Triton X-100 System

Zhi-Kun Si, Gui-Yun Zhu and Jie Li
Department of Applied Chemistry, Shandong University, Jinan, China

The europium–thenoyltrifluoroacetone (TTA)–cetyltrimethylammonium bromide (CTAB)–Triton X-100 system at pH 5.5–7.5 was studied and used for the spectrofluorimetric determination of europium. The excitation and emission wavelengths were 370 and 612 nm, respectively. Fluorescence intensity was a linear function of the concentration of europium in the range 1.0×10^{-7}–1.0×10^{-9} mol dm^{-3}. The detection limit was 2.0×10^{-12} mol dm^{-3}. The standard additions method was used for the determination of europium in synthetic rare earth oxides and gave satisfactory results. The molar ratio method was carried out spectrofluorimetrically for the determination of the stoichiometric composition of the fluorescent species. A ratio of 1 : 4 : 1 for the ternary Eu–TTA–CTAB complex was found.

Keywords: *Europium; micellar-enhanced spectrofluorimetric method; cetyltrimethylammonium bromide*

Spectrofluorimetric procedures for the determination of europium have been reported previously.[1,2] The ternary complexes formed in aqueous solution by the reaction of europium or samarium with thenoyltrifluoroacetone (TTA) and certain substituted ammonium cations or neutral ligands, such as 1,3-diphenylguanidine (DPG) and 1,10-phenanthroline, have also been investigated.[3,4] In recent years interest in the application of the micellar system has increased.[5,6] The micellar-enhanced spectrofluorimetric method is an enhanced spectrofluorimetric method that can be used for the determination of trace amounts of lanthanide ions.

In this paper, the fluorescence characteristics of the ion associate formed by the reaction of europium with TTA and cetyltrimethylammonium bromide (CTAB) in the presence of Triton X-100 are reported, and a spectrofluorimetric method for the determination of europium is described. The fluorescence intensity of the Eu–TTA–CTAB micellar system is about three orders of magnitude greater than that of the Eu–TTA–DPG system. The stoichiometric composition of the fluorescent species has also been studied.

Experimental

Apparatus

All fluorescence intensity measurements were made on an RF-540 fluorescence spectrophotometer (Shimadzu, Kyoto, Japan), using 1.0 cm silica cells.

Reagents

Analytical-reagent grade chemicals were used and solutions were prepared in distilled water.

The lanthanide oxides were obtained from the Yuelong Chemical Plant (Shanghai, China) in purities of at least 99.9%. Stock solutions of the lanthanide ions (0.01 or 0.001 mol dm^{-3}) were prepared by dissolving a known amount of the appropriate rare earth oxide in hydrochloric acid. Working solutions were obtained by further appropriate dilution with water.

Aqueous solutions of 2.0×10^{-3} mol dm^{-3} TTA (Shanghai Reagent Factory, Shanghai, China), 1.0×10^{-3} mol dm^{-3} CTAB (Beijing Chemical Plant, Beijing, China) and 0.5% Triton X-100 were used. Hexamine–hydrochloric acid (pH 6.0) at a concentration of 1.0 mol dm^{-3} was used as a buffer.

Procedure

To a 25 ml test-tube, a standard solution of Eu^{3+}, 1.0 ml of TTA, 1.0 ml of CTAB and 1.0 ml of Triton X-100 solutions were added sequentially. The mixture was diluted to 10 ml with distilled water and allowed to stand for 10 min. The fluorescence intensity was measured in a 1.0 cm silica cell at excitation and emission wavelengths of 370 and 612 nm, respectively.

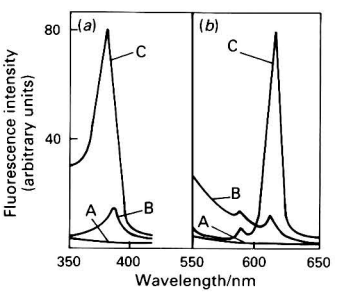

Fig. 1 (*a*) Excitation and (*b*) emission spectra. A, Eu–TTA–Triton X-100; B, Eu–TTA–DPG; and C, Eu–TTA–CTAB–Triton X-100. [Eu] = 1.0×10^{-8} mol dm^{-3}; [TTA] = 2.0×10^{-4} mol dm^{-3}; [CTAB] = 1.0×10^{-4} mol dm^{-3}; [DPG] = 2.0×10^{-4} mol dm^{-3}; and [Triton X-100] = 0.05%. pH 6.0; instrument setting: for peak B, gain = 2^{10}; for peaks A and C, gain = 2^7

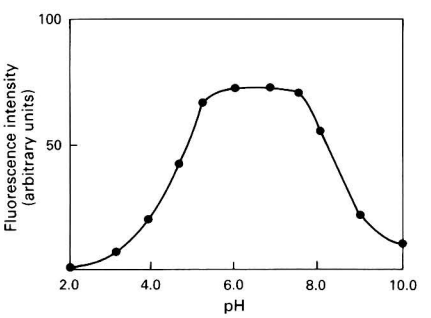

Fig. 2 Effect of pH on fluorescence intensity. [Eu] = 1.0×10^{-8} mol dm^{-3}; [TTA] = 2.0×10^{-4} mol dm^{-3}; [CTAB] = 1.0×10^{-4} mol dm^{-3}; and [Triton X-100] = 0.05%

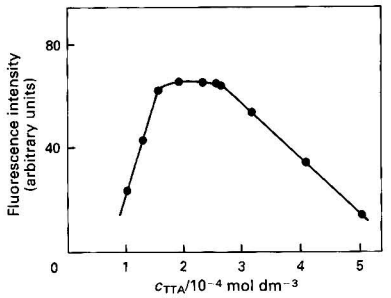

Fig. 3 Effect of TTA concentration on fluorescence intensity. [Eu] = 1.0×10^{-8} mol dm^{-3}; [CTAB] = 1.0×10^{-4} mol dm^{-3}; and [Triton X-100] = 0.05%. pH = 6.0

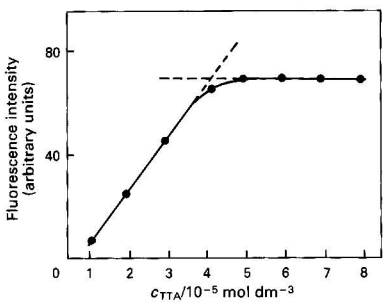

Fig. 4 Determination of the composition of the complex. [Eu] = 1.0×10^{-5} mol dm^{-3}; [CTAB] = 1.0×10^{-4} mol dm^{-3}; and [Triton X-100] = 0.05%. pH = 6.0

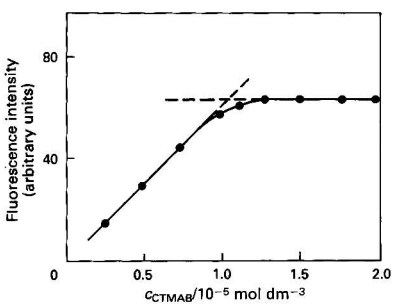

Fig. 5 Determination of the composition of the complex. [Eu] = 1.0×10^{-5} mol dm^{-3}; [TTA] = 2.0×10^{-4} mol dm^{-3}; and [Triton X-100] = 0.05%. pH = 6.0

Results and Discussion

Fluorescence Spectra

The excitation and emission spectra of the system investigated are shown in Fig. 1. The results indicated that in the presence of CTAB and Triton X-100 the fluorescence intensity of the system is about three orders of magnitude higher than that of the Eu–TTA–DPG–organic solvent system,[3] and the maximum excitation wavelength changed from 380 nm in the Eu–TTA–DPG system to 370 nm in the Eu–TTA–CTAB–Triton X-100 system. In the emission spectrum the emission line at 612 nm was the most intense, hence, this wavelength was used in all subsequent experiments.

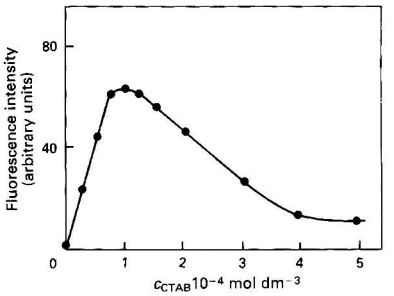

Fig. 6 Effect of CTAB concentration on fluorescence intensity. [Eu] = 1.0×10^{-8} mol dm^{-3}; [TTA] = 2.0×10^{-4} mol dm^{-3}; and [Triton X-100] = 0.05%. pH = 6.0

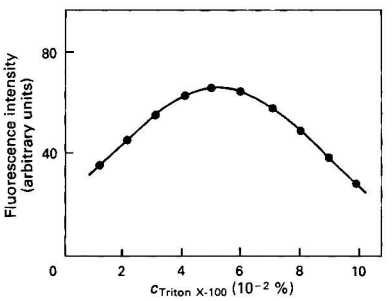

Fig. 7 Effect of Triton X-100 concentration on fluorescence intensity. [Eu] = 1.0×10^{-8} mol dm^{-3}; [TTA] = 2.0×10^{-4} mol dm^{-3}; and [CTAB] = 1.0×10^{-4} mol dm^{-3}. pH = 6.0

Effect of pH

A study of pH was carried out in the range 2–10. The results indicated that the maximum fluorescence intensity was obtained at a pH between 5.5 and 7.5 (Fig. 2).

For the system used here, hexamine–hydrochloric acid was chosen as the buffer solution and the pH was adjusted by use of either hydrochloric acid or sodium hydroxide solution.

Effect of TTA Concentration

The effect of the concentration of TTA on the fluorescence intensity at a fixed concentration of europium (1.0×10^{-8} mol dm^{-3}) was examined. A maximum and constant fluorescence intensity was obtained for TTA at a concentration of between 1.5×10^{-4} and 2.5×10^{-4} mol dm^{-3} (Fig. 3). In the absence of TTA no intrinsic europium emission was observed.

Effect of CTAB and Triton X-100 Concentrations

The effect of the concentrations of the surfactant CTAB and Triton X-100 on the fluorescence intensity of the system was investigated. The CTAB plays a part not only in its activity as a surfactant, but also as a cation. It forms a ternary ion associate with the Eu–TTA complex. A ratio of 1:4:1 for the ternary Eu–TTA–CTAB complex was found using the molar ratio method[7] (Figs. 4 and 5), therefore, the intramolecular transfer of energy from TTA* (the excited state of TTA) to Eu^{3+} is considerably enhanced,[8] resulting in an increase in the fluorescence intensity. The fluorescence intensity of this system is 15% higher than that of the Eu–TTA–1,10-phenanthroline–Triton X-100 system (1:3:1 for Eu–TTA–1,10-phenanthroline). In the absence of CTAB, no fluorescence was

Table 1 Determination of europium in rare earth oxides

Synthetic sample—

Europium present/μg	Europium found/μg	Mean ± SD*
11.0	11.3, 10.7, 11.0 11.0, 11.0, 10.9	11.0 ± 0.2

Commercial oxides—

Europium present/μg	Europium found/μg	Mean ± SD*
0.40	0.40, 0.39, 0.39 0.40, 0.39	0.39 ± 0.01

* SD = standard deviation.

Table 2 Recovery of europium from synthetic samples of rare earth oxides

Europium added/μg	Europium found/μg	Mean ± SD*
12.2	12.8, 12.2, 12.2 12.2, 11.6, 12.4	12.2 ± 0.4
25.0	24.8, 24.5, 25.2 25.5, 25.0, 25.0	25.0 ± 0.3

* SD = standard deviation.

observed in the system. The Triton X-100 also plays an important part in the dissolution of the complex and in protecting the complex against collision with solvent (water) molecules, which would result in a loss of energy. The maximum fluorescence intensity was obtained with CTAB at a concentration of 1.0×10^{-4} mol dm^{-3} (Fig. 6) and 0.05% Triton X-100 (Fig. 7).

Analytical Characteristics

Under the optimum conditions, the fluorescence intensity was a linear function of the concentration of europium in the range 1.0×10^{-7}–1.0×10^{-9} mol dm^{-3}. The detection limit (signal to noise ratio = 2) found was 2.0×10^{-12} mol dm^{-3}.

The effect of foreign ions on the fluorescence intensity of the Eu–TTA–CTAB–Triton X-100 system was studied for 5.0×10^{-9} mol dm^{-3} europium. A variation in the fluorescence intensity of ±5% was allowed. The other trivalent rare earth ions were examined, and it was found that the following molar excesses of these ions caused no interference: La, 5; Ce, 100; Pr, 100; Nd, 100; Sm, 10; Gd, 5; Tb, 10; Dy, 50; Ho, 100; Er, 100; Tm, 5; Yb, 10; and Lu, 5.

The Eu–TTA–CTAB–Triton X-100 system was applied to the determination of trace amounts of europium in synthetic rare earth oxides. The results obtained are given in Tables 1 and 2.

The synthetic mixture was prepared on the basis of the amount of each rare earth element in the Earth's crust. The amounts of rare earth ions in μg per 100 ml of the synthetic mixture were as follows: La, 190; Ce, 440; Pr, 56; Nd, 240; Sm, 105; Eu, 11; Gd, 63; Tb, 10; Dy, 43; Ho, 12; Er, 24; Tm, 2.1; Yb, 26; Lu, 7; and Y, 310.

References

1 Fisher, R. P., and Winefordner, J. D., *Anal. Chem.*, 1975, **43**, 454.
2 Lyle, S. J., and Maghzian, R., *Anal. Chim. Acta*, 1975, **80**, 125.
3 Melent'eva, E. V., Poluektov, N. S., and Kononenko, L. I., *Zh. Anal. Khim.*, 1967, **22**, 187.
4 Zapkina, L. L., and Stbepvuova, S. A., *Zh. Anal. Khim.*, 1971, **26**, 1764.
5 Zhu, G.-Y., Yang, J.-H., and Si, Z.-K., *Anal. Chim. Acta*, 1988, **215**, 331.
6 Zhu, G.-Y., Si, Z.-K., and Ding, J., *Anal. Chim. Acta*, 1990, **231**, 157.
7 Ci, Y.-X., and Lan, Z.-H., *Anal. Lett.*, 1988, **21**, 1499.
8 Zhu, G.-Y., Yang, J.-H., and Si, Z.-K., *Zhongguo Xitu Xuebao*, 1989, **7**, 73.

Paper 0/03558K
Received August 6th, 1990
Accepted October 17th, 1990

Ultraviolet–Visible Photodiode Array Spectrophotometer Wavelength Calibration Method. A Practical Computer Algorithm

Pedro E. Berlot and Guillermo A. Locascio*
Laboratory of Biological Instrumentation, Facultad de Ciencias Exactas y Naturales, University of Buenos Aires, Ciudad Universitaria, Pab. 2, CP 1428, Buenos Aires, Argentina

A method is proposed for wavelength calibration of the reversed-optics polychromators of photodiode array spectrophotometers. The central wavelength of each diode is determined using classical line emission sources and an appropriate algorithm. The method can be used even when the light from the slit image formed on the detector falls on several diodes, whether due to a large slit to diode ratio, detector window effects or other causes.

Keywords: *Polychromator; wavelength calibration; diode array detector; line source; calibration algorithm*

Wavelength calibration of normal ultraviolet (UV)–visible spectrophotometers usually involves the use of line emission sources,[1–4] often low-pressure mercury discharge lamps are used to determine the wavelengths at which maximum signal (energy) from the detector is obtained for each spectral emission line. This is possible because the position of the dispersing element (prism or grating) can be continuously adjusted and therefore any wavelength within the instrumental operating range can be selected as the central wavelength of the instrumental bandpass.

Clearly this is not possible in instruments with fixed optics, *e.g.*, polychromator–diode array systems. In fact, as far as we know, no standard method or practice has yet been proposed for wavelength calibration of these instruments.

Various solid and liquid filters, giving fairly sharp absorption peaks caused by electronic transitions of incomplete f orbitals of rare earth salts and oxides (Ho, Sm, Dy, Eu, Nd, *etc.*),[1,2,4–9] have often been recommended for verification purposes.

In a photodiode array system such a test or verification procedure would, in principle, only be taken as a first approximation because of the selective integration effect of the device on the absorption peaks of finite natural bandwidth. Therefore, maximum displacements are often produced due to the asymmetry of the absorption peaks.[4]

The proposed calibration technique could be applied to any UV–visible linear array photodiode detector reversed optics instrument, *e.g.*, spectrophotometers or liquid chromatography detectors. It employs a pen-ray type, low-pressure mercury discharge lamp. There is no need for it to be substituted for the normal light source of the lamphouse. It is sufficient to introduce the lamp into the sample compartment and to record the data from the detected energy spectrum. A simple algorithm is then applied to calculate the nominal central wavelength of each diode. This algorithm takes into account the spatial distribution of energy on the detector surface, regardless of the number of diodes illuminated by a given wavelength. However, a previous examination of the data is required to know the number of illuminated diodes in order to select the correct calculation procedure.

Experimental

Materials

A pen-ray quartz lamp (Ultraviolet Products, San Gabriel, CA, USA) was used as the emission line source. One of the spectrophotometers studied was a laboratory-built prototype (details to be published), which employs a Hamamatsu S 994-17 linear array detector consisting of 32 photodiodes, with optical mirrors and lenses supplied by Laboratorios Rodriguez Corswant (Bernal, Buenos Aires, Argentina). The other was a Hewlett-Packard Model 8451A spectrophotometer which was tested for comparison purposes.

Holmium and 'didymium' glass filters were obtained from Philips, Cambridge, UK.

Holmium(III) perchlorate and samarium(III) perchlorate solution filters were prepared according to Burgess and Knowles,[2] Burgess,[8] and Fog and Osnes.[9] Holmium oxide and samarium oxide were obtained from Fluka, Buchs, Switzerland. Perchloric acid (analytical-reagent grade) was obtained from Merck, Darmstadt, Germany.

An Apple II Europlus microcomputer equipped with the appropriate interfaces was also used.

Previous Assumptions

The following conditions were assumed to be fulfilled by the instrument or system under test. (*i*) The light beam from the line source reaching a given diode or group of neighbouring diodes is monochromatic, has the rectangular shape of the slit image and its energy is uniformly distributed over its area, *i.e.*, the irradiance is constant. (*ii*) All diodes have the same spectral response curve and sensitivity. The signal from each individual diode, both under dark and illuminated conditions, can be measured; the gain or electronic amplification corresponding to each diode is known and the signal can thus be expressed in nA or equivalent appropriate units, corrected for its gain. (*iii*) Detector geometry, *i.e.*, the width, D, of each diode and the separation, d, between diodes is known and is the same for all diodes (Fig. 1).

Strictly, a diode can be considered to be illuminated if the net signal, I_i, produced, *i.e.*, with the dark current discounted, is equal to or greater than twice the standard deviation of the signal of that diode under dark conditions then

$$I_i > 2 \times \text{standard deviation}$$

However, for various reasons (*e.g.*, the background continuum emission of low pressure discharge lamps being

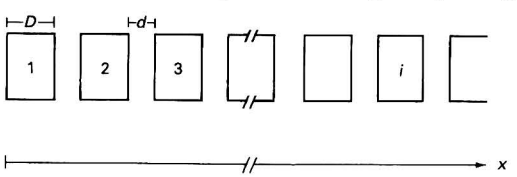

Fig. 1 Schematic diagram of the geometry of the linear photodiode array detector (LPDA). Diode width D, interdiode spacing d, diode numbering i and axis x are shown

* To whom correspondence should be addressed.

superimposed on the sharp emission lines, different types of 'crosstalk' between diodes, light scattering on the detector surface or other optical surfaces) it is convenient, in order to define the limits of a given group of illuminated diodes, to adopt a more restrictive criterion. For example, to consider only those diodes with a signal equal to or greater than one tenth of the highest signal within that group.

Deduction

The position of a given point along the array is designated x, measured from the beginning of the first photodiode; diodes are assigned a number i, beginning with 1. Thus, x_i denotes the position of the centre of diode i.

$$x_i = (D + d)(i - 1) + D/2 \quad (1)$$

$$i = 1 + \frac{x_i - D/2}{D + d} \quad (2)$$

The three possible cases are considered.

(1) A given isolated, spectral emission line reaches three or more diodes [slit comparatively wide, *i.e.*, a slit whose width produces an image greater than the sum of the width D of a single diode plus twice the width d of the separation between diodes, as this is the minimum slit width that can produce a monochromatic slit image large enough to reach three (or more) diodes]. In this case, at least one diode is fully covered by the light image. It is thus convenient, for the sake of clarity, to differentiate two sub-cases: (*a*) The first and last diode are only partially illuminated, *i.e.*, their signals are smaller than that of the central diode(s). It will be shown that the exact position of the centre x_m of the light image of width M can be known in this case (Fig. 2). (*b*) The first, the last or both diodes are fully illuminated. (2) The monochromatic image covers two diodes. (3) Only one diode is illuminated.

The situations described under (1*b*), (2) and (3) introduce a small but unavoidable uncertainty in the position of x_m, the importance of which depends upon the ratio of the 'blind' interdiode gap size d to the individual photodiode width D.

First case

Three or more diodes partially or fully illuminated by a given monochromatic image.

Considering only a group of n fully illuminated diodes, to the first, the number j is assigned, and the central position is called x_c. It will correspond to the centre of the real diode number c if n is odd, but to an equidistant position intermediate between two diodes, if c is an odd multiple of 1/2. If n is even then

$$c = j + (n - 1)/2 \quad (3)$$

In Fig. 2, $j = k + 1$; $n = 2$, *i.e.*, $c = k + 1 + 1/2$

To calculate the values of x_c for each case. When n is even, c falls exactly between two diodes

$$x_c = (D + d)(c - 1/2) - d/2 \quad (4)$$

and when n is odd, c coincides with a diode centre and

$$x_c = (D + d)(c - 1) + D/2 \quad (5)$$

Note, however, that equations (4) and (5) are identical when re-written.

In order to take the shift S between x_c and x_m into account for a given group of diodes illuminated by a monochromatic slit image, let us examine the net signals I_A and I_B (dark current subtracted) of the diodes located at the extremes of that group, and the net signal I_M of any fully illuminated, maximum signal diode in the same group.

At constant irradiance and spectral sensitivity, these signals are proportional to the areas illuminated. From Fig. 2, it can be seen that

$$M/2 = a + c_1 + S = b + c_2 - S \quad (6)$$

S must be added to x_c to calculate x_m; note that in Fig. 2 $x_c > x_m$, and therefore $S < 0$, as S is defined as the distance from x_c to x_m in the right hand direction.

In Fig. 2, $c_1 = c_2$,

$$S = (b - a)/2 \quad (7)$$

$$\frac{I_A}{I_M} = \frac{a}{D} \quad (8)$$

$$\frac{I_B}{I_M} = \frac{b}{D} \quad (9)$$

Substituting in equation (7) we obtain

$$S = (D/2)(I_B/I_M - I_A/I_M) \quad (10)$$

It is necessary to point out that if a, b or both are zero the exact position of the extremes of the slit image cannot be determined, for they can fall in any 'blind' position between two diodes and therefore some unavoidable uncertainty will be present whose importance depends upon the ratio d/D of the detector. [It must be remembered that the value of I_A/I_M and/or I_B/I_M is 1 in case (1*b*), as the signal from the extreme diodes must be considered to be equivalent to that from a fully illuminated diode, as stated previously.]

Second case

Two diodes illuminated. It is not possible to ascertain whether or not the diode that gives the greatest signal is fully covered.

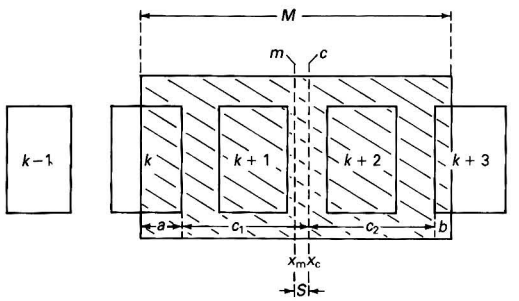

Fig. 2 Case 1. Outline of LPDA region (three or more diodes) illuminated by a monochromatic image of width M, showing image centre m and corresponding position x_m; fully illuminated diodes $k+1$ and $k+2$, its centre c (central position x_c), and shift S between them. a and b: illuminated fraction of extreme diodes k and $k+3$

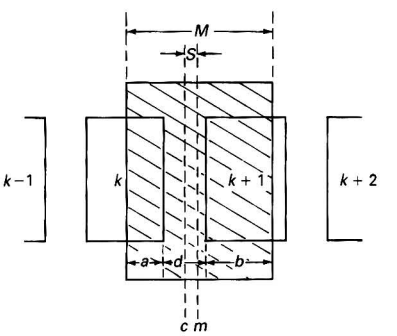

Fig. 3 Case 2. Schematic diagram of the LPDA showing only two diodes illuminated. Symbols as in Figs. 1 and 2

In this case, c lies obviously in the middle of d. If we number, as in Fig. 3, the first diode (left) as k, then

$$c = \frac{k + (k + 1)}{2} \quad (11)$$

and x_c can be calculated by means of equation (4).

From Fig. 3

$$M = a + d + b \quad (12)$$

Let us define the ratio R between the net signals (and covered areas) of the first and last diode of a given group,

$$R = I_A/I_B = a/b \quad (13)$$

Hence,

$$b = \frac{M - d}{R + 1} \quad (14)$$

$$a = \frac{M - d}{R + 1} R \quad (15)$$

Substituting in equation (7)

$$S = \frac{M - d}{2}\left(\frac{1 - R}{1 + R}\right) \quad (16)$$

Rearranging, we obtain

$$M = d + 2S\frac{1 + R}{1 - R} \quad (17)$$

Obviously if R tends to 1 the image becomes centred and S tends to zero.

Fig. 4 shows the case in which the size and position of the light image produce maximum shift S_{max} (if a tends to, but does not actually reach zero value). An interdiode gap d (on the right) is fully covered but the next diode on the right is not illuminated; on the other hand the left interdiode gap is also fully covered; the light also reaches the next diode to the left, just enough to produce a minimum detectable signal.

$$M/2 + S < d + D + d/2 \quad (18)$$

Hence

$$M_{max} = 2D + 3d - 2S_{max} \quad (19)$$

From equations (17) and (19), and solving for S_{max}

$$S_{max} = (D + d)/\left(1 + \frac{1 + R}{1 - R}\right) \quad (20)$$

The minimum value of M is not likely to be less than D if a sensible design is employed for the polychromator, for if the slit image cannot fully cover a diode, a loss of signal (and degradation of signal to noise ratio) without any improvement in resolution would occur.

$$M_{min} = D \quad (21)$$

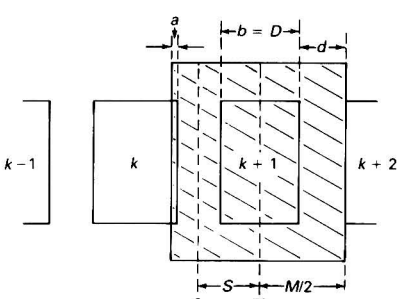

Fig. 4 Case 2. Situation in which a tends to a minimum and maximum shift S is produced

From equations (16) and (21), for M_{min} corresponding to S_{min}, we obtain

$$S_{min} = \frac{D - d}{2}\left(\frac{1 - R}{1 + R}\right) \quad (22)$$

For a given pair of diodes the value of R is calculated from the measured signals, correcting both for the dark current and the electronic gain. Then, the value of S, taken as $(S_{max} + S_{min})/2$ for that value of R, is calculated from equations (20) and (21). The maximum possible error thus introduced is less than or equal to the difference between that mean value of S and S_{max} or S_{min}.

Third case

Only one diode is illuminated. It is assumed that $x_c = x_m$ and therefore $S = 0$. The centre of the light image is assigned to the centre of the diode.

Procedure

A convenient number of measurements is made for each determination in order to obtain statistically significant values of the mean and standard deviation. (*a*) By means of an occluder, baffle or similar device, light is prevented from reaching the detector. The dark signal of each diode is measured. (*b*) The dark current of each diode is obtained by dividing its previously measured signal by the corresponding electronic amplification or gain. The corresponding standard deviation is calculated. (*c*) A line emission source, *i.e.*, a pen-ray, is placed in the cell holder, turned on and its light allowed to reach the detector. (*d*) The signal of each diode is measured. (*e*) The net current I_i of each diode is obtained by dividing its signal by the corresponding gain, as before, and subtracting its dark current. (*f*) For each wavelength (emission line) a central position x_c and the corresponding shift S (where applicable) are calculated. The values of x and S with sign are summed. The data are tabulated. (*g*) A linear regression analysis is performed, $\lambda(nm) = Px + Q$. (*h*) The wavelength corresponding to the centre of each diode is calculated according to equation (1), $\lambda(nm) = P[(D + d)(i - 1) + D/2] + Q$. (*i*) The final calibration is then obtained, $\lambda_i = f(i)$.

For some particular instruments it may be necessary to alter or modify details of one or more of the procedures described above.

Results and Discussion

The present calibration procedure has been employed for wavelength calibration studies on two linear array spectrophotometers, as described under Experimental. The coefficient of correlation, r, and the standard error of estimation (σ) are compared with those obtained by a less elaborate method based on direct assignation of the wavelengths of the emission lines to those diodes that give the highest signals. Wavelength verifications carried out on both instruments, making use of the absorption maxima of holmium and 'didymium' glass filters and of holmium and samarium perchlorate solutions, are also shown for comparison purposes; the reference peak wavelengths were taken from sources mentioned previously.[2-4] The results are summarized in Table 1.

It can be seen from the figures that the proposed calibration procedure gives slightly but consistently higher coefficients of correlation and considerably better values of σ compared with those obtained by the direct assignation of wavelengths to diodes at which maximum light intensity is detected. It has to be pointed out that these improvements are much greater for the Hamamatsu S 994-17 detector, a 'low resolution' device of only 32 diodes (D = 0.585 mm; d = 0.05 mm) operating between approximately, 340 and 700 nm, than for the HP 8451A detector consisting of 328 photodiodes (D = 50 μm; d = 4 μm). Light from the spectral operating range of the

Table 1 Comparison of correlation coefficient (r) and the standard error of estimation (σ) on two linear array spectrophotometers

	Instrument detector			
	HP 8451A		Hamamatsu S 994-17	
Method	*r*	σ	*r*	σ
Hg lamp, this method	0.99999	0.52	0.9999	1.70
Hg lamp, single diode assignation	0.99998	0.67	0.9996	3.21
Ho glass	0.99993	1.56	0.9997	3.30
Dy glass	0.99996	1.19	0.9977	5.21
Ho solution	0.99994	1.35	0.9997	4.75
Sm solution	0.99990	0.77	0.9983	3.95

instrument falls on 316 of these (190–820 nm). As can be expected, the results obtained with rare earth filters were less precise, although the σ value corresponding to the samarium perchlorate filter was remarkably low when used with the higher resolution instrument.

Analysis of the data obtained both with emission sources and absorption filters showed several unresolved fused peaks due to insufficient instrumental resolution. Therefore, among the wavelengths of emission lines of mercury arcs suitable for calibration purposes as recommended by Mavrodineanu,[3] only ten could be employed for the Hewlett-Packard instrument and five for our experimental prototype, within the wavelength operating range of each spectrophotometer.

The same instrumental limitations restricted use to seven and four absorption peaks of Ho glass, six and four of 'didymium' glass, ten and seven of Ho perchlorate and 11 and four of Sm perchlorate solutions, for the Hewlett-Packard spectrophotometer and our prototype, respectively.

It is appropriate to remember that the observed wavelength of an absorption maximum as obtained in a 'normal' spectrophotometer is affected by the spectral slit-width of the instrument and also by the asymmetry of the absorption band.[4] However, it seems that a full and comprehensive study of these displacements or shifts for reversed optics linear array spectrophotometers is still needed.

The regression analysis (results not shown) performed for the different absorption filters employed, indicates some displacement of the wavelength values, corresponding to the first diode (taken as a reference) calculated as a fraction of *D*, of about half for the HP instrument and of more than three units for our experimental prototype. This leads to the conclusion that in spite of the more or less acceptable values of the coefficients of correlation and standard error of the estimate obtained, 'calibration' with filters is rather unreliable. In addition, as is already well known, a mercury discharge lamp, if available, is always to be preferred even if only a single wavelength check is desired.

We thank the Programa Nacional de Informatica y Electronica, (PNIE, SECyT) Argentina, for financial support and Laboratorios Rodriquez Corswant SRL for the generous gift of some optical components. Thanks also to Dra. R. E. Balsells and Dr. E. G. Gros (Department of Organic Chemistry, Facultad de Ciencias Exactas y Naturales, Universidad de Buenos Aires), for providing the Hewlett-Packard facilities. We are indebted to Dr. J. C. Monge for valuable discussion and preparation of figures.

References

1 *Standard Method for Describing and Measuring Performance of Ultraviolet, Visible and Near Infrared Spectrophotometers, Annual Book of ASTM Standards*, Vol. 14.01, 1987, E 275–83, American Society for Testing and Materials (ASTM), Philadelphia, PA, 1987, p. 408.
2 *Standards in Absorption Spectrometry*, eds., Burgess, C., and Knowles, A., Chapman and Hall, London and New York, 1981, p. 130.
3 Mavrodineanu, R., *NBS Spec. Publ.* 260–51, Washington, DC, 1975, pp. 54–64.
4 *Advances in Standards and Methodology in Spectrophotometry*, eds., Burgess, C., and Mielenz, K. D., Elsevier, Amsterdam, 1987, pp. 99, 125 and 303.
5 *Standard Practice for the Periodic Calibration of Narrow Band-Pass Spectrophotometers, Annual Book of ASTM Standards*, Vol. 14.01, 1987, E 925–83, American Society for Testing and Materials (ASTM), Philadelphia, PA, 1987, p. 824.
6 McNeirney, J., and Slavin, M., *Appl. Opt.*, 1962, **1**, 365.
7 *Practical Absorption Spectrometry*, eds., Knowles, A., and Burgess, C., Chapman and Hall, London and New York, 1984, p. 221.
8 Burgess, C., *UV Spectrom. Group Bull.*, 1977, **5**, 77.
9 Fog, J., and Osnes, E., *Analyst*, 1962, **87**, 760.

Paper 0/03278F
Received July 20th, 1990
Accepted October 12th, 1990

Spectrophotometric Investigation of Palladium(II)–Disulfoton Complexes in Aqueous Ethanolic Media

Breda Simonovska
Tobacco Institute, 97500 Prilep, Macedonia, Yugoslavia
Jože Marsel
Department of Chemistry, Faculty of Natural Sciences and Technology, University of Ljubljana, 61000 Ljubljana, Yugoslavia

The systemic insecticide disulfoton {*O,O*-diethyl *S*-[2-(ethylthio)ethyl] phosphorodithioate} forms stable complexes with Pd^{II} in ethanol. With an excess of disulfoton in solution, Pd^{II} forms 1 : 1 or 2 : 2 complexes. With an excess of $PdCl_2$, an equilibrium between 2 : 2 and 3 : 2 complexes is maintained; further addition of $PdCl_2$ leads to a situation where the 3 : 2 complex prevails. With a large excess of $PdCl_2$, an additional complex of unknown composition, probably 4 : 2, can be observed. The most characteristic absorption maxima for these complexes are exhibited between 270 and 300 nm. Hence, the spectrophotometric determination of disulfoton with $PdCl_2$ in ethanolic media is possible. By measuring the absorbance at 278 nm, disulfoton can be determined in the concentration range from 2 to 17 mg l^{-1} (a correlation coefficient of 0.9958 for nine standard solutions was calculated). As $PdCl_2$ interferes slightly with disulfoton at this wavelength, the measurement can be performed at 390 nm with lower sensitivity. Further, disulfoton can also be determined in ethyl acetate by shaking an ethyl acetate–disulfoton solution with aqueous $PdCl_2$, whereby the Pd^{II}–disulfoton complex is extracted into ethyl acetate. This procedure is sensitive and precise, with an optimum concentration range of disulfoton between 1 and 15 mg l^{-1} at 268 nm ($r = 0.9999$). However, it must be noted that this method is inadequate for residue analysis of disulfoton with regard to the specificity and detection limit.

Keywords: *Disulfoton insecticide; palladium–disulfoton complex; spectrophotometry*

Palladium(II) chloride is a well known reagent for the detection of organothiophosphoric insecticides in thin-layer chromatography (TLC), where microgram amounts of thiophosphates exhibit coloured spots with $PdCl_2$.[1]

This paper describes a study of the complexation of $PdCl_2$ with disulfoton, *i.e.*, *O,O*-diethyl *S*-[2-(ethylthio)ethyl] phosphorodithioate. It seems that complexation of disulfoton with metal ions in soil plays an important role in the transport of water-insoluble disulfoton from the soil into plants. In addition, the possibility of the spectrophotometric determination of this insecticide as its Pd^{II} complex is outlined.

Experimental and Results

Reagents

A standard solution of $PdCl_2$–$HClO_4$ was prepared by dissolving 0.5 g of $PdCl_2$ in warm water with the addition of 2 ml of concentrated $HClO_4$ and diluting with water to 100 ml. Owing to its instability, working solutions were prepared by dilution of the standard solution with ethanol immediately before the experiments.

In the same way, a $PdCl_2$–HCl standard solution, *i.e.*, the reagent for TLC, was prepared. Working solutions prepared with ethanol or water were stable (these were subsequently used only for the determination of disulfoton in ethyl acetate media).

Commercial-grade disulfoton (Sandoz, 96% purity) was purified by TLC on a 0.5 mm silica gel G (unactivated) plate in hexane solution with hexane–acetone (4 + 1) as the mobile phase. Disulfoton was detected by exposure to iodine vapour and was extracted, after evaporation of the iodine, into ethanol or ethyl acetate. In contrast to its stability in ethanolic media, disulfoton is very stable in hexane.

Apparatus

A Pye Unicam 1800 B spectrophotometer was used for absorbance and absorption spectra measurements.

Composition of the Pd^{II}–Disulfoton Complexes

On mixing ethanolic disulfoton solutions with a $PdCl_2$ solution of appropriate concentration, stable yellow complexes can immediately be observed at room temperature. The absorption spectra, with a maximum at about 300 nm, are influenced by the absorbance of $PdCl_2$, especially below 280 nm, whereas the absorbance of disulfoton above 260 nm is negligible.

Although the method of continuous variations and the corresponding molar ratio method yield results that are only approximate, both methods are often used for the investigation of the composition of complexes in solutions.[2] For the continuous method, *i.e.*, Job's method,[3] a $PdCl_2$–$HClO_4$ solution, with a constant concentration of 0.005 mol dm^{-3} of $HClO_4$ in all working solutions, was used. From the spectra of isomolar solutions of $PdCl_2$–disulfoton ($\Sigma n = 0.1$ mmol dm^{-3}), it could be concluded that different complexes are formed with an excess of $PdCl_2$ in solution. This evidence is supported by the irregularity on the left-hand side of the Job plot shown in Fig. 1(*a*).

With an excess of disulfoton, a complex exhibiting an absorption maximum at 295 nm is formed. From the spectra, shown in Fig. 1(*b*), a complex with a Pd^{II}: disulfoton ratio of 1 : 1 could be predicted. As the continuous variations method of Job is of little value if several complexes with the same ligand are present in solution, further investigations were performed by using the molar ratio method. By raising the concentration of disulfoton, at a constant concentration of $PdCl_2$, absorption maxima were obtained towards higher wavelengths, at a 1 : 1 molar ratio, in a broad region of wavelengths (Fig. 2). In spite of the absorbance of $PdCl_2$ itself, careful investigation of the spectra leads to the conclusion that two types of complex are formed at equilibrium.

Some difficulties arise if the concentration of disulfoton is kept constant and the concentration of $PdCl_2$ is varied. Because of the absorbance of $PdCl_2$, which is pronounced near the absorption maximum of the second complex (about 275 nm), and the absorbance of the 1 : 1 complex formed at

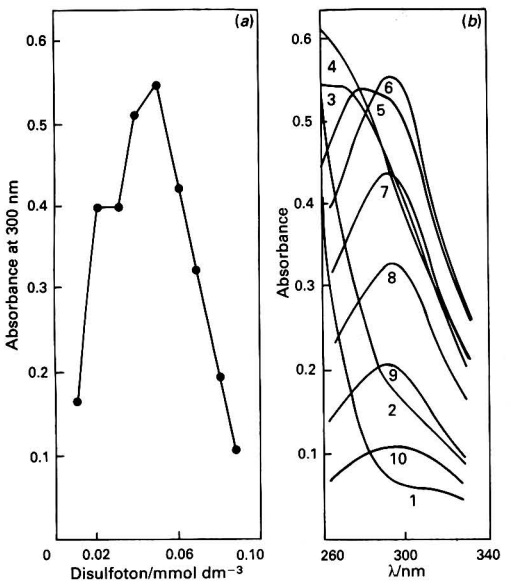

Fig. 1 (*a*) Continuous variations graph: $PdCl_2$ + disulfoton concentration, 0.1 mmol dm^{-3}. Wavelength, 300 nm. Reference, ethanol. (*b*) Continuous variations spectra of $PdCl_2$–disulfoton complexes, Σn_i = 0.1 mmol dm^{-3}. 1; $PdCl_2$ alone, 0.1 mmol dm^{-3}. 2–9: $PdCl_2$, 0.09–0.02 mmol dm^{-3}; disulfoton, 0.01–0.09 mmol dm^{-3}; 10: $PdCl_2$, 0.01 mmol dm^{-3}; disulfoton, 0.09 mmol dm^{-3}. Curves 2 and 3 show the absorption spectra of $PdCl_2$ superimposed on the spectra of the $PdCl_2$–disulfoton complex (probably 4 : 2); curve 4 corresponds to the absorption spectrum of $PdCl_2$ superimposed on the spectrum of the 3 : 2 $PdCl_2$–disulfoton complex, whereas curve 5 corresponds to the absorption spectra of the 3 : 2 and 1 : 1 $PdCl_2$–disulfoton complexes; curves 6–10 correspond to the absorption spectra of the 1 : 1 $PdCl_2$–disulfoton complex. Reference, ethanol

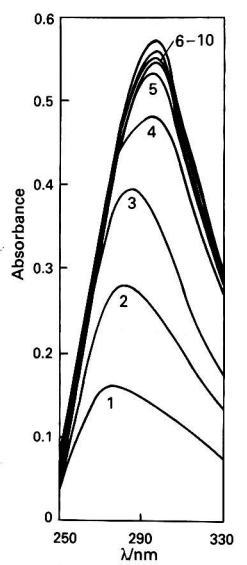

Fig. 2 Molar ratio spectra of $PdCl_2$–disulfoton complex in ethanol. $PdCl_2$ concentration, 0.05 mmol dm^{-3}; disulfoton concentrations from 0.01 to 0.10 mmol dm^{-3} (curves 1–10). Reference, 0.05 mmol dm^{-3} $PdCl_2$ ('saturation' at 0.05 mmol dm^{-3} disulfoton, curves 5–10)

equilibrium, no 'saturation' could be observed in the ultraviolet region. By choosing appropriate higher concentrations of both components, 'saturation' could be observed at 390 nm, where the absorbance of $PdCl_2$ is negligible [Fig. 3(*a*)]. Additionally, the second complex could be confirmed by the characteristic absorption maximum at 275 nm.

Inspecting the absorption spectra, it could be shown that mixtures of the 1 : 1 (or 2 : 2) and 3 : 2 complexes are present before saturation. It is of interest that, from the observed absorbances at 390 nm, the 1 : 1 complex could not be identified if disulfoton were in excess, as the absorbance regularly changes until saturation is reached. However, at 295 nm, the absorption maximum shifted towards 275 nm when the molar ratio reached 3 : 2, thereby indicating formation of this complex at saturation.

Absorption spectra of the 1 : 1 complex were obtained by scanning solutions containing an excess of disulfoton in the range from 40 : 1 to 4 : 1 [Fig. 3(*b*)].

The spectra of solutions containing $PdCl_2$ in excess are shown in Fig. 3(*c*). Although disulfoton concentrations were varied regularly from 1×10^{-5} to 1×10^{-4} mol dm^{-3}, two groups of spectra with regard to the molar absorptivity could be observed. The upper part of the absorbance (above 0.6) can be attributed to the 3 : 2 complex (some uncertainty arises from the absorbance of $PdCl_2$), whereas the lower part of the absorbance (below 0.6) could correspond to another complex, *e.g.*, a 4 : 2 complex. This finding is consistent with the Job plot [Fig. 1(*a*)], where a break appears in the lower part of the region in which an excess of $PdCl_2$ is present. Unfortunately, it was not possible to isolate the two complexes pure in the solid state to perform further investigations (by infrared analysis) on the character of the complexation with $PdCl_2$.

In order to avoid the influence of complexes of the type $PdCl_{2+x}$ (where x = 1 or 2) in the presence of HCl, all the experiments described in this section were performed with $HClO_4$ added to the solution. Nevertheless, almost the same results were obtained with HCl. As $PdCl_2$–HCl solutions are more stable, they were used for analytical purposes.

Spectrophotometric Determination of Disulfoton

Although most of the reports on the determination of pesticides describe the application of different chromatographic techniques,[4,5] the chromogenic properties of Pd^{II}–disulfoton complexes can be utilized in the spectrophotometric determination of disulfoton.

For this purpose, four sets of standard solutions were prepared for calibration measurements under different conditions, as given in Table 1. All absorbance measurements were performed immediately after mixing the reagents, in 1 cm silica cells, as there was a gradual change in absorbance with time.

The excellent linearity of the calibration graphs, $A_\lambda = a + bc$, where c is the concentration of disulfoton, is clear from the correlation coefficients (r), calculated from the linear regression for n regularly ordered standard solutions with resulting absorbances between 0.1 and 1 or 0.75, at 390 nm.

A concentration of 50 mg l^{-1} of $PdCl_2$ allows the formation of the 3 : 2 complex. At lower concentrations the equilibrium is shifted towards 1 : 1 complex formation, which influences the calibration graphs, owing to the differences in molar absorptivity for the two complexes at 278 and 305 nm. As the absorption maximum of the 3 : 2 complex lies close to 278 nm, the sensitivity is high, but, unfortunately, at this wavelength the absorbance of $PdCl_2$ is very pronounced. In this respect, measurement at 305 nm is more favourable, but the sensitivity is lower. In order to avoid interference from the absorbance of $PdCl_2$, the most favourable wavelength is 390 nm. However, at higher concentrations of disulfoton, the solutions become turbid, allowing measurement of absorbance only below 0.75.

The best results were obtained by extraction of the 3 : 2 complex into ethyl acetate: 10.0 ml of a standard disulfoton

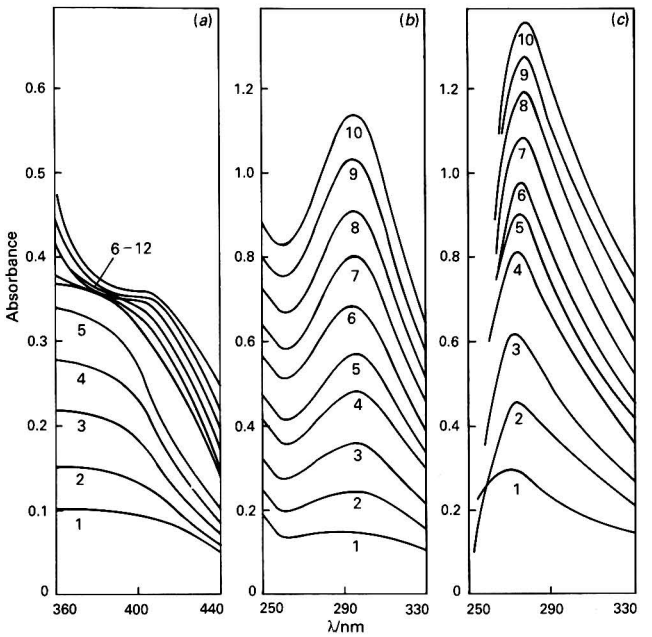

Fig. 3 (*a*) Molar ratio spectra of the $PdCl_2$–disulfoton complexes in ethanol. $PdCl_2$ concentration, 0.025–0.30 mmol dm^{-3} (curves 1–12); disulfoton concentration, 0.10 mmol dm^{-3}. Reference, ethanol ('saturation' at 0.15 mmol dm^{-3} $PdCl_2$, curves 6–12). (*b*) Spectra of the 1:1 $PdCl_2$–disulfoton complex in ethanol. $PdCl_2$ concentration, 0.01–0.10 mmol dm^{-3} (curves 1–10); disulfoton concentration, 0.4 mmol dm^{-3}. Reference, ethanol. (*c*) Spectra of the 3:2 $PdCl_2$–disulfoton complex in ethanol. $PdCl_2$ concentration, 0.3 mmol dm^{-3}; disulfoton concentration, 0.01–0.10 mmol dm^{-3} (curves 1–10). Reference, 0.3 mmol dm^{-3} $PdCl_2$ in ethanol

Table 1 Conditions for the spectrophotometric determination of disulfoton with the $PdCl_2$–HCl reagent

Concentration of $PdCl_2$/ mg l^{-1}	Concentration of disulfoton/ mg l^{-1}	Solvent	*n*	λ/nm	*a*	*b*	*r*
50	2–17	Ethanol	9	278	0.073	0.0534	0.9958
50	2–26	Ethanol	9	305	0.018	0.0370	0.9984
100	8–66	Ethanol	8	390	−0.014	0.0116	0.9994
100*	1–15	Ethyl acetate	9	268	0.034	0.0631	0.9999

* As a solution in water.

solution were shaken for 1 min with 5.0 ml of aqueous $PdCl_2$–HCl. After separation, moisture was removed from the upper ethyl acetate phase by filtration, and the absorbance was measured at 268 nm.

The concentration range of disulfoton (Table 1) shows that the proposed spectrophotometric determination can be used in formulation analysis. A similar method for this purpose was proposed earlier,[6] but without any explanation being given about the composition of the complexes, which is emphasized in the present study. It is very probable that the insecticides phorate and terbufos, closely related to disulfoton, react with $PdCl_2$ in the same manner.

As Pd^{II} is a known complexing agent,[7] the method described is not specific (oxidation and hydrolysis products of disulfoton react also). Therefore, disulfoton must be present in a relatively pure form, which can be easily achieved by extraction from silica gel G after TLC, as described. The extraction is quantitative with ethanol or ethyl acetate (and even with diethyl ether, as proposed for the extraction of the chemically related insecticide isothioate in the TLC–phosphorus spectrophotometric method of formulation analysis[8]).

For residue analysis of disulfoton, the method based on the use of $PdCl_2$ is not applicable, not only because of the requirement for a lower limit of detection and better specificity, but also because of the need to consider its toxic oxidative metabolites (sulphoxide, sulphone, oxon sulphoxide and oxon sulphone[9,10]).

The financial support of the Research Community of Slovenia is gratefully acknowledged.

References

1 Lichtenstein, E. P., and Schultz, K. R., *J. Econ. Entomol.*, 1964, **57**, 618.
2 Murphy, R. J., and Svehla, G., *Anal. Chim. Acta*, 1978, **99**, 115.
3 Schläfer, H. L., *Komplexbildung in Lösung*, Springer-Verlag, Berlin, 1961, p. 233.
4 Sherma, J., *Anal. Chem.*, 1987, **59**, 18R.
5 Pasarela, N. R., in *Analytical Methods for Pesticides and Plant Growth Regulators*, ed. Zweig, G., Academic Press, New York, San Francisco and London, 1977, vol. VI, p. 107.
6 Fujimoto, M., and Tsujino, Y., *Sankyo Kenykynsho Nempo*, 1966, **18**, 144; *Chem. Abstr.*, 1966, **66**, 114892k.
7 Morelli, B., *Analyst*, 1984, **109**, 47.

8 Nakagawa, T., and Kanauchi, M., in *Analytical Methods for Pesticides and Plant Growth Regulators*, eds. Zweig, G., and Sherma, J., Academic Press, New York, San Francisco and London, 1978, vol. X, p. 77.
9 Bowman, M. C., Beroza, M., and Gentry, C. R., *J. Assoc. Off. Anal. Chem.*, 1969, **52**, 157.
10 Wilkins, J. P. G., Hill, A. R. C., and Lee, D. F., *Analyst*, 1985, **110**, 1045.

Paper 0/02582H
Received June 11th, 1990
Accepted September 27th, 1990

Spectrophotometric Determination of Dissolved Oxygen in Water by the Formation of a Dicyanoaurate(I) Complex With Gold Sol

Tarasankar Pal,* Nikhil R. Jana and Pradip K. Das
Department of Chemistry, Indian Institute of Technology, Kharagpur 721 302, India

A simple and sensitive spectrophotometric method for the determination of dissolved oxygen (DO) in water has been developed involving the dissolution of a gelatin-stabilized gold sol formed with cyanide ion in the presence of oxygen. The coloured sol is converted into the colourless dicyanoaurate(I) ion at the end-point. The reagent solution is fairly stable over the experimental time scale and the change in absorbance at 540 nm gives a measure of the concentration of DO in water. The effects of foreign ions on the determination indicated that the method is suitable for determining DO in both drinking and effluent waters. It has the advantage of being capable of determining DO down to a concentration of 60 ppb in water samples. The slope of the calibration graph is 0.16 A ml μg^{-1}. The molar absorptivity of the solution is 5.12×10^3 dm^3 mol^{-1} cm^{-1} with a relative standard deviation of 0.85%; the confidence limit (95%) for 0.20 ppm of DO (ten replicates) is 0.20 ± 0.002 ppm.

Keywords: *Dissolved oxygen determination; gold sol; dicyanoaurate(I) ion; spectrophotometry*

The determination of dissolved oxygen (DO) plays a key role in water pollution control activities and waste treatment process control. In natural and waste waters, DO levels depend on the physical, chemical and biological activities. Hence, there is a need for a method for the determination of DO in water that is sufficiently sensitive to dispense with microtechniques and special glassware and apparatus. This is particularly true in situations where only small samples are available, or where a number of different analyses must be made on a limited amount of sample. This paper describes a procedure for the determination of DO utilizing a very stable sol system.

Many methods[1–8] are available for the determination of DO in water. An extensive review including a comparative study of the various techniques for the determination of DO has been carried out by Lindstrom *et al.*[7] However, the standard classical method is still that of Winkler[1] or one of its modifications, all of which suffer from serious drawbacks in that they require large sample volumes, are time consuming and suffer serious interferences from foreign ions. Recently, we reported a simple and sensitive method[9] for the determination of DO involving the dissolution of a gelatin-stabilized yellow silver sol formed with cyanide ion in the presence of oxygen. However, a disadvantage of the method is the instability of the silver sol to visible light: even interior lighting can cause a change in the absorbance of the reduced silver sol; hence the silver sol must be kept in amber-coloured bottles.

In this paper, a pink gold sol which is largely insensitive to light was used as the colour reagent for the determination of trace amounts of DO in water by following the oxygen- and cyanide-dependent decrease in intensity of the coloured gold sol at 540 nm. We are currently attempting to develop a fibre optic based remote sensing technique to measure the DO level in water samples utilizing this gold sol dissolution principle. Although the chloroauric acid used for the preparation of the gold sol is an expensive reagent, the concentration of gold ion used (1×10^{-3} mol dm^{-3}) is such as to make the proposed method very economical. Moreover, the concentration of cyanide ion used to produce the reaction products means that the toxicity of the method is negligible. Further, the gold can be reclaimed from the cyano complex.[10] The method is best suited to the routine determination of DO in industrial and natural waters at concentrations down to 60 ppb.

* Present address: Health and Safety Research Division, Oak Ridge National Laboratory, Oak Ridge, TN 37831-6101, USA.

Experimental

Apparatus

All absorbance measurements were made with a Shimadzu UV-160 digital spectrophotometer with 1 cm quartz cells.

A digital (ECIL, Hyderabad, India, Government of India Enterprise) pH meter was used for pH measurements.

Reagents

All reagents used were of analytical-reagent grade. A stock solution of gold(III) chloride was prepared by dissolving 1 g of chloroauric acid (Johnson Matthey, Royston, Hertfordshire, UK) in 500 ml of doubly distilled water. The solution was standardized using a literature method[11] and diluted to about 1×10^{-3} mol dm^{-3}. A fresh stock solution of hydrazine (0.1 mol dm^{-3}) was prepared by dissolving hydrazine sulphate in distilled water and was standardized by a classical procedure.[12] Gelatin solution (1%) was prepared by dissolving 1 g of powdered gelatin (Merck, Darmstadt, Germany) in 100 ml of warm, distilled water. Glycine buffer of pH 9.5 was prepared by mixing 50 ml of 0.2 mol dm^{-3} glycine and 16.8 ml of 0.2 mol dm^{-3} sodium hydroxide and was diluted with water to obtain a final volume of 200 ml; the pH was adjusted using the pH meter. Sodium cyanide (May and Baker, Dagenham, Essex, UK) (0.1 g) was dissolved in 100 ml of distilled water and the solution was standardized with silver nitrate.[13] The gold–gelatin complex was prepared by placing 5.0 ml of 1×10^{-3} mol dm^{-3} chloroauric acid, 25 ml of 1% gelatin and 25 ml of glycine buffer (pH 9.5) in a 100 ml calibrated flask. The

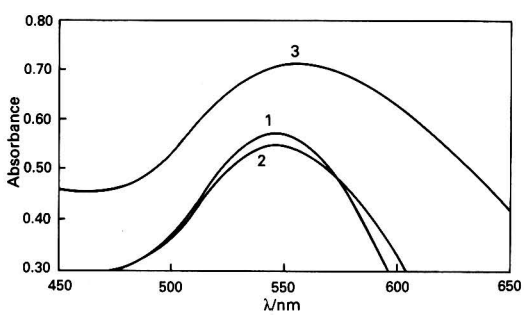

Fig. 1 Absorption spectra of gold sol. pH: 1, 10.6; 2, 10.0; and 3, 8.6

complex was reduced to the gold sol with 1 ml of hydrazine sulphate solution (0.1 mol dm^{-3}) at 35 °C. The gold sol is very stable at room temperature. At the maximum wavelength (λ_{max}) (540 nm) the sol solution shows negligible scattering. A gold sol of reproducible particle size (λ_{max} = 540 nm) can best be obtained in a buffered medium of pH 9.5–11.0 (see Fig. 1). The sol system, particularly the gold sol, might be able to act as a unique adsorbate in diverse chemical studies.[14] The absorbance values are proportional to the sol concentration. For the purpose of de-gassing, oxygen-free nitrogen was used, which was further purified by passing it over hydrogen-reduced copper powder at 350 °C and through two consecutive solutions of alkaline pyrogallol.[9]

Procedure

Gelatin-stabilized gold sol and sodium cyanide were studied as reagents for the determination of DO. As mentioned in a previous paper,[9] de-gassed reagents were used and other precautionary measures taken in order to avoid contamination by oxygen. Then, appropriate aliquots of the two reagents (gold sol : sodium cyanide ratio = 50 : 1 v/v) were placed in the spectrophotometer cell under a nitrogen atmosphere. Air-saturated water was employed to obtain a calibration graph.

The concentration of DO in the sample tube containing air-saturated water was calculated from the equation used previously.[9] Hence the temperature-dependent DO concentration in water can easily be found.

Results and Discussion

The reaction of the gold sol with cyanide may be represented as follows:

$$4Au + 8CN^- + 2H_2O + O_2 \rightarrow 4[Au(CN)_2]^- + 4OH^- \quad (1)$$

The gold sol solution is pink when stabilized by the gelatin solution, but the dicyanoaurate(I) complex, which is readily formed in alkaline medium, is colourless. Therefore, if gold sol and cyanide are taken in a 50 : 1 ratio in the concentration range mentioned earlier, the decrease in intensity of the pink gold sol in the presence of oxygen is a measure of the concentration of DO in water. As the disappearance of the pink colour is both DO- and cyanide-dependent, the sol concentration in the test system should be sufficient for the final absorbance values to lie within the sensitive spectrophotometric region. The advantage of the method is that as little as 60 ppb of DO can be determined using a minimum volume (about 0.03 ml) of water while recording the absorbance values.

Advantages of the Proposed Method

The methods described in the literature for the spectrophotometric determination of DO in water samples suffer from serious interferences from common ions. The proposed method has advantages not only over the method of Winkler[1] but also over other spectrophotometric methods as mentioned previously.[9] The reagent solutions can be stored for at least 2 months; further, as the reaction is carried out with a very dilute solution of gold sol (1×10^{-5} mol dm^{-3}) and a sodium cyanide solution of 0.1 mol dm^{-3} in a ratio of 50 : 1 v/v, the cost of chemicals and the toxicity of the method are negligible.

Precision and Accuracy

The method is suitable for the determination of DO in water when the DO concentration is very low (60 ppb) even in a few microlitres of analyte. The slope of the calibration graph is 0.16 A ml μg^{-1}. The molar absorptivity of the solution is 5.12×10^3 dm^3 mol^{-1} cm^{-1} with a relative standard deviation of 0.85% and the confidence limit (95%) for 0.20 ppm of DO (ten replicates) is 0.20 ± 0.002 ppm.

Interferences and Applications

A brief investigation was carried out into the influence of common organic and inorganic compounds which usually interfere with the determination of DO. The DO content of several water samples was determined by the standard method[1] and the proposed method. The results were comparable to the data reported previously.[9]

References

1 Winkler, L. W., *Ber. Dtsch. Chem. Ges.*, 1888, **21**, 2843.
2 Fadrus, H., and Maly, J., *Analyst*, 1971, **96**, 591.
3 Duncan, A., Harriman, A., and Parter, G., *Anal. Chem.*, 1979, **51**, 2206.
4 Hamlin, P. A., and Lambert, J. L., *Anal. Chem.*, 1971, **43**, 618.
5 Rahim, S. A., and Mohamed, S. A., *Talanta*, 1978, **25**, 519.
6 Sastry, G. S., Hamm, R. E., and Pool, K. H., *Anal. Chem.*, 1969, **41**, 857.
7 Lindstrom, R. E., Patel, S. N., and Wilkinson, P. K., *J. Parenter. Drug Assoc. (Philadelphia)*, 1980, January/February.
8 Malaiyandi, M., and Sastri, V. S., *Talanta*, 1983, **30**, 983.
9 Pal, T., and Das, P. K., *Analyst*, 1988, **113**, 1601.
10 Perman, C. A., *Talanta*, 1979, **26**, 603.
11 Vogel, A. I., *A Text-Book of Quantitative Inorganic Analysis*, Longman, London, 1973, p. 464.
12 Vogel, A. I., *A Text-Book of Quantitative Inorganic Analysis*, Longman, London, 1969, p. 380.
13 Vogel, A. I., *A Text-Book of Quantitative Inorganic Analysis*, Longman, London, 1969, p. 272.
14 Pal, T., Pal, A., and Vo-Dinh, T., *Science*, submitted for publication.

Paper 0/02711A
Received June 18th, 1990
Accepted October 4th, 1990

Sensitive Spectrophotometric Determination of Osmium With Pyrocatechol and Hydroxyamidine

Manas Kanti Deb, Neera Mishra, Khageshwar Singh Patel and Rajendra Kumar Mishra
Department of Chemistry, Ravishankar University, Raipur-492 010, M.P., India

An ethanolic solution of pyrocatechol in the presence of hydroxyamidine and osmium(VIII), on heating at a pH between 7.0 and 9.0, gives a very sensitive colour reaction. The coloured species formed is extracted into dichloromethane and gives molar absorptivities with N^1-hydroxy-N^1,N^2-diphenylbenzamidine and its eight derivatives in the range 0.80×10^6–3.45×10^6 dm^3 mol^{-1} cm^{-1} with the wavelengths of maximum absorption at 400–430 nm. The method is extremely sensitive and free from interference from the ions commonly associated with osmium. The method is applicable to the recovery of the metal from ores containing osmium at ppb levels and also from synthetic matrices.

Keywords: *Osmium(VIII) spectrophotometric determination; solvent extraction; pyrocatechol; hydroxyamidines; low-grade ore*

Osmium is a precious metal that occurs, with other platinum-group metals and other base metals, in the Earth's crust in trace amounts ranging from ppb to ppm levels. It is a metal of electronic,[1] industrial[2] and environmental[3] interest. Therefore, a very sensitive method for its determination is required in order to detect the metal in geological, metallurgical, environmental and industrial waste samples. Many sensitive spectrophotometric methods for the determination of osmium have been reported; the reagents utilized included [values given are molar absorptivity (dm^3 mol^{-1} cm^{-1}) and wavelength (nm)]: Methylene Blue (2.2×10^5, 655);[4] 7-amino-1-hydroxynaphthalene-3-sulphonic acid (5.08×10^5, 500);[5] Rhodamine 6G (4.0×10^5, 530);[6] Brilliant Green (1.95×10^5, 640);[7] 2-thiobarbituric acid (1.4×10^6, 332);[8] Rhodamine B (4.1×10^5, 560);[9] and Malachite Green (1.6×10^6, 690).[10] However, these methods suffer interference from some of the platinum-group metals and other base metals, hence their sensitivity is poor. In this work, the most sensitive compound, N^1-hydroxy-N^2-(3-chlorophenyl)-N^1-(4-chlorophenyl)-2-chlorobenzamidine (HCPCPCBA), was chosen for detailed investigation. The method used is based on heating an ethanolic solution of Os^{VIII} in the presence of pyrocatechol [$C_6H_4(OH)_2$] and hydroxyamidine (HOA), over a water-bath to near dryness at pH 8.0 ± 0.2, and then re-dissolving the coloured species in dichloromethane.

Experimental

Apparatus

A Carl Zeiss Jena Spekol Model 856 and a Cecil ultraviolet/visible spectrophotometer with matched 1 cm quartz cells were used for the absorbance measurements. A Systronic Model 322 pH meter was employed for the pH measurements.

Reagents

All chemicals used were of analytical-reagent grade and were obtained from either grade and were obtained from either BDH or Merck.

A standard solution of Os^{VIII} was prepared by dissolving 1.0 g of osmium tetroxide in about 100 ml of 0.2 mol dm^{-3} NaOH,[11] diluting to 1 l with distilled water and standardizing with KI and $Na_2S_2O_3$.[12] The stock solution was kept in a refrigerator, and a working solution (0.25 μg ml^{-1} of Os) prepared by appropriate dilution with distilled water.

Hydroxyamidines were synthesized as described previously,[13] and used at a concentration of 0.4% m/v in ethanol. A 0.4% m/v solution of pyrocatechol in water was also employed. A pH 8.0 NaOH–H_3BO_3 buffer[14] was used for pH adjustment.

Procedure

An aliquot of the standard solution containing up to 0.4 μg of Os^{VIII} was placed in a 25 ml beaker, followed by 2 ml of pyrocatechol and 5 ml of HCPCPCBA solutions. The pH was adjusted to about 8.0 by the addition of 1 ml of NaOH–H_3BO_3 buffer, and the volume made up to 10 ml with 0.4% m/v ethanol solution.

The solution was evaporated over a boiling water-bath to near dryness (otherwise full colour development was not observed). The dried residue was re-dissolved in water (5 ml) with heating. The solution was then cooled and transferred into a 100 ml separating funnel and the pH adjusted to about 5 ± 1. The aqueous solution was shaken with 5 ml of dichloromethane and washed with a fresh 2 ml portion of dichloromethane. The extract was dried, in a 25 ml beaker, over anhydrous sodium sulphate (1 g). All of the extract was then transferred into a 10 ml calibrated flask and diluted to the mark with dichloromethane. The spectrum of the coloured species was recorded against the reagent blank; the absorbance was measured at λ_{max}.

Results and Discussion

Formation of Coloured Species

The optimum pH range of the aqueous solution for maximum colour development of the species in dichloromethane was evaluated, and found to be between pH 7.0 and 9.0. Further work was carried out, at a pH of 8.0 ± 0.2, on the effect of the addition of buffer solution; addition of 0.5–3 ml had no adverse effect.

Maximum colour development only occurred when the solution containing Os, $C_6H_4(OH)_2$ and HCPCPCBA was heated to near dryness over a water-bath at 80 ± 5 °C. Increasing the water-bath temperature to 100 °C had no adverse effect on the maximum colour development. However, heating of the dried mass for more than 3 min tended to decrease the formation of the coloured species; this may have been due to the evaporation of some of the osmium content or the thermal decomposition of the coloured species.

The effect of $C_6H_4(OH)_2$ and HCPCPCBA concentrations on the maximum colour development of the species in dichloromethane was examined. Concentrations of greater than 0.33×10^{-3} mol dm^{-3} $C_6H_4(OH)_2$ and 0.38×10^{-2} mol dm^{-3} HCPCPCBA in a 50% v/v ethanolic solution were

necessary for full colour development, and concentrations of up to 1.35×10^{-2} mol dm^{-3} $C_6H_4(OH)_2$ and 1.0×10^{-2} mol dm^{-3} HCPCPCBA had no adverse effect. The ratio of the volume of ethanol to water was examined and it was found that the ratio of the volumes can be varied from 1:4 to 4:1 with no effect.

Extraction of Coloured Species

Various solvents, *i.e.*, pentan-1-ol, ethyl acetate, cyclohexane, chloroform, carbon tetrachloride, benzene, toluene, dichloromethane and trichloroethane, were tested for the extraction of the coloured species formed by Os^{VIII}, $C_6H_4(OH)_2$ and HCPCPCBA. All of the solvents, except carbon tetrachloride and cyclohexane, extracted the coloured species with different values for the molar absorptivity [ε (dm^3 mol^{-1} cm^{-1})] and the wavelength of maximum absorption [λ_{max} (nm)]: pentan-2-ol ($\varepsilon = 3.60 \times 10^6$, $\lambda_{max} = 430$); ethyl acetate ($\varepsilon = 3.75 \times 10^6$, $\lambda_{max} = 415$); chloroform ($\varepsilon = 4.02 \times 10^6$, $\lambda_{max} = 430$); benzene ($\varepsilon = 2.00 \times 10^6$, $\lambda_{max} = 435$); toluene ($\varepsilon = 2.80 \times 10^6$, $\lambda_{max} = 430$); dichloromethane ($\varepsilon = 3.45 \times 10^6$, $\lambda_{max} = 430$); and trichloroethane ($\varepsilon = 2.95 \times 10^6$, $\lambda_{max} = 430$). In this investigation, dichloromethane was chosen as it was the least toxic diluent (among the various non-polar organic solvents) and it gave more selective extraction than either ethyl acetate or pentan-1-ol.

Variation in the volume of the aqueous phase used on the extraction of the brown species with dichloromethane was studied. A ratio of the volume of the aqueous to the organic phase of between 1:2 and 2:1 is required for maximum extraction of the coloured species. An equilibration period of 1 min is sufficient for full colour development of the species in the organic solution; prolonged extraction of up to 30 min has no adverse effect. During extraction the pH of the aqueous solution should be maintained between 3.5 and 9.5. The temperature of the aqueous phase can be varied from 10 to 40 °C without any adverse effect. The extract, in dichloromethane at room temperature (22 ± 2 °C), is stable for at least 2 h.

The colour reaction of Os^{VIII} with N^1-hydroxy-N^1,N^2-diphenylbenzamidine and its eight derivatives in the presence

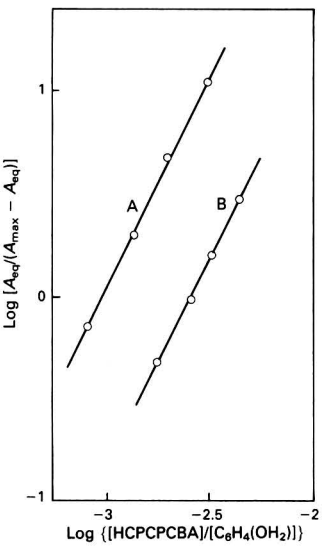

Fig. 2 Determination of the ratio of osmium to pyrocatechol and HCPCPCBA in the formation of the coloured species. A, Log distribution ratio $[A_{eq}/(A_{max} - A_{eq})]$ of the coloured species in dichloromethane *versus* log$[C_6H_4(OH)_2]$; and B, log distribution ratio $[A_{eq}/(A_{max} - A_{eq})]$ of the coloured species in dichloromethane *versus* log[HCPCPCBA]

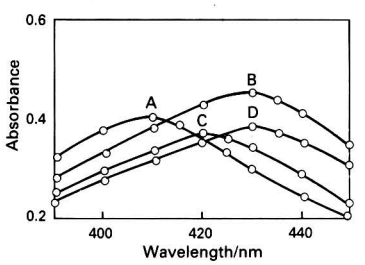

Fig. 1 Absorption spectra of the coloured species with different hydroxyamidines in dichloromethane. [Os^{VIII}] = 0.25 μg per 10 ml of aqueous ethanolic solution, [$C_6H_4(OH)_2$] = 7.25×10^{-3} mol dm^{-3}, pH = 8.0 ± 0.2. A, N^1-Hydroxy-N^1,N^2-diphenylbenzamidine; B, N^1-hydroxy-N^2-(3-chlorophenyl)-N^1-(4-chlorophenyl)-2-chlorobenzamidine; C, N^1- hydroxy-N^1-(2-chlorophenyl)-N^2-phenyl-2-chlorobenzamidine; and D, N^1-hydroxy-N^1-(3-chlorophenyl)-N^2-(3-chlorophenyl)-2-chlorobenzamidine

Table 2 Effect of foreign ions on the determination of Os^{VIII} (0.25 μg per 10 ml) with pyrocatechol and HCPCPCBA

Ion	Tolerance limit*/ μg
V^V	0.4
Ru^{III}	2.8
Ti^{IV}	6.0
Ni^{II}	18
Pd^{II}	23
Fe^{III}	55
Ir^{III}, Cu^{II}, Pt^{IV}, Mo^{VI}	80
Sb^{III}	100
Cd^{II}	150
W^{VI}	180
Sr^{II}, CH_3COO^-, NO_3^-, SCN^-	225
Pb^{II}, Sn^{IV}, Re^{VII}, $C_2O_4^{2-}$	310
Ag^I	330
Zn^{II}, Bi^{III}, Th^{IV}, I^-, F^-	400
Al^{III}, As^V	460
Ethylenediaminetetraacetic acid	5500

* Causing an error of less than 2%.

Table 1 Spectral data of the coloured species formed between Os^{VIII}, pyrocatechol and hydroxyamidines [$R^1C(R^3NOH)NR^2$] in dichloromethane

Hydroxyamidine			λ_{max}/ nm	$\varepsilon/10^6$ dm^3 mol^{-1} cm^{-1}
R^1	R^2	R^3		
2-Cl-C_6H_4	3-Cl-C_6H_4	4-Cl-C_6H_4	430	3.45
2-Cl-C_6H_4	3-Cl-C_6H_4	3-Cl-C_6H_4	430	2.90
2-Cl-C_6H_4	C_6H_5	2-Cl-C_6H_4	430	2.84
2-Cl-C_6H_4	C_6H_5	4-Cl-C_6H_4	425	2.40
C_6H_5	3-Cl-C_6H_4	C_6H_5	415	1.90
C_6H_5	4-CH_3-C_6H_4	C_6H_5	410	2.66
4-Cl-C_6H_4	2,3-$(CH_3)_2$-C_6H_3	4-Cl-C_6H_4	420	0.80
C_6H_5	C_6H_5	4-CH_3-C_6H_4	400	2.35
C_6H_5	C_6H_5	C_6H_5	410	3.10

Table 3 Recovery of osmium from synthetic matrices

Synthetic matrix sample*	Composition reported (%)	Composition added/μg	Osmium found/μg	Recovery (%)
South Africa—				
Ru	8.9	0.0308	—	—
Ir	17	0.0608	—	—
Pd	0.2	0.0007	—	—
Os	69.9	0.25	0.245	98.0
Australia—				
Ru	5.22	0.0467	—	—
Ir	58.13	0.521	—	—
Pd	3.04	0.0272	—	—
Os	33.46	0.3	0.298	99.3
California—				
Ru	0.5	0.003	—	—
Ir	53.5	0.308	—	—
Pd	2.6	0.0145	—	—
Os	43.4	0.25	0.256	102.4
Urals—				
Ru	8.49	0.053	—	—
Ir	43.28	0.27	—	—
Pt	0.62	0.0039	—	—
Pd	5.73	0.038	—	—
Os	41.88	0.25	0.260	104.0
Colombia—				
Ru	6.37	0.055	—	—
Ir	57.8	0.50	—	—
Pd	0.63	0.0055	—	—
Os	35.1	0.30	0.298	99.3

* The locations given indicate the actual composition of the ores from the Earth's crust in these locations. The synthetic mixtures were prepared according to these compositions.

Table 4 Recovery of osmium from synthetic water samples and a low-grade ore sample

Sample	Osmium concentration (ppb)	Osmium found (ppb)	Recovery (%)
Tap water, 1 l	5*	4.8	96.0
Tap water, 2 l	2.5*	2.6	104.0
US Bureau of Mines Reference Material, Platinum Ore (USBM-Pt-A)	103 ± 7†	112	—

* Concentration of osmium added.
† Concentration of osmium reported.

of pyrocatechol was investigated as described under Procedure. Spectral data show that the values for the molar absorptivity and absorption maximum of the coloured species are markedly affected by the nature of the hydroxyamidine (Fig. 1). The molar absorptivities of the coloured species, *i.e.*, for osmium with the nine different hydroxyamidines, lie in the range 0.80×10^6–3.45×10^6 dm^3 mol^{-1} cm^{-1} (see Table 1). The most sensitive colour reaction is seen with the derivative having a chloro group in each of the three phenyl rings of the hydroxyamidine. Hence, this derivative was chosen for detailed investigation. The value of the molar absorptivity of the coloured species in dichloromethane with HCPCPCBA was found to be 3.45×10^6 dm^3 mol^{-1} cm^{-1} at a λ_{max} of 410 nm. The system followed Beer's law in the range 0–40 ppb of Os, with a correlation coefficient of 0.9. Ten replicate determinations at a level of 25 ppb of Os gave a relative standard deviation of 1.9%.

The stoichiometry of the colour reaction occurring between Os^{VIII}, $C_6H_4(OH)_2$ and HCPCPCBA was determined by a curve-fitting method which plotted the log of the distribution ratio of the coloured species *versus* the log of the molar concentration of the reagent taken. Slopes of 2.1 and 2.0, close to the integer 2, were obtained for the pyrocatechol and hydroxyamidine reactions, respectively (see Fig. 2). The reaction ratio of Os : $C_6H_4(OH)_2$: HCPCPCBA in the formation of the coloured species in dichloromethane is expected to be 1 : 2 : 2.

The influence of foreign ions on the determination of 0.25 μg of Os^{VIII} with $C_6H_4(OH)_2$ and HCPCPCBA was examined using the method described under Procedure. A considerable amount of precious metal ions and a large amount of other ions are tolerated; their tolerance limits are summarized in Table 2.

Procedure for Determination of Osmium

The validity of the proposed method was tested for the recovery of the metal from a low-grade ore (platinum metal ore) and synthetic matrices. An accurately weighed sample of ore was digested by the acid-treatment method described by Haskell and Wright.[15] The residue obtained was dissolved in 1% m/v tartaric acid and diluted to 50 ml with the same solution. An aliquot (10 ml) of this solution was transferred into a 50 ml beaker containing 2 ml of pyrocatechol, 5 ml of HCPCPCBA, 1 ml of buffer solution and the standard solution of Os^{VIII}. The solution was heated to near dryness and dissolved in 10 ml of water and the pH adjusted to about 5. The solution was transferred into a 100 ml separating funnel and washed with 2 ml of water; it was then shaken with 5 ml of dichloromethane. The organic layer containing the coloured species was transferred, over 1 g of anhydrous sodium sulphate (to dry the extract), into a 25 ml beaker and the aqueous phase washed with a fresh 2 ml portion of dichloromethane. All of the extract, after drying, was transferred into a 10 ml calibrated flask and diluted to the mark with dichloromethane. Five replicate determinations were carried out with different known amounts of Os^{VIII}. A calibration graph was prepared by plotting the absorbance *versus* the concentration of Os^{VIII} added, and the metal content in the solution determined by extrapolation from the graph. Similarly, the metal contents in the synthetic matrices were determined. The results obtained are summarized in Tables 3 and 4.

We thank the Council of Scientific amd Industrial Research (CSIR), New Delhi, for financial support of this work through grant-in-aid 1(1067)/87/EMR-II.

References

1 Belousova, T. P., and Telezhkin, S. A., *New Materials in Electronic Instrument Making*, Izd. Ontipribor, 1965.
2 Das, M. S., *Trace Analysis and Technological Development*, Wiley Eastern, New Delhi, 1981.
3 Sax, N. I., *Dangerous Properties of Industrial Materials*, Van Nostrand Reinhold, New York, 6th edn., 1984.
4 Marczenko, Z., and Uscinska, J., *Anal. Chim. Acta*, 1981, **123**, 271.
5 Yeh, S., *Gaodeng Xuexiao Huaxue Xuebao*, 1981, **2**, 548.
6 Marczenko, Z., Balcerzak, M., and Pasek, H., *Mikrochim. Acta, Part II*, 1982, 371.
7 Balcerzak, M., and Marczenko, Z., *Microchem. J.*, 1984, **30**, 397.
8 Morelli, B., *Analyst*, 1987, **112**, 1395.
9 Balcerzak, M., *Analyst*, 1988, **113**, 129.
10 Li, Z., and Zhao, M., *Fenxi Huaxue*, 1989, **17**, 118.
11 Ayers, G. H., and Wells, W. N., *Anal. Chem.*, 1950, **22**, 317.
12 Klobbie, E. A., *Chem. Zentralbl.*, 1898, **11**, 65.
13 Satyanarayana, K., and Mishra, R. K., *Anal. Chem.*, 1974, **46**, 1609.
14 Lange, N. A., *Handbook of Chemistry*, McGraw-Hill, New York, 10th edn., 1967, p. 971.
15 Haskell, R. J., and Wright, J. C., *Anal. Chem.*, 1987, **59**, 427.

Paper 0/02469D
Received June 4th, 1990
Accepted November 13th, 1990

High-pressure Flow-injection Assembly. Indirect Determination of Glycine by Atomic Absorption Spectrometry

J. Martinez Calatayud
Departamento de Quimica Analitica, Universidad de Valencia, Valencia, Spain
J. V. Garcia Mateo
Departamento de Quimica, Colegio Universitario CEU, Moncada, Valencia, Spain

A procedure for the determination of glycine is described. The method is based on the reaction of the analyte with finely powdered, solid copper(II) carbonate in a continuous-flow assembly. The optimum experimental conditions of pH, temperature, sample volume, flow-rate, column length and internal diameter, and the linear range of calibration, were studied. Interference from foreign substances that accompany this amino acid in pharmaceutical formulations was studied, and the method was applied to the determination of glycine.

Keywords: *Glycine determination; atomic absorption spectrometry; on-line conversion*

A recent trend in flow injection (FI) techniques is the use of solid or immobilized reagents. Although it is preferable to allow each sample to react with a fresh portion of reagent solution, this approach is not always possible if the reagent is available only in the solid form. Hence, the solid particles of reagent are packed into a column, which can be easily integrated into a continuous-flow manifold, and the sample plug moves through the packed reactor, producing the species sensed by the detector.

The use of solid reactors has some advantageous features, however, such as simplification of manifolds by eliminating one or more streams, and enhancement of both the sensitivity of the transient signal and the injection rate as a consequence of reduction in the dilution of the sample plug. Solid reactors are also required for reducing the consumption of expensive reagents such as enzymes. The use of solid or immobilized reagents in FI is likely to increase markedly in the next few years. A solid can be incorporated at various points along an FI manifold for a variety of purposes,[1] namely, (*a*) sample pre-treatment prior to injection by using adsorbents or ion exchangers;[2,3] (*b*) reaction with the sample between injection valve and detector or inside the detector flow cell;[4,5] and (*c*) *in situ* preparation of unstable reagents.[6]

In relation to the application of packed-bed reactors to pharmaceutical analysis, the potential of FI atomic absorption spectrometry (AAS) for the indirect automated determination of drugs should be emphasized.[7-9] Classical methods based on a reaction between the pharmaceutical compound and a metal ion are usually tedious and time consuming, as they rely on outdated methodologies that are generally non-automated and hence incur high personnel and reagent costs.

The strategies that can be adopted in order to utilize immobilized reagents in continuous-flow systems are varied. The general use of immobilized reagents is associated with: (*a*) a simple construction procedure; and (*b*) lack of problems (derived from variations in the pressure) when the assembly is working; FI has been defined as a low-pressure methodology, the size or external diameter of the particle should be large enough to allow the use of peristaltic pumps. A comparative study on immobilized enzyme reactors emphasized the importance of the aspect ratio and recommended that, for the best results, the reactor should be filled with beads of a diameter equal to 90% of the tube diameter.[10]

This paper deals with a reactor containing a finely powdered solid, that requires pressures greater than those obtained with peristaltic pumps. This is an attempt to provide a variety of solid–liquid reactions, which can be considered for use with FI manifolds, and for which no additional effort is required in order to adapt the reagent, commercially available with a small particle diameter, for use in larger columns (*i.e.*, tedious recrystallization processes are avoided). No chemical or physical bonding is needed for immobilization and a larger surface area per unit length of reactor can be offered and hence, shorter column lengths can be used.

Amino acids are considered to be the main indicators of the nutritional requirements in various pathological states.[11,12] Much information on the levels of free and total amino acids in biological matrices has been accumulated by classical ion-exchange liquid chromatography based on post-column reaction with ninhydrin. A number of reagents have been introduced, such as fluorescamine, *o*-phthalaldehyde, dansyl chloride and phenylthiohydantoin. An automated on-line high-performance liquid chromatographic method, based on pre-column derivatization with *o*-phthalaldehyde in the presence of 2-mercaptoethanol, has recently been developed.[13] Titrimetry with sodium hydroxide using Bromothymol Blue as indicator, has been officially recommended for the determination of amino acids in vitamin preparations.[14] The Edman method[15] is widely used for the sequential determination of amino acids in a peptide chain.

This paper describes the determination of glycine by means of on-line conversion with copper(II) carbonate packed into a column, the complex formed being fed to an AAS detector. Different types of columns containing copper(II) carbonate were tested, and the chemical and FI parameters were optimized for the determination of glycine in pharmaceutical preparations. The influence of foreign compounds was also studied.

Experimental

Reagents and Apparatus

All solutions were prepared with de-ionized water. Aqueous solutions of glycine (Probus, analytical-reagent grade), caffeine (Fluka), acetylsalicylic acid (Panreac, pure), ascorbic acid (Merck, analytical-reagent grade), sorbitol (Acofarma, pure), and copper(II) carbonate, sodium carbonate and sodium hydrogen carbonate (Probus, analytical-reagent grade) were used. The packed-bed reactor was prepared with $CuCO_3 \cdot Cu(OH)_2 \cdot 10H_2O$ (Panreac, analytical-reagent grade).

Flow injection assembly

Fig. 1 shows the continuous-flow manifold; the sample injector (Model 5041) was from Rheodyne, and a Shimadzu LC-GA high-performance liquid chromatographic pump was used. The determination of Cu^{II} was carried out by means of

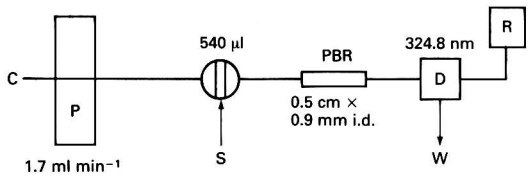

Fig. 1 Continuous-flow assembly: C, carrier; P, pump; S, sample; PBR, packed-bed reactor; D, detector; R, recorder; and W, waste

an AAS instrument, Model SP-1900 (Pye Unicam), at a wavelength of 324.8 nm. The PTFE tube coils in the FI assembly were of 0.8 mm i.d. The laboratory-built reactor was constructed by perforating a methacrylate or plastic block to form a column (0.5 cm long) with an i.d. of 0.9 mm.

Procedures

Preparation of the packed-bed reactor

The methacrylate column was filled with solid copper(II) carbonate by means of a mini-funnel; it was then inserted into the FI manifold. The column was conditioned for 15 min with a carbonate–hydrogen carbonate buffer solution of pH 9.5, containing 100 ppm of glycine, prior to sample injection.

Aliquots, of 540 µl, of the aqueous drug solution were directly injected into the carrier stream and, after flowing through the solid mini-reactor, were carried towards the AAS detector.

Determination of glycine in pharmaceutical formulations (tablets)

The required amount of powdered tablets was dissolved in de-ionized water. If some precipitate remained the solution was filtered, and the volume of the filtrate re-adjusted with de-ionized water. Calibration graphs were prepared from measurements with pure glycine in de-ionized water.

Results and Discussion

Preliminary experiments were carried out under static conditions; 0.1 g of copper(II) carbonate was introduced into a beaker, then 10 ml of aqueous glycine, with the pH previously adjusted (HCl or NaOH), were added. Absorption spectra of the resulting solution were monitored over the range 450.0–700.0 nm. An absorption band was observed with a maximum at 632.0 nm. The pH was studied over the range 2.0–12.0. These experiments revealed that the greatest absorbance values were produced by the solution at pH 9.5 (see Fig. 2). The beaker was then immersed in a water-bath at different temperatures: 20.0, 40.0, 60.0 and 80.0 °C, and absorption spectra were recorded when thermal equilibrium was reached. The best results were observed at 40 °C.

The optimization of chemical and FI parameters was carried out by means of the univariate method and with the aim of a suitable compromise between peak height, sample throughput, reproducibility and lifespan of the column. The preliminary tests on the FI assembly were carried out by means of the assembly represented in Fig. 1; hydrodynamic problems, such as the required pressure, did not allow the packed-bed reactor to be inserted into the sample loop.

Preliminary tests on the FI assembly revealed the influence of the pH and basic media; tests were carried out at 40.0 °C, and the study was effected by adjusting the pH of the carrier or sample solution prior to injection. The optimization of the carrier medium was obtained by using different mixtures. Higher transient signals were observed with a basic carrier stream (pH range 9–11). A set of experiments carried out over the selected pH range and with use of sodium hydroxide or several buffer mixtures, led to the following results and

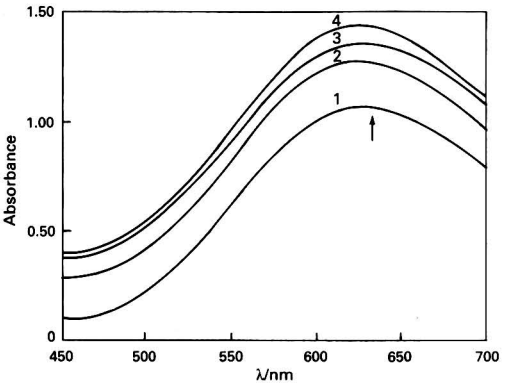

Fig. 2 Influence of pH on the absorbance spectra of the copper–glycine complex. pH: 1, 8.0; 2, 8.5; 3, 9.0; and 4, 9.5. The arrow indicates the wavelength of maximum absorption (632 nm)

conclusions. The sodium hydroxide solution at pH 9.5 appeared to be adequate, but the column darkened, perhaps because of CuO formation; this also meant a shorter lifespan. The carbonate–hydrogen carbonate solution, buffered at pH 9.5, was selected for further experiments. It must be pointed out that the ionic strength (adjusted with NaCl) had no effect on the outputs.

The influence of the basic media in the sample solution was tested by injecting the previously pH adjusted sample into the buffered carrier stream. Three different sets of experiments were carried out at 40.0 °C: the first with NaOH; the second with NaOH plus NaCl (in order to have the same ionic strength as the carrier); and the third with carbonate–hydrogen carbonate mixture (the same as the carrier). No significant differences were observed, however, all of them produced higher peaks than those obtained from the injection of glycine in de-ionized water.

The influence of temperature on the continuous-flow procedure was shown to be a non-critical parameter; it was tested by adjusting the temperature with the aid of a water-bath. Two different sets of experiments were carried out: (*a*) with the carrier solution container in the bath; and (*b*) with the sample loop immersed in the bath. No significant enhancement of the outputs was observed when the temperature was increased; bearing in mind that a plain (single-channel) manifold was being used, room temperature was selected for further work.

The size of the packed-bed reactor was studied by testing two parameters simultaneously, namely, length and i.d. of the column. The ranges tested were: 0.5–1.6 mm for the i.d. and 5–25 mm for the column length. The set of experiments carried out led to the following results and conclusions: (*a*) the longest columns were not suitable, as the peak height was slightly decreased; (*b*) the i.d. was the main parameter influencing sample dispersion, *e.g.*, in experiments with columns of three different i.d. values (0.5, 0.9 and 1.6 mm), all with the same length, the absorbance readings for the 0.9 and 1.6 mm column, respectively, were 85 and 1.1% of that obtained with the 0.5 mm column; and (*c*) the high pressure required for small i.d. values, *e.g.*, 0.5 mm, could not be tolerated by the plastic connection devices used in the manifold. Therefore, a column of 0.9 mm i.d. and 5 mm in length was selected for further work.

The influence of the sample volume on the peak height was considered; the range tested was from 90–990 µl. The results were compared with the maximum possible output, *i.e.*, that arising from continuous sample passage. Fig. 3 shows higher outputs as sample volume was increased, but these points were not suitable as the base peak was too wide. Therefore, 540 µl

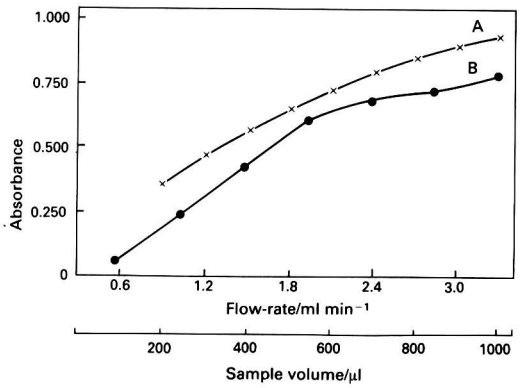

Fig. 3 Optimization of FI parameters: A, flow-rate; and B, sample volume

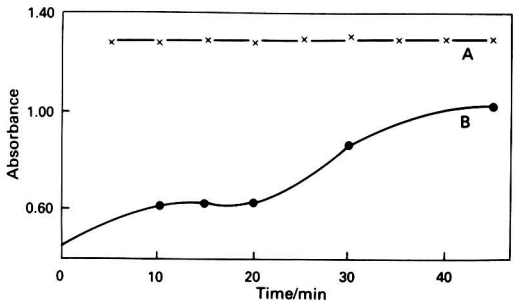

Fig. 4 Stability of the column and influence of pre-conditioning. Glycine, 100 ppm. A, Continuous passage of glycine solution; and B, mean values (20 replicates) of transient signals after different column pre-conditioning times

was selected for further work as the volume affording the best compromise between sensitivity and sample throughput.

The FI peaks were higher as the flow-rate was increased, but reproducibility of outputs was clearly worse at elevated flow-rates. The range tested was between 0.4 and 3.2 ml min^{-1}; the selected value was 1.7 ml min^{-1}.

The stability of the column was checked using the FI assembly and with two different sets of experiments. In the first set, the column was subjected to rapid consumption (*i.e.*, to a continuously flowing analyte solution instead of discrete sample volumes); the carrier solution, which contained 100.0 ppm of the amino acid at pH 9.5 flowed continuously (flow-rate 1.5 ml min^{-1}) through the column, no injections were performed. The flow-rate was kept constant for 45 min, and a total volume of 67.5 ml (6.750 mg of glycine) was forced through the column. The outputs were recorded at 5 min intervals; the mean absorbance was 1.280 and the relative standard deviation (RSD) was 0.8%. (Fig. 4.)

The results were considered as indicative only, as the flow assembly includes a washing step between injections. In the second set of experiments, the stability of the column was further tested by injection into the proposed assembly, with normal operation, of six different series of 20 injections containing 100 ppm of glycine in buffered solution, the difference being the time employed for column pre-treatment (0, 10, 15, 20, 30 and 45 min prior to injection). The column was conditioned as described under Procedures. The peak height was clearly influenced by the preliminary treatment of the column. The results obtained, shown in Fig. 4, demonstrate that (*a*) the pre-treatment interval is not a critical parameter in the range 10–20 min; and (*b*) the column remains stable (same outputs) for any series of injections tested.

Analytical Application

The calibration graph was found to be linear over the range 10–90 ppm of glycine; $A = -88.389 + 12.798c$ [where A is the absorbance ($\times 10^3$) and c the concentration of glycine in ppm]; the correlation coefficient was 0.9994.

The repeatability of the determination and sample throughput were tested by injecting into the reagent stream 30 samples containing 50.0 ppm of glycine. The calculated RSD was 1.9%, and a sample injection rate of 40 h^{-1} was achieved.

The tolerance of the method to interfering compounds, which are commonly found in glycine pharmaceutical formulations, was investigated by preparing mixtures of 50 ppm of glycine and different amounts of the foreign compound. The results of these studies are as follows (interfering species, maximum amount tested in ppm and relative error): caffeine, 500 and 0.37%; NaCl, 1000 and 1.98%; acetylsalycilic acid, 500 and 1.5%; ascorbic acid, 54 and 1.4%; and sorbitol, 800 and 4.6%.

Glycine was determined in the pharmaceutical formulation Okal (from Puerto Galiano) containing 100 mg of glycine per tablet as the label claims. A typical result was 105.4 mg per tablet.

Conclusions

An indirect FI-AAS procedure has been developed for the determination of glycine, with application to the analytical control of pharmaceutical formulations. The method is based on the reaction of glycine with solid copper(II) carbonate and is applicable to low concentrations of glycine.

The use of the solid reagent enables a simple FI manifold to be used. The preparation of the column is rapid and easy, and the lifespan of the reactor is sufficiently long to allow the processing of a number of samples. The large surface area of the packed reactor allows the column length to be shorter than that usually employed in similar FI packed-bed reactors (0.5 cm as against more than 1 m).

The precision of the procedure is competitive with that of other established techniques, with no serious interference from compounds usually found in formulations of glycine.

References

1 Mottola, H. A., *Quim. Anal.*, 1989, **8**, 119.
2 Marshall, M. A., and Mottola, H. A., *Anal. Chem.*, 1983, **55**, 2089.
3 Luhrmann, M., Shelter, N., and Kettrup, A., *Fresenius Z. Anal. Chem.*, 1985, **322**, 476.
4 Faizullah, A. T., and Townshend, A., *Anal. Chim. Acta*, 1985, **167**, 225.
5 Faizullah, A. T., and Townshend, A., *Anal. Chim. Acta*, 1985, **172**, 291.
6 Den Boef, G., *Anal. Chim. Acta*, 1989, **216**, 289.
7 Lazaro, F., Luque de Castro, M. D., and Valcárcel, M., *Anal. Chim. Acta*, 1988, **214**, 227.
8 Martinez Calatayud, J., and Sagrado Vives, S., *J. Pharm. Biomed. Anal.*, 1989, **7**, 1165.
9 Martinez Calatayud, J., and Gomez Benito, C., *Anal. Chim. Acta*, 1990, **231**, 259.
10 Bower, L. B., *Anal. Chem.*, 1986, **58**, 513A.
11 Greenstein, J. P., and Winitz, M., *Chemistry of the Amino Acids*, Wiley, New York, 1961.
12 Galjarrd, H., *Genetic Metabolic Disorders*, Elsevier, Amsterdam, 1980.
13 Ali Qureshi, G., and Qureshi, A. R., *J. Chromatogr.*, 1989, **491**, 281.
14 *Official Methods of Analysis of the Association of Official Analytical Chemists*, ed. Williams, S., Association of Official Analytical Chemists, Arlington, VA, 14th edn., 1984.
15 Pine, S. H., and Hendricson, J. B., *Quimica Organica*, McGraw-Hill, New York, 1988.

Paper 0/04768F
Received August 21st, 1990
Accepted October 23rd, 1990

BOOK REVIEWS

Analytical Absorption Spectrophotometry in the Visible and Ultraviolet. The Principles

L. Somer. *Studies in Analytical Chemistry 8.* Pp. 311. Elsevier. 1989. Price $129.95; Dfl265.00. ISBN 0-444-98882-3.

The subject of this book has been very extensively covered, both from the point of view of the theory of spectrophotometry and the associated instrumentation and from the analytical procedures covered, a fact acknowledged by the Author in his 'Preface'. It is therefore difficult to see the need for yet another volume on the subject, except in the context of the series '*Studies in Analytical Chemistry*' of which this is the eighth volume. Such a series would certainly look incomplete without a contribution from ultraviolet–visible spectrophotometry, but it is difficult to see what this current volume adds to the literature on the subject.

The volume starts with two chapters (92 pages) covering the 'Basis of Spectrophotometry' and 'Principles of Instrumentation'. The first of these is a concise account of the principles of spectrophotometry, although some of the terminology is non-standard, the second, the chapter on instrumentation is very brief and would have been better omitted in order to allow space for a more detailed treatment of some of the other areas of the subject, which (one suspects due to limitations of space) also receive a rather superficial treatment.

The two chapters on 'Errors in Spectrophotometry' and 'Evaluation of the Analyte Concentration . . . ' are adequate if a little dated. (Stray light levels are now much better than indicated, while the presence of the microprocessor and/or the dedicated PC on practically all instruments makes apparently complex procedures routine.)

A chapter on 'Optimization of Spectrophotometric Procedures' is over brief, 16 pages are devoted to complex equilibrium, while experimental optimization takes little more than one page! About 90 pages are devoted to 'Special Approaches in Spectrophotometry', covering topics such as difference spectrophotometry, multicomponent analysis, elimination of blocks, derivative spectrophotometry (rather brief), dual-wavelength spectrophotometry, spectrophotometric titration, automation (including flow injection analysis in three pages!) and high-sensitivity spectrophotometry. 'Complexation and Spectrophotometry' covers organic analytical reagents, ternary species, ion pairs and the use of surfactants, in about 20 pages using some very selective examples for illustrative purposes.

The volume concludes with a 40 page section on applications which is far too brief to be of any real use. For example, analysis of light purity materials is covered in two pages, while amplification reactions are covered in half a page! Analysis of organic substances gets a two page treatment while environmental chemistry gets two pages and a four page table, while clinical chemistry is dealt with in one page with a one page table.

In general the book is produced very well with only a few typographical errors such as 'CO' for Co which would cause few readers any real problems. It is referenced up to 1988, but comparatively few references are post-1980, which probably reflects the lack of real advances in the subject except in data processing in recent years, despite the voluminous literature on the subject.

The Author has made a valiant attempt to cover the subject in a minimum of space and any criticism should be directed to those who produced his remit rather than the author! The price of the book is not excessive by today's standards and it should be of use to those who need a thoroughly referenced, if limited, treatment of the subject.

C. A. Watson

Selectivity and Detectability Optimizations in HPLC

Satinder Ahuja. *Volume 104 in Chemical Analysis. A Series of Monographs on Analytical Chemistry and Its Applications.* Pp. xi + 610. Wiley-Interscience. 1990. Price £70.00. ISBN 0-471-62645-7.

Selecting the conditions for the successful chromatographic separation of a complex mixture can be a laborious and time-consuming task. The task is often hampered by a lack of experience with all the potential methods that could be used, but unfortunately also, by a lack of guidance from the theory of chromatography because of our often poor understanding of the mechanism of retention.

In this book the author draws on his own, and the experience of others, to illustrate the factors that can affect a separation and how the different modes of liquid chromatography operate. For each mode the stationary phases are described, the mechanism of retention is discussed and finally, a series of applications are given. However, he concludes that in many instances selection of conditions is still mainly a matter of trial and error.

However, rather disappointingly it appears that this book has taken a long time to publish. Most of the sections seem to have been essentially completed by 1984 with only minor later additions. Out of 132 references in the chapter on reversed-phase chromatography only eight (two of which are the author's own work) are post-1984 and similar distributions apply in other chapters. This is particularly noticeable in the sections on adsorption and normal-phase chromatography, which still refer to separations using ODPN and Carbowax coated columns, and almost all of the applications were published between 1975 and 1983; 'a recent review' was published in 1984. Ion chromatography stops at about 1984 and omits all three of the comprehensive books on the topic published between 1983 and 1987, but pleasingly the section on isomeric separations, including chiral chromatography, goes up to 1987. Snyder and Kirkland (1979 Edition) and the author's own texts are the primary references in most chapters and few of the many more recent monographs on HPLC are included. The last section on detection seems out of place and although interesting adds little to other previous publications.

Overall, the style is often that of a referenced review and there is a tendency to return to topics two or three times (such as Pirkle columns) increasing the coverage on each occasion. The applications sections are a series of representative examples rather than co-ordinated surveys.

However, despite these failings this book contains much good advice and basic information and it should be useful to the practising chromatographer as a reminder of the great flexibility of liquid chromatography and of the wide range of variables that can be employed.

Roger M. Smith

CUMULATIVE AUTHOR INDEX

JANUARY–MARCH 1991

The XXVII Colloquium Spectroscopicum Internationale

XXVII CSI

1991
NORWAY

will be held in

Grieg Hall, Bergen, Norway
June 9–14 1991

IUPAC

This traditional biennial conference in analytical spectroscopy will once again provide a forum for atomic, nuclear and molecular spectroscopists worldwide to encourage personal contact and the exchange of experience.

Participants are invited to submit papers for presentation at the XXVII CSI, dealing with the following topics:

Basic theory and instrumentation of—

- Atomic spectroscopy (emission, absorption, fluorescence)
- Molecular spectroscopy (UV, VIS and IR)
- X-ray spectroscopy
- Gamma spectroscopy
- Mass spectrometry (inorganic and organic)
- Electron spectroscopy
- Raman spectroscopy
- Mössbauer spectroscopy
- Nuclear magnetic resonance spectrometry
- Methods of surface analysis and depth profiling
- Photoacoustic spectroscopy

Application of spectroscopy in the analysis of—

- Metals and alloys
- Geological materials
- Industrial products
- Biological samples
- Food and agricultural products

Special emphasis will be given to trace analysis, environmental pollutants and standard reference materials.
The scientific programme will consist of both plenary lectures and parallel sessions of oral presentation. Specific times will be reserved for poster sessions.

PRE- AND POST-SYMPOSIA

In connection with the XXVII CSI the following symposia will be organised:

Pre-symposia—

I. GRAPHITE ATOMISER TECHNIQUES IN ANALYTICAL SPECTROSCOPY
June 6–8, 1991, Hotel Ullensvang, Lofthus, Norway.

II. CHARACTERISATION OF OIL COMPONENTS USING SPECTROSCOPIC METHODS
June 6–8, 1991, Hotel Hardangerfjord, Øystese, Norway.

III. MEASUREMENT OF RADIO-NUCLIDES AFTER THE CHERNOBYL ACCIDENT
June 6–8, 1991, Hotel Solstrand, Bergen, Norway.

Post-symposium—

IV. SPECIATION OF ELEMENTS IN ENVIRONMENTAL AND BIOLOGICAL SCIENCES
June 17–19, 1991, Hotel Alexandra, Loen, Norway.

For further information contact:

THE SECRETARIAT
XXVII CSI
HSD Congress-Conference
P.O. Box 1721 Nordnes
N-5024 Bergen, Norway.
Tel. 47-5-318414, Telex 42607 hsd n, Telefax 47-5-324555

FIRST FOLD HERE

THE ANALYST READER ENQUIRY SERVICE
For further information about any of the products featured in the advertisements in this issue, write the appropriate number on the postcard, detach and post.

FOLD HERE

THE ANALYST READER ENQUIRY SERVICE MARCH'91

For further information about any of the products featured in the advertisements in this issue, please write the appropriate number in one of the boxes below.
Postage paid if posted in the British Isles but overseas readers must affix a stamp.

PLEASE USE BLOCK CAPITALS LEAVING A SPACE BETWEEN WORDS *Valid 12 months*

1 NAME

2 COMPANY

PLEASE GIVE YOUR BUSINESS ADDRESS IF POSSIBLE. IF NOT, PLEASE TICK HERE ☐

3 STREET

4 TOWN

5 COUNTY
POST CODE

6 COUNTRY

7 DEPARTMENT
DIVISION

8 YOUR JOB TITLE
POSITION

9 TELEPHONE NO

OFFICE USE ONLY REC'D PROC'D

FOLD HERE

Postage will be paid by Licensee

Do not affix Postage Stamps if posted in Gt. Britain, Channel Islands, N. Ireland or the Isle of Man

BUSINESS REPLY SERVICE
Licence No. WD 106

Reader Enquiry Service
The Analyst
The Royal Society of Chemistry
Burlington House, Piccadilly
LONDON
W1E 6WF
England

ANALAO 116(3) 221–332 (1991) March 1991

The Analyst

The Analytical Journal of The Royal Society of Chemistry

CONTENTS

Typeset and printed by Black Bear Press Limited, Cambridge, England